ICPMG 2010 – volume 1

Physical Modelling in Geotechnics

Editors
Sarah Springman, Jan Laue and Linda Seward

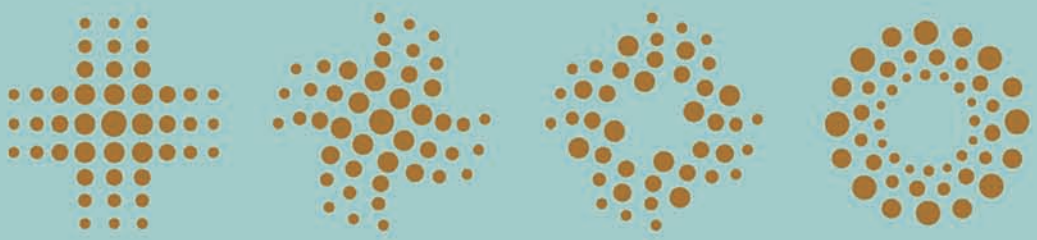

CRC Press
Taylor & Francis Group
A BALKEMA BOOK

This page intentionally left blank

PROCEEDINGS OF THE 7TH INTERNATIONAL CONFERENCE ON PHYSICAL MODELLING IN GEOTECHNICS 2010 (ICPMG 2010), ZURICH, SWITZERLAND, 28 JUNE–1 JULY 2010

Physical Modelling in Geotechnics

Editors
Sarah Springman, Jan Laue & Linda Seward
Institut für Geotechnik, ETH Zürich, Zürich, Switzerland

VOLUME 1

CRC Press
Taylor & Francis Group
Boca Raton London New York Leiden

CRC Press is an imprint of the
Taylor & Francis Group, an **informa** business

A BALKEMA BOOK

CRC Press
Taylor & Francis Group
6000 Broken Sound Parkway NW, Suite 300
Boca Raton, FL 33487-2742

Version Date: 20131028

International Standard Book Number-13: 978-1-4665-5742-0 (eBook - PDF)

Physical Modelling in Geotechnics – Springman, Laue & Seward (eds)
© 2010 Taylor & Francis Group, London, ISBN 978-0-415-59288-8

Table of contents

Physical Modelling in Geotechnics – Springman, Laue & Seward (eds)
© 2010 Taylor & Francis Group, London, ISBN 978-0-415-59288-8

Preface

The International Conferences on Physical Modelling in Geotechnics, held under the auspices of Technical Committee 2 (TC2: *Physical modelling in geotechnics*) of the International Society of Soil Mechanics and Geotechnical Engineering, provide a roughly quadrennial focus for diverse and internationally significant scientific and technical research on many aspects relating to geotechnical physical modelling. Following preliminary workshops in Manchester, California and Tokyo, all in 1984, TC2 conferences were held in Paris, France (1988), Boulder, Colorado (1991), Singapore (1994), Tokyo, Japan (1998), St Johns, Canada (2002) and Hong Kong, HKSAR (2006). TC2 returned to Europe after 22 years for the 7th International Conference (ICPMG 2010), which was held in Zurich between 28th June and 1st July, celebrating 75 years of soil mechanics and geotechnical engineering at the host institution, ETH Zurich. The next conference will be held in Perth, Western Australia in 2014.

The 7th ICPMG Proceedings reflect progress made since the last international conference, held in Hong Kong in 2006 under the leadership of Professor Charles Ng, and contain 3 keynote lectures and 228 reviewed contributions from 32 countries. The papers document the state of the art in soil-structure-interaction, natural hazards, earthquake and soft soil engineering, with ever increasing complexity of modelling, challenging existing understanding of similitude, as many problems hover on the boundaries of mechanics, hydraulics, physics and chemistry. Our community revels in this opportunity and takes great joy in benefitting from modern technology in improving our modelling and analytical techniques, while managing massive quantities of data. However, it is important that we communicate our passion for physical modelling and how we can use it to solve ongoing problems for industry, and then share our progress across the world. These aspirations are investigated, and progress reported, in papers representing focus areas of the TC2 working groups over the last four years, such as similitude, industry relationships, data management and education.

The organisation of the conference was a collaborative effort by volunteers from all continents, including key contributions to the peer review process and to the administration. Close contact was also maintained with the Board of the International Society of Soil Mechanics and Geotechnical Engineering, to which TC2 reports. Deep appreciation is due to all who worked to make the conference a success, particularly the core members of the Local Organising Committee. I am especially grateful to my hardworking co-editors, Jan Laue and Linda Seward, and the outstanding review editors of the two proceedings volumes, the assistant editors and numerous reviewers, all of whom devoted their valuable time and expertise to ensure that the papers published are of the highest possible quality.

The conference venue, Zurich, is a lively and colourful city within a small, densely populated, country in the heart of Europe that offers a perfect field laboratory for geotechnical engineers. Conference participants were able to enjoy an innovative public lecture, in which the impact of physical modelling on understanding and dealing with the hazards of climate change was presented alongside the work of a famous Swiss artist, who modelled erosion in the ETH Geotechnical Drum Centrifuge, which was inaugurated in 2000. A special state-of-the-art-lecture, plenary keynote presentations, oral and poster sessions on specific topics, parallel sessions for the centrifuge technicians, exhibits and social events made up the main programme of the conference.

I hope that these proceedings will provide an inspiration to future generations of geotechnical engineers.

Sarah M. Springman
Chair, Technical Committee 2 on Physical Modelling in Geotechnics, 2005–2010
(of the International Society of Soil Mechanics and Geotechnical Engineering)
Chair, 7th International Conference on Physical Modelling in Geotechnics, 2010
ETH Zurich, Switzerland

This page intentionally left blank

Physical Modelling in Geotechnics – Springman, Laue & Seward (eds)
© 2010 Taylor & Francis Group, London, ISBN 978-0-415-59288-8

Committees

LOCAL ORGANISING COMMITTEE

S.M. Springman, *Chair* (ETH Zurich, TC2)
J. Laue, *Vice Chair* (ETH Zurich, TC2)
M. Amberg, *Excursions* (ETH Zurich)
M.F. Bransby (University of Dundee, UK)
E.A. Ellis (Plymouth University, UK)
S.K. Haigh (Cambridge University, UK)
R. Herzog, *IT support* (ETH Zurich)
D. König (Ruhr-University Bochum, Germany)
G. Laios, *Conference Secretariat* (ETH Zurich)
P.-A. Mayor, *Finances* (ETH Zurich)
A. McNamara (City University, London, UK, TC2)
L.J. Seward, *Publications* (ETH Zurich)
B. Teymur (Istanbul Technical University, Turkey, TC2)
L. Thorel (Laboratoire Central des Ponts et Chaussées, Nantes, France)
D.J. White (University of Western Australia, Perth, TC2)
S. Zwahlen, *Finances* (ETH Zurich)

INTERNATIONAL ADVISORY BOARD

T. Abdoun (Rensselaer Polytechnic Institute, Troy, NY, USA)
M.S.S. Almeida (Federal University of Rio de Janeiro, Brazil, TC2)
G. Anagnostou (ETH Zurich, Switzerland)
A. Bezuijen (Deltares, The Netherlands, TC2)
M.D. Bolton (Cambridge University, UK)
E.T. Bowman (University of Canterbury, New Zealand, TC2)
B. Caicedo (Universidad de los Andes, Bogotà, Colombia, TC2)
P. Culligan (Columbia University, USA, TC2)
A. El Nimr (Mansoura University, Egypt)
A. Elgamal (University of California, San Diego, USA)
V. Fioravante (Ferrara University, Italy, TC2)
P. Foray (Institut National Polytechnique de Grenoble, France, TC2)
J. Garnier (LCPC, France, TC2)
C. Gaudin (University of Western Australia, Perth, Australia, TC2)
J. Grabe (Technische Universität Hamburg-Harburg, Germany)
O. Hededal (Technical University of Denmark, Lyngby, Denmark)
C. Hird (University of Sheffield, UK, TC2)
Y. Hou (China Institute of Water Resources and Hydropower Research, Beijing, China, TC2)
A.B. Huang (National Chiao Tung University, Taiwan, TC2)
S. Iai (Kyoto University, Japan)
R. Katzenbach (Technische Universität Darmstadt, Germany)
D.S. Kim (KOCED Geocentrifuge Center at KAIST, Daejeon, Korea)
O. Kusakabe (Tokyo Institute of Technology, Japan, TC2)
B. Kutter (University of California, Davies, USA, TC2)
C.J. Lee (National Central University, Taiwan, TC2)

F.H. Lee (National University of Singapore, Singapore)
C.C.F. Leung (National University of Singapore, TC2)
S.P.G. Madabhushi (Cambridge University, UK, TC2)
R.J. Mair (Cambridge University, UK)
D. Muir Wood (University of Dundee, UK)
C.W.W. Ng (Hong Kong University of Science and Technology, Hong Kong, TC2)
C. O'Loughlin (Institute of Technology Sligo, Ireland, TC2)
R. Phillips (C-CORE, St Johns, Canada, TC2)
J.C. Portugal (Laboratorio Nacional de Engenharia Civil, Lisbon, Portugal, TC2)
M.F. Randolph (University of Western Australia, Perth, Australia)
H. Salehzadeh (Iran University of Science and Technology, Iran)
T. Schanz (Ruhr-Universität Bochum, Germany)
J.S. Sharma (University of Saskatchewan, Canada)
K. Soga (University of Cambridge, UK)
W.A. Take (Queen›s University, Kingston, Canada, TC2)
R.N. Taylor (City University, London, UK)
V. Vinogradov (Moscow State University of Railway Engineering MIIT, Russia, TC2)
B.V.S. Viswanadham (Indian Institute of Technology Bombay, India, TC2)
A.A. Zaitsev (Moscow State University of Railway Engineering MIIT, Russia)
J. Zornberg (University of Texas at Austin, Texas, USA)

Physical Modelling in Geotechnics – Springman, Laue & Seward (eds)
© 2010 Taylor & Francis Group, London, ISBN 978-0-415-59288-8

External review editors

M.F. Bransby
(University of Dundee, UK)

M.J.Z. Brown
(University of Dundee, UK)

B. Caicedo
(Universidad de los Andes, Bogotà, Colombia)

E.A. Ellis
(Plymouth University, UK)

V. Fioravante
(Ferrara University, Italy)

C. Gaudin
(University of Western Australia, Australia)

J. Grabe
(Technical University Hamburg-Harburg, Germany)

S.K. Haigh
(Cambridge University, UK)

D. König
(Ruhr University Bochum, Germany)

A. McNamara
(City University, London, UK)

C. O'Loughlin
(Institute of Technology Sligo, Ireland)

R. Phillips
(C-CORE, St Johns, Canada)

W.A. Take
(Queen's University, Kingston, Canada)

B. Teymur
(Istanbul Technical University, Turkey)

T. Tobita
(Disaster Prevention Research Institute, Uji, Kyoto, Japan)

B.V.S. Viswanadham
(Indian Institute of Technology Bombay, India)

D.J. White
(University of Western Australia, Australia)

D. Muir Wood
(University of Dundee, UK)

J. Zornberg
(University of Texas at Austin, USA)

Internal assistant editors

M. Amberg

A. Arnold

A. Askarinejad

G. Laios

A. Marin

F. Morales

Y. Yamamoto

Physical Modelling in Geotechnics – Springman, Laue & Seward (eds)
© 2010 Taylor & Francis Group, London, ISBN 978-0-415-59288-8

List of reviewers

The editors are most grateful to the following people, who helped to review the manuscripts and assisted in improving the quality and presentation of the papers in these proceedings.

T. Abdoun
M. Achmus
D. Airey
P. Allan
G. Anagnostou
I. Anastasopoulos
N. Baker
A. Basha
P. Becker
R. Berardi
A. Bezuijen
S. Bhattacharya
B. Bienen
E. Bilotta
J. Black
M. Bouazza
E.T. Bowman
N. Boylan
S. Brandenberg
M.F. Bransby
A. Brennan
M.J.Z. Brown
C. Budach
B. Byrne
B. Caicedo
L. Caldeira
P. Carrubba
F. Casini
F. Castelli
A. Cerato
V.S. Chandrasekaran
J.-L. Chazelas
J. Cheuk
U. Cilingir
C. O'Loughlin
E. Conte
W.H. Craig
P. Culligan
A. Deeks
O. Detert
M. Dewoolkar
A. Dietmar
J. Dijkstra
S. Dwyer
A. El Nimr
E.A. Ellis
N. Estrada
J. Fannin
V. Fioravante
A. Flora
J. Garnier
C. Gaudin
K. Gavin
M. Ghazavi
B. Ghosh
A. Ghosh
C. Gnanendran
R. Goodey
G. Gottardi
S. Gourvenec
L. Govoni
W.D. Guo
S.K. Haigh
A. Heath
O. Hededal
S. Henke
A. Hettler
Y. Higo
C. Hird
M.S. Hossain
Y. Hu
A. Hyde
J. Izawa
R. Jagow-Klaff
A. Juneja
K. Kelesoglu
S. Kessler
D.S. Kim
K. Kita
J. Knappett
S.-I. Kobayashi
D. König
J. Laue
C.-J. Lee
F.H. Lee
B. Lehane
N. Levy
L. Li
S. Lobo-Guerrero
M. Long
F. Lopez-Caballero
X. Ma
G. Madabhushi
I. Manzella
J. Marcelino
D. Marot
R. McAffee
J. McCartney
A. McNamara
R. Merifield
I. Moore
R. Motamed
D. Muir Wood
C. Murillo
D. Murty
A. Mwasha
P. Naughton
T. Newson
C.W.W. Ng
C. Nogueira
M. Okamura
M. Pando
V. Pane
R. Phillips
E. Pimentel
J. Portugal
F. Rackwitz
K. Rajagopal
M. Rayhani
D. Richards
M. Richardson
R.G. Robinson
L. Röchter
F. Saboya
S. Sassa
R. Schäfer
P.E.L. Schaminée
J. Schneider
M. Senders
L.J. Seward
M. Shah
J.S. Sharma
R. Shen
S. Tamura
L.S. Sze Yue
G. Siemens
B.-H. Silva
C. Smith
J. Speerli
S.M. Springman
K. Stone
M. Stringer
A. Taboada
A. Takahashi
H. Takahashi
W.A. Take
J. Takemura
R.N. Taylor
K.L. Teh
B. Teymur
L. Thorel
T. Tobita
L.E. Vallejo
A. Valsangkar
V. van Beek
S. Vanapalli
G. Venkatachalam
G.M.B. Viggiani
B.V.S. Viswanadham
A. Volkwein
D. Wang
J. Wartman
D. White
D. Wilson
A.A. Zaitsev
A. Zakeri
X. Zeng
J. Zornberg

This page intentionally left blank

Physical Modelling in Geotechnics – Springman, Laue & Seward (eds)
© 2010 Taylor & Francis Group, London, ISBN 978-0-415-59288-8

Conference sponsors

PLATINUM SPONSORS

http://www.actidyn.com/

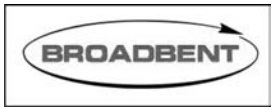

http://www.broadbent.co.uk/

SILVER SPONSOR

Solexperts http://www.solexperts.ch

BRONZE SPONSOR

Tekscan http://www.tekscan.com/

CO-SPONSORS

Kanton Zürich http://www.ktzh.ch/
Stadt Zürich http://www.stadt-zuerich.ch/portal/en/index.html

SUPPORTERS

Tencate service.ch@tencate.com
Swiss http://www.swiss.com
ETH Zurich http://www.ethz.ch/index_EN
Institute for Geotechnical Engineering http://www.igt.ethz.ch

This conference is held under the auspices of the International Society for Soil Mechanics and Geotechnical Engineering ISSMGE (http://www.issmge.org).

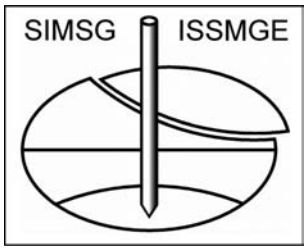

This page intentionally left blank

1 *Keynotes and TC 2 contributions*

This page intentionally left blank

Physical Modelling in Geotechnics – Springman, Laue & Seward (eds)
© 2010 Taylor & Francis Group, London, ISBN 978-0-415-59288-8

Physical modelling of natural hazards

M.C.R. Davies
Faculty of Engineering, The University of Auckland, Auckland, New Zealand

E.T. Bowman
Department of Civil and Natural Resources Engineering, University of Canterbury, Christchurch, New Zealand

D.J. White
Centre for Offshore Foundation Systems, The University of Western Australia, Perth, Australia

ABSTRACT: In order to assess the risks associated with a natural hazard, it is necessary that as full an understanding as possible is available about the mechanisms associated with it. This paper considers how physical modelling may be used to study the mechanisms associated with natural hazards that have direct geotechnical implications. Physical modelling may be conducted to understand trigger mechanisms as well as the mechanisms they initiate, and this knowledge may be used to inform the processes of geotechnical risk assessment. Close control over material properties and well defined boundary conditions in physical models enable repeatability that permits parametric studies to be conducted. Physical model testing can also be used to validate analytical and numerical methods and assess techniques for hazard reduction or rehabilitation. Examples of physical modelling studies to obtain a greater understanding of the mechanisms associated with sliding slopes, earthquake surface fault rupture and slope instabilities due to climate change driven permafrost degradation are presented and the current state-of-the-art assessed.

1 INTRODUCTION

The term "natural hazards" may be applied to a wide range of natural phenomena. It has been defined more specifically by Burton et al. (1978) as "those elements of the physical environment, harmful to man and caused by forces extraneous to him". It has now become accepted generally that there are seven major classes of natural hazard, i.e. earthquakes, floods, hurricanes, landslides, tsunamis, volcanoes, and wildfires. Whilst all could, to a greater or lesser extent, result in a potential geotechnical hazard, this paper will concentrate on natural hazards that have direct geotechnical implications. It is important that fundamental mechanisms associated with such natural hazards are well understood because this knowledge forms a vital component of geotechnical risk assessment. These mechanisms can be studied in a number of ways. The most direct is through field observation. However, since generally this can be done only after a catastrophic event, it is not always possible to establish reliably trigger mechanisms that initiated the phenomenon or how subsequent mechanisms developed in the immediate aftermath of the trigger. Long term field monitoring provides a possible solution to this, but it is not generally possible to determine when and where a physical event (e.g. an intense rainfall or earthquake induced landslide) will result; rendering scientific study of such hazards somewhat serendipitous.

An alternative to field studies is to model the natural hazard either analytically (including numerical studies) or physically, or in a combination of both. Both approaches have their limitations and strengths and a detailed comparison is outside the scope of this paper. In the case of analytical/numerical modelling, it is necessary to define the constitutive behaviour of the geomaterials and the boundary conditions of the physical process (e.g. such as the volume of a slope and the run out area for a flow slide) together with modelling accurately the trigger for the process. In physical models, it is necessary to use appropriate materials and to be aware of scaling conflicts. It is necessary also to ensure that, with due regard to the appropriate scaling laws (and the potential conflicts within these), the scale of the model and its boundary conditions are appropriate to replicate accurately the physical phenomena being studied. The combination of physical and analytical modelling to investigate a potential natural geohazard is a particularly powerful technique because—as real events in their own right—physical models may be used to validate numerical or other analytical techniques that may then be used to model a field

(i.e. full scale or "prototype") situation where the scale is too large or the boundary conditions too complex to model satisfactorily in a physical model, (e.g. Anastasopoulos et al. 2007).

Despite the limitations of scale (i.e. the limiting dimensions of a prototype that can be modelled in a specialist facility, the laboratory or in a geotechnical centrifuge), physical models have significant beneficial characteristics compared to full scale monitoring for conducting fundamental studies of mechanisms. Close control over material properties and well defined boundary conditions in physical models enable repeatability that permits parametric studies to be conducted. In addition, simulations of processes that would otherwise be highly time consuming or almost impossible to achieve can be conducted (e.g. modelling rock falls in permafrost resulting from an increase in mean annual air temperature over a 50 year period, Davies et al. 2001) and, also, remediation techniques and techniques for hazard reduction or rehabilitation may be assessed.

The majority of physical modelling of mechanisms associated with natural hazards that has been reported in the literature has described investigations of phenomena related to earthquakes and mass movements of soil and rock. The earthquake phenomena that have been studied most in physical models—particularly in geotechnical centrifuge modelling—are related to ground shaking. This includes the development of both liquefaction and lateral spreading, which can lead to geotechnical hazards such as foundation failure. There have been extensive studies of the response of structures and foundation systems to ground shaking using both laboratory floor models (e.g. Knappett et al. 2006) and centrifuge modelling (e.g. Gajan et al. 2005) and this area of soil structure interaction is outside the scope of this paper. However, earthquakes can also give rise to ground shaking that can trigger events such as landslides and also result in surface fault rupture. Both topics have been the subject of physical model studies and are, therefore, considered herein.

The most comprehensive recent study of the global climate system (IPCC 2007) indicates that global average temperatures have risen by nearly 0.8°C since the late 19th century, and in the last 25 years have been rising at a rate of about 0.2°C/decade. A consequence of this is that other aspects of climate will be affected. For example, global climate models predict changes in the amount and intensity of rainfall in some parts of the world which will, clearly, have an effect on the temporal stability of slopes in affected regions (IPCC 2007). A more direct consequence of the rise in average air temperature in high latitudes and altitudes is that this can lead to degradation of permafrost that can result in reductions in slope stability and an increased hazard potential.

Notwithstanding the experimental difficulties and limitations associated with the physical modelling of natural geotechnical hazards, the authors have conducted successfully a variety of studies in this area. This paper considers and critically assesses the outcomes of examples of physical model studies conducted by the authors and reported in the literature that focus on understanding mechanisms associated with natural hazards resulting from mass movements, earthquake surface fault rupture and permafrost degradation.

2 MASS MOVEMENTS: SLIDING SLOPES

2.1 *Background*

2.1.1 *Types and scales of mass movement*

Mass movements constitute the large-scale translation of soil, rock, ice and water in varying proportions and over varying timescales under the influence of gravity. They pose risks to life and infrastructure in all areas of relatively steep terrain—in particular where earthquakes and/or heavy rainfall are also a factor. Sub-aerial mass movements are accorded various names according to type: rock avalanches, landslides, debris flows and rock falls, to name a few. Submarine mass movements are sometimes also referred to as debris flows, and can transform into turbidity currents. Although typically only ~10% of a submarine slide is mobilised into a turbidity current, these currents can travel over very large distances—up to hundreds of kilometres—and last for long periods of time—up to several days.

The mechanics of a particular type of mass movement relates to its trigger, constituent materials, volume and speed of movement. Clearly there are some mechanical processes, which are common to all types of movement, while others are peculiar to one type.

As summarized by Coussot & Meunier (1996) for sub-aerial mass movements, the speed of a particular type of movement tends to relate to its proportion of water, with higher water content often leading to faster flows (except in the case of rock avalanches, where water does not appear to be a factor). Grain size is also important, with slides and flows involving coarse granular materials tending to be more finely balanced with regard to their motion—progressing from failure to rapid speeds with little apparent change in water content—compared to those that are clay dominated. There is a wide range of typical velocities and of typical volumes of material pertinent to each type of mass movement. These are summarized in Table 1 and the volume ranges are shown schematically across the top of Figure 1.

Also shown on Figure 1 are a set of data showing the typical scales of subaerial and subaqueous mass movements, reproduced from De Blasio et al. (2006). The runout ratio, H/L, is a dimensionless measure of the reach of a mass movement. The height H, is the vertical distance from the crest of the intact material to the base of the slide, after running out. L is the horizontal distance, usually measured from the rear of the intact block to the tip (rather than the centroid) of the deposited material. This ratio is inversely proportional to the coefficient of friction mobilised within the slide (which serves to dissipate the potential energy of the slide)—whether modelled as basal sliding or through internal deformation (Dade & Huppert 1998; Issler et al. 2005).

Table 1. Typical range of velocities and sizes of events for mass movements. Note, some extreme events may exceed the "typical" range.

Mass movement	Volume magnitude (m^3)	Average velocity (m/s)
Landslide	10^3–0^7	0.001–10
Rockfall	10^2–0^5	5–50
Mudflow/lahar	10^3–0^9	1–25
Debris flow	10^2–0^6	0.5–20
Rock avalanche	10^4–0^9	10–90
Submarine slide	10^7–0^{12}	5–50

There is a clear dependency of the runout ratio on the absolute size of the mass movement, which highlights the existence of an underlying effect of scale. Models of slide runout based on sliding Coulomb friction indicate that the equivalent friction coefficient controlling the runout must reduce significantly as the size of the slide increases. Alternatively, other mechanisms of slide mobility must be invoked, such as lubrication by trapped air (Shreve 1968), molten material (Erismann 1979), or heat-generated pore pressure (Habib 1967, 1975; Goguel 1978; Vardoulakis 2000). Acoustic fluidisation has also been proposed as a weakening mechanism within larger slides (Melosh 1979). The need to invoke these additional mechanisms, beyond the conventional behaviour of a drained or undrained continuum of soil means that the scaling of physical models to prototype scale is likely to be more challenging than for more conventional geotechnical problems.

The runout ratio of a mass movement is also affected by the presence of pore water as opposed to pore air. Subaqueous slides invariably show a greater runout distance than subaerial slides of the same volume and the same initial properties. This observation that a viscous pore fluid (and ambient

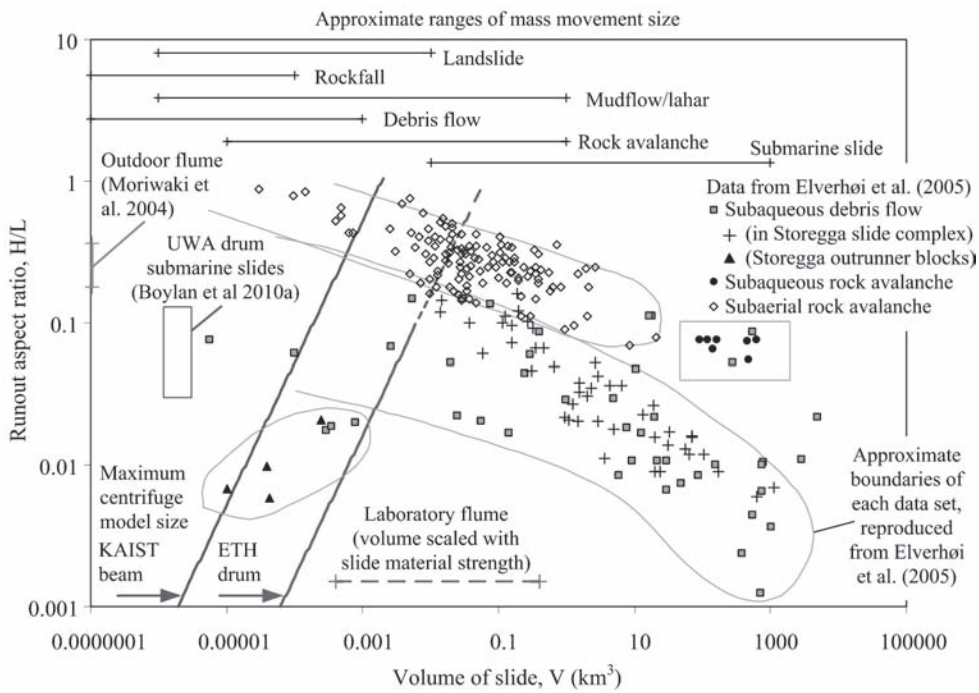

Figure 1. Mass movements: Natural scales and proportions, relative to physical modelling capabilities.

fluid) increases the runout is counter-intuitive in some respects: (i) energy is dissipated through viscous shearing in the fluid, (ii) energy is dissipated through drag effects on the upper surface of the flow, and (iii) the gravitational driving shear stresses are reduced due to buoyancy.

This increased mobility in the presence of water can be linked to geotechnical processes such as static liquefaction of the slide material, which is prevented in subaerial conditions due to the higher 'permeability'. However, studies have shown that hydroplaning at the front of the slide is a mechanism observed in physical modelling of slurry flows—as discussed in Section 2.4.3. Hydroplaning and fluid drag are further mechanisms of behaviour that are challenging to scale from manageable laboratory dimensions to prototype mass movement events.

Despite the difficulties of scaling, it is inevitable that physical modelling of mass movements must be undertaken at a reduced scale relative to prototype conditions, even if the conventional scaling laws for centrifuge modelling are assumed to be relevant and are applied. The maximum dimensions of mass movement that can be simulated in two of the largest beam and drum centrifuges are indicated in Figure 1. The KAIST beam centrifuge (Kim et al. 2006) has a very large swinging platform (1.2 m square) and can operate at an acceleration of 130 g. Ignoring the need to avoid boundary effects, the maximum volume of slide, for various runout ratios, is indicated. This limit encompasses small landslides and rockfalls, but falls short of permitting typical submarine slides. Drum centrifuges are often favoured for mass movement research because of their narrow aspect ratio. However, even if the large (2.2 m diameter) ETH drum centrifuge (Springman et al. 2001) is entirely filled with soil and used at the maximum g-level, the largest slides remain at the lower end of natural events.

In practice it is not possible to fill a centrifuge entirely with soil since space is required for instruments, and model packages are often unable to survive the maximum rated g-level of the centrifuge. Boylan et al. (2010) report submarine slides composed of kaolin clay that have been simulated in the UWA drum centrifuge—which is somewhat smaller than the ETHZ facility. The runout ratios of these slides varied with the intact strength but fell within the zones of the natural submarine slide data, albeit at the lower limit of the volume range (Figure 1).

An alternative to the use of a centrifuge is to address the challenge of scale by counteracting the reduced size of a laboratory model with a reduction in the material strength—typically by 2–3 orders of magnitude. Modelling of this kind, using analogue materials, is a well-established technique for simulating gross deformations in structural geology (e.g. Koyi 1997). However, it is rarely used in geotechnical engineering, where the smaller deformations mean that replication of the correct constitutive behaviour through the use of real soil is considered more important.

The resulting volume range of slides that can be simulated in the laboratory via a reduction in the material strength is indicated approximately by the green dotted line in Figure 1. This indication is based on the scaling of material strength providing a proportional reduction in the linear dimensions (because the self-weight stresses scale in this way) (e.g. Hubbert 1937). This approach to scaling has been widely adopted in the interpretation of submarine slide mobility experiments (Section 2.4.2).

A large outdoor flume can be used for research that is concerned with the triggering of slides, rather than great lengths of runout. One of the largest such flumes is at NIED, in Japan and is 20 m long, and is operated in combination with a rainfall simulator, to assess rainfall-induced landslides (Moriwaki et al. 2004). This flume contains 100 m^3 of soil, and features on the margin of Figure 1.

2.1.2 *Triggers of mass movements*

The triggering of a mass movement also has a bearing on how it will behave subsequently. Typical triggers of subaerial slides are earthquake and volcanic activity, freeze-thaw action, heavy rainfall and glacial melting. Of these, rainfall is the most common, tending to result in lower volume cases of slope instability, landslides, mudflows, and debris flows.

Earthquake-triggered events are less common, however, per event, the consequences are usually far more severe as a result of greater volumes being mobilised. Specifically, earthquakes are usually responsible for high-velocity, large volume rock avalanches. These are destructive in their own right; however, in addition, they also can entrain ice, soil and water into their paths, which can result in high speed large-volume debris flows or "debris avalanches" being generated downslope. So it is seen that two types of debris flow can be generated: the first is more common, rainfall-induced, slower moving and small-scale and the second is less common, earthquake induced, fast-moving and large-scale. While they tend to be grouped under one type of movement, the mechanics central to these two sizes of event may be somewhat different.

Volcanic-driven mass movements (lahars) are clearly limited to areas of volcanic activity and thus may be considered as "rare" in terms of geographical occurrence. However, because of the addition of heat and gas into the mix, the large

accumulations of loose debris on steep volcanic slopes, the abundance of water in the form of glaciers or rainfall, and the potentially explosive nature of volcanoes, lahars can be catastrophic. While lahars behave somewhat as debris flows (often they are referred to as volcanic debris flows), their volumes typically tend to be two orders of magnitude greater. As a result they constitute some of the largest mass movements on Earth.

For submarine slides, other triggers include (i) the dissociation of gas hydrates, (ii) rapid rates of deposition (leading to trapped pore pressures), (iii) storm-wave loading, and (iv) diapirism (leading to upthrust and over steepening) (e.g. Orange et al. 2003; Tripsanas et al. 2004).

Rapid deposition, so that the sediment forms faster than trapped pore pressure can escape, creates weak under-consolidated sediments. Failure in these slopes can occur at slope angles lower than angle of friction. Fluid or gas expulsion—associated with gas hydrates or from trapped excess pore pressure—has been widely recognised as a driver of mass movements. The characteristic pockmarks that identify regions of gas or fluid expulsion have been widely recognised as a potential geohazard (King & Maclean 1970; Harrington 1985; Forsberg et al. 2007). Physical modelling of pockmark formation is reviewed in Section.

2.2 *Drivers of physical modelling of mass movements: Who and why?*

As noted above, it is difficult to model mass movements faithfully at the correct scale, so physical modelling studies are focussed more on establishing the individual mechanisms that govern the global behaviour. The aim is typically to calibrate one aspect of a numerical model, which can ultimately be used to simulate the full response of a mass movement. Project-specific studies are rarely undertaken.

In light of this, most of the major physical modelling studies into mass movements are funded by a consortium of sources, ranging from government agencies to large oil companies; examples are international projects known by the acronyms as PODS, COSTA, and STRATAFORM.

One of the most studied submarine slides is the Storegga complex in the North Sea off the coast of Norway. Although this slide has long been identified (Bugge et al. 1988), research intensified following the discovery of the Ormen Lange gas field, downslope from the headwall, in 1997. The most recent slide within the Storegga complex took place only ~7000 years ago, so intensive efforts were made to establish the stability of the current topography. Much of the associated physical modelling focussed on the dynamics of the runout process, with a series of studies being undertaken at the St Antony Falls laboratory, in collaboration with Norwegian researchers (e.g. Ilstad et al. 2004a-c; Elverhøi et al. 2005). This research focussed on the dynamics of slurry flowing down an open flume as an analogue for the flow of stronger sediment at larger scale.

These physical modelling studies provided insights that have clarified why submarine slides exhibit such great runout lengths compared to subaerial slides, contributing to the risk assessment process associated with the Ormen Lange development. There remain, however, aspects of the behaviour that cannot yet be captured by physical models, as discussed in Section 2.4.2.

Onshore mass movements, triggered principally by rainfall, have been widely studied using physical modelling, by groups in Japan and in southern Europe, as reviewed by Olivares & Picarelli (2006) at the previous ICPMG. This research has been motivated by the hazard presented by landslides in rugged terrain, and has generally been supported by government agencies.

2.3 *Physical modelling techniques*

The physical modelling of mass movements is usually carried either to determine the validity of a particular failure/runout hypothesis or to verify and calibrate a numerical model. The setting up of known and controllable boundary conditions is one of the prime reasons to model a mass movement physically. To obtain this may mean testing under centrifuge conditions, the use of comparatively large-scale testing facilities or the use of unusual materials to allow testing at small scale while maintaining mechanical relevance. Calibration chamber testing is clearly not an option since a free surface is a prerequisite for mass movements.

The testing of a particular mechanical hypothesis is the most straightforward use of physical modelling. For mass movement processes, there is still a large degree of uncertainty associated with movement mechanisms—in particular for debris flows and rock avalanches. In the event that mechanisms are being investigated, modelling is therefore often parametric, and may involve only one or two stages in a process, such as initiation, transition from slow to rapid movement or flow and arrest (e.g. Wang & Sassa 2001). With regard to centrifuge testing, the development of scaling laws is of particular interest—this is both because there are limitations as to what can be achieved in a centrifuge and advantages in being able to vary g for parametric studies.

Physical modelling for calibration of numerical models usually assumes that the mechanisms of behaviour are already understood, and a set of

mathematical rules is now sought to describe this behaviour. Mechanistically-based numerical models for mass movement behaviour are usually of the Savage-Hutter type, involving modification to the shallow-water equations (Savage & Hutter, 1989). Calibration against physical models rather than field cases is often preferred for mechanistically-based (as opposed to statistically-based) models, because they provide controlled boundary conditions and more easily measurable loads, pore pressures and displacements velocities. The physical models for this purpose are often very simplified, with flowing dry granular material being the most common experimental arrangement (e.g. Hungr 2008), although results are sometimes used to make far broader comments on geophysical flows. There have been some attempts to link more complex physical model results to complex numerical models (e.g. Denlinger & Iverson 2001), although these attempts remain relatively few.

2.4 *Key results from physical modelling of mass movements*

Scaling is a central issue to physical modelling of mass movements because:

i. conventional scaling laws relevant to static geotechnical constructions are inadequate to capture fluid dynamics and thermomechanical effects that underlie some aspects of mass movement mobility;
ii. trends within data sets of natural mass movement imply scale effects for which there is no accepted consensus on the underlying mechanism; and
iii. simulations of mass movements in the laboratory—including centrifuge models, with conventional scaling applied—are generally far smaller than natural mass movements.

The use of physical models therefore relies heavily on understanding or determining the scaling laws involved, and this in turn depends on the mechanical processes behind each type of mass movement. The physical modelling of different types of mass movement, their scaling issues and other practicalities, are described below.

2.4.1 *Slope stability and slow moving landslides*

The stability of slopes in clay soil was one of the first geotechnical problems to be modelled physically using a geotechnical centrifuge (Taylor 1984). Testing at enhanced g (with the g-level factor 'N' equal to that of the model scale) ensures that the stresses felt in the model slope are the same as that of the prototype. This in turn is important for the correct stress-strain behaviour of the soil within the slope. Given the relative "simplicity" of the problem—i.e. slopes without reinforcement represent one of the more simple of geotechnical structures—there has been extensive research to establish the general applicability of conventional scaling laws, using modelling of models with respect to grain size effects and boundary issues by examining this problem (Goodings & Gillette 1996). For clay slopes, an additional advantage of centrifuge testing is that consolidation scales with the square of the scale factor—N^2. Hence processes, which can take years at the prototype scale (such as seepage and pore pressure dissipation), can take place in a matter of hours in the centrifuge.

Recent work on slope failures and slow moving landslides using centrifuges has benefited from developments in the technology used, providing *inter alia*, miniature pore pressure sensors that can measure both positive pore pressures and suctions (Take & Bolton 2003), robust digital cameras to provide imaging and photogrammetry techniques for deformation measurement (White et al. 2003, 2005), and environmental chambers and rainfall devices adjusted to take account of Coriolis (Take & Bolton 2002; Hudacsek et al. 2009). As a result of this, centrifuge studies have elucidated mechanisms of "rubblisation" and creep in saturated clay slopes due to seasonal moisture cycles (Take & Bolton 2004; Hudacsek et al. 2009), brittle failure of fill slopes due to permeable tongues (Take et al. 2004), freeze-thaw action on hillslope instability (Harris et al. 2008) and most recently rainfall induced slope instability on sandy and sandy-clay slopes (Ling et al. 2009). Centrifuge modelling has also been used to study the embankment failures that occurred during Hurricane Katrina, clarifying the failure mechanisms that led to collapse of sections of the flood defences in New Orleans (Ubilla et al. 2008; Sasanakul et al. 2008).

Examples from this research, which has been facilitated by recent advances in modelling technology, are shown in Figure 2. Physical modelling is now a well-established technique for faithfully reproducing slope processes, when driven by hydraulic or atmospheric boundary conditions. In these experiments, the stress history of the soil, the geometry of the slope, and the imposed changes in humidity, temperature and rainfall are all known and controlled, and the resulting pore pressure and the detailed ground movements are continuously monitored. Due to the maturity of this technique, physical modelling is now used to provide data supporting the analysis and refinement of new slope stabilisation works (Sonnenberg et al. 2010; Yoon & Ellis 2009), and occasionally site-specific simulations (Zhou et al. 2006).

The physical modelling of slopes in fine-grained deposits, without the use of a centrifuge, is relatively rare. Small-scale models without g-scaling

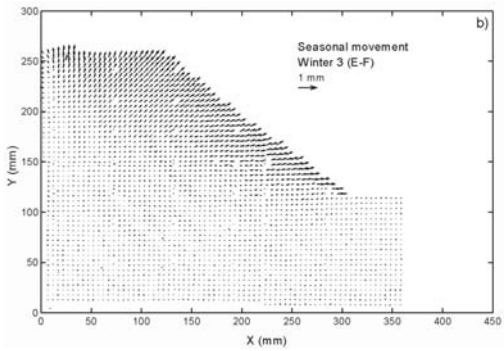

(a) Swelling of an intact clay embankment during a simulated transition from summer to winter (Take & Bolton 2007).

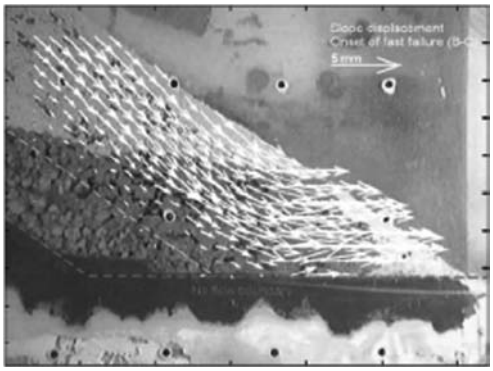

(b) Sudden failure of a loose fill slope due to elevated pore pressure in a buried permeable layer (Take et al. 2004).

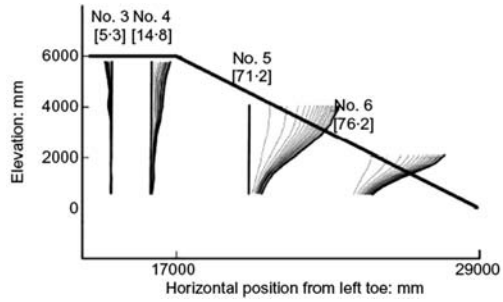

(c) Deformation of virtual inclinometers in a compacted clay embankment over 18 seasonal cycles (Hudacsek et al. 2010).

Figure 2. Examples of physical modelling of the deterioration of clay slopes.

tend to produce failure surfaces that are shallow compared to the field-scale although due to the ease of construction and control of boundary conditions, small models have been used for some investigations such as investigating the process of slope failure under rainfall conditions (Tohari et al. 2007) and the transition of a landslide to flow (Wang & Sassa 2001).

These physical modelling studies have clarified the static liquefaction mechanism in a way that soil element tests could not. Element tests show that loose sands can suddenly soften, due to rapid pore pressure generation, when sheared under undrained conditions. However, it remained unclear whether the failure of unsaturated slopes is generally a consequence of pore pressure rise, or whether the rapid pore pressure rise occurs due to the onset of post-failure shear strains. Detailed measurements of pore pressure and deformation within physical models of slopes has resolved this conundrum. In general, the slope fails as a consequence of progressive saturation and the mobilisation of strength; failure then occurs, and the consequent shear strain leads to collapse of the soil, and a rapid generation of pore pressure (Eckersley 1990; Wang & Sassa 2001; Olivares & Picarelli 2006).

Large-scale models are resource and time consuming to construct, which can lead to a lack of control over boundary conditions. In addition, in fine-grained soils, the time taken for pore pressures to build and equilibrate can render the test length excessive. However in Japan a number of large-scale tests have been undertaken, again with a view to understanding the role of rainfall infiltration on partially saturated slopes (Ling et al. 2009; Hori et al. 2004; Moriwaki et al. 2007; Figure 3a).

2.4.2 *Mudflows and submarine slides*

After a slope fails, it may transform into a dynamic sliding mass, depending on the downslope topography and the tendency for the material to soften. Sections 2.4.2 to 2.4.6 describe the various forms of dynamic mass movement that can follow slope failure.

Smaller magnitude mudflows are often generated by rain falling on already saturated soft or sensitive clayey slopes. In this sense they are somewhat like small debris flows (see below). The major difference between mudflows and debris flows is that, owing to their main constituents being suspended clay and water, mudflows tend to be more consistent in their behaviour than debris flows. Very little consolidation and seepage can occur during motion, compared with the event timescale (Mohrig et al. 1998), and the rheology of the slide material is usually described via a Bingham or Herschel-Bulkeley viscous fluid model (Huang & Garcia 1999; de Blasio et al. 2003) rather than as a rate-dependent solid (although these models can be virtually equivalent, Boukpeti et al. 2008).

A mudflow is therefore usually considered as a single phase material from commencement through to arrest. This provides a convenient definition to distinguish mudflows, including submarine slides

(a) Rainfall-induced landslides (~1:1) (Moriwaki et al. 2004).

(b) Submarine slides runout (~1:1000) (Toniolo et al. 2004).

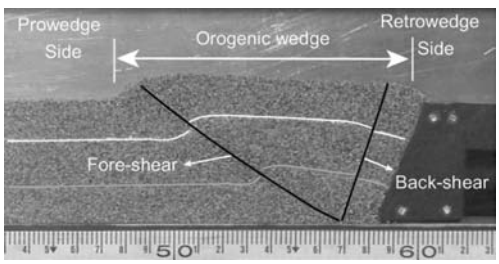

(c) Mountain building orogeny (~1:300,000) (Cruz et al. 2008).

Figure 3. Physical models of mass movements at varying scale.

(which are discussed in this section), and debris flows (which are covered in Section 2.4.3).

Submarine slides have similar characteristics to subaerial mudflows except that they are generally larger when triggered by earthquakes or slow overpressurisation. The greater volume of soil mobilised by these low-recurrence triggers is partly a reflection of the longer period over which the unstable deposit has accumulated. Small submarine slides are also triggered during storm events, due to the hydrodynamic pressure imposed on the seabed (Henkel 1970; Gilbert et al. 2007).

As discussed in Section 2.1.1, the scale of large submarine slides prevents the entire process being simulated in a physical model (Figure 1). To investigate the increased lengths of runout associated with submarine slides as opposed to subaerial slides, researchers have focussed on the behaviour of 'pre-failed' sediments that are injected into a flume in the form of a slurry, with a yield strength typically in the range 10–100 Pa.

A 10 m long flume at the St Antony Falls laboratory in the University of Minnesota has been widely used to investigate various aspects of the behaviour of submarine slides and the resulting turbidity currents (Mohrig et al. 1998, 1999; Marr et al. 2001; Mohrig & Marr 2003; Toniola et al. 2004) (Figure 3b). The effect of slurry composition on the runout length and deposition profile was studied, as well as the mixing of a debris flow with the ambient water, generating a turbidity current.

Measurements of the total stress and pore water pressure have been made at the base of the slide in further studies, in which the dynamics of the slide front, where hydroplaning is evident, have been investigated in detail (Ilstad et al. 2004a, 2004b, 2004c). These experimental studies identified hydroplaning as the most likely mechanism to explain the great runout distances of submarine slides. However, in order to match the observed profiles of runout, it was also necessary to invoke a significant reduction in the internal strength of the sediments to well below the undrained remoulded strength (de Blasio et al. 2003). The physical mechanism of this effect—termed 'wetting'—and its scaling, remain to be quantified (Elverhoi et al. 2005).

The scaling approach used to interpret these types of flume study is based on preservation of the relative magnitudes of the hydrodynamic inertia and the gravitational forces, so that the densimetric Froude number Fr is kept constant, where v is the fluid velocity, s is the bulk density ratio between slide and fluid (i.e. ρ_s/ρ_f), g is gravitational acceleration and H is the slide thickness:

$$Fr = \frac{v^2}{(s-1)gH} \quad (1)$$

The slurry used to model the debris has a reduced strength relative to the prototype sediments, so similitude is maintained between gravitational forces and material strength via the Johnson number Jn, where τ_y is the yield stress (when describing the slide using

a fluid rheology such as a Bingham model), s_u is the undrained shear strength (when using conventional soil mechanics terms):

$$Jn = \frac{\rho_w v^2}{\tau_y} \text{ or } \frac{\rho_w v^2}{s_u} \quad (2)$$

The Johnson number controls the tendency for frontal fluid pressure to deform a slide, and features in analyses for frontal stability derived from physical modelling (Ilstad et al. 2004c).

However, this use of strength-scaling, with a reduction in scale typically of 100, means that the model 'soil' does not exhibit some of the characteristics that are likely to govern the behaviour of prototype material. In particular, slurry materials that are prepared as fluids with a consistency typically of 50 Pa, do not have the capability to soften significantly during runout.

Strength-scaling does not therefore allow rapid remoulding or 'wetting' behaviour to be simulated. This means that the second element of the solution to the mystery of long submarine slide runout distances cannot be explored in small scale flume experiments unless new soil analogue materials are derived.

An alternative to strength-scaling, which allows both Froude and Johnson similarity, is to perform reduced scale experiments in a geotechnical centrifuge, notwithstanding the limitations of size illustrated in Figure 1. Pilot studies of submarine slides in 'intact' sediments, which can soften on remoulding, are reported by Boylan et al. (2010). Despite the limitations of scale evident in Figure 1, the morphological features evident in submarine slides can be replicated at reduced scale (Fig. 4).

The use of a centrifuge also provides improved similitude of erosion from the surface of a slide via a process of scour. The critical fluid velocity for the onset of scour in fine-grained (i.e. 'cohesive') sediments varies non-linearly with soil strength, but not in a manner that would be preserved by Johnson similitude (Kamphuis & Hall 1983). Centrifuge modelling, with retention of both prototype material strengths and velocities, provides similitude of scour in cohesive soils (Goodings 1985).

Other research related to onshore mudflows has also treated the material behaviour as that of a Bingham or similar model fluid with a measurable and definable rheology. The physical modelling of mudflows has, in the main, been undertaken by hydraulics researchers as an extension of fluid behaviour. Because the mechanical behaviour of mudflows is reasonably well-constrained, much research has focussed in recent years on comparison with numerical models to predict flow velocity and overall runout (Jin & Fread 1999). In recent

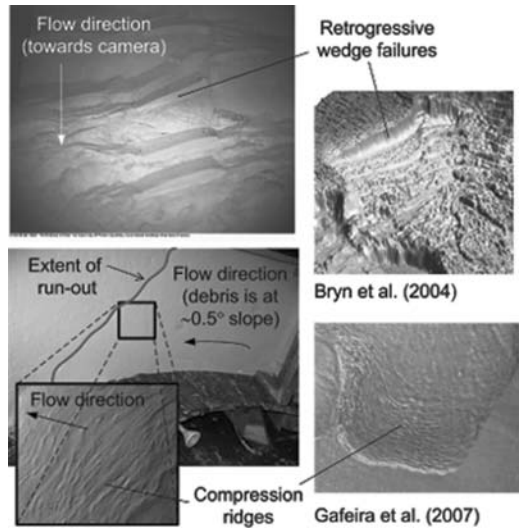

Figure 4. Replication of submarine slide features in centrifuge models. Images on left are from centrifuge models in stiff (top) and soft (bottom) clay (Boylan et al. 2010); images on the right show bathymetry at the headwall (top) and runout region (bottom) of the Storegga slide.

times, this work has extended to 3-dimensions. There also has been some progress on understanding the forces imparted to structures in the path of such flows (Tiberghien et al. 2007).

2.4.3 *Debris flows*

In this paper, a debris flow is defined as a "rapid to extremely rapid flow of saturated non-plastic debris in a steep channel" following Hungr (2004). The magnitude of such a flow can vary widely, even during the same event, growing by entraining material in its path and diminishing via deposition. This situation renders the boundary conditions rather indeterminate. One major factor separating the behaviour of debris flows from mud flows is the range of particle sizes involved in a single event, which can range from silt through to boulders. The segregation of particle sizes during motion, where large particles tend to focus towards the front of the flow, appears to result in a greater mobility of the flow (Bowman & Sanvitale 2009).

The clasts within a debris flow are considered to be in constant frictional contact rather than colliding with each other as in more dispersed flows, while segregation causes high pore pressures to be maintained within the flow, reducing the effective stress and hence frictional resistance. With regard to dimensional scaling, there has been much debate on "correct" scaling laws. Typically it is considered to be important to match various non-dimensional

numbers (e.g. the Bagnold and Savage numbers) at laboratory scale with those found at field or prototype scale (Iverson 1997) in order to produce flow behaviour that is in the correct regime (e.g. frictional rather than collisional). There are difficulties with this, in that, while it has been shown to be important to have a large range of clast sizes to capture key aspects of debris flow behaviour, the use of very large particles is not possible at laboratory scale, while the use of fine particles can introduce unwanted viscous effects and lead to undrained behaviour. Recent research using a drum centrifuge (Fig. 5), suggests that testing at enhanced g can overcome some of these problems (Bowman et al. 2010, in press), although added complexity such as a varying g-field and Coriolis forces, may be introduced.

Despite the concerns mentioned above, considerable useful physical model research on debris flows has been conducted at laboratory scale at 1 g. Studies have been instigated to examine for example, the role of porosity and fluid viscosity on runout of debris flows, the effect of particle size on runout and erosion, and the influence of bed topography, saturation and density on overall behaviour (e.g. Armanini et al. 2000; Rombi et al. 2006; Takahashi 2005; Tognacca & Minor 2000).

Figure 5. Aftermath of erodible bed debris flow experiment on the ETH Zurich drum centrifuge carried out at a centrifugal acceleration equivalent to 40 g (approx.). Photo is taken from the bottom fan area of the horizontally mounted flume. Earth's gravity acts in the leftward direction relative to the picture.

Physical models have also been linked to numerical model development and calibration—attempting to match, for example the velocity of flow surges as well as the overall extent of a model flow (Takahashi 2005; Hungr 2008; Denlinger & Iverson 2001). There are, however, few attempts to reproduce the behaviour found during specific debris flow events fully in the laboratory. The exception to this has been the occasional use of "typical" debris flow materials (less their largest fractions for the sake of practicality) obtained from real debris flow channels for use in laboratory flows (e.g. Rickenmann 2003). The advantage of using such materials is that realistic particle shapes are obtained, however, there can be considerable problems associated with dimensional scaling in terms of particle size.

2.4.4 *Lahars*

A lahar can simply be a mud or debris flow that is generated on the flanks of a volcano, or it can be a far more complex event, beginning life as a pyroclastic surge of high velocity hot ash and gas. It may then entrain melting snow and various fine and coarse solids, and thus be transformed into a hyperconcentrated stream flow, a coarse-grained debris flow, or anything in between. Lahars are often grouped with mudflows, because at their most simple and common, this is largely how they behave.

True lahars are rarely modelled physically, however, extreme forms are investigated. Simple mudflows have been examined (above) and this has been extrapolated to the behaviour of lahars (Hayashi & Self 1992). Debris flow behaviour is also sometimes assumed. Pyroclastic surges have also been studied in physical model experiments (e.g. Wilson 1984).

It would appear that the sheer complexity of their mechanics precludes the study of lahar behaviour that is intermediate to the mudflow, debris flow and pyroclastic flow cases. In comparison with the dearth of physical model research on rock avalanches, however, it is of interest that these three processes are being investigated at all.

2.4.5 *Rockfalls*

Rockfalls can be considered to be small magnitude events where single or multiple discrete blocks of rock become detached from the parent rock and slide, bounce and roll downhill under gravity. Rockfall studies utilising physical modelling are relatively uncommon in comparison with numerical simulation (e.g. Kobayashi et al. 1990). This may be attributable rock impact phenomena being relatively well-constrained in terms of scaling with few non-dimensional groups to consider, in comparison with say, debris flows.

Some examples of small-scale experiments include those by Chau et al. (2002) at 1 g, which assessed the influence of angular rotation and coefficient of restitution on rockfall hazards and Chikatamarla et al. (2006) in the centrifuge, which assessed impacts on different types of rockfall protection structure. Large-scale experiments have been conducted by Pichler et al. (2005) amongst others to understand the energy absorbency of gravel better. Such studies are usually aimed at the specifics of mitigating a relatively well-understood hazard, so that, as with slope stability, modelling in this area has reached a maturity, where particular arrangements and realistic and complex case studies can be examined.

2.4.6 *Rock avalanches*

Rock avalanches are large volume, high velocity events involving masses travelling for up to tens of kilometres horizontally while travelling up to a kilometre vertically. Field evidence suggests avalanche average speeds can sometimes exceed free-fall velocity, while their deposits can spread far beyond limits suggested by Coulomb friction. In particular, the normalised runout (i.e. where the runout extent is normalised by the cube root of volume, to take account of spreading; Davies & McSaveney 1999) is found to increase with the volume of the avalanche.

This fact has discouraged much small-scale physical modelling from being undertaken until recently, and it is a reflection of the view by some, that modelling should involve the whole process, rather than focussing on one aspect. One effect of this lack of research has been that various competing hypotheses regarding the extreme runout of avalanches still prevail in the literature, fifty years or more after they were first proposed, among them those involving air fluidization (Shreve 1968), acoustic fluidization (Melosh 1979), frictional melting (Erisman 1986), and dynamic fragmentation (Davies & McSaveney 2003).

Some recent work has sought to address this problem by focussing on particular aspects of rock avalanche behaviour or factors that may be of influence using physical models. Small-scale model avalanche investigations have been used to examine the influence of initial volume, basal friction and particle size, block geometry and arrangement using sand, gravel and regular blocks (Davies & McSaveney 1999; Manzella & Labiouse 2008). While in general, tests at 1 g at small scale have not been shown to produce any clear volumetric effects other than those due to spreading, Manzella & Labiouse (2008) did show that having blocks arranged in a closely packed regular arrangement caused an increase in runout via a reduction in spent energy during downslope shearing.

A few tests have been conducted at very large scale to examine volumetric effects on small rock avalanche runout (Okura et al. 2007) using up to 1000 closely packed granite blocks. These tests showed that the number of blocks, and overall volume correlated positively with runout of the blockfalls, while the centre of gravity was negatively correlated with runout. In addition, a few studies have also been conducted in the geotechnical centrifuge, with the aim of examining the role of fragmentation on run-out behaviour (Bowman 2006; Imre 2010).

These investigations used materials that could break or disintegrate under the action of enhanced gravity made possible in the centrifuge as the mass travelled downslope. The results of these tests suggest, as shown in Figure 6 (Bowman & Hann,

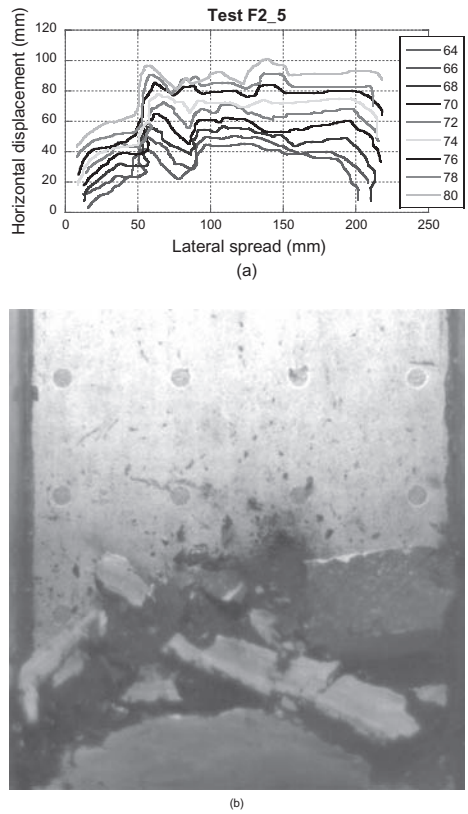

Figure 6. Example of the fragmentation spreading of coal (a low-strength analogue for rock) during a centrifuge test (Bowman & Hann, in prep.). (a) Viewed from above the prototype, the front of the avalanche as it spreads through time at 2 msec intervals. (b) Photograph taken using a high-speed camera mounted on the centrifuge from which the front analyses are later derived, taken at point corresponding to "74" in (a) Note the fractured and broken slabs.

in prep.), that dynamic fragmentation can lead to an increase in the areal spreading of rock avalanches, however the mechanics of this process are complex and are the matter of on-going research.

Taken as a whole, while they do not model whole events, these disparate studies have begun to build a picture of what essential elements are required to generate long runout rock avalanche behaviour and the centrifuge appears to offer some possibilities to model particular high energy mechanisms such as fragmentation at small scale. Improvements in high speed digital imaging and subsequent analysis have enhanced the data outcomes that can be gained from such experiments at both 1 g and on centrifuge, for example, by use of geoPIV (White et al. 2003) or similar systems.

2.4.7 *Slope destabilisation mechanisms*

Three further processes that can destabilise slopes have been the subject of novel physical modelling: (i) gas or fluid expulsion, (ii) diapirism—for example, from salt domes—and (iii) tectonic action.

Gas and fluid expulsion is recognised as a potential trigger of submarine slides, as well as a natural hazard to offshore foundations and oil wells (Tjelta et al. 2007). The presence of pock marks on the seabed is a tell tale sign of current or previous expulsion events. Pock marks are also commonly observed in clay samples that have been poorly de-aired prior to normal consolidation in a centrifuge.

The same form of feature can also be observed in centrifuge models following earthquake simulations, where coarser material—sand boils—may also be expelled through a surface vent created by escaping pore fluid (Brennan & Madabhushi 2005). A systematic study of sand boils is reported by Brennan (2008). A novel investigation into the escape of gas through a transparent clay is reported by de Vries et al. (2007) and Gylland & de Vries (2008). The hydraulic fracture path generated by the gas followed the directions of maximum principal stress, being therefore attracted to foundations in compression but diverted away from foundations loaded in tension.

Structural geologists have long recognised the scaling laws relevant to reduced scale physical models, through the use of analogue modelling of tectonic processes (Hubbert 1937; Koyi 2007). The importance of maintaining the ratio of strength to self-weight was recognised (i.e. gH/s_u, or gH/τ_y—which is the third combination of gravitational, inertial and plastic strengths, besides the dimensionless Fr and Jn numbers). This led to the use of centrifuge modelling techniques in the 1960s to study structural geology (Ramberg 1967), concurrent with its development within geotechnical engineering.

The tectonic distortion of rock and diapirism, leading to the steepening of slopes, remains actively studied using analogue materials at scale factors that far exceed those that we are accustomed to in geotechnical engineering. As an example, Cruz et al. (2008) simulate 15 km of the Earth's crust using an analogue 5 cm 'deposit' of walnut shells, at a scale factor of 300,000. They maintain, it is argued, similarity of self-weight stresses and (cohesive) shear strength (Fig. 3c).

The novel studies described in this section explore behaviour that controls many natural geohazards, which are faced in frontier areas of offshore development (Jeanjean et al. 2005). Ambitious future physical modelling might tackle the effects on seabed slopes of gas and fluid expulsion, diapirism and rapid sedimentation.

2.5 *Conclusions—mass movements*

The physical modelling of high-energy mass movements is a valuable tool in identifying mechanisms central to their behaviour. For some types of mass movement—e.g. rockfalls and cases of slope stability—physical modelling has reached a stage where it is now used as a direct adjunct to numerical modelling of relatively complex cases, because the mechanics of the basic problem are mostly well-constrained and understood. For other types of movement—e.g. mudflows—physical modelling is helping engineers to identify and mitigate the effects of field cases through, for example, the calibration of new numerical models.

For research into the most mechanically complex of mass movements—i.e. rock avalanches, lahars and, to a lesser extent, submarine slides and debris flows, however, the physical models remain relatively crude and the latest modelling technologies are not fully utilised. Physical modelling has successfully reproduced certain mechanisms observed in the field, and has provided quantitative data for validating analytical and numerical models that are used for design—such as for the hydroplaning of submarine slides. However, other aspects of behaviour—such as the 'wetting' or severe remoulding of submarine slides—are inferred from prototype relic slides, but are yet to be quantified in small scale physical models.

The relative crudeness of many physical modelling studies of complex mass movements is in part due to the scale and costs associated with such modelling. It is also in part due to self-imposed restrictions of researchers, whereby, because it is impossible to match every aspect of behaviour non-dimensionally, it is not deemed worthwhile to attempt to reproduce any aspect in isolation. For these cases, the optimal approach is to determine parametrically via physical modelling, which

non-dimensional groups are of *most* importance to the generic material behaviour inherent in each type of mass movement (an example is fragmentation in rock avalanches). By separating and isolating different mechanical phenomena, the complexity of each problem will be reduced, allowing engineers to focus on the variables of most influence, and hence to determine the most suitable strategies to mitigate the risks posed.

3 EARTHQUAKE FAULT RUPTURE

3.1 *Background*

As indicated in the introduction to this paper, the earthquake phenomena that have been studied most in physical models—and in geotechnical centrifuge modelling in particular—are related to ground shaking. However, another earthquake hazard is caused when a fault rupture extends to, or very near to, the ground surface resulting in a permanent offset. This is a serious hazard to the serviceability of infrastructure (e.g. Bray 2001; O'Rourke 2003) such as vital lifeline systems that are located across a fault line or structures located at the surface above or adjacent to the location of the surface rupture. Post earthquake investigations (e.g. Ulusay et al. 2002) have revealed complex interactions between earthquake faults and buildings supported by shallow foundations and in some cases the buildings appeared to be able to divert the earthquake fault rupture emergence away from the buildings. This has led to the conclusion that in certain circumstances it might be possible to design buildings founded on shallow foundations to survive the natural hazard of surface fault rupture (e.g. Anastasopoulos & Gazetas 2007; Anastasopoulos et al. 2007).

Studies using physical model testing of dip-slip earthquake faults through soil layers have been conducted to gain a greater understanding of how fault ruptures propagate through the soil above faulted bed rock. In the earliest recorded study, reported by Cole & Lade (1984), laboratory floor models were used to investigate the influence of soil properties, depth of layer and dip angle in the bed rock on the propagation of both normal and reverse faults and in particular the location of their final emergence.

In this study, it was observed that the position of the fault propagation was governed by the dilation angle of the soil. Since for a particular relative density the dilation angle is a function of effective stress (e.g. Bolton 1986), if the position of the fault rupture is to be modelled correctly in a reduced scale model then effective stresses need to be reproduced appropriately. This can only be achieved at elevated acceleration in a geotechnical centrifuge.

Fundamental studies of fault rupture propagation in normal faulting using centrifuge models have been conducted by Stone & Wood (1992) and Hu et al. (2009). However, whilst they provide valuable information about the development of fault ruptures, these studies do not address the hazard resulting from the interaction of the fault rupture with the foundation of a structure or a lifeline system. Investigations of the interaction of both normal and reverse faults with shallow foundations have been conducted as part of the "QUAKER" European research project to quantify and reduce seismic risk to foundation systems (Davies 2003). In this project, parametric studies were conducted in plane strain models to examine how the magnitude of thrust displacements affects foundation systems. The variables considered in the study were proximity of the fault to the foundations together with the foundation loading and its breadth (Bransby et al. 2008a, b). A schematic view the centrifuge model tests for normal fault testing is shown in Figure 7.

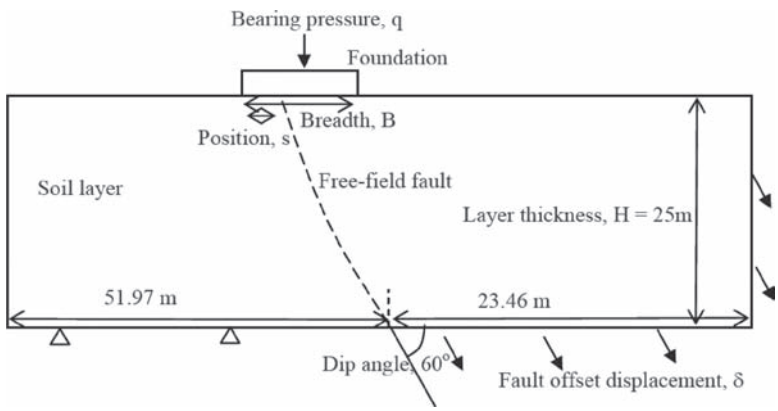

Figure 7. Geometry of normal fault rupture emergence adjacent to a shallow foundation (after Bransby et al. 2008a).

A normal fault of dip angle 60° was propagated through a dry sand layer of depth, H = 25 m (at prototype scale when the model was accelerated to 115 g) in a quasi-static, drained manner. The study also considered the case of reverse faults, in which case the sand layer was modelled to be 15 m thick in order to allow the fault rupture to propagate to the surface. In both series of experiments, tests were conducted both without a foundation (a "free field" test) and with a foundation resting on the surface with its centre line located at varying distances from the location of free field surface rupture. During the model tests, soil and structure displacements were measured both visually from images obtained using digital cameras and with displacement transducers.

3.2 *Modelling normal faults*

Figure 8 (Bransby et al. 2008a) shows typical images obtained in a centrifuge model experiment conducted to investigate the interaction of a normal fault with a shallow foundation. Figure 8a shows the location of the foundation relative to the free field fault rupture. The three further images shows the gradual evolution of the fault rupture as the fault in the bedrock displaces. The presence of the foundation results in the fault rupture being diverted away from the hanging wall to the left of the foundation when the throw of the fault is approximately 2 m (Fig. 8d). The calculated soil displacements for the final mechanism (when h ≈ 2 m) are shown on Figure 9, demonstrating that there are negligible deformations outside the shear plane once the final mechanism forms. However, despite deviating the fault rupture, all foundations underwent significant rotation whilst the final fault-rupture mechanism was developing. This rotation appeared to be reduced with increasing bearing pressures, as shown in Figure 10.

3.3 *Conclusions—earthquake fault rupture*

The example presented above illustrates how physical modelling may be used to investigate the previously little studied phenomenon of fault rupture interaction with foundations. In addition to the studies of normal faulting, similar investigations have been conducted for reverse faulting (Bransby et al. 2008b). Preliminary studies of the performance of deep foundations and flexible, continuous pipelines that cross fault ruptures have been conducted also (Bransby et al. 2007). Data from these experimental studies have been used successfully to validate numerical simulations of fault rupture—structure interaction (Anastasopoulos et al. 2008).

Investigations to date have indicated that centrifuge modelling is a powerful tool for investigating the phenomena of earthquake fault rupture. Since many important lifeline systems that cannot be relocated, such as water pipelines or bridges, cross potentially active faults, further programmes of physical modelling would provide importance data for use in risk assessments of these (and other forms of) infrastructure assets.

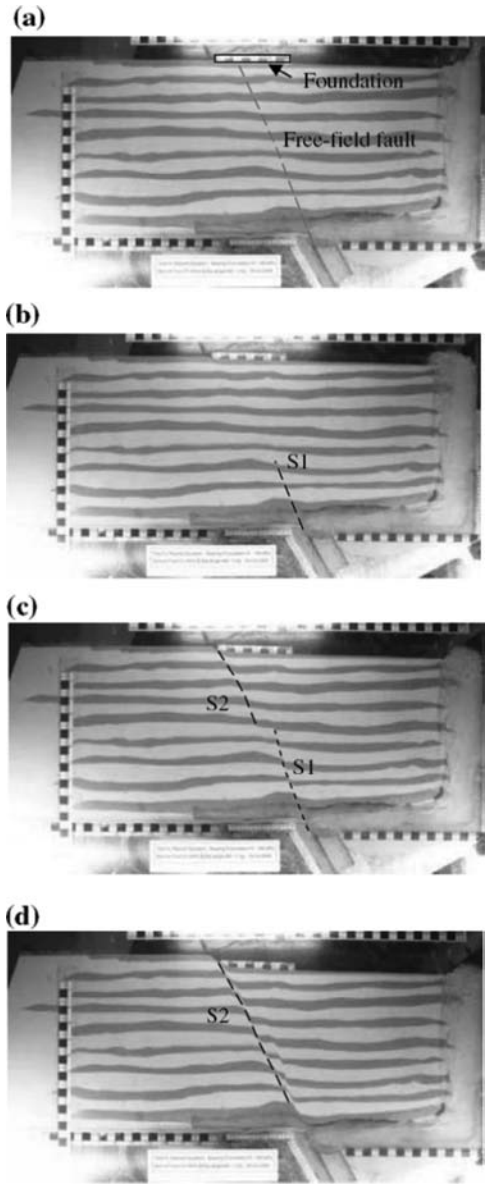

Figure 8. Photographs taken during normal fault propagation: (a) Fault throw, h = 0.48 m (h_{model} = 4.2 mm). (b) h = 0.80 m (h_{model} = 6.9 mm). (c) h = 1.15 m (h_{model} = 10.0 mm). (d) h = 2.16 m (h_{model} = 18.8 mm) (after Bransby et al. 2008a).

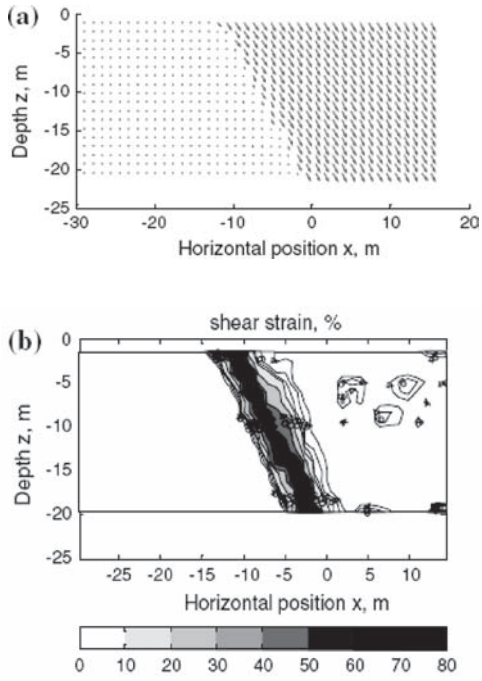

Figure 9. Cumulative soil displacements after h = 2.01 m (h_{model} = 17.5 mm). (a) Displacements (b) Maximum shear strain (γ_{max}) (after Bransby et al. 2008a).

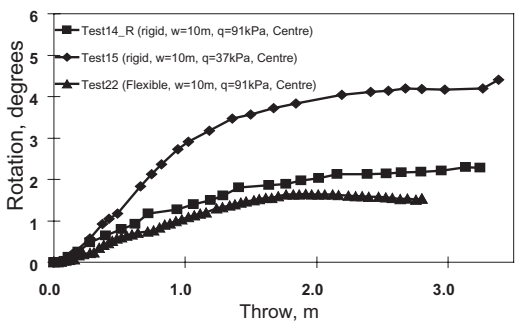

Figure 10. Foundation rotation against fault throw (adapted from Bransby et al. 2008a).

4 PERMAFROST DEGRADATION

4.1 *Background*

Seasonal thawing of the active layer on sloping ground may be associated with a range of mass movement mechanisms, depending on gradients, soil properties, ice contents and thermal regime (e.g. Lewkowicz 1988). As indicated in Section 2.4.1, above, these processes, which range from progressive downslope movements caused by solifluction to mudflow in non-cohesive silt and active layer detachment sliding in overconsolidated silt–clay, may be replicated correctly in physical models both in the laboratory and tested at elevated acceleration using a geotechnical centrifuge (e.g. Harris et al. 1995; Harris et al. 2008 a, b).

Measurement of permafrost temperatures in European Mountains—and other cold regions throughout the world—indicates clearly that permafrost is warming as a response to global climate change (Vonder Mühll et al. 1998, 2000). The result of this warming is the development of "active layer thickening" as during the warmer months of the year, the thickness of the annual thawing layer of soil above (and in some cases below) the zone of permafrost increases. This has the effect of exacerbating and accelerating mass movement processes, thus increasing potential geotechnical hazards (Harris et al. 2001).

4.2 *Rockfall hazard*

Another natural hazard phenomena resulting from permafrost warming is the potential for jointed rock masses, in which joints are filled with ice, to become unstable (Davies et al. 2001; Gude & Barsch 2005). Laboratory tests conducted by Davies et al. (2000) showed that the shear strength of an ice-filled frozen joint is, as would be expected from consideration of the properties of ice (e.g. Barnes et al. 1971), a function of both temperature and normal stress.

However, the experiments indicated that as ice in a joint warms, at certain temperatures and pressures, the ice-filled joint can display less shear strength than an ice free joint. These results suggest that, in slope stability assessment, if the presence of ice in a joint is ignored (on the grounds that ice will always add to shear strength and its absence represents the most unstable conditions) then as this ice warms, conditions may arise where unexpected failure could occur. This implies that the slope stability is more sensitive to changes in the thermal environment than previously envisaged in certain circumstances.

This hypothesis has been tested in series of centrifuge model tests (Davies et al. 2001, 2003) in which frozen jointed rock slopes were formed from concrete blocks. To ensure consistency in joint roughness between models, Davies et al. (2001) developed a technique for constructing slopes from concrete having similar physical properties to granite. This involved casting blocks forming the slope in moulds of the appropriate geometry and internal roughness. A range of models, which had one or more potentially unstable blocks, have been investigated. Figure 11 shows the typical geometry

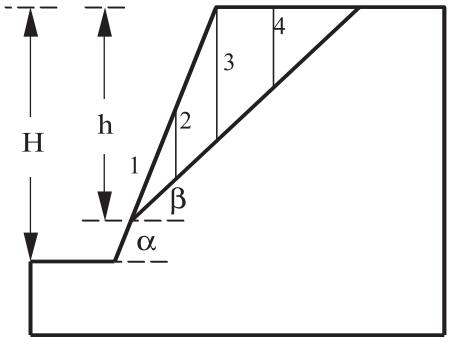

Figure 11. Geometry of the centrifuge model containing a single ice-filled discontinuity inclined at an angle, β, with three vertical joints (blocks forming slope are numbered 1 to 4).

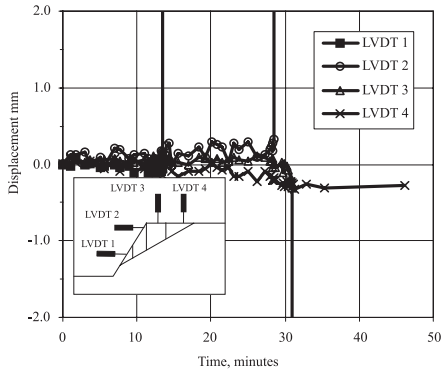

Figure 12. Displacement of the slope following acceleration to 120 g, Slope B-1 frozen model (α = 60°, β = 35°).

of a centrifuge model tested at 120 g; the prototype dimensions of the model were H = 43.8 m and h = 29 m. In this case, the potential sliding zone contained three vertical discontinuities and four potentially sliding blocks. The inclination of the discontinuity was β = 35°; which in control tests conducted without ice in the joints resulted in a slope that was stable.

During testing of the frozen slopes, displacement of the potentially unstable blocks were monitored as the air temperature (and hence the temperature in the slope) was permitted to increase. Typical results, shown in Figure 12, demonstrate that whilst blocks 1, 2 and 3 slid off the bed rock (indicated by rapid large displacements) as the ice in the joint increased in temperature, block 4 remained stable. Since the joint beneath block 4 was at a shallower depth than block 3, the joint beneath it was able to close during warming and eventual melting of the ice, whilst block 4 was supported by the still stable block 3.

4.3 *Conclusions—rockfall resulting from permafrost degradation*

Although the geometry in these models was simple, the findings of the study, which includes quantitative assessment of the slope stability, provides a means for interpretation of the mechanisms associated with the warming of ice-bonded discontinuities and may be used to inform the assessment of the long term stability of rock slopes in permafrost regions, which are subject to permafrost degradation (Harris et al. 2001; Gude & Barsch 2005). In addition, centrifuge modelling has also been conducted to assess mechanisms associated with hazard mitigation methods (Günzel & Davies 2006).

5 CONCLUSIONS

Physical modelling—in laboratory or centrifuge models—may be used to investigate the mechanics associated with a range of natural hazards that have direct geotechnical implications together with the trigger mechanisms that initiate these hazards. Close control over material properties and well defined boundary conditions in physical models enable repeatability that permits parametric studies to be conducted. However, care has to be taken when designing a model testing programme to ensure that the model scaling laws are appropriate to permit mechanisms to be replicated faithfully.

The level of complexity of a model depends very much on the nature of the hazard. Where the mechanics of the basic problem are mostly well-constrained and understood, such as the development of earthquake induced surface fault rupture, it is possible to design and execute highly sophisticated model tests of complex boundary value problems. Quantitative results obtained in such tests may be applied directly in design or used to develop or assess analytical techniques. However physical models of mechanically complex hazards, such as mass movements associated with rock avalanches, submarine slides and debris flows, are relatively crude and they do not fully utilise the latest modelling technologies. Nevertheless, these models permit important generic mechanisms to be identified and explained.

REFERENCES

Anastasopoulos, I., Callerio, A., Bransby, M.F., Davies, M.C.R., Gazetas, G., Masella, A., Paolucci, R., Pecker, A. & Rossignol, E. 2008. Numerical analyses of fault-foundation interaction. *Bull Earthquake Eng.* 6: 645–675.

Anastasopoulos, I. & Gazetas, G. 2007a. Foundation-structure systems over a rupturing normal fault: I. Observations after the Kocaeli 1999 Earthquake. *Bull Earthquake Eng* 5(3): 253–275.

Anastasopoulos I. & Gazetas, G. 2007b. Behaviour of structure-foundation systems over a rupturing normal fault: II. Analyses, experiments, and the Kocaeli case histories. *Bull Earthquake Eng* 5(3): 277–301.

Anastasopoulos, I., Gazetas, G., Bransby, M.F., Davies, M.C.R. & Nahas, E.A. 2007. Fault rupture propagation through sand: finite element analysis and validation through centrifuge experiments. *Journal of Geotechnical and Geoenvironmental Engineering*, ASCE 133(8): 943–958.

Armanini, A. & Gregoretti, C. 2000. Triggering of debris-flow by overland flow: A comparison between theoretical and experimental results. In Wieczorek, G., & Naeser, N.D., (eds). *2nd International conference on Debris Flow Hazards Mitigation: Mechanics, Prediction and Assessment*: 117–124.

Barnes, P., Tabor, D. & Walker, J.C.F. 1971. The friction and creep of polycrystalline ice. *Proc. Roy. Soc. Lond.* A. 324: 127–155.

Bolton, M.D. 1986. The strength and dilatancy of sands. *Géotechnique* 36(1): 65–78.

Boukpeti, N., White, D.J. & Randolph, M.F. 2009. Characterization of the solid-liquid transition of fine-grained sediments. *Proc. Conf. on Offshore Mechanics and Arctic Engineering*, Honolulu. OMAE2009–79738.

Bowman, E.T., Laue, J., Imre, B. & Springman, S.M. (in press). Experimental modelling of debris flow behaviour using a geotechnical centrifuge. *Canadian Geotechnical Journal*.

Bowman, E.T. & Sanvitale, N. 2009. The role of particle size in the flow behaviour of saturated granular materials. *Paper read at 17th International Conference on Soil Mechanics and Geotechnical Engineering*, at Alexandria.

Bowman, E.T. 2006. A note on the micromechanics of long runout rock avalanches. *Paper read at International Symposium on Geomechanics and Geotechnics of Particulate Media*, at Ube, Yamaguchi.

Boylan N., Gaudin C., White D.J. & Randolph M.F. 2010. Modelling of submarine slides in a geotechnical centrifuge *Int. Conf. on Physical Modelling in Geotechnics*. Zurich, Switzerland, (this proceedings).

Bransby, M.F., Davies, M.C.R., Mickovski, S.B., Sonnenberg, R., Bengough, A.G. & Hallett, P.D. 2006. Stabilisation of slopes by vegetation reinforcement. In C.W.W. Ng, L.M. Zhang & Y.H. Wang (eds). *6th International Conference on Physical Modelling in Geotechnics*. Hong Kong: Taylor Francis.

Bransby, M.F., Davies, M.C.R. & El Nahas, A. 2008a. Centrifuge modelling of normal fault-footing interaction. *Bulletin of Earthquake Engineering* 6: 585–605.

Bransby, M.F., Brennan, A.J., Davies, M.C.R., El Nahas, A. & Nagaoka, S. 2008b. Centrifuge modelling of reverse fault-foundation interaction. *Bulletin of Earthquake Engineering* 6: 607–628.

Bransby, M.F., El Nahas, A., Turner, E. & Davies, M.C.R. 2007. The interaction of reverse fault ruptures with flexible, continuous pipelines. *International Journal of Physical Modelling in Geotechnics* 7: 25–40.

Bray, J.D. 2001. Developing mitigation measures for the hazards associated with earthquake surface fault rupture. In A workshop on seismic fault-induced failures—possible remedies for damage to urban facilities. *Japan Society for the promotion of science*, University of Tokyo, Japan, January 11–12: 55–79.

Brennan, A.J. & Madabhushi, S.P.G. 2005. Liquefaction and drainage in stratified soil. *Journal of Geotechnical and Geoenvironmental Engineering, ASCE* 131: 876–885.

Brennan, A.J., Moran, D. & Ritchie, N. 2008. Observations on sand boils in simple model tests. *Proc. Geotechnical Earthquake Engineering and Soil Dynamics IV*, ASCE GSP 181 Sacramento, USA, 10pp.

Bugge, T., Belderson, R.H. & Kenyon, N.H. 1988. The Storegga slide, Philos. Trans.-R. Soc. A325: 357–388.

Burton, I., Kates, R.W. & White, G.F. 1978. *The Environment as Hazard*. Oxford University Press.

Chau, K.T. Wong, R.H.C. & Wu, J.J. 2002. Coefficient of restitution and rotational motions of rockfall impacts, *International Journal of Rock Mechanics and Mining Sciences* 39: 69–77.

Chikatamarla, R., Laue, J. & Springman, S.M. 2006. Modelling of rockfall on protection galleries. In Ng, C.W.W., Zhang, L.M. & Wang, Y.H. (eds). *6th International Conference on Physical Modelling in Geotechnics*: 331–336. Hong Kong: Taylor Francis.

Cole, D.A. Jr. & Lade, P.V. 1984. Influence zones in alluvium over dip-slip faults. *J Geotech Eng* 110: 599–615.

Coussot, P. & Meunier, M. 1996. Recognition, classification and mechanical description of debris flows. *Earth-Science Reviews* 40: 209–227.

Cruz, L., Tweyssier, C., Perg, L., Take A. & Fayon, A. 2008. *Journal of Structural Geology* 30: 98–115.

Dade, W.B. & Huppert, H.E. 1998. Long-runout rockfalls, *Geology* 26: 803–806.

Davies, M.C.R. 2003. Quantification and reduction of seismic risk though the application of advanced geotechnical engineering techniques. In M. Yeroyanni (ed.) *Seismic and landslide risk in the European Union*, EUR 20592, 2003, Office for Official Publications of the European Communities, Luxembourg, 50–56.

Davies, M.C.R., Hamza, O. & Harris, C. 2001. The effect of rise in mean annual temperature on the stability of rock slopes containing ice filled discontinuities. *Permafrost and Periglacial Processes* 12: 137–144.

Davies, M.C.R., Hamza, O. & Harris, C. 2003. Physical modelling of permafrost warming in rock slopes. In M. Phillips, S.M. Springman & L.U. Arenson (eds). *Proceedings of the 8th International Conference on Permafrost*, Zurich: 169–173. Lisse, Netherlands: Balkema.

Davies, M.C.R., Hamza, O., Lumsden, B.W. & Harris, C. 2000. Laboratory measurement of the shear strength of ice filled rock joints. *Annals of Glaciology* 31: 463–467.

Davies, T.R. & McSaveney, M.J. 1999. Runout of dry granular avalanches. *Canadian Geotechnical Journal* 36: 313–320.

Davies, T.R.H., McSaveney, M.J. & Hodgson, K.A. 1999. A fragmentation-spreading model for long-runout rock avalanches. *Canadian Geotechnical Journal* 36(6): 1096–1110.

de Blasio, F.V., Issler, D., Elverhøi, A., Harbitz, C.B., Ilstad, T., Bryn, P., Lien, R. & Løvholt, F. 2003. Dynamics, velocity and runout of the giant Storegga slide. In Locat, J. & Mienert (eds). *Submarine Mass Movements and Their Consequences, J., Adv. Natural Technol. Hazards Res.* 19: 223–230.

de Blasio, F.V., Elverhøi, A., Engvik, L.E., Issler, D., Gauer, P. & Harbitz, C. 2006. Understanding the high mobility of subaqueous debris flows. *Norwegian Journal of Geology* 86: 275–284. Trondheim.

de Vries, M.H., Svanø, G. & Tjelta, T.I. 2007. Small scale model testing of gas and fluid migration in a soft seabed as a basis for developing a mechanical model for gas migration. *Proc. 6th International Conference on Offshore Site Investigation and Geotechnics*. Society for Underwater Technology. London.

Denlinger, R.P., & Iverson, R.M. 2001. Flow of variably fluidized granular masses across three-dimensional terrain, 2. Numerical predictions and experimental tests. *Journal of Geophysical Research* 106(B1): 553–566.

Eckersley, J.D. 1990. Instrumented laboratory flowslides. *Géotechnique* 40(3): 489–502.

Elverhoi, A., Issler, D., De Blasio, F.V., Ilstad, T., Harbitz, C.B. & Gauer, P. 2005. Emerging insights into the dynamics of submarine debris flows. *Natural Hazards and Earth System Sciences* 5: 633–648.

Erismann, T.H. 1979. Mechanisms of large landslides. *Rock Mechanics* 12: 5–46.

Erismann, T.H. 1986. Flowing, rolling, bouncing, sliding: synopsis of basic mechanisms. *Acta Mechanica* 64: 101–110.

Forsberg, C.F., Planke, S., Tjelta, T.I., Svanø, G., Strout, J. & Svensen, H. 2007. Formation of pockmarks in the Norwegian Channel. *In: Proc. 6th Int. Conf. on Offshore Site Investigation and Geotechnics*. London, Society for Underwater Technology: 221–230.

Gajan, S., Kutter, B.L., Phalen, J.D., Hutchinson, T.C. & Martin, G.R. 2005. Centrifuge modeling of load-deformation behaviour of rocking shallow foundations. *Soil Dynamics and Earthquake Engineering* 25: 773–783.

Gilbert, R.B., Nodine, M.C., Wright, S.G., Cheon, J.Y., Wrzyszczynski, M., Coyne, M. & Ward, E.G. 2007. Impact of hurricane-induced mudslides on pipelines. *Proc. Offshore Technology Conference, Houston, Paper OTC 18983.*

Goguel, J. 1978. Scale-dependent rockslide mechanisms. In: Voight, B. (ed.). *Rockslides and Avalanches, 1 Dev. Geotech. Eng.* 14 A: 693–705. Elsevier.

Goodings, D.J. 1984. Relationships for modelling water effects in geotechnical models. In W.H. Craig. (ed.). *Proc. Symposium on the Application of Centrifuge Modelling to Geotechnical Design,* Manchester: 1–24.

Goodings, D.J. & Gillette, D.R. 1996. Model size effects in centrifuge models of granular slope instability. *Geotechnical Testing Journal* 19(3): 277–285.

Gude, M. & Barsch, D. 2005. Assessment of geomorphic hazards in connection with permafrost occurrence in the Zugspitze area (Bavarian Alps, Germany). *Geomorphology* 66: 85–93.

Günzel, F.K. & Davies, M.C.R. 2006. Influence of thawing permafrost on the stability of ice filled rock slopes, In Ng, Zhang & Wang (eds). *Physical Modelling in Geotechnics, 6th International Conference on Physical Modelling in Geotechnics:* Hong Kong: 343–348. London: Taylor and Francis Group.

Gylland, A.S. & de Vries, M.H. 2008. The effect of a gas blow-out on shallow offshore foundations. *In: Proc. 2nd BGA Int. Conf. on Foundations*. Dundee, Scotland: 885–896.

Habib, P. 1967. Sur un mode de glissement des massifs rocheaux. *C.R. Acad. Sci.* 264: 151–153.

Habib, P. 1975. Production of gaseous pore pressure during rock slides. *Rock Mechanics* 7: 193–197.

Harrington, P.K. 1985. Formation of pockmarks by pore-water escape. *Geo-Marine Letters* 5: 193–197.

Harris, C., Davies, M.C.R. & Coutard, J.-P. 1995. Laboratory simulation of periglacial solifluction: significance of porewater pressure, moisture contents and undrained shear strength during thawing. *Permafrost and Periglacial Processes* 6: 293–311.

Harris, C., Davies, M.C.R. & Etzelmüller, B. 2001. The assessment of potential geotechnical hazards associated with mountain permafrost in a warming global climate. *Permafrost and Periglacial Processes* 12: 145–156.

Harris, C., Kern-Luetschg, M., Murton, J., Font, M., Davies, M.C.R. & Smith, F.W. 2008. Solifluction processes on permafrost and non-permafrost slopes: results of a large scale laboratory simulation. *Permafrost and Periglacial Processes* 19: 359–378.

Harris, C., Smith, J.S. Davies, M.C.R. & Rea, B. 2008. An investigation of periglacial slope stability in relation to soil properties based on physical modelling in the geotechnical centrifuge. *Geomorphology* 93(3–4): 437–459.

Hayashi, J.N. & Self, S. 1992. A comparison of pyroclastic flow and debris avalanche mobility, *Journal of Geophysical Research—Solid Earth* 97 (B6): 9063–9071.

Henkel, D.J. 1970. The role of waves in causing submarine landslides, *Géotechnique* 20(1): 75–80.

Hori, T., Mohri, Y., Bowman, E.T. & Soga, K. 2004. Model test for progressive failure of a sandy embankment dam by seepage. In W.A. Lacerda, M. Ehrlich, S. Fontoura & A. Sayao (eds). *Landslides: Evaluation and Stabilization. Proc. 9th International Symposium on Landslides*. Rio de Janeiro: AA Balkema.

Hu, P., Cai, Q.P., Luo, G.Y., Ding, Y.H., Dong, M., Hu, L.W., Hou, Y.J. & Ng, C.W.W. 2009. Centrifuge modeling of failure patterns in mixed soil layers induced by normal faults. In *Proceedings of the 17th International Conference on Soil Mechanics and Geotechnical Engineering*, Alexandria, Egypt, 694–597.

Huang, X. & Garcia, M.H. 1999. Modeling of non-hydroplaning mudflows on continental slopes. *Marine Geology* 154: 131–142.

Hubbert, M.K. 1937. Theory of scale models as applied to the study of geologic structures. *GSA Bulletin* 48: 1459–1520.

Hudacsek, P., Bransby, M.F., Hallett, P.D. & Bengough, A.G. 2009. Centrifuge modelling of climatic effects on the long-term performance of compacted clay embankments. *ICE Journal of Engineering Sustainability* 162(2): 91–100.

Hungr, O. 2005. Classification and terminology. In Jakob, M., & Hungr, O. (eds). *Debris-flow hazards and related phenomena*: 9–23.

Hungr, O. 2008. Simplified models of spreading flow of dry granular material. *Canadian Geotechnical Journal* 45: 1156–1168.

Ilstad, T., Marr, J.G., Elverhøi, A., & Harbitz, C.B. 2004a. Laboratory studies of subaqueous debris flows by measurements of pore-fluid pressure and total stress. *Marine Geology* 213: 403–414.

Ilstad, T., Elverhøi, A., Issler, D. & Marr, J.G. 2004b. Subaqueous debris flow behaviour and its dependence on the sand/clay ratio: a laboratory study using particle tracking. *Marine Geology* 213: 415–438.

Ilstad, T., DeBlasio, F.V., Elverhøi, A., Harbitz, C.B., Engvik, L., Longva, O., & Marr, J.G. 2004c. On the frontal dynamics and morphology of submarine debris flows. *Marine Geology* 213: 481–497.

IPCC, 2007. Climate Change 2007: The physical science basis. In Solomon, S., Qin, D., Manning, M., Marquis, M., Averyt, K.B., Tignor, M., & Miller, H.L. (eds). *Contribution of Working Group I to the Fourth Assessment Report of the Intergovernmental Panel on Climate Change*. Cambridge University Press, Cambridge, United Kingdom and New York, NY, USA, 996pp.

Issler, D., De Blasio, F.V., Elverhøi, A., Bryn, P. & Lien, R. 2005. Scaling behaviour of clay-rich submarine debris flows. *J. Marine Petrol. Geol.* 22: 187–194.

Iverson, R.M. 1997. The physics of debris flows. *Reviews of Geophysics* 35: 245–296.

Jeanjean, P., Liedtke, E. & Clukey, E.C. 2005. An operator perspective on offshore risk assessment and geotechnical design in geohazard-prone areas. *Proc. International Sym-posium on Frontiers in Offshore Geotechnics (ISFOG 2005)*, Perth, 115–143.

Jin, M. & Fread, D.L. 1999. 1D modeling of mud/debris unsteady flows. *Journal of Hydraulic Engineering, ASCE* 125(8): 827–834.

Kamphuis, J.W. & Hall, K.R. 1983. Initiation of erosion of consolidated cohesive materials by unidirectional current. *J. of Hydraulics (ASCE)* 109: 49–61.

Kim, D.S., Cho, G.C. & Kim, N.R. 2006. Development of KOCED geotechnical centrifuge facility at KAIST. In Ng, Zhang & Wang (eds). *Physical Modelling in Geotechnics—6th ICPMG '06*. London: Taylor and Francis Group.

King, L.H. & MacLean, B. 1970. Pockmarks on the Scotian Shelf. *Geological Society of America Bulletin* 81: 3141–3148.

Knappett, J.A., Haigh, S.K. & Madabhushi, S.P.G. 2006. Mechanisms of failure for shallow foundations under earthquake loading, *Soil Dynamics and Earthquake Engineering* 26: 91–102.

Kobayashi, Y., Harp, E.L. & Kagawa, T. 1990. Simulation of rockfalls triggered by earthquakes. *Rock Mechanics and Rock Engineering* 23(1): 1–20.

Koyi, H. 1997. Analogue modeling: from a qualitative to a quantitative technique, a historical outline. *Journal of Petroleum Geology* 20(2): 223–238.

Lewkowicz, A.G. 1988. Slope processes. In Clark, M.J. (ed.). *Advances in Periglacial Geomorphology:* 325–368. Chichester: Wiley.

Ling, H.I., Wu, M.H., Leshchinsky, D. & Leshchinsky, B. 2009. Centrifuge Modeling of Slope Instability. *Journal of Geotechnical and Geoenvironmental Engineering* 135(6): 758–767.

Manzella, I. & Labiouse, V. 2008. Qualitative analysis of rock avalanches propagation by means of physical modelling of not-constrained gravel flows. *Rock Mechanics and Rock Engineering* 41(1): 133–151.

Marr, J.G., Harff, P.A., Shanmugam, G. & Parker, G. 2001. Experiments on subaqueous sandy gravity flows: the role of clay and water content in flow dynamics and depositional structures. *GSA Bulletin*, 113: 1377–1386.

Melosh, H.J. 1979. Acoustic fluidization: A new geological process? *Journal of Geophysical Research* 84: 7513–7520.

Mohrig, D., Whipple, K.X., Hondzo, M., Ellis, C. & Parker, G. 1998. Hydroplaning of subaqueous debris flows. *GSA Bulletin*, 110: 387–394.

Mohrig, D., Elverhøi, A. & Parker, G. 1999. Experiments on the relative mobility of muddy subaqueous and subaerial debris flows, and their capacity to remobilize antecedent deposits. *Marine Geology* 154: 117–129.

Moriwaki, H., Inokuchi, T., Hattanji, T., Sassa, K., Ochiai, H. & Wang, G. 2004. Failure processes in a full scale landslide experiment using a rainfall simulator. *Landslides* 4: 277–288.

Okura, Y., Kitahara, H., Sammori, T. & Kawanami, A. 2000. The effects of rockfall volume on runout distance. *Engineering Geology* 58(2): 109–124.

Olivares, L. & Picarelli, L. 2006. Modelling of flowslides behaviour for risk mitigation. *Proc. of the Physical Modelling in Geotechnics—6th ICPMG '06* 1: 99–112. Hong Kong: Taylor and Francis/Balkema.

Orange, D., Angell, M., Brand, J., Thompson, J., Buddin, T., Williams, M., Hart, B. & Berger, B. 2003. Shallow geological and salt tectonic setting of the Mad Dog and Atlantis field: relationship between salt, faults and seafloor geomorphology. *Proc. Offshore Tech. Conf*. Paper OTC15157.

O'Rourke, M.J. 2003. Buried pipelines. In: Chen W-F, Scawthorn C (eds) *Earthquake engineering handbook*. Boca Raton: CRC Press.

Pichler, B., Hellmich, Ch. & Mang, H.A. 2005. Impact of rocks onto gravel: Design and evaluation of experiments. *Journal of Impact Engineering* 39: 559–578.

Ramberg, H. 1967. *Gravity, deformation and the Earth's crust.* Academic Press, London (2nd edition 1981).

Rickenmann, D., Weber, D. & Stephanov, B. 2003. Erosion by debris flows in field and laboratory experiments. In Rickenmann, D., & Chen, C.-l., (eds). *3rd International conference on Debris-flow Hazards Mitigation: Mechanics Prediction and Assessment:* 883–894.

Rombi, J., Pooley, E.J. & Bowman, E.T. 2006. Factors influencing granular debris flow behaviour: an experimental investigation. In Ng, C.W.W., Zhang, L.M. & Wang, Y.H. (eds). 6th *International Conference on Physical Modelling in Geotechnics:* 379–384.

Sasanakul, I., Vanadit-Ellis, W., Sharp, M., Abdoun, T., Ubilla, J., Steedman, S. & Stone, K. 2008. New Orleans levee system performance during Hurricane Katrina: 17th Street Canal and Orleans Canal North. *ASCE Journal of Geotechnical and Geoenvironmental Engineering* 134(5): 657–667.

Savage, S.B. & Hutter, K. 1989. The motion of a finite mass of granular material down a rough inclined plane. *Journal of Fluid Mechanics* 199: 177–215.

Shreve, R.L. 1968. The Blackhawk landslide. *Geological Society of America Special Paper* 108: 1–47.

Sonnenberg, R., Bransby, M.F., Hallett, P.D., Bengough, A.G. & Davies, M.C.R. 2010. Centrifuge modelling of slope reinforcement by roots. *Proc. Int. Conf. on Phys. Modelling in Geotechnics*, Zurich (this proceedings).

Springman, S.M., Laue, J., Boyle, R., White, J. & Zweidler, A. 2001. The ETH Zurich geotechnical drum centrifuge. *Int. J. of Phys. Modelling in Geotechnics* 1: 59–70.

Stone, K.J.L. & Wood, D.M. 1992. Effects of dilatancy and particle size observed in model tests on sand. *Soils and Foundations* 32(4): 43–57.

Takahashi, T. 2007. *Debris Flow: Mechanics, Prediction and Countermeasures*. Taylor and Francis.

Take, W.A., & Bolton, M.D. 2002. An atmospheric chamber for the investigation of the effect of seasonal moisture changes on clay slopes. In Phillips R. et al., (eds). *Int. Conf. Physical Modelling Geotechnics,* St. John's: 765–770. Rotterdam: Balkema.

Take, W.A. & Bolton, M.D. 2003. Tensiometer saturation and the reliable measurement of matric suction. *Géotechnique*. 53(2): 159–172.

Take, W.A. & Bolton, M.D. 2004. Identification of seasonal slope behaviour mechanisms from centrifuge case studies, *Skempton Memorial Conference*, London, UK, 2: 992–1004.

Take, W.A., Bolton, M.D., Wong, P.C.P. & Yeung, F.J. 2004. Evaluation of landslide triggering mechanisms in model fill slopes. *Landslides* 1(3): 173–184.

Taylor, R.N. ed. 1984. *Geotechnical Centrifuge Technology*. Taylor and Francis.

Tiberghien, D., Laigle, D., Naaim, M., Thibert, E. & Ousset, F. 2007. In Chen, C.L. & Major, J.J. (eds). *4th International Conference on Debris-Flow Hazards Mitigation: Mechanics, Prediction and Assessment*: 281–292.

Tjelta, T.I., Svanø, G., Strout, J.M., Forseberg, C.F. & Johansen, H. 2007. Shallow gas and its multiple impact on a North Sea production platform. *Proc. 6th International Conference on Offshore Site Investigation and Geotechnics*, Society for Underwater Technology. London. 205–220.

Tognacca, C. & Minor, H.-E. 2000. Role of surface tension, fluid density and fluid viscosity on debris-flow dynamics. In Wieczorek, G. & Naeser, N.D. (eds). *2nd International Conference on Debris-Flow Hazards Mitigation: Mechanics, Prediction and Assessment*: 229–235.

Tohari, A., Nishigaki, M. & Komatsu, M. 2007. Laboratory rainfall-induced slope failure with moisture content measurement. *Journal of Geotechnical and Geoenvironmental Engineering* 133(5): 575–587.

Toniolo, H., Harff, P., Marr, J.G., Paola, C. & Parker, G. 2004. Experiments on reworking by successive unconfined subaqueous and subaerial muddy debris flows. *Journal of Hydraulic Engineering, ASCE* 130(1): 38–48.

Tripsanas, E.K., Bryant, W.R. & Phaneuf, B.A. 2004. Slope-instability processes caused by salt movements in a complex deep-water environment, Bryant Canyon area, northwest Gulf of Mexico. *AAPG Bulletin* 88(6): 801–823.

Ubilla, J., Abdoun, T., Sasanakul, I., Sharp, M., Steedman, S., Vanadit-Ellis, W. & Zimmie, T. 2008. New Orleans levee system performance during Hurricane Katrina: London Avenue and Orleans Canal South. *ASCE Journal of Geotechnical and Geoenvironmental Engineering* 134(5): 668–680.

Ulusay, R., Aydan, O. & Hamada, M. 2002. The behaviour of structures built on active fault zones: examples from the recent earthquakes of Turkey. *Struct Eng Earthquake Eng. JSCE* 19(2): 149–167.

Vardoulakis, I. 2000. Dynamic thermo-poro-mechanical analysis of catastrophic landslides. *Géotechnique* 52(3): 157–171.

Vonder Mühll, D., Delaloye, R., Haeberli, W., Hölzle, M. & Krummenacher, B. 2000. *Permafrost Monitoring Switzerland PERMOS, annual report 1999/2000*.

Vonder Mühll, D., Stucki, T. & Haeberli, W. 1998. Borehole temperatures in Alpine permafrost: A ten year series. *Proc. Seventh International Conference on Permafrost, Yellowknife, Canada*: 1089–1095.

Wang, G. & Sassa, K. 2001. Factors influencing rainfall-induced landslides in laboratory flume tests. *Géotechnique* 51(7): 587–599.

White, D.J., Take, W.A. & Bolton, M.D. 2003. Soil deformation measurement using particle image velocimetry (PIV) and photogrammetry. *Géotechnique* 53(7): 619–631.

White, D.J., Randolph, M.F. & Thompson, B. 2005. An image-based deformation measurement system for the geotechnical centrifuge. *Int. J. Phy. Modelling in Geotechnics* 5(3): 1–12.

Wilson, C.J.N. 1984. The role of fluidisation in the emplacement of pyroclastic flows 2: Experimental results and their interpretation. *Journal of Volcanology and Geothermal Research* 20(1–2): 55–84.

Yoon, B.S. & Ellis, E.A. 2009. Centrifuge modelling of slope stabilisation using a discrete pile row. *Geomechanics and Geoengineering: An International Journal* 4(2): 103–108.

Zhou, R.Z.B., Ng, C.W.W., Zhang, M., Pun, W.K., Shiu, Y.K. & Chang, G.W.K. 2006. The effects of soil nails in a dense steep slope subjected to rising groundwater, In Ng, C.W.W, Zhang, L.M. & Wang, Y.H. (eds). *6th International Conference on Physical Modelling in Geotechnics*: 397–402. Hong Kong: Taylor Francis.

Physical Modelling in Geotechnics – Springman, Laue & Seward (eds)
© 2010 Taylor & Francis Group, London, ISBN 978-0-415-59288-8

Recent trends in geotechnical earthquake engineering experimentation

A. Elgamal
Department of Structural Engineering, University of California, San Diego, La Jolla, CA, USA

A.B. Huang
Department of Civil Engineering, National Chiao Tung University, Hsin Chu, Taiwan

M. Okamura
Department of Civil and Environmental Engineering, Ehime University, Matsuyama, Japan

ABSTRACT: Experimental facilities and related research have been expanding dramatically, with efforts underway in small-scale centrifuge modeling, large-scale 1-g testing, and full-scale dynamic/seismic investigations. In parallel, the advances in instrumentation and Information Technologies (IT) are allowing for increased insights. Within this framework, researchers are able to increasingly focus on soil-structure system response, gleaning new outlooks that more effectively address current challenges. In view of the possibilities allowed by these current advances, this paper presents an overview of such current activities, findings, and future trends.

1 INTRODUCTION

Major advances in experimental techniques, instrumentation, and information technologies are facilitating an accelerated pace of innovation and discovery. An effort will be made to present the big picture, in order to highlight the potential inter-play opportunities among a wide range of experimentation options. In the following sections, an overview of developments and advances will be presented to address: i) novel testing facilities and instrumentation, ii) ongoing research directions, and iii) related research outcomes as facilitated by these developments. A discussion of current findings and future trends is also included.

2 RECENT DEVELOPMENTS IN TESTING TECHNIQUES

2.1 *Testing facilities and sites*

2.1.1 *In situ mobile testing facilities*

In the United States, two new mobile laboratories have become available to provide relatively high levels of dynamic excitation (Elgamal et al. 2007). A summary of the equipment at each of these two US Network for Earthquake Engineering Simulation (NEES) facilities is included below.

2.1.1.1 NEES@UCLA (http://nees.ucla.edu)

NEES at UCLA operates a set of mobile shakers for dynamic excitation, and a data acquisition laboratory with satellite Internet transmission capabilities. In addition, a Cone Penetration (CPT) truck is available for estimation of soil properties in-situ.

Eccentric mass shakers impart controlled harmonic excitation. Using this technique, earlier geotechnical studies were conducted by Keightley (1964, 1966), Jennings & Kuroiwa (1968), and Abdel-Ghaffar & Scott (1978, 1981). The UCLA laboratory includes (Fig. 1) two uni-directional eccentric mass vibrators (Model MK-15) with a wide frequency range (0–25 Hz) and large force capability (100 kips). Synchronization between the two shakers is possible with the use of Vector motor drives. Two or more vibrators, spaced apart

Figure 1. NEES@UCLA large eccentric shaker and Cone Penetration Testing truck (http://nees.ucla.edu).

on a structure, can provide the tested structure with torsional as well as translational force, or enhance the response of one particular mode over another by force appropriation, which can be very helpful in distinguishing between closely spaced modes of vibration. Recent research using NEES@UCLA includes the studies reported by Stewart et al. (2002, 2005), Luco et al. (2004), Ozcelik (2008), Runnels (2007), Valentine (2007), and Cummins (2009).

The UCLA NEES equipment portfolio also includes a Hogentogler cone penetration testing truck, equipped with a seismic-piezocone to characterize soil consistency, pore-water pressure and shear wave velocity (Fig. 1). The rig has a 20-ton hydraulic push capacity, weighs 6 tons approximately, with side augers to provide additional reaction force. A fully automatic data acquisition system records measurements of cone tip resistance, sleeve friction, probe inclination, pore-water pressure and shear wave velocity.

2.1.1.2 NEES@UTexas (http://nees.utexas.edu)
NEES at the University Texas is an equipment site that specializes in dynamic field testing using large-scale shakers. The equipment includes three mobile shakers that have diverse force and frequency capabilities, a satellite linked instrumentation van that houses a data acquisition system, and a large collection of field instrumentation capabilities.

The mobile shakers include (Stokoe et al. 2004, 2006a, b, 2008; Menq et al. 2008): i) Thumper, a dynamic source for urban applications with a useful frequency range of up to 500 Hz, and peak force of about 6000 lbs (up to 17 Hz), ii) T-Rex, a Tri-Axial Vibrosies (Fig. 2), which allows axis transformation between vertical, inline, and cross-line (peak force of 60,000 lbs or about 267 kN vertical, and about half this value in the horizontal directions starting at 12 Hz), and is fitted with a cone penetrometer, and iii) Liquidator, a low frequency Vibrosies (Fig. 2) with a peak force (at 1 Hz) of 10,000 lbs or 45 kN, in the vertical or the horizontal directions (also is fitted with a cone penetrometer).

This field equipment is being used in a variety of applications, including linear and nonlinear ground shear loading (Rathje et al. 2004; Stokoe et al. 2006a, b; Kurtulus et al. 2006, 2007), liquefaction testing (Rathje et al. 2005; Chang et al. 2007; Cox et al. 2009), geophysical testing (Stokoe et al. 2006a, b; Rosenblad et al. 2007, 2008; Lerch et al. 2008), and dynamic testing of soil-structure systems (Agarwal et al. 2006; Rix et al. 2007).

Figure 2. UTexas T-Rex (Tri-axial) vibroseis, and liquidator (low frequency) vibroseis (http://nees.utexas.edu).

2.1.2 *Large-scale testing facilities*
Four new large-scale testing laboratories are presented in this section (Elgamal et al. 2007). A special fault-crossing system and three new large shake-tables have recently become available.

2.1.2.1 NEES@Cornell (http://nees.cornell.edu)
The Cornell facility is a unique world-class resource for research and education, focused on underground lifeline response to large ground deformation.

Large-scale experiments were successfully completed to evaluate the effects of earthquake-induced ground rupture on welded steel pipelines with elbows. The experimental set-up involved the largest full-scale replication of ground deformation effects on pipelines ever performed in the laboratory. Figure 3 shows two experimental basins with a total of 60–65 metric tons of soil that were displaced 1 m relative to each other to simulate the type of abrupt displacement generated by liquefaction-induced lateral spread, landslides, and surface faulting.

2.1.2.2 NEES@UCSD (http://nees.ucsd.edu)
The University of California, San Diego (UCSD) outdoor shake table has been developed at the

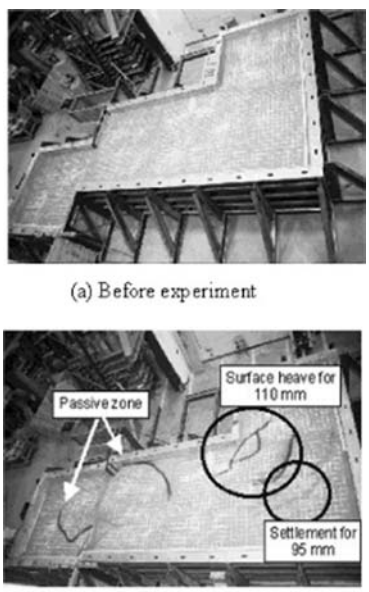

Figure 3. Overhead view of test basin (over 10 m long, max. 5 m wide and 1.2 m deep) before and after the experiment (http://nees.cornell.edu).

Englekirk Field Station (Fig. 4), a site located 15 km away from the main UCSD campus (Van Den Einde et al. 2004; Restrepo et al. 2005). The shake table, acting in combination with equipment and facilities separately funded by the California Department of Transportation (Caltrans), includes a large laminar soil shear box (inside dimensions of the box are 6.71 m long by 2.90 m wide by as much as 5 m in height) and two refillable soil pits (Figs. 4, 5).

This unique facility enables next generation seismic experiments to be conducted on very large structural and Soil-Foundation-Structure-Interaction (SFSI) systems. Moreover, the proximity of a soil pit to the Shake Table allows hybrid shake table-soil pit experiments to be conducted. This innovative shake-table in conjunction with the Caltrans SFSI facility adds unique testing capabilities to NEES and consolidates the leadership of the NEES collaboratory (http://www.nees.org) as a worldwide predominant earthquake testing consortium.

The UCSD Outdoor Shake Table is a 7.6 m wide by 12.2 m long single Degree-of-Freedom (DOF) system with the capability of upgrading to 6-DOF. The specifications for the first phase of the facility include a stroke of ±0.75 m, a peak horizontal velocity of 1.8 m/s, a horizontal force capacity of 6.8 MN, an overturning moment capacity of 50 MN-m for a 400 ton specimen, and a vertical payload capacity of 20 MN. The testing frequency range is 0–20 Hz. While not the largest of its kind, the velocity, frequency range, and stroke capabilities make it the largest table outside Japan and the world's first outdoor shake table. The facility adds a significant new dimension to existing US testing capabilities, with no overhead space and lifting constraints.

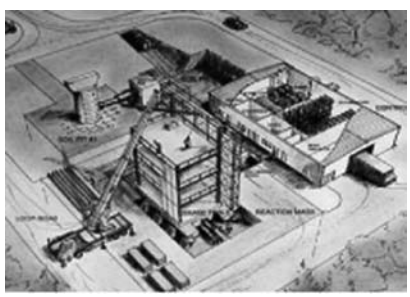

Figure 4. Facility layout including shake-table and adjacent large soil pits (http://nees.ucsd.edu).

Figure 5. UCSD NEES large high performance outdoor shake table (LHPOST), with soil container on shake table during model construction.

2.1.2.3 Japan E-Defense shake table

E-Defense of the National Research Institute for Earth Science and Disaster Prevention (NIED), the largest earthquake engineering shaking table in the world (Fig. 6), was opened in 2005, commemorating the tenth anniversary of the 1995 Kobe earthquake. This shaking table facility is located at the Hyogo Earthquake Engineering Research Center, (http://www.bosai.go.jp/hyogo/ehyogo/), Miki City, Japan.

The E-Defense shaking table platform has dimensions of 20 m in length and 15 m in width. It is supported on fourteen vertical hydraulic actuators and is connected to ten horizontal hydraulic actuators (five in each lateral direction), allowing three-dimensional motion. It has a payload capacity of 1200 tons with maximum acceleration, velocity, and displacement of 9 m/s^2, 2 m/s, and 1 m in both horizontal directions and of 15 m/s^2, 0.7 m/s, and 0.5 m in the vertical direction. To record data during an experiment, about 900 data acquisition channels are available (http://www.bosai.go.jp/hyogo/ehyogo/).

2.1.2.4 PWRI hybrid shaking table

In 1998, the Public Works Research Institute (PWRI) in Japan developed a large shaking table (Fig. 7) with a hybrid testing experimental system (Tamura et al. 2004). The PWRI shaking table has a platform of 6 m in length and 6 m in width with a payload capacity of 300 tons. The hybrid testing system achieves the capability for modeling of real time interaction between huge superstructures and foundation-soil systems. In this system, numerical analysis takes the role of evaluating response of structures such as bridge piers and superstructures which are large but relatively easy to handle computationally. Within this framework, the highly non-linear behavior of

Figure 6. E-Defense shake table schematic with schematic of liquefaction SFSI experiments in a 2D circular laminar container, and a waterfront pile-supported structure (from Tokimatsu et al. 2007).

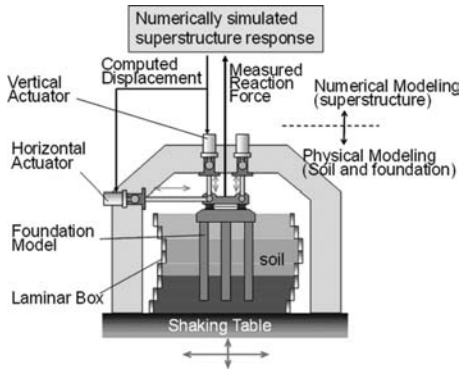

Figure 7. PWRI hybrid vibration experiment system.

the soil-foundation system is physically simulated by the shaking table experimental setup.

2.1.3 *Instrumented sites*

For monitoring and recording earthquake generated motions, instrumented sites deploy sensors including accelerometers and pore-pressure transducers at various depths within the ground (Nigbor et al. 2004). The three sites described below (Elgamal et al. 2007) have been recording such data sets, which have constituted the basis for numerous informative studies. Along with the seismic ground response, SFSI investigations have been undertaken with the actual recorded earthquake motions as the source of dynamic excitation.

2.1.3.1 NEES@UCSB (http://nees.ucsb.edu)

At the University of California, Santa Barbara (UCSB), the Garner Valley and the Wildlife refuge sites have been instrumented and are available for research (Steidl 2007; Steidl et al. 2008; Steidl and Seale 2010). A brief description is included below.

The NEES field site in the Garner Valley (Fig. 8) is very well suited to the study of soil-foundation-structure interaction and liquefaction. The area is located near active faults, on low density alluvial soil with a near surface water table. The site has been thoroughly characterized recently through borehole geotechnical investigations over the last ten years.

Additionally, the valley bedrock is basin shaped and late arriving surface waves have been observed, traveling from the edge of the basin. Thus, this field site provides a possibility to observe surface waves on fully instrumented structures.

The NEES Wildlife Refuge Liquefaction Field Site (Fig. 9) has been thoroughly characterized through geotechnical borehole samples, as was a nearby site that was previously studied by the United States Geological Survey (Youd et al. 2004, 2007, 2008). Located in California's Imperial

Figure 8. Garner Valley SFSI field site and SFSI structure (http://nees.ucsb.edu).

Figure 9. Wildlife refuge instrumented site (http://nees.ucsb.edu).

Valley, the Wildlife Liquefaction Array (WLA) field site records numerous earthquakes in this seismically active area at the southern most terminus of the San Andreas Fault system. The WLA array is located on the west bank of the Alamo River 13 km due north of Brawley, California and 160 km due east of San Diego. This area has been frequently shaken by earthquakes with six events in the past 75 years generating liquefaction effects within 10 km of the WLA site. Currently, researchers are using earthquakes that occur on a daily basis near this site, as well as active testing using mobile shakers to try to better understand how the near-surface geologic conditions affect the ground shaking at this location (http://nees.ucsb.edu).

2.1.3.2 Euroseis project

EUROSEIS is a large physical laboratory (Test Site), located at a distance of 30 km from Thessaloniki (at the epicentral area of the M 6.5 1978 earthquake), in northern Greece (Fig. 10). About 150 seismic events have been recorded. Of those, about 5 events are considered of moderate strength with peak acceleration of as much as 130 gals. The EUROSEIS-RISK project encompasses integrated experimental and theoretical research studies in seismology, applied geophysics, engineering seismology, earthquake engineering, soil dynamics, and structural engineering (Raptakis et al. 1998; Pitilakis et al. 1999; Chavez-Garcia et al. 2000; 2000, 2005; Guéguen & Bard 2005; Makra et al. 2005). Specific topics include seismic hazard assessment, monitoring of seismicity, design of two-dimensional (2D) and 3D soil models for site response evaluation, 2D/3D theoretical computations, site effects, Soil-Structure-Interaction (SSI) effects in the presence of yielding buildings or bridges, and validation of retrofitting

Figure 10. Map with the surface accelerographs (green rectangles) and the geological background (http://euroseis.civil.auth.gr, Pitilakis et al. 1999).

techniques (Euroseistest 1993–1995, Euroseismod 1996–1998, EUROSEISRISKSeismic 2002–2005 http://euroseis.civil. auth.gr).

2.1.4 *Geotechnical centrifuges*

As many as 30 large geotechnical centrifuges or more (radius larger than 3 m) are in operation in the world (Ng & Kutter 2001). Payload is in the range of 0.5–2 tons and models may be tested at g-levels of the order of 100–200 gravities. Earthquake simulators (shakers) are an integral part of centrifuge testing for earthquake engineering applications. For instance, Kimura (2000) reports that nearly half of 32 operating centrifuges in Japan are equipped with shakers.

The most common dynamic actuators installed on geotechnical centrifuges are 1-dimensional (1D) shaking tables using servo-hydraulic actuators. At Cambridge University, the Stored Angular Momentum (SAM) actuator (Madabhushi et al. 1998, 2006; Coelho et al. 2006) is being employed (Fig. 11). An innovative shaker (Fig. 12) has recently been deployed on the LCPC, France centrifuge (Chazelas et al. 2008). It is manufactured by Actidyn Systems and allows for generation of arbitrary earthquake-like motions. Major effort was expended in achieving a high level of isolation between the shaker and the centrifuge machine (leading to cleaner generated signals and long-term preservation of the centrifuge structural integrity).

For more realistic earthquake input excitation scenarios, horizontal and vertical 2D shakers already exist in Hong-Kong (Ng et al. 2001a), and in Korea (Kim et al. 2006). An in-flight robot exists at Hong Kong (Ng et al. 2002; Zhang & Kong 2006).

In addition, a great step forward has been taken thanks to the North American project NEES, launched in October 2000. More than US $ 9 million of investment allowed for upgrading the UC Davis (UCD) and RPI (New York) centrifuges (Figs. 12–14). In the UCD facility (Wilson et al. 2004), upgrades include the 2D (horizontal and vertical) shaker and a robot. A robot has also been installed (Ubilla et al. 2006; Saunders et al. 2007) at RPI (http://nees.rpi.edu/) along with a new 2D shaker (horizontal X- and Y- axes).

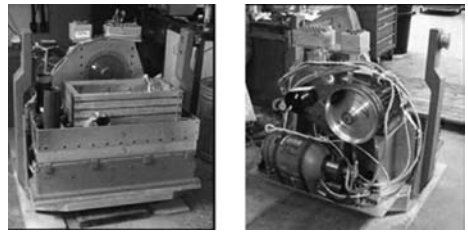

Figure 11. Model container mounted on the SAM actuator shaking system.

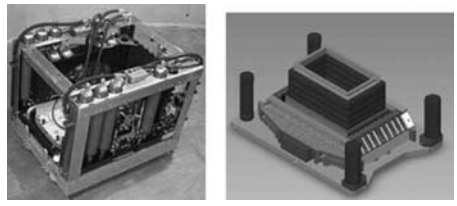

Figure 12. Left: LCPC shaker (http://www.lcpc.fr/en/presentation/moyens/centrifugeuse/index.dml), and Right: 2D shaker of UC Davis that can deliver horizontal and vertical shaking.

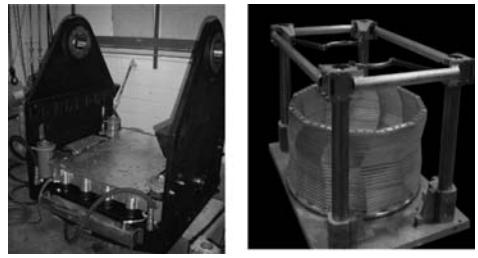

Figure 13. 2D shaker at RPI (two horizontal directions), and RPI 2D Laminar Container (http://nees.rpi.edu).

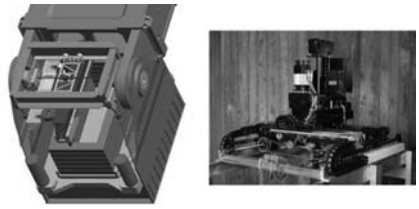

Figure 14. UCD (left), and RPI (right) in-flight Robots.

2.2 *Novel instrumentation techniques*

2.2.1 *Measurement of contact normal stress (Tactile pressure sensor)*

In conducting physical tests, direct measurement of soil pressure is frequently an important consideration. For that purpose, pressure cells and load cells have been conventionally employed. In order to reduce disturbance at the measurement location of interest, much attention is given to minimizing the space occupied by such devices. This matter has been of even greater significance in centrifuge testing where the reduced small-scale model may require sub-mm level accuracy, and even the cable connections may result in disruptions.

To accomplish this goal, a relatively un-intrusive technology has been proposed for use in geotechnical engineering applications (Paikowsky & Hajduk 1997; Paikowsky et al. 2000, 2003, 2006), in the form of thin sheets of small stress sensors (e.g., Tekscan Inc., http://www.tekscan.com/pressure-distribution.html). Known as Tactile force/pressure sensors, this technology has been adapted and employed for the first time in centrifuge testing, for static and dynamic applications, in the pioneering research of Springman et al. (2002). More recently, it has also been employed in 1 *g* and in the centrifuge for measurement of normal stress on buried pipelines (Abdoun et al. 2008c, 2009; Choo 2007; Ha et al. 2008a, b; O'Rourke et al. 2008; Palmer et al. 2006, 2009), due deformation of the surrounding soil (Fig. 15).

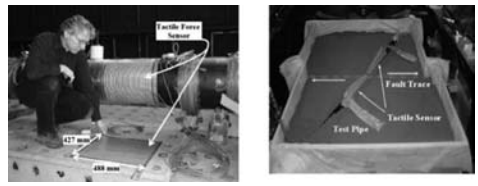

Figure 15. Tactile force sensor sheet wrapped around full-scale pipeline (from O'Rourke et al. 2008), and around centrifuge model pipeline (from Ha et al. 2008b).

2.2.2 *Direct measurement of relative displacement*

Estimation of the dynamic ground relative displacement (at and/or below the ground surface) is conventionally done by integrating recorded accelerations (from actual downhole arrays and during centrifuge experiments). Unfortunately, this approach involves the invocation of adhoc assumptions and approximations due to technical considerations associated with sensor orientation, electronic low and high frequency noise, and a multitude of digitization considerations. Two relatively new direct measurement approaches are discussed below.

2.2.2.1 Shape acceleration array (Shape tape)

Recently, a new technology for measuring acceleration and relative displacement (http://www.measurand.com/products/ShapeTape.html) has been adapted for use in geotechnical engineering applications (Abdoun et al. 2007a; Bennett et al. 2009). A synchronized array of micro-machined electro mechanical (MEMS) detects lateral and rotational motion (Fig. 16) and uses this information to measure acceleration as well as relative spatial location (Shape Acceleration Array).

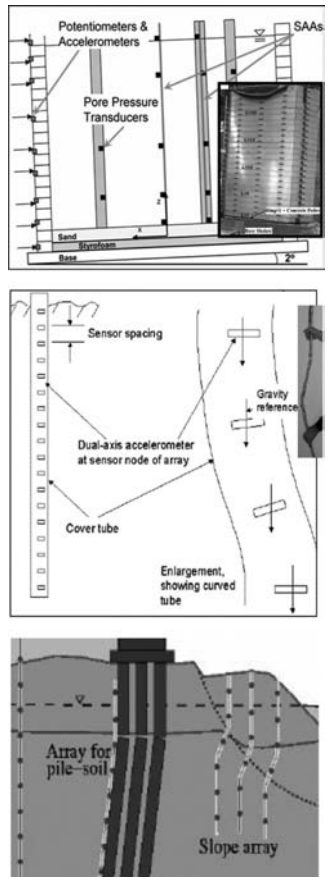

Figure 16. SAA in large 1 g shake-table experiment (after Bennett et al. 2009), for dynamic in-situ measurement of acceleration and displacement (after Zeghal et al. 2004), and for detection of slope movements (after Abdoun et al. 2007a).

Full-scale deployment of this technology has been underway for possible detection of static and dynamic motions (Zeghal et al. 2004; Abdoun et al. 2008a; Bennett et al. 2007; Jung et al. 2007). In addition, the technology has been proven to be quite effective in large 1 g shake table experiments

(Abdoun et al. 2007b, 2008b; Bennett et al. 2009). Along with other testing applications (e.g., Kutter & Wilson 2006), wireless connectivity may be resorted to.

2.2.2.2 Vision-based image monitoring

With the aid of an image recording system (e.g., standard camera images), versatile and robust procedures are being developed (Garnier et al. 1998; White et al. 2003; Zhang et al. 2009) for direct measurement of relative displacement (static and dynamic). Video can also be used to monitor targets that may be affixed on measurement locations of interest (Hutchinson et al. 2006; Natase et al. 2008; Doerr et al. 2005, 2008), or highlighted by a laser beam (Wahbeh et al. 2003). Currently, standard Matlab software may be used for image subtraction to extract and document the displacement field (to a high level of accuracy, depending on the employed camera system resolution). Among other studies, this approach is being used to record displacements of a laminar container during 1 g shake table lateral spreading experimentation (Thevanayagam et al. 2009).

2.2.3 *Distributive monitoring with fiber optic sensors*

Significant developments have been made in ground monitoring technologies using optic fiber as a means for data transmission and sensing. The optic fibers are durable and small in size (typical diameters less than 300 mm), and are not prone to damage by lightning. The optic signal can be transmitted for a long distance without amplification; it is immune to electromagnetic interference and short-circuit considerations under water. These characteristics make fiber optic sensors ideal for long term, field monitoring in the ground as well as in laboratory experimental studies where submersible and miniaturized sensors are usually preferred. Depending on the techniques applied, monitoring can be fully or partially distributive. In the case of fully distributive sensing, all parts of the optic fiber transmission line are capable of performing as sensors. Available techniques can include the optical time domain reflectometry (OTDR) or Brillouin Optical time domain reflectometry (BOTDR) (Bao et al. 2001; Mohamad et al. 2007). A single optic fiber with length in the 10's of kilometers can be laid in the field to detect ground failure/displacement. The magnitude of ground displacement is related to light intensity (OTDR) or frequency of the back scattered lightwave (BOTDR). The event location is resolved according to the speed and arrival time of the reflected light. However, OTDR or BOTDR are not suitable for high frequency data logging which is usually required for monitoring seismic events.

Optic Fiber Bragg Grating (FBG) is a partially distributive strain sensing technique where multiple sensors can be connected via a single optic fiber. The optic fiber has sensing capability only when an FBG is present. In an FBG, a periodic variation of fiber core refractive index is formed on a 1 to 20 mm segment of the optic fiber (Rao 1998). When the FBG is illuminated by a wideband light source, a fraction of the light is reflected back upon interference by the FBG. The peak wavelength of the reflected light is linearly related to the strain experienced by the FBG. Each of the FBG's on the same optic fiber occupies a separate wavelength domain to enable multiplexing among the connected FBG's according to wavelength. Taking advantage of these unique capabilities, Ho et al. (2006) developed an FBG-segmented deflectometer (FBG-SD) to monitor the profile of ground displacement. The FBG-SD is equipped with spring-loaded wheels that are compatible with the inclinometer casings. For field monitoring, a series of FBG-SD's are connected as they are inserted into a pre-installed inclinometer casing.

In a FBG-SD, two rigid segments are connected at a hinge. A flexible rod fixed to one of the segments extends through the hinge and is simply supported by a pin in the other segment. A pair of FBG's are fixed to the opposite sides of the flexible rod to measure the flexural strains as a result of deflection between the two segments caused by ground movement. The length and sensitivity of the FBG-SD can be adjusted by changing the configurations of the segments and flexible rod. Figure 17 shows the installation of FBG-SD in an inclined borehole at a Yellow River dike in Henan Province of China and ground deflections detected by the FBG-SD's as a result of removal of 9.7 m^3 of rock pile placed on the surface of the dike.

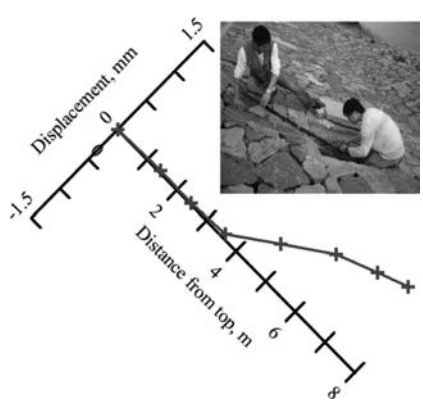

Figure 17. Field installation of the FBG-SD and displacement profile after removal of 9.7 m^3 of rock pile (Ma et al. 2007).

Using FBG to sense the deflection of a diaphragm in response to pressure variation against a sealed chamber, Ho et al. (2008) reported the design of an FBG based pressure sensor. Using this technique, Huang et al. (2009) placed 10 FBG based pressure sensors as piezometers in a single 100 mm diameter, 60 m deep borehole at 5 m intervals. Figure 18 shows the change of pore pressure profile with time during typhoon Morakot in Alishan, Taiwan where the accumulated rainfall reached 2600 mm in three days.

Using FBG to sense the deflection of a spring loaded mass, Mita & Yokoi (2000) developed an FBG accelerometer. FBG signal interrogation devices capable of recording data at frequencies in excess of the kHz rage are readily available commercially. It is thus conceivable that the down-hole-array typically used to monitor ground response in an earthquake event can be fully instrumented with FBG based sensors. Using the FBG's, profile measurements can include displacement, pore pressure and acceleration, with significantly improved stability and durability over the conventional electric sensors. With reasonable miniaturization, the same system can be installed in physical models for laboratory studies.

2.3 *Experiment databases*

A large-scale archival repository has been created for compiling research data and information related to the US George E. Brown Network for Earthquake Engineering Research (NEES, http://www.nees.org). This network currently includes 15 large-scale testing laboratories that conduct earthquake engineering research throughout the United States. Accessible via the internet (https://central.nees.org/), this database currently serves users in the thousands. Various modes of connectivity and accessibility are available to suit the data owner and the data user communities.

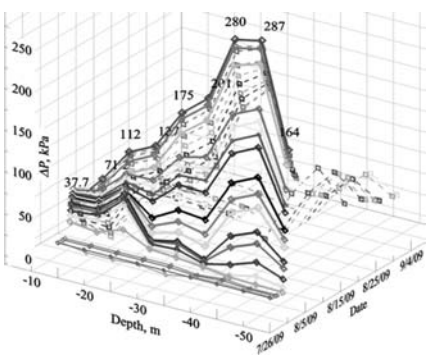

Figure 18. Change of pore pressure profile with time during typhoon Morakot.

As such, NEES initiated a curated data repository for experimental as well as computational simulations (Kutter et al. 2002). For NEES, it was evident that robust professional long-term preservation of data in a readily accessible format was simply a necessity. An integral component for NEES is data curation, in the form of a standard procedure to provide certification as to a data set's viability for general use.

For that purpose, a robust database archiving environment and an Internet accessible interface, along with an extensible Data Model was developed to systematically allow for organizing this data and all relevant related information (Kutter et al. 2002) of interest (i.e., the metadata). Basically, the Data model (Peng & Law 2004) allows for availability of data sets along with all associated relevant knowledge of interest. Ideally, an interested user would have all they need available for conducting further studies using the data. In addition, the metadata can provide digital identification to support archiving and preservation (Peng & Law 2004). Upon completion of a formal process of data curation (conducted independently after any data set upload), the information (data and metadata) would be deemed complete, and can be formally made available as such. Implementation of the data model in the form of an internet accessible database further allows for capabilities such as (Van Den Einde et al. 2007; Elgamal et al. 2009a, b): i) robust organization and storage of the data, ii) convenient searching and downloading, iii) availability of the data in common standard format(s), iv) ability to set different levels of access for different user groups, v) automated backup and archiving, and vi) instant accessibility without need for intermediate storage media that may become obsolete or outdated.

2.3.1 *Export to data viewers*

With the availability of this data repository, various tools may be developed to facilitate usage and the knowledge extraction process. For instance, through NEES central (https://central.nees.org/), data can be exported for use in N3DV, an advanced stereo-graphic application developed by UC Davis (Fig. 19) for visualizing the experimental response (Weber et al. 2003).

Similar applications can be added for automated linkages to other visualization tools and/or data processing algorithms/codes. Capabilities for increased integration between numerical and experimental simulation may be also added. Processed data may in turn be uploaded back to NEES central for archival and sharing, as a means of promoting collaboration on a world-wide scale.

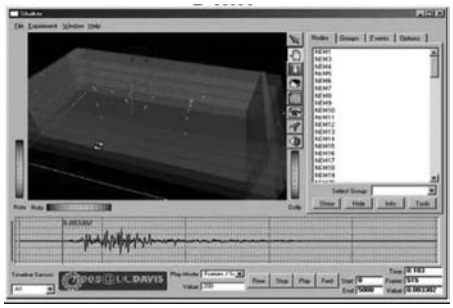

Figure 19. N3DV visualization tool, UC Davis (from http://www.nees.org, Weber et al. 2003).

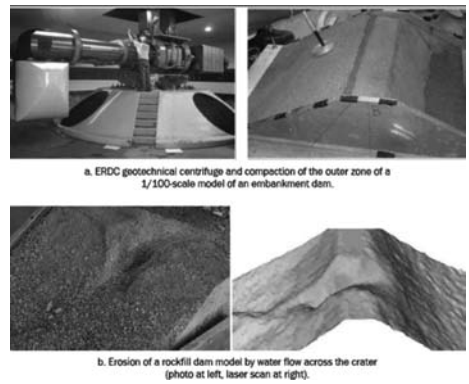

Figure 20. Examples of the tests conducted in the 2007–08 ERDC centrifuge test program of embankment cratering: a) ERDC geotechnical centrifuge and compaction of the outer zone of a 1/100-scale model of an embankment dam, and b) Erosion of a rockfill dam model by water flow across the crater showing photo at left, and laser scan at right (from Davis 2008; Seda-Sanabria et al. 2009).

Figure 21. Small-scale 1-g embankment dam model (left) under a VBIED dynamic loading (from Davis 2008; Seda-Sanabria et al. 2009), and small-scale embankment dam model (right) under waterborne improvised explosive device (WBIED) loading (from Davis 2008; Seda-Sanabria et al. 2009).

3 RESEARCH DIRECTIONS

3.1 *Blast loading*

Related to earthquake engineering research, there has been an increased interest in blast-induced dynamic effects and resulting damage. Related classical research (Davis 2003) had been primarily focused on the threats from either conventional air-delivered weapons or nuclear weapon attacks (Davis 2008). Currently, the focus was somewhat shifted to address (Davis 2008): i) cratering effects from potential Vehicle Borne Improvised Explosive Devices or (VBIED's), ii) the possibility of a waterside attack on Dams and Levees, from vessels carrying explosive charges, and iii) detonations within underground structures (tunnels). For that purpose, centrifuge testing and 1-g physical models have been under investigation.

For dams and levees, a main concern lies in the possible formation of an explosion crater that could possibly breach the embankment. Insights were gained as to the influence of the embankment characteristics and design on the ensuing damage (Zimmie et al. 2005; Davis 2008; Seda-Sanabria et al. 2009). Craters formed by detonations along the embankment crest, on a water bottom, or by surface detonations in shallow water were studied in 1-g and in the centrifuge (Figs. 20, 21). On this basis, analytical/numerical crater models were further developed and verified (Davis 2008).

Underground pipelines and tunnels were also studied in 1-g and centrifuge tests. Blast effects inside tunnels (Bakhtar 1997), and surface explosion scenarios (De et al. 2005; De & Zimmie 2006, 2007) were addressed.

3.2 *In-situ and large-scale testing*

3.2.1 *Liquefaction by blast loading*

Extensive research on ground liquefaction by blast loading was highlighted by the pioneering full-scale experiment CANLEX (Robertson et al. 2000a, b; Byrne et al. 1995; Puebla et al. 1997). Thereafter, major research on lateral response of pile foundations in liquefied ground was undertaken (Ashford et al. 2004, 2006; Kamijo et al. 2004; Miyamoto et al. 2004; Tanaka et al. 2005; Rollins et al. 2005a, b; Weaver et al. 2005; Juirnarongrit & Ashford 2006; Charlie 2009). In addition, this type of loading mechanism has allowed for insights related to liquefaction countermeasures (Ashford et al. 2000a, b). Stone columns were deployed around a deep foundation system, with favorable outcomes denoting the increased ability of the treated ground to resist the detrimental effects of liquefaction.

3.2.2 *Monotonic and cyclic loading*

In order to assess the behavior and lateral resistance characteristics of piles and pile groups, a

series of studies were undertaken in a wide range of soil profiles. Monotonic and cyclic loads were applied (Fig. 22). Pile testing in sands and clays demonstrated salient pile-group interaction effects, compared to the single pile scenario (Ahlberg et al. 2005; Rollins et al. 2005c, 2006a, b; Khalili-Tehrani et al. 2007; Stewart et al. 2007; Lemnitzer et al. 2008). Studies were also conducted to document the influence of pile diameter (Ng et al. 2001b; Ashford & Juirnarongrit 2003).

Evaluation of passive earth pressure was also a topic that received much attention (Duncan & Mokwa 2001). Specifically, effort was directed towards development of force-displacement relationships, as the wall gradually moved (Fig. 23) into the adjacent backfill (Cole & Rollins 2006; Rollins & Cole 2006; Runnels 2007; Shamsabadi et al. 2007; Valentine 2007; Cummins 2009; Lemnitzer et al. 2009). Such relationships allow for development of computational models to assess the involved soil-structure interaction considerations (e.g., bridge-abutment interaction during strong earthquake excitation).

3.2.3 *Liquefaction*

3.2.3.1 NIED

The National Research Institute for Earth Science and Disaster Prevention (NIED), Japan operates one of the largest shaking tables worldwide. A laminar container is available at NIED with dimensions of about 12 m length, 6 m height and 3.5 m width (Fig. 24). Earlier, Kagawa et al. (2004) and Tokimatsu & Suzuki (2004) employed this container in related soil-structure interaction studies. Recently, model piles in laterally flowing ground with (Cubrinovski et al. 2006) and without (He 2005; He et al. 2006, 2008, 2009) an upper non-liquefiable stratum, were also tested.

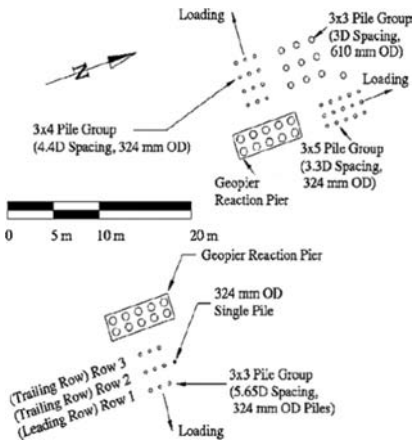

Figure 22. Layout of single piles and pile groups at test site below South Temple overpass on I-15 corridor in Salt Lake City (modified from Rollins et al. 2006a).

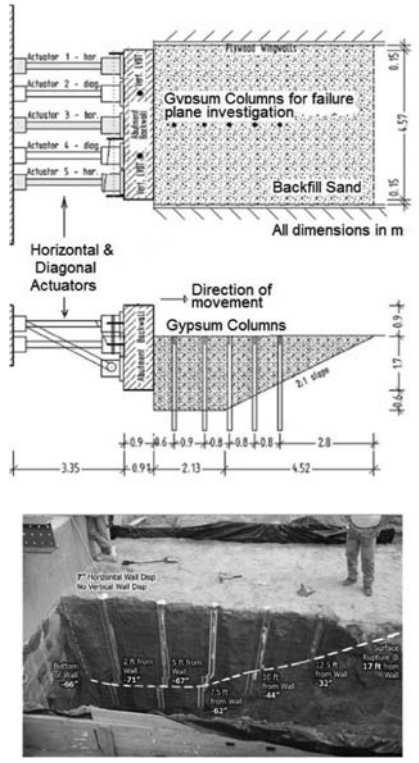

Figure 23. Plan view and cross-section of passive bridge abutment wall test and colored gypsum columns showing backfill deformation (modified from Lemnitzer et al. 2009).

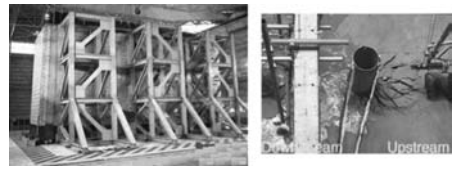

Figure 24. The NIED large size laminar box (Kagawa et al. 2004), and passive bulge of soil upslope of the flexible pile due to liquefaction-induced lateral ground displacement (He 2005).

3.2.3.2 UCSD

A series of one-g shake-table experiments was conducted to explore the response of piles due to liquefaction-induced lateral soil flow. A rigid and a laminar container were employed (Figs. 25, 26). The laminar container was about 4 m long, 2 m high and 1.8 m wide, and the rigid wall soil

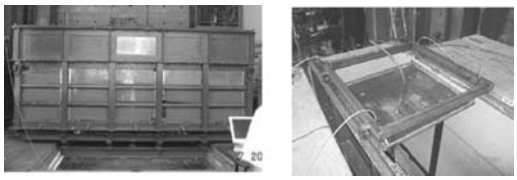

Figure 25. Rigid box and screen for the hydraulic fill model construction process (He 2005).

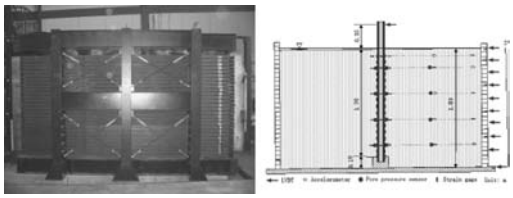

Figure 26. Laminar container and pile lateral spreading shake table test configuration (He 2005).

container was about 4 m long, 2 m high and 1.8 m wide (Meneses et al. 2002). The piles were embedded in fully saturated Medium Relative Density (D_r) sand strata in the range of 1.7 m in thickness (He 2005; He et al. 2006, 2008, 2009). Single pile and 2 × 2 pile groups were subjected to liquefaction-induced lateral flow with and without an upper non-liquefiable stratum (Meneses et al. 2002). Peak lateral pile displacements and bending moments were recorded and analyzed.

On the basis of the experiments reported by He et al. (2009), a triangular soil pressure was found to more closely represent the peak lateral load on single piles due to liquefaction-induced lateral soil flow. Specifically, the observed levels of pile bending moment (upon liquefaction of the employed Medium D_r sand layers), suggested a hydrostatic lateral pressure approximately equal to that due to the total overburden stress (He et al. 2009).

3.2.3.3 E-defense

Using the E-defense facility, recent research has been conducted to investigate the inertial and kinematic response of pile systems during three-dimensional shaking. A 3 × 3 steel pile group (each pile had a diameter of 152.4 mm and a wall thickness of 2.0 mm) supporting a foundation (Tabata & Sato 2006), with or without a superstructure, was set in a dry sand deposit prepared in a cylindrical laminar box (consisting of 41 laminates) with a height of 6.5 m and a radius of 8.0 m (Fig. 27). The piles were installed at a spacing of four-pile diameter center to center. Tests were conducted under one-, two-or three-dimensional shaking with three types of ground motion having a peak acceleration in the range of 0.3 m/s^2 to 8.0 m/s^2.

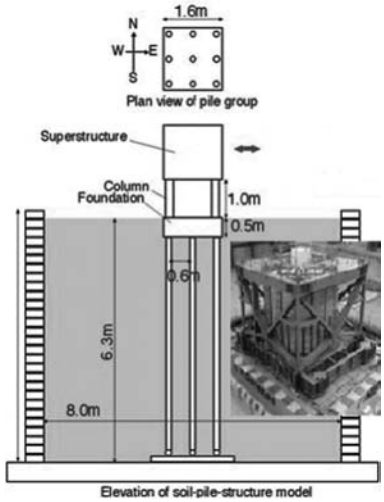

Figure 27. Test layout in laminar container mounted on the E-Defense shake table (modified from Tokimatsu et al. 2007).

At the end of this experimental program (Tokimatsu et al. 2007), the superstructure was observed to sustain significant damage (Fig. 28). Piles yielded down to depth in the range of 0.7 m to 1.2 m during the final stage of shaking resulting in permanent deformation and inclination of the superstructure.

More recently, shaking table tests were conducted in this laminar box to investigate the response and failure of a nearly full-scale pile-structure system in a liquefiable sand deposit subjected to multi-dimensional loading (Suzuki et al. 2008, 2009). To minimize the occupation time of the shaking table platform, the soil model was built off the shaking table platform, and the laminar box including the dry sand-pile-foundation system was then moved onto the shaking table platform by two large cranes. The dry sand was then saturated on the shaking table platform with water under a vacuum. A 3 × 3 steel pile group was tested, and the pile heads yielded, causing residual deformation and settlement of the foundation (Suzuki et al. 2008, 2009).

3.2.3.4 U Buffalo

Thevanayagam et al. (2009) report details of a large scale modular 1-g laminar box system (Fig. 29) capable of simulating seismically induced liquefaction and lateral spreading response of deposits of up to 6 m depth. The internal dimensions of the largest module are 5 m in length and 2.75 m in width. This two dimensional laminar box is made of 24 laminates stacked on top of each other supported by ball bearings, with a base shaker resting on a strong floor. The stacks of laminates slide on

Figure 28. Superstructure before and after test (from Tokimatsu et al. 2007).

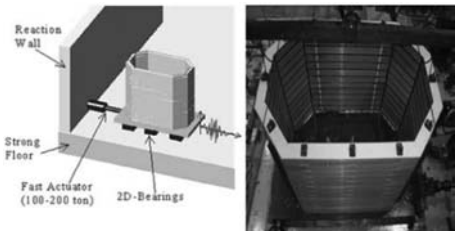

Figure 29. Laminar container testing at U Buffalo (from Thevanayagam et al. 2009).

each other using a low-friction high-load capacity ball bearing system placed between each laminate.

3.2.3.5 NCTU

Huang & Hsu (2004) reported the development of 1-g pressure chambers at National Chiao Tung University (NCTU) of Hsin Chu, Taiwan. These chambers are used mainly for the calibration of cone penetration tests (CPT) in sands. A system, referred to as the NCTU field simulator, had a physical cylindrical specimen, as in the conventional cavity-wall calibration chamber, and a numerically-simulated soil mass that extended laterally from the physical boundary to infinity. The physical specimen, 790 mm in diameter and 1600 mm high was surrounded by a stack of 20 rings (each at 80 mm in height), as shown in Figure 30. These rings are lined with an inflatable silicone rubber membrane on the inside to facilitate boundary displacement measurement and stress control. The pressure in each ring is individually servo controlled according to measurements of membrane expansion during CPT and theory of cylindrical cavity expansion. CPTs can be performed in dry sand in the field simulator with practically no boundary effects and thus no need for boundary effect corrections (Huang & Hsu 2005).

For CPT calibration in silty sands, a relatively small chamber was built for ease of specimen saturation, back pressuring and handling. It was designed for a 525 mm diameter and 760–815 mm high specimen, as shown in Figure 31. The chamber was designed to provide constant stress lateral boundary conditions only. For compressible sands (which is often the case for silty sand), these chamber dimensions were

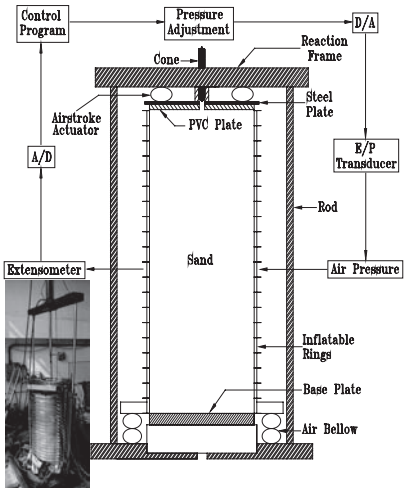

Figure 30. Design and operation of the NCTU field simulator.

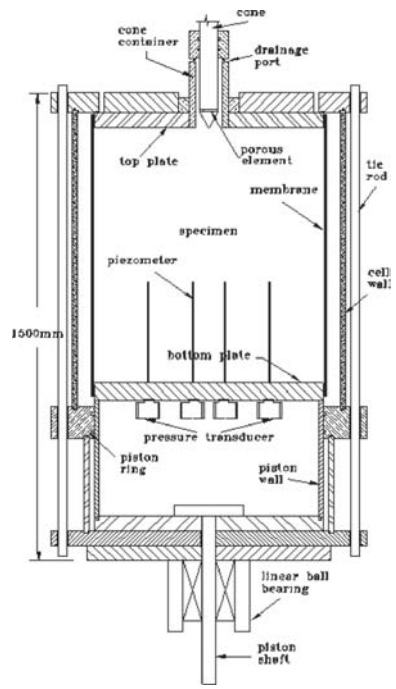

Figure 31. The NCTU medium sized calibration chamber.

sufficient in offsetting the boundary effects. The chamber provided top and bottom drainage and six open-ended piezometers to monitor the pore pressure development within the specimen.

The cone tip resistance (q_c)—cyclic resistance ratio (CRR) relationships can be obtained by comparing CPTs performed in the calibration chamber

and cyclic triaxial test results on sand specimens prepared under similar density and stress states.

Issues such as the effects of intrinsic properties and fines contents on q_c-CRR correlations for sands can be verified without the confusion generally involved in field observation and empirical approaches (Ishihara & Harada 2008; Huang 2009; Huang et al. 2009a, b).

3.2.4 *Liquefaction mitigation by de-saturation*

Although degree of saturation (S_r) has a significant effect on liquefaction resistance of soils (Okamura & Soga 2006; Okamura & Noguchi 2009), researchers have not always measured S_r of the model ground for shaking table tests and dynamic centrifuge tests. Okamura & Inoue (2010) developed a highly accurate measurement procedure and showed that only a few percent reduction in S_r changes the seismic behavior of the model, except for at shallower depths. In the light of this fact, soil de-saturation as an innovative liquefaction countermeasure technique (e.g., by air injection into liquefiable soil layers) has attracted much attention in recent years (Okamura & Teraoka 2005; Okamura et al. 2009; Yasuhara et al. 2008). This was triggered by a report of site investigation that injected air into a sand stratum has survived for more than 20 years (Okamura et al. 2006).

3.2.5 *Earth pressure*

An experimental investigation was conducted in a large soil container (Wilson & Elgamal 2006, Wilson 2009) in order to measure the characteristics of passive and dynamic earth pressure. The soil container was placed on a large outdoor shake table (Figs. 32–35). Well graded silty sand was compacted (Fig. 34) in

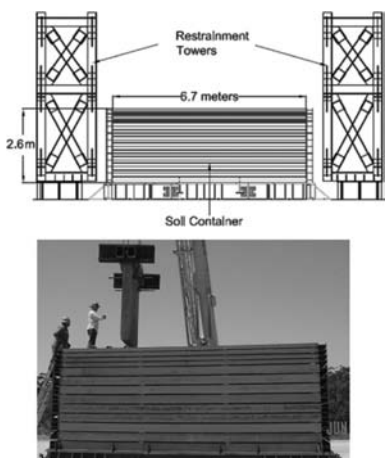

Figure 32. Schematic elevation view of soil container and restraining towers, and insertion of test wall into container (Wilson 2009).

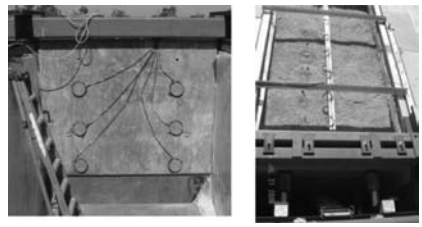

Figure 33. Soil container inside lining (left and right sides) and test wall with pressure sensors, and test setup overhead-view showing jacks and load cells behind wall (Wilson 2009).

Figure 34. Backfill compaction inside container, and soil model container on the NEES outdoor shake table at UCSD (Wilson 2009).

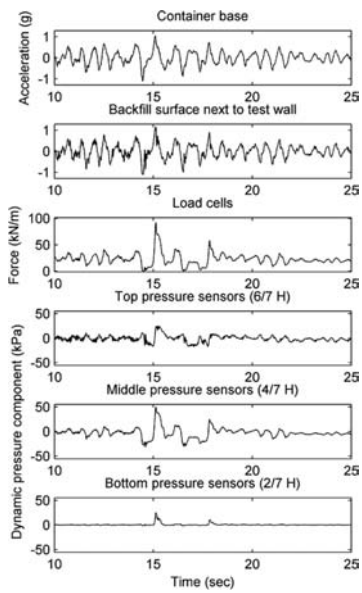

Figure 35. Test results from scaled earthquake record input motion with peak acceleration of about 1 g (Wilson 2009).

the container behind a 1.7 meter tall vertical wall section. The wall was first displaced laterally to record the peak passive earth pressure and the corresponding force-displacement relationship (Wilson & Elgamal 2006; Wilson 2009). Dynamic lateral earth

pressure was recorded next, during a series of shake table experiments with amplitudes reaching in excess of 1 g (Wilson & Elgamal 2008, 2009a, b, c; Wilson 2009). Data was recorded, including the input and surface accelerations, the pressure at different depths and the total lateral force (Fig. 35). In this stiff compacted backfill scenario, earth pressure remained close to the static value for low to moderate input excitations. For larger input acceleration levels, the backfill shear strength was progressively mobilized, and the change in the measured dynamic earth pressure became quite significant.

3.3 *Centrifuge testing*

Along with the extensive in-situ and large-scale studies reported above on liquefaction and effects on pile foundations, major insights were also derived from centrifuge testing investigations. In the centrifuge, actual dynamic earthquake-like motions may be imparted, thus providing a complementary venue to assess the response of the ground and of the supported foundation systems (Bhattacharya et al. 2004, 2005; Boulanger et al. 2006, 2007; Brandenberg 2005; Brandenberg et al. 2005, 2007a, b; Chang et al. 2005, 2006; Escoffier et al. 2008). Effect of permeability and soil compressibility were highlighted in the studies by Gonzalez (2005), and Gonzalez et al. (2006, 2008).

At the soil system level, studies were conducted to highlight the potentially significant effects of soil layering on the observed patterns of shear deformation (Kulasingam et al. 2004; Kutter et al. 2004; Malvick et al. 2006, 2008). Strength loss and shear strain localization were evident immediately below any low permeability strata or inter-layers.

Recently, soil-structure interaction research on shallow foundations has also shown the potentially beneficial outcomes of foundation rocking. Valuable studies have shed light on this mechanism and have allowed for development of appropriate modeling procedures (Gajan et al. 2005; Gajan 2006; Gajan and Kutter 2008, 2009a, b; Paolucci et al. 2007; Algie et al. 2008).

Studies that address underground structures and systems have also been underway. At RPI, parallel efforts to look at pipeline fault crossing have complemented the near full-scale studies of NEES@Cornell (O'Rourke et al. 2008; Abdoun et al. 2008c, 2009). Studies of tunnels crossing under waterways have been effective for verification of numerical codes (Yang et al. 2004), constituting an example of strong linkage between academia and the state of practice.

4 SUMMARY AND CONCLUSIONS

The sections above have attempted to provide a partial overview of ongoing developments in testing facilities/techniques, and related research. Experimental investigations today address contemporary needs with in-situ instrumented sites, full-scale and near full-scale in-situ tests, large-scale 1-g shake table tests, and centrifuge testing. Each technique complements the other, and provides important pertinent perspectives.

Centrifuge testing continues to allow for system-level studies, analysis of large deformation, and the evolution of insightful failure mechanisms. The in-situ instrumented sites bring actual earthquake response into the picture. Field testing and large 1-g experiments allow the actual natural soil materials to influence the outcomes and provide a closer representation of the state of practice (including construction procedures). Closer representations of the structural elements (e.g., HDPE pipelines, reinforced concrete piles), and use of field soil materials (e.g., engineered backfills composed of available native soils) are also possible. In addition, the structural-soil interface characteristics are appropriately captured (e.g., soil-pile interface, soil-wall interface).

As such, among the main characteristics to be highlighted are:

i. Natural soils that may be employed in 1-g testing have shown strength derived from friction as well as cohesion/cementation, which might be also somewhat age dependent (for instance, c-ϕ soils). Emulation of such characteristics is encouraged for small scale experimentation.
ii. In addition to the shear strength and stiffness characteristics, recent liquefaction studies have shown permeability and compressibility to play a significant role. This is in turn necessitating the continued attention towards more accurate representation of such actual in-situ conditions.
iii. Modeling and testing of entire soil-foundation-structure systems has generated new valuable insights. Examples include the potentially beneficial effects of rocking in shallow foundation systems.
iii. Formal experimentation databases stand to facilitate unprecedented collaborative research efforts. While currently at its infancy stage, the prospects are quite positive and advancements in this direction are highly encouraged.
iv. Facilitating the use of data from hundreds/thousands of channels by powerful visualization tools, and for more routine data-mining, system-identification, and computational simulation/verification efforts is an additional important frontier.
v. Novel sensors and IT technologies continue to play an increasingly important role. Major

strides have been made in terms of wireless connectivity, direct measurement of relative displacements and deformations, and unintrusive measurement of normal contact stresses.

vi. Increased attention in modeling soil-soil and soil-structure interfaces has been producing valuable new insights. Examples include the major influence of permeability in stratified soil formations, and behavior of soil at the interface with the structural components.

vii. Continued interaction with Industry and the state of practice can infuse critical salient insights into the overall scope of testing, with benefits to the academic and practical sides alike. Recent examples include research on tunnels and pipelines crossing below major waterways and fault systems.

viii. Increased use of robots in centrifuge testing will substantially increase the range of research applications, particularly for the important scenarios of site characterization, staged construction, and ground modification.

ACKNOWLEDGEMENTS

The assistance provided by Dr. Michael Sharp (ERDC), and Professors T. Abdoun and R. Dobry (RPI), R. Boulanger and B. Kutter (UC Davis), J. Garnier (LCPC), S.P.G. Madabhushi (Cambridge University), K. Pitilakis (Aristotle University), E. Rathje and K. Stokoe II (U. Texas), S. Thevanayagam (U. Buffalo), K. Tokimatsu (Tokyo Institute of Technology), J. Steidl (UCSB), H. Stewart (Cornell University), and J. Wallace (UCLA) is most appreciated. Research by the author and co-workers was supported by NSF grants No. CMMI 0420347 and 0529995.

REFERENCES

Abdel-Ghaffar, A.M. & Scott, R.F. 1978. An Investigation of the dynamic characteristics of an earth dam. *Technical Report: EERL-78–02*, California Institute of Technology, Pasadena, CA.

Abdel-Ghaffar, A.M. & Scott, R.F. 1981. Vibration tests of full-scale earth dam. *Journal of the Geotechnical Engineering Division,* March 107(3): 241–269.

Abdoun, T., Bennett, V., Danisch, L., Shantz, T. & Jang, D. 2007a. Field installation details of a wireless shape-acceleration array system for geotechnical applications. *Proceedings of SPIE*, San Diego, CA, March 19–22, Volume 6529.

Abdoun, T., Abe, A., Bennett, V., Danisch, L., Sato, M., Tokimatsu, K. & Ubilla, J. 2007b. Wireless real time monitoring of soil and soil-structure systems. *Proceedings of Sessions of Geo-Denver 2007, Embankments, Dams, and Slopes*, ASCE GSP 161, Colorado, USA.

Abdoun, T., Bennett, V., Danisch, L. & Barendse, M. 2008a. Real-time construction monitoring with a wireless shape-acceleration array system. *Proc. of GeoCongress 2008: Characterization, Monitoring, and Modeling of GeoSystems*, ASCE GSP 179, New Orleans, LA, March 9–12, pp. 533–540.

Abdoun, T., Bennett, V. Dobry, R., Thevanayagam, S. & Danisch, L. 2008b. Full-scale laboratory tests using a shape-acceleration array system. *Proceedings of the Geotechnical Earthquake Engineering and Soil Dynamics IV Congress*, Geotechnical Earthquake Engineering and Soil Dynamics (GSP 181), ASCE.

Abdoun, T.H., Ha, D., & O'Rourke, M.J. 2008c. Behavior of moderately buried HDPE pipelines subject strike-slip faulting. *The 12th International Conference of International Association for Computer Methods and Advances in Geomechanics (IACMAG),* 1–6 October, 2008, Goa, India.

Abdoun, T.H., Ha, D., O'Rourke, M.J., Symans, M.D., O'Rourke, T.D., Palmer, M.C. & Stewart, H.E. 2009. Factors influencing the behavior of buried pipelines subjected to earthquake faulting. *Soil Dynamics and Earthquake Engineering* 29(3): 415–427.

Agarwal, P., Black, J.S., Wood, S.L., Kurtulus, A., Menq, F.Y., Rathje, E.M. & Stokoe, II, K.H. 2006. Dynamic field tests of small-scale bridge bents supported on drilled shaft. *8th U.S. National Conference on Earthquake Engineering,* April 18–21, 10 pp.

Ahlberg, E., Stewart, J.P., Wallace, J.W., Rha, C. & Taciroglu, E. 2005. Response of a reinforced concrete embedded pile under lateral loading. I: Field-testing. *2005 Caltrans Bridge Research Conference,* October 1, 2005, Sacramento CA, Paper 01–505.

Algie, T.B., Deng, L., Erduran, E., Kutter, B.L. & Kunnath, S. 2008. Centrifuge Modeling of Innovative Foundation Systems to optimize seismic behavior of bridge structures. *14th World Conference on Earthquake Engineering,* Beijing, China.

Ashford, S.A., Rollins, K.M. & Baez, J.I. 2000a. Comparison of deep foundation performance in improved and non-improved ground using blast-induced liquefaction. *Soil Dynamics and Liquefaction 2000*, ASCE GSP 107, Proceedings of Sessions of Geo-Denver.

Ashford, S.A., Rollins, K.M., Bradford, V.S.C., Weaver, T.J. & Baez, J.I. 2000b. Liquefaction mitigation using stone columns around deep foundations: full-scale test results. *Transportation Research Record: Journal of the Transportation Research Board* 1736: 110–118.

Ashford S.A. & Juirnarongrit, T. 2003. Evaluation of pile diameter effect on initial modulus of subgrade reaction. *Journal of Geotechnical and Geoenvironmental Engineering* 129(3): 234–242.

Ashford, S.A., Rollins, K.M. & Lane, J.D. 2004. Blast-Induced Liquefaction for Full-Scale Foundation Testing. *J. Geotech. and Geoenvir. Engrg.* (130)8: 798–806.

Ashford, S., Juirnarongrit, T., Sugano, T. & Hamada, M. 2006. Soil–pile response to blast induced lateral spreading. I: field test. *Journal of Geotechnical and Geoenvironmental Engineering* 132(2): 152–162.

Bakhtar, K. 1997. Impact of joints and discontinuities on the blast-response of responding tunnels studied under physical modeling at 1-g. *International Journal of Rock Mechanics and Mining Sciences* 34(3–4), April-June, Paper No. 021.

Bao, X., DeMerchant, M., Brown, A. & Bremner, T. 2001. Tensile and compressive strain measurement in the lab and field with the distributed brillouin scattering sensor. *Journal of Lightwave Technology* 19(11).

Bennett, V., Zeghal, M., Abdoun, T. & Danisch, L. 2007. A wireless shape-acceleration array system for local identification of soil and soil-structure systems. *Transportation Research Record: Journal of the Transportation Research Board, Soil Mechanics*, 2004: 60–66.

Bennett, V., Abdoun, T., Shantz, T., Jang, D. & Thevanayagam, S. 2009. Design and characterization of a compact array of MEMS accelerometers for geotechnical instrumentation. *J. Smart Structures and Systems* 5(6), November.

Bhattacharya, S., Madabhushi, S.P.G. & Bolton, M.D. 2004. An alternative mechanism of pile failure in liquefiable deposits during earthquakes. *Géotechnique* 54(3): 203–213.

Bhattacharya, S., Bolton, M.D. & Madabhushi, S.P.G. 2005. A reconsideration of the safety of the existing piled bridge foundations in liquefiable soils. *Soils and Foundations*, August 45(4).

Boulanger, R.W. & Tokimatsu, K. 2006. Seismic performance and simulation of pile foundations in liquefied and laterally spreading ground. *Geotechnical Special Publication No. 145*. ASCE, Reston, Va.

Boulanger, R.W., Chang, D., Brandenberg, S.J., Armstrong, R.J. & Kutter, B.L. 2007. Seismic design of pile foundations for liquefaction effects. K.D. Pitilakis (ed.), *Earthquake Geotechnical Engineering*, Chapter 12, 277–302. Springer.

Brandenberg, S.J. 2005. Behavior of pile foundations in laterally spreading ground. Ph.D. dissertation, Univ. of California at Davis, Davis, California.

Brandenberg, S.J., Boulanger, R.W., Kutter, B.L. & Chang, D. 2005. Behavior of pile foundations in laterally spreading ground during centrifuge tests. *J. Geotech. Geoenviron. Eng.* 131(11): 1378–1391.

Brandenberg, S.J., Boulanger, R.W., Kutter, B.L. & Chang, D. 2007a. Liquefaction-induced softening of load transfer between pile groups and laterally spreading crusts. *J. Geotech. and Geoenvir. Engrg.*, ASCE, January 133(1): 91–103.

Brandenberg, S.J., Boulanger, R.W., Kutter, B.L. & Chang, D. 2007b. Static pushover analyses of pile groups in liquefied and laterally spreading ground in centrifuge tests. *J. Geotech. and Geoenvir. Engrg.*, ASCE, September 133(9): 1055–1066.

Byrne, P.M., Robertson, P.K., Plewes, H.D., List, B. & Tan, S. 1995. Liquefaction event planning. *Proceedings 48th Canadian Geotechnical Conference*, Vancouver, B.C., 25–27 Sept. 1: 341–352.

Chang, D., Boulanger, R.W., Kutter, B.L. & Brandenberg, S.J. 2005. Experimental observations of inertial and lateral spread loads on pile groups during earthquakes. *Earthquake Engineering and Soil Dynamics, Proc. GeoFrontiers 2005 Congress*, ASCE GSP 133.

Chang, B.J, Raychowdhury, P., Hutchinson, T., Thomas, J., Gajan, S. & Kutter, B.L. 2006. Centrifuge testing of combined frame-wall-foundation structural systems. *Proc. 8th US National Conference on Earthquake Engineering*, April 18–22, San Francisco, CA, paper No. 998.

Chang, W.-J., Rathje, E.M., Stokoe, K.H. & Hazirbaba, K. 2007. In situ pore pressure generation behavior of liquefiable sand. *Journal of Geotechnical and Geoenvironmental Engineering*, ASCE 133(8): 921–931.

Charlie, W.A., Allard, D.J. & Doehring, D.O. 2009. Pile Settlement and Uplift in Liquefying Sand Deposit, *Geotechnical Testing Journal*, March, 32(2).

Chávez-García, F.J., Raptakis, D., Makra, K. & Pitilakis, K. 2000. Site effects at Euroseistest II. Results from 2D numerical modeling and comparison with observations, *Soil Dyn. Earthq. Engrg.* 19: 23–39.

Chazelas, J.L., Escoffier, S., Garnier, J., Thorel, L. & Rault, G. 2008. Original technologies for proven performances for the new LCPC earthquake simulator, *Bull Earthquake Eng* 6:723–728.

Choo, Y.W., Abdoun, T.H., O'Rourke, M.J. & Da, H. 2007. Remediation for buried pipeline systems under permanent ground deformation. *Soil Dynamics and Earthquake Engineering,* December, 27(12): 1043–1055.

Coelho P.A.L.F., Haigh, S.K. & Madabushi G. 2006. Effects of successive earthquakes on saturated deposit of sand. 6th ICPMG'06, Ng et al; (Ed.), Hong-Kong, 4–6 August, Taylor & Francis, Vol. 1, 443–448.

Cole, R. & Rollins, K. 2006. Passive earth pressure mobilization during cyclic loading. *Journal of Geotechnical and Geoenvironmental Engineering*, 132(9):1154–1164.

Cox, B.R., Stokoe, K.H. & Rathje, E.M. 2009. An Active, strain-based, in-situ test method for evaluating the coupled pore pressure generation and nonlinear shear modulus behavior of liquefiable soils. *ASTM Geotechnical Testing Journal* 32(1): 11–21.

Cubrinovski, M., Kokusho, T. & Ishihara, K. 2006. Interpretation from large-scale shake table tests on piles undergoing lateral spreading in liquefied soils. *Soil Dynamics and Earthquake Engineering* 26: 275–286.

Cummins, C.R. 2009. Behavior of a Full-Scale Pile Cap with Loosely and Densely Compacted Clean Sand Backfill Under Cyclic and Dynamic Loading, MS thesis, Department of Civil and Environmental Engineering, Brigham Young University, April.

Davis, L.K. 2003. Blast effects on dams: An historical perspective. *Proc. 73rd Shock and Vibration Symposium*, October, San Diego, CA.

Davis, L.K. 2008. Civil Works Infrastructure Security and Protection R&D Program. *Report 2: Development of an embankment cratering model for atplanner/dams*, Geotechnical and structures laboratory, U.S. army engineer research and development center, 3909 Halls Ferry Road, Vicksburg, MS, ERDC/GSL TR-09-X, December.

De, A., Zimmie, T.F. & Vamos, K.E. 2005. Centrifuge experiments to study blast effects on underground pipelines. *Pipelines 2005, Proc. of the Pipeline Div. Specialty Conf.,* Vipulanandan, C. and Ortega, R. (eds.), Aug., Houston, TX, ASCE, 362–370.

De, A. & Zimmie, T.F. 2006. Modeling of surface blast effects on underground structures. *GeoCongress 2006: Geotechnical engineering in the information technology age,* ASCE, Atlanta, Georgia.

De, A. & Zimmie, T.F. 2007. Centrifuge modeling of surface blast effects on underground structures. *Geotechnical Testing Journal*, American Society of Testing and Materials (ASTM) 30(5): 427–431.

Doerr, K., Hutchinson, T., & Kuester, F. 2005. Methodology for image-based tracking of seismic-induced

motions, *Proc. SPIE—Smart Structures/NDE* 321–332.

Doerr, K.-U., Kuester, F., Nastase, D. & Hutchinson, T.C. 2008. Development and evaluation of a seismic monitoring system for building interiors—Part II: Image data analysis and results. *IEEE Transactions on Instrumentation and Measurement* 57(2): 345–354.

Duncan, M. & Mokwa, R. 2001. Passive earth pressures: theories and tests. *Journal of Geotechnical and Geoenvironmental Engineering* 127(3): 248–257.

Elgamal, A., Pitilakis, K., Dimitrios, R., Garnier, J., Madabhushi, SP G, Pinto, A., Steidl, J., Stewart, H.E., Stokoe, K.H., Taucer, F., Tokimatsu, K. & Wallace, J.W. 2007. A review of large-scale testing facilities in geotechnical earthquake engineering, Chapter 5, *Earthquake geotechnical engineering, 4th international conference on earthquake geotechnical engineering*-invited lectures, Pitilakis, K.D., ed., June, Thessaloniki, Greece, Springer, Berlin.

Elgamal, A., Van Den Einde, L., Baru, C., Fowler, K. & Rowley, J. 2009a. The NEES web-accessible database for earthquake engineering research. *Proceedings of the International Symposium on Geo-informatics and Zoning for Hazard Mapping (GIZ2009)*, Kyoto, Japan, Dec. 3–4, 27–34.

Elgamal, A., Baru, C., Van Den Einde, L., Krishnan, S., Fowler, K. & Tadepalli, T.P. 2009b. NEESit: An IT framework for collaboration in earthquake engineering research. B.H.V. Topping, L.F. Costa Neves, R.C. Barros, (eds), *Trends in Civil and Structural Engineering Computing, The Twelfth International Conference on Civil, Structural and Environmental Engineering Computing,* Chapter 11, 225–241. Saxe-Coburg Publications, Stirlingshire, UK.

Escoffier, S., Chazelas, J.-L. & Garnier, J. 2008. Centrifuge modelling of raked piles. *Bull Earthquake Eng*, 6:689–704.

Euroseistest Volvi—Thessaloniki: a European test site for engineering, Seismology, Earthquake Engineering and Seismology. Commission of the European Communities, Project EV5V-CT93-0281 (DIR 12 SOLS), 1993–1995.

Euroseismod Volvi-Thessaloniki: development and experimental validation of advanced modeling techniques in engineering seismology, Earthquake Engineering. Commission of the European Communities, 1996–1998.

EUROSEISRISKSeismic Hazard assessment, site effects and soil structure interaction studies in an instrumented basin (EVG1-CT-2001-00040), 2002–2005.

Gajan, S., Kutter, B.L., Phalen, J.D., Hutchinson, T.C. & Martin, G.R. 2005. Centrifuge modeling of load-deformation behavior of rocking shallow foundations. *Soil Dynamics and Earthquake Engineering* 25(7–10): 773–783.

Gajan, S. 2006. Physical and numerical modeling of nonlinear cyclic load-deformation behavior of shallow foundations supporting rocking shear walls. Ph.D. Dissertation, Dept. of Civil and Environmental Engineering, Univ. of California, Davis, California.

Gajan, S. & Kutter, B.L. 2008. Capacity, settlement, and energy dissipation of shallow footings subjected to rocking. *J. Geotech. Geoenviron. Eng.*, ASCE 134(8): 1129–1141.

Gajan, S. & Kutter, B.L. 2009a. Contact interface model for shallow foundations subjected to combined cyclic loading. *J. Geotech. and Geoenvir. Engineering* 135(3): 407–419.

Gajan, S. & and Kutter, B.L. 2009b. Effects of moment-to-shear ratio on combined cyclic load-displacement behavior of shallow foundations from centrifuge experiments. *J. Geotech. and Geoenvir. Engrg.*, ASCE 135: 1044–1055.

Garnier, J., Chambon, P., Ranaivoson, D., Charrier, J. & Mathurin, R. 1998. Computer image processing for displacement measurement. In: Kimura, Kusakabe and Takemura, eds, *Centrifuge 98*, 543–550. Rotterdam: Balkema.

Gonzalez, L. 2005. Centrifuge modeling of permeability and pinning reinforcement effects on pile response to lateral spreading. Ph.D. dissertation, Rensselaer Polytechnic Institute, Troy, N.Y.

González, L., Abdoun, T. & Dobry, R. 2006. Effect of soil permeability on centrifuge modeling of pile response to lateral spreading. *Seismic Performance and Simulation of Pile Foundations*, ASCE GSP 145, Boulanger, R.W. and Tokimatsu, K. (eds), March 16–18, Davis, California, USA.

González, M., Ubilla, J., Abdoun, T. & Dobry, R. 2008. The role of soil compressibility in centrifuge model tests of piles foundation undergoing lateral spreading of liquefied soil. *Proceedings of the Geotechnical Earthquake Engineering and Soil Dynamics IV Congress*, ASCE.

Guéguen, P. & Bard, P.-Y. 2005. Soil-structure and soil-structure-soil interaction: Experimental evidence at the Volvi test site. *J Earthquake Engineering* 9(4): 1–36.

Ha, D., Abdoun, T,H., O'Rourke, M.J., Symans, M.D., O'Rourke, T.D., Palmer, M.C. & Stewart, H.E. 2008a. Buried high-density polyethylene pipelines subjected to normal and strike-slip faulting—a centrifuge investigation. *Canadian Geotechnical J.* 45(12): 1733–1742.

Ha, D., Abdoun, T.H., O'Rourke, M.J., Symans, M.D., O'Rourke, T.D., Palmer, M.C. & Stewart, H.E. 2008b. Centrifuge modeling of earthquake effects on buried high-density polyethylene (HDPE) pipelines crossing fault zones, *Journal of Geotechnical and Geoenvironmental Engineering* 134(10): 1501–1515.

He, L. 2005. Liquefaction-induced lateral spreading and its effects on pile foundations, Ph.D. Dissertation, Department of Structural Engineering, University of California, San Diego, La Jolla, California.

He, L., Elgamal, A., Abdoun, T., Abe, A., Dobry, R., Meneses, J., Sato, M. & Tokimatsu, K. 2006. Lateral load on piles due to liquefaction-induced lateral spreading during one-g shake table experiments. *Proceedings, 100th anniversary earthquake conference commemorating the 1906 San Francisco earthquake*, San Francisco, CA, April 18–22.

He, L., Elgamal, A., Hamada, M. & Meneses, J. 2008. Shadowing and group effects for piles during earthquake-induced lateral spreading. *Proc. 14th World Conference on Earthquake Engineering,* October 12–17, Beijing, China.

He, L., Elgamal, A., Abdoun, T., Abe, A., Dobry, R., Hamada, M., Meneses, J., Sato, M., Shantz, T. & Tokimatsu, K. 2009. Liquefaction-induced lateral

load on pile in a medium Dr sand layer, *Journal of Earthquake Engineering* 13(7): 916–938.

Ho, Y.T., Huang, A.B. & Lee, J.T. 2006. Development of a fiber Bragg grating sensored ground movement monitoring system. *Journal of Measurement Science and Technology*, Institute of Physics Publishing 16): 1733–1740.

Ho, Y.T., Huang, A.B. & Lee, J.T. 2008. Development of a chirped/differential optical fiber Bragg grating pressure sensor. *Journal of Measurement Science and Technology*, Institute of Physics Publishing, Vol. 19, 6pp.

Huang, A.B. & Hsu, H.H. 2004. Advanced calibration chambers for cone penetration testing in cohesionless soils. *Proceedings, ISC-2 on Geotechnical and Geophysical Site Characterization*, Keynote Lecture, Porto, Portugal 1: 147–167.

Huang, A.B., & Hsu, H.H. 2005. Cone penetration tests under simulated field conditions. *Géotechnique* LV(5): 345–354.

Huang, A.B. 2009. Lessons learned from sampling and CPT in silt/sand soils. *Proceedings, IS-Tokyo, Performance-Based Design in Earthquake Geotechnical Engineering*, Tokyo, Japan, eds. Kokusho, Tsukamoto & Yoshimine, CRC Press., 209–220.

Huang, A.B., Lee, J.T., Ho, Y.T., Chiu, Y.F. & Tsai, T.L. 2009a. Field monitoring of pore-water pressure profile in a slope subjected to heavy rainfalls. *Proceedings XVII International Conference on Soil Mechanics and Geotechnical Engineering*, Alexandria, Egypt, 1931–1934.

Huang, A.B., Tai, Y.Y., Lee, W.F. & Huang, Y.T. 2009b. Field evaluation of the cyclic strength versus cone tip resistance correlation in silty sands. *Soils and Foundations* 49(4): 557–568.

Hutchinson, T.C., Kuester, F., Doerr, K.-U. & Lim, D.H. 2006. Optimal hardware and software design of an image-based system for capturing dynamic movements. *IEEE Transactions on Instrumentation and Measurement* 55(1): 164–175.

Ishihara, K. & Harada, K. 2008. Effects of lateral stress on relations between penetration resistances and cyclic strength to liquefaction, *The 3rd International Conference on Site Characterization*, Taipei, 1043–1050.

Jennings, P.C. & Kuroiwa, J.H. 1968. Vibration and soil-structure interaction tests of a nine-storey reinforced concrete building. *Bull. Seism. Soc. Am.* 58: 891–916.

Juirnarongrit, T. & Ashford, S. 2006. Soil-pile response to blast-induced lateral spreading. II: analysis and assessment of the p–y Method. *Journal of Geotechnical and Geoenvironmental Engineering* 132(2): 163–172.

Jung, S., Choo, Y. & Kim, D. 2007. Monitoring ground vibration and displacement using SAA sensor. *The twentieth KKCNN symposium on civil engineering,* October 4–5, Jeju, Korea.

Kagawa, T., Sato, M., Minowa, C., Abe, A. & Tazoh, T. 2004. Centrifuge simulations of large-scale shaking table tests: Case studies. *J. Geotech. and Geoenviron. Eng* 130(7): 663–672.

Kamijo, N., Saito, H., Kusama, K., Kontani, O. & Nigbor, R. 2004. Seismic tests of a pile-supported structure in liquefiable sand using large-scale blast excitation. *Nuclear Engineering and Design* 228(1–3): 367–376.

Keightley, W.O. 1964. A dynamic investigation of Bouquet Canyon Dam. *Report, Earthquake Eng. Res. Lab.*, California Institute of Technology, Pasadena, CA.

Keightley, W.O. 1966. Vibrational characteristics of an earth dam. *Bulletin of the Seismological Society of America* 56(6): 1207–1226.

Khalili-Tehrani, P., Ahlberg, E., Rha, C., Lemnitzer, A., Salamanca, A., Nigbor, R., Stewart, J., Wallace, J. & Taciroglu, E. 2007. Field-testing and modeling of soil-structure interaction for highway support structures. *Structural Engineering Research Frontiers, Proceedings of Sessions of the 2007 Structures Congress,* ASCE.

Kim, D.S., Cho, G.C. & Kim, N.R. 2006. Development of KOCED geotechnical centrifuge facility at KAIST. *Physical Modelling in Geotechnics—6th ICPMG '06,* Ng, Zhang & Wang (eds), Taylor & Francis Group, London, 147–150.

Kulasingam, R., Malvick, E.J., Boulanger, R.W. & Kutter, B.L. 2004. Strength loss and localization at silt interlayers in slopes of liquefied sand. *J. Geotech. Geoenviron. Eng.* 130(11): 1192–1202.

Kimura T. 2000. Development of geotechnical centrifuges in Japan. *Centrifuge 98*, Tokyo, Kimura et al. (ed.), 2: 945–954. Balkema.

Kurtulus, A. & Stokoe, K.H., II, 2006. Field Evaluation of the nonlinear shear modulus of soil. *8th U.S. National Conference on Earthquake Engineering*, San Francisco, CA, April.

Kurtulus, A. & Stokoe, II, K.H. 2007. Field method for measuring nonlinear soil behaviour at depth using a dynamically loaded drill shaft. *Geotechnical Testing Journal* 26(4).

Kutter, B.L., Wilson, D.W. & Bardet, J.P. 2002. Metadata structure for geotechnical physical model tests. *Proc. Int. Conf. On Physical Modelling in Geotechnics,* St. Johns, Canada, Phillips, Guo, Popescu (eds), 137–142. Lisse, Netherlands: Balkema.

Kutter, B.L., Gajan, S., Manda, K.K. & Balakrishnan, A. 2004. Effects of layer thickness and density on settlement and lateral spreading. *J. Geotech. Geoenviron. Eng.*, 130(6): 603–614.

Kutter, B.L. & Wilson, D.W. 2006. Physical modelling of dynamic behavior of soil-foundation-superstructure systems. *International Journal of Physical Modeling in Geotechnics*. 1: 1–12.

Lemnitzer, A., Ahlberg, E..I, Khalili-Tehrani, P., Rha, C., Taciroglus, E., Stewart, J.P., Wallace, J.W. 2008. Experimental testing of a full-scale pile group under lateral loading. *14th World Conference on Earthquake Engineering*, Beijing, China.

Lemnitzer, A., Ahlberg, E., Nigbor, R., Shamsabadi, A., Wallace, J. & Stewart, J. 2009. Lateral performance of full-scale bridge abutment backwall with granular backfill. *Journal of Geotechnical and Geoenvironmental Engineering,* ASCE 506–514.

Lerch, D.W., Klemperer, S.L., Stokoe, K.H., II, & Menq, F.-Y. 2008. Integration of the NEES T-Rex vibrator and PASSCAL texan recorders for seismic profiling of shallow and deep crustal targets. *Seismological Research Letters* 79(1): 791–809.

Luco, J.E., Conte, J.P., Moaveni, B., Mendoza, L. & Whang, D. 2004. Forced vibration tests of the foundation block and surrounding soil at the NEES/UCSD large high-performance shake table. *Proc. of 3rd UJNR Workshop on Soil-Structure Interaction*, Menlo Park, California, USA.

Ma, J., Zhang B., Cao J. & Huang, A.B. 2007. Safety monitoring of the yellow river dike: a feasibility study on various instrumentation schemes. *Proceedings, 7th International Symposium on Field Measurement in Geomechanics*, Boston, MA, USA.

Madabhushi, S.P.G., Schofield, A.N. & Lesley, S. 1998. A new Stored Angular Momentum (SAM) based earthquake actuator. *Centrifuge 98*, Kimura et al. (eds), 111–116, Balkema.

Madabhushi, S.P.G., Ghosh, B. & Kutter, B.L. 2006. Role of input motion in excess pore pressure generation in dynamic centrifuge modeling. *International Journal of Physical Modelling in Geotechnics*, Japan.

Malvick, E.J., Kutter, B.L., Boulanger, R.W. & Kulasingam, R. 2006. Shear localization due to liquefaction-induced void redistribution in a layered infinite slope. *J. Geotech. Geoenviron. Eng.* 132(10): 1293–1303.

Malvick, E.J., Kutter, B.L. & Boulanger, R.W. 2008. Post-shaking shear strain localization in a centrifuge model of a saturated sand slope. *J. Geotech. and Geoenvir. Engrg.* (2): 164–174.

Makra, K., Chávez-García, F.J., Raptakis, D. & Pitilakis, K. 2005. Parametric analysis of the seismic response of a 2D sedimentary valley: Implications for code implementations of complex site effects. *Soil Dyn. Earthq. Engrg.* 25: 303–315.

Meneses, J., Hamada, M. & Elgamal, A. 2002. Shake Table Testing of Liquefaction and Effect on Concrete Pile. *Proc. 4th US-China-Japan Symposium on Lifeline Earthquake Engineering, Qingdao*, China, October.

Menq, F-Y, Stokoe, K.H., II, Park, K., Rosenblad, B. & Cox, B.R., 2008. Performance of mobile hydraulic shakers at nees@UTexas for earthquake studies, *14th World Conference of Earthquake Engineering,* October 12–17, Beijing, China.

Miyamoto, Y., Hijikata, K. & Tanaka, H. 2004. Seismic design of a structure supported on pile foundation considering dynamic soil-structure interaction. *Proceedings Third UJNR Workshop on Soil-Structure Interaction,* March 29–30, *2004, Menlo Park, California, USA*.

Mita, A. & Yokoi, I. 2000. Fiber bragg grating accelerometer for structural health monitoring. *Proceedings, Fifth International Conference on Motion and Vibration Control (MOVIC 2000)*, 4–8 Dec., Sydney, Australia.

Mohamad, H., Bennett, P.J., Soga, K., Klar, A. & Pellow, A. 2007. Distributed optical fiber strain sensing in a secant piled wall. *Proceedings, 7th International Symposium on Field Measurements in Geomechanics*, Boston, MA, USA.

Nastase, D., Chaudhuri, S.R., Chadwick, R., Hutchinson, T.C., Doerr, K.-U. & Kuester, F. 2008. Development and evaluation of a seismic monitoring system for building interiors—Part I: Experiment design and results. *IEEE Transactions on Instrumentation and Measurement* 57(2): 332–344.

Ng, C.W.W. & Kutter, B.L., eds. 2001. Proceedings, International symposium on geotechnical centrifuge modelling and networking—focusing on the use and application in the Pan-Pacific region. *Hong Kong University of Science and Technology, and University of California, Davis*, December 8–9, Center for Geotechnical Modeling, UCD/CGMPRC-01/01 and Hong Kong University of Science and Technology, Clear Water Bay, Kowloon, Hong Kong.

Ng, C.W.W., Van Laak, P.A., Tang, W.H., Li, X.S. & Shen, C.K. 2001a. The Hong Kong Geotechnical centrifuge and its unique capabilities. *Sino-Geotechnics*, Taiwan, (83): 5–12.

Ng, C.W.W., Zhang, L. & Nip, D.C.N. 2001b. Response of laterally loaded large-diameter bored pile groups. *Journal of Geotechnical and Geoenvironmental Engineering,* 127(8): 658–669.

Ng, C.W.W., Van Laak, P.A., Zhang, L.M., & Tang, W.H. 2002. Development of a four-axis robotic manipulator for centrifuge modeling at HKUST, in: Phillips, Guo, Popescu (eds.), *Physical Modelling in Geotechnics*, 71–76. Lisse: Balkema.

Nigbor, R.L., Steidl, J.H. & Youd, T.L. 2004. Permanently instrumented field sites in NEES: a resource for future geotechnical research. *Geotechnical Engineering for Transportation Projects (GSP 126), Proceedings of GeoTrans,* ASCE.

Okamura, M. & Teraoka, T. 2005. Shaking table tests to investigate soil desaturation as a liquefaction countermeasure. *Seismic Performance and Simulation of Pile Foundations in Liquefied and Laterally Spreading Ground, GSP 145*, ASCE, 282–293.

Okamura, M. & Soga, Y. 2006. Effects of pore fluid compressibility on liquefaction resistance of partially saturated sand. *Soils and Foundations* 46(5): 695–700.

Okamura, M., Ishihara, M. & Tamura, K. 2006. Degree of saturation and liquefaction resistances of sand improved with sand compaction pile. *Journal of Geotechnical and Geoenvironmental Engineering* 132(2): 258–264.

Okamura, M. & Noguchi, K. 2009. Liquefaction resistances of unsaturated non-plastic silt. *Soils and Foundations* (49)2: 221–229.

Okamura, M., Takebayashi, M., Nishida, K., Fujii, N., Jinguji, M., Imasato, T., Yasuhara, H. & Nakagawa, M. 2009. In-situ test on desaturation by air injection and its monitoring. *Proc. Int. Symp. Ground Improvement Technologies and Case Histories*, 151–158, Singapore.

Okamura, M. & Inoue, T. 2010. Preparation of fully saturated model ground. *Proc. ICPMG 2010, 7th International Conference on Physical Modelling in Geotechnics*, Zurich, Switzerland (to appear).

O'Rourke, T.D., Jezerski, J.M., Olson, N.A., Bonneau, A.L., Palmer, M.C., Stewart, H.E., O'Rourke, M.J. & Abdoun, T., 2008. Geotechnics of pipeline system response to earthquakes. *Proceedings Geotechnical Earthquake Engineering and Soil Dynamics IV*, ASCE, Sacramento, CA, May.

Ozcelik, O. 2008. A mechanics-based virtual model of NEES-UCSD shake table: theoretical development and experimental validation, Ph.D. Thesis, University of California, San Diego, Department of Structural Engineering, La Jolla, CA, 496 pages.

Paikowsky, S.G. & Hajduk, E.L. 1997. Calibration and use of grid-based tactile pressure sensors in granular material. *Geotech. Test. J.,* 20(2): 218–241.

Paikowsky, S.G., Palmer, C.J. & Dimillio, A.F. 2000. Visual observation and measurement of aerial stress distribution under a rigid strip footing. ASCE GSP 94, 148–169.

Paikowsky, S.G., Rowles, L.E. & Tien, H.S. 2003. Visualization measurements of stress around a trap door. *Proc., 12th Pan American Conf. and 39th Rock*

Mechanics Symp., 1171–1177. Cambridge, Mass.: VGE Publications.

Paikowsky, S.G., Palmer, C.J. & Rowles, L.E. 2006. The use of tactile sensor technology for measuring soil stress distribution. *Proc. GeoCongress 2006–Geotechnical Engineering in the Information Technology Age*, ASCE, Atlanta.

Palmer, M.C., O'Rourke, T.D., Stewart, H.E., O'Rourke, M.J. & Symans, M. 2006. Large displacement soil-structure interaction test facility for lifelines. *Proc. 8th US National Conf. on Earthquake Engineering and 100th Anniversary Earthquake Conf. Commemorating the 1906 San Francisco Earthquake*, EERI, San Francisco.

Palmer, M.C., O'Rourke, T.D., Olson, N.A., Abdoun, T., Ha, D. & O'Rourke, M.J. 2009. Tactile pressure sensors for soil-structure interaction assessment. *Journal of Geotechnical and Geoenvironmental Engineering* 135(11): 1638–1645.

Paolucci, R., Shirato, M. & Yilmaz, M.T. 2007. Seismic behavior of shallow foundations: shaking table experiments vs numerical modeling. *Earthquake Eng. Struct. Dyn.* 37(4): 577–595.

Peng, J. & Law, K. 2004. Reference NEESgrid data model. *Technical Report NEESgrid-2004–40*, Network for Earthquake Engineering Simulation (NEES), https://www.nees.org/images/doc_library/TR-2004–40.pdf.

Pitilakis, K., Raptakis, D., Lontzetidis, K., Tika-Vassilikou, T.H. & Jongmans, D. 1999. Geotechnical and geophysical description of EURO-SEISTEST, using field, laboratory tests and moderate strong motion recordings. *J. Earthq. Engrg.* 3: 381–409.

Puebla, H., Byrne, P.M. & Phillips, R. 1997. Analysis of CANLEX liquefaction embankments: prototype and centrifuge models. *Can. Geotech. J.* 34: 641–657.

Rao, Y.-J. 1998. Fiber Bragg grating sensors: principles and applications. *Optic Fiber Sensor Technology*, K.T.V. Gattan and B.T. Meggitt, eds., 2: 355–379. London: Chapman and Hall.

Raptakis, D., Theodulidis, N. & Pitilakis, K. 1998. Data analysis of the EURO-SEISTEST strong motion array in Volvi (Greece): Standard and horizontal to vertical spectral ratio techniques. *Earthq. Spectra* 14: 203–224.

Raptakis, D., Chávez-García, F.J., Makra, K. & Pitilakis, K. 2000. Site effects at Euroseistest I. Determination of the valley structure and confrontation of observations with 1D analysis. *Soil Dyn. Earthq. Engrg.* 19: 1–22.

Raptakis, D., Manakou, M., Chávez-García, F.J., Makra, K. & Pitilakis, K. 2005. 3D Configuration of Mygdonian basin and preliminary estimate of its site response. *Soil Dyn. Earthq. Engng.* 25: 871–887.

Rathje, E.M., Chang, W.-J., Stokoe, K. & Cox, B. 2004. Evaluation of ground strain from in situ dynamic testing. *13th World Conference on Earthquake Engineering*, CD-ROM Paper No. 3099, August, Vancouver, Canada.

Rathje, E.M., Chang, W.-J. & Stokoe II, K.H. 2005. Development of an In Situ Dynamic Liquefaction Test. *ASTM Geotechnical Testing Journal*, 28(1): 50–60.

Restrepo, J.I., Conte, J.P., Luco, J.E., Seible, F. & Van Den Einde, L. 2005. The NEES@UCSD large high performance outdoor shake table. *Earthquake engineering and soil dynamics (GSP 133), Proc. Geo-Frontiers 2005*, ASCE, Austin, TX.

Rix, G., Boulanger, R., Conlee, C., Gallagher, P., Kamai, R., Kano, S., Marinucci, A. & Rathje, E. 2007. Large-Scale Geotechnical Simulations to Advance Seismic Risk Management for Ports,. *4th International Conference on Earthquake Geotechnical Engineering*, Thessaloniki, Greece, June (CD-ROM).

Robertson, P.K., Wride (Fear), C.E., List, B.R., Atukorala, U., Biggar, K.W., Byrne, P.M., Campanella, R.G., Cathro, D.C., Chan, D.H., Czajewski, K., Finn, W.D.L., Gu, W.H., Hammamji, Y., Hofmann, B.A., Howie, J.A., Hughes, J., Imrie, A.S., Konrad, J.-M., Küpper, A., Law, T., Lord, E.R.F., Monahan, P.A., Morgenstern, N.R., Phillips, R., Piché, R., Plewes, H.D., Scott, D., Sego, D.C., Sobkowicz, J., Stewart, R.A., Watts, B.D., Woeller, D.J., Youd, T.L. & Zavodni, Z. 2000a. The canadian liquefaction experiment: an overview. *Canadian Geotechnical Journal* 37: 499–504.

Robertson, P.K., Wride (Fear), C.E., List, B.R., Atukorala, U., Biggar, K.W., Byrne, P.M., Campanella, R.G., Cathro, D.C., Chan, D.H., Czajewski, K., Finn, W.D.L., Gu, W.H., Hammamji, Y., Hofmann, B.A., Howie, J.A., Hughes, J., Imrie, A.S., Konrad, J.-M., Küpper, A., Law, T., Lord, E.R.F., Monahan, P.A., Morgenstern, N.R., Phillips, R., Piché, R., Plewes, H.D., Scott, D., Sego, D.C., Sobkowicz, J., Stewart, R.A., Watts, B.D., Woeller, D.J., Youd, T.L. & Zavodni, Z. 2000b. The CANLEX project: summary and conclusions. *Canadian Geotechnical Journal* 37: 563–591.

Rollins, K.M., Lane, J.D., Dibb, E., Ashford, S.A. & Mullins, A.G. 2005a. Pore pressure measurement in blast-induced liquefaction experiments. *Journal Transportation Research Record: Journal of the Transportation Research Board* 1936: 210–220.

Rollins, K.M., Gerber, T.M., Lane, J.D. & Ashford, S.A. 2005b. Lateral resistance of a full-scale pile group in liquefied sand. *J. Geotech. and Geoenvir. Engrg.* 131(1): 115–125.

Rollins, K.M., Lane, J.D. & Gerber, T.M. 2005c. Measured and computed lateral response of a pile group in sand. *Journal of Geotechnical and Geoenvironmental Engineering* 131(1): 103–114.

Rollins, K. & Cole, R. 2006. Cyclic lateral load behavior of a pile cap and backfill. *Journal of Geotechnical and Geoenvironmental Engineering*, 132(9): 1143–1153.

Rollins, K.M., Olsen, R.J., Egbert, J.J., Jensen, D.H., Olsen, K.G. & Garrett, B.H. 2006a. Pile spacing effects on lateral pile group behavior: load tests, *Journal of Geotechnical and Geoenvironmental Engineering* 132(10): 1262–1271.

Rollins, K.M., Olsen, K.G., Jensen, D.H., Garrett, B.H., Olsen, R.J. & Egbert, J.J. 2006b. Pile spacing effects on lateral pile group behavior: analysis. *Journal of Geotechnical and Geoenvironmental Engineering* 132(10): 1272–1283.

Rosenblad, B.L., Li, J., Menq, F.Y. & Stokoe, II, K.H. 2007. Deep shear wave velocity profiles from surface wave measurements in the Mississippi embayment. *Earthquake Spectra*, EERI 23(4): 791–809.

Rosenblad, B., Stokoe, K.H., II, Li, J., Wilder, B. & Menq, F.-Y. 2008. Deep shear wave velocity profiling

of poorly characterized soils using the nees low-frequency vibrator. *Geotechnical Earthquake Engineering and Soil Dynamics IV*, ASCE, Sacramento, CA, May 18–22.

Runnels, I.K. 2007. Cyclic and dynamic full-scale testing of a pile cap with loose silty sand backfill, MS thesis, Department of Civil and Environmental Engineering, Brigham Young University, August.

Saunders, G., Derby, S. & Abdoun, T. 2007. Auxiliary axis for rensselaer's geotechnical centrifuge center in-flight robot—design considerations. *Proceedings of ASME 2007, International Design Engineering Technical Conferences & Computers and Information in Engineering Conference (IDETC/CIE 2007)*, September 4–7, Las Vegas, Nevada, USA.

Seda-Sanabria, Y., Matheu, E.E., Rickman, D.D., Akers, S.A., O'Daniel, J., McMahon, G.W. & Davis, L.K. 2009. Research and development efforts for dams, navigation locks, and levees. *ASDSO Annual Conference—National Dam Security Forum*, Sept 27-Oct 1, Hollywood, FL.

Shamsabadi, A., Rollins, K. & Kapuskar, M. 2007. Nonlinear soil-abutment-bridge structure interaction for seismic performance-based design. *Journal of Geotechnical and Geoenvironmental Engineering* 133(6): 707–720.

Springman, S.M., Nater, P., Chikatamarla, R. & Laue, J. 2002. Use of flexible tactile pressure sensors in geotechnical centrifuges. *Proc. of the International conference of Physical Modelling in Geotechnics,* Phillips et al. (eds.), St. John's, 113–118. Rotterdam: Balkema.

Steidl, J.H. 2007. Instrumented geotechnical sites: current and future trends, *Proceedings of the 4th International Conference on Earthquake Geotechnical Engineering*, June 25–28, 2007, Paper No. W1-1009, 234–245, Aristotle University of Thessaloniki, Greece.

Steidl, J.H., Nigbor, R.L. & Youd, T.L. 2008. Observations of insitu soil behavior and soil-foundation-structure interaction at the George E. Brown, Jr. network for earthquake engineering simulation (NEES) permanently instrumented field sites. *Proceedings of the 14th World Conference on Earthquake Engineering*, October 12–17, Beijing, China.

Steidl, J.H. & Seale, S.H. 2010. Observations and analysis of ground motion and pore pressure at the NEES Instrumented geotechnical field sites. *Fifth International Conference on Recent Advances in Geotechnical Earthquake Engineering and Soil Dynamics,* San Diego, CA.

Stewart, J.P., Whang, D.H., Fox, P.J. & Wallace, J.W. 2002. Applications of UCLA NEES equipment for testing of soil-foundation-structure interaction. *Proc. 7th U.S. National Conference on Earthquake Engineering*, Boston, MA, Paper 00018, July 21–25.

Stewart, J.P., Whang, D.H., Wallace, J.W. & Nigbor, R.L. 2005. Field testing capabilities of nees@UCLA equipment site for soil-structure interaction applications. *Proc. Geo-Frontiers 2005,* Austin Texas, ASCE Geotechnical Special Publication 130–142, January 24–26.

Stewart, J.P., Taciroglu, E., Wallace, J.W., Ahlberg, E.R., Lemnitzer, A., Rha, C., Tehrani, P.K., Keowen, S., Nigbor, R.L. & Salamanca, A. 2007. Full scale cyclic testing of foundation support systems for highway bridges. Part II: Abutment b1s. *UCLA – SGEL, Report 2007/02*, Department of Civil Engineering, University of California, Los Angeles, Los Angeles, CA.

Stokoe, K.H., Rathje, E.M., Wilson, C.R., Rosenblad, B.L. & Menq, F.Y. 2004. Development of the NEES large-scale mobile shakers and associated instrumentation for in situ evaluation of nonlinear characteristics and liquefaction resistance of soils. *13th World Conference on Earthquake Engineering*, Vancouver, B.C. Canada, August 1–6, Paper No. 535, (CD-ROM).

Stokoe, K.H., Cox, B.R., Lin, Y.-C., Jung, M.J., Menq, F.-Y., Bay, J.A., Rosenblad, B. & Wong, I. 2006a. Use of intermediate to large vibrators as surface wave sources to evaluate Vs profiles for earthquake studies. *19th symposium on the application of geophysics to engineering and environmental problems,* Seattle, Washington.

Stokoe, K.H., II, Kurtulus, A. & Park, K. 2006b. Development of field methods to evaluate the nonlinear shear modulus of soil. *Earthquake Geotechnical Engineering Workshop*, November, Canterbury, Christchurch, New Zealand.

Stokoe, K.H., II, Menq, F-Y, Wood, S.L., Park, K., Rosenblad, B. & Cox, B.R. 2008. Experience with nees@UTexas large-scale mobile shakers in earthquake engineering studies. *Third International Conference on Site Characteristic,* Taipei, Taiwan, April 1–4, 6 pp.

Suzuki, H., Tokimatsu, K., Sato, M. & Tabata, K. 2008. Soil-pile-structure interaction in liquefiable ground through multi-dimensional shaking table tests using the E-Defense facility. *Proc. of 14th World Conference on Earthquake Engineering*, Beijing, China, 8 pp.

Suzuki, H., Tokimatsu, K., Sato, M. & Tabata, K. 2009. Kinematic and inertial effects on deformation modes of piles during liquefaction in shaking table tests using e-defense facilities. *Earthquake Geotechnical Engineering Satellite Conference, XVIIth International Conference on Soil Mechanics & Geotechnical Engineering*, 2–3 October, Alexandria, Egypt.

Tabata, K. & Sato, M. 2006. Report of special project for earthquake disaster mitigation in urban areas. Ministry of Education, Culture, Sports Science and Technology, 489–554 (in Japanese).

Tamura, K., Okamura, M. & Tanimoto, S. 2004. Hybrid vibration experiment on interactive response of superstructure and foundation of highway bridge. *Proc. 13th WCEE*, Vancouver, B.C., Canada, August 1–6, Paper No. 1206.

Tanaka, H., Hijikata, K., Hashimoto, T., Fujiwara, K., Kontani, O., Miyamoto, Y. & Suzuki, A. 2005. Vibration tests on pile-group foundations using large-scale blast excitation. *Nuclear Engineering and Design* 235: 2087–2098.

Thevanayagam, S., Kanagalingam, T., Reinhorn, A., Tharmendhira, R., Dobry, R., Pitman, M., Abdoun, T., Elgamal, A., Zeghal, M., Ecemis, N. & El Shamy, U. 2009. Laminar box system for 1-g physical modeling of liquefaction and lateral spreading. *Geotechnical Testing Journal* 32(5).

Tokimatsu, K. & Suzuki, H. 2004. Pore water pressure response around pile and its effects on p-y behavior during soil liquefaction. *Soils and Foundations* 44(6): 101–110.

Tokimatsu, K., Suzuki, H., Tabata, K. & Sato, M. 2007. Three dimensional shaking table tests on soil-pile-structure models using e-defense facility. *4th International Conference on Earthquake Engineering*, June 25–28, Thessaloniki, Greece.

Ubilla, J., Abdoun, T. & Zimmie, T. 2006. Application of in-flight robot in centrifuge modeling of laterally loaded stiff pile foundations. in: Ng, Zhang, Wang (eds.), *Physical Modeling in Geotechnics, Sixth ICP-MG'06*, 259–264. London: Taylor and Francis Group.

Valentine, T.J. 2007. Dynamic testing of a full-scale pile cap with dense silty sand backfill, MS thesis, Department of Civil and Environmental Engineering, Brigham Young University, August.

Van Den Einde, L., Restrepo, J., Conte J.P., Luco, E., Seible, F, Filiatrault, A., Clark, A., Johnson, A., Gram, M., Kusner, D. & Thoen, B. 2004. Development of the George E. Brown Jr. network for earthquake engineering simulation (NEES) large high performance outdoor shake table at the University of California, San Diego. *Proceedings of the 13th World Conference on Earthquake Engineering*, Paper No. 3281. Vancouver, BC, Canada, 1–6 August.

Van Den Einde, L., Kinderman, T.L., Masuda, M. & Elgamal, A. 2007. NEES IT tools to advance earthquake engineering research and practice. *Proc. Structures Congress 2007, Structures 2007: Structural Engineering Research Frontiers*, ASCE, Wallace, J.W., ed., Long Beach, California, USA, May 16–19.

Wahbeh, A.M., Caffrey, J.P. & Masri, S.F. 2003. A vision-based approach for the direct measurement of displacements in vibrating systems, *Smart Mater. Struct.* 12: 785–794.

Weaver, T.J., Ashford, S. & Rollins, K. 2005. Response of 0.6 m cast-in-steel-shell pile in liquefied soil under lateral loading. *Journal of Geotechnical and Geoenvironmental Engineering* 131(1): 94–102.

Weber, G.H., Schneider, M., Wilson, D.W., Hagen, H., Hamann, B. & Kutter, B.L. 2003. Visualization of experimental earthquake data. Visualization and Data Analysis 2003. *Proc. SPIE*, (Boerner, K., Chen, P.C., Erbacher, R.F., Groehn, M. & Roberts, J.C., eds.), August, Vol. 5009, Bellingham, Washington.

White, D.J., Take, W.A. & Bolton, M.D. 2003. Soil deformation measurement using particle image velocimetry (PIV) and photogrammetry. *Géotechnique* 53(7):619–631.

Wilson, D.W., Boulanger, R.W., Feng, X., Hamann, B., Jeremic, B., Kutter, B.L., Ma, K.-L., Santamarina, C., Sprott, K.S., Velinsky, S.A., Weber, G. & Yoo, S.J.B. 2004. The NEES geotechnical centrifuge at UC Davis. *Proceedings 13th World Conference on Earthquake Engineering*, Vancouver, BC, Canada, August, paper 2497, pp. 14.

Wilson, P. & Elgamal, A. 2006. Large scale measurement of lateral earth pressure on bridge abutment backwall subjected to static and dynamic loading. *Proc. NZ Workshop on geotechnical earthquake engineering,* Cubrinovski, M., ed., University of Canterbury, New Zealand, 307–315.

Wilson, P. & Elgamal, A. 2008. Full scale bridge abutment passive earth pressure tests and calibrated models. *Proc. 14th World Conference on Earthquake Engineering,* October 12–17, Beijing, China.

Wilson, P. 2009. Large scale passive force-displacement and dynamic earth pressure experiments and simulations, Ph.D. thesis, Dept. of Structural Eng., University of California, San Diego, La Jolla, CA.

Wilson, P. & Elgamal, A. 2009a. Bridge abutment lateral earth pressure experiments. *Sixth international conference on urban earthquake engineering, Center for urban earthquake engineering, Tokyo Institute of Technology*, March 3–4, Tokyo, Japan, 287–291.

Wilson, P. & Elgamal, A. 2009b. Large scale shake table lateral earth pressure experiments. *17th International Conference on Soil Mechanics & Geotechnical Engineering*, ISSMGE, Alexandria, Egypt, 5–9 Oct.

Wilson, P. & Elgamal, A. 2009c. Full-scale shake-table investigation of bridge abutment lateral earth pressure. *Bull. New Zealand Society Earthquake Engineering, NZSEE*, March 42(1): 39–46.

Yang, D., Naesgaard, E., Byrne, P.M., Adalier, K. & Abdoun, T. 2004. Numerical model verification and calibration of George Massey Tunnel using centrifuge models. *Can. Geotech. J.* 41(5): 921–942.

Yasuhara, H., Okamura, M. & Kochi, Y. 2008. Experiments and predictions of soil desaturation by air-injection technique and the implications mediated by multiphase flow simulation. *Soils and Foundations* 48(6): 791–804.

Youd, T.L., Steidl, J.H. & Nigbor, R.L. 2004. Lessons learned and need for instrumented liquefaction sites. *Soil Dynamics and Earthquake Engineering* 24(9–10): 639–646.

Youd, T.L., Steidl, J.H. & Steller, R.A. 2007. Instrumentation of the wildlife liquefaction array. Earthquake Geotechnical Engineering, K.D. Pitilakis (ed.), Paper No. 1251. Springer.

Youd, T.L., Bartholomew H.W. & Steidl, J.H. 2008. SPT hammer energy ratio versus drop height. *Journal of Geotechnical and Geoenvironmental Engineering* 134(3): 397–400.

Zeghal, M., Abdoun, T. & Oskay, C. 2004. A novel-shaped-acceleration array and local identification of geotechnical systems. *Consortium of Organizations for Strong-Motion Observation Systems, COSMOS International workshop for site selection, installation and operation of geotechnical strong-motion arrays, workshop 1, inventory of current and planned arrays*, October 14–15.

Zhang, L.M. & Kong, L.G. 2006. Centrifuge modeling of torsional response of piles in sand. *Can. Geotech. J.* 43: 500–515.

Zhang G., Hu Y., & Zhang, J.-M. 2009. New image analysis-based displacement-measurement system for geotechnical centrifuge modeling tests, Measurement. *Journal of the International Measurement Confederation* 42(1): 87–96.

Zimmie, T.F., Sausville, M.J., Simpson, P.T. & Abdoun, T.H. 2005. Blasting studies on dams using the geotechnical centrifuge. *Dam Safety 2005, Proc. of the ASDSO Annual Conf. on Dam Safety*, Assoc. of State Dam Safety Officials-conference moved to Orlando, FL. due to Hurricane Katrina, New Orleans, LA, September.

Physical Modelling in Geotechnics – Springman, Laue & Seward (eds)
© 2010 Taylor & Francis Group, London, ISBN 978-0-415-59288-8

Physical modelling of soft ground problems

F.H. Lee
National University of Singapore, Singapore

M.S.S. Almeida
Federal University of Rio de Janeiro, Brazil

B. Indraratna
University of Wollongong, Australia

ABSTRACT: This paper reviews the application of physical modelling to soft ground engineering problems. The problems discussed include foundations and bearing problems, consolidation and preloading problems, ground improvement and underground constructions.

1 INTRODUCTION

Physical modelling has been used to study soft soil problems since the early days of centrifuge modelling. For instance, one of the earliest reported centrifuge model studies was that by Mikasa and Takada (1966) and involved a series of self-weight consolidation tests of clay in a centrifuge to validate Mikasa's (1963) self-weight consolidation theory. Since then, many soft soil problems have been studied using physical modelling. An examination of the soft soil engineering papers published in the last two International Conferences on Physical Modelling in Geomechanics shows that most of the papers can be grouped several categories, namely foundations, consolidation and preloading, ground improvement, retaining structures, excavations and underground constructions.

In the discussion below, the application of physical modelling to these categories of problems, as well as some of the relevant issues, will be discussed.

2 FOUNDATIONS AND BEARING PROBLEMS (*CONTRIBUTED BY ALMEIDA*)

2.1 *Pipelines*

Studies on the bearing capacity of pipelines quite often rely on physical modelling. A good example of the interplay between physical modelling and offshore engineering practice is the SAFEBUCK JIP Project (Bruton et al. 2006). In this project, use was made of 1 g and centrifuge tests to investigate the following factors: (a) embedment of the pipe at installation; (b) breakout during buckle formation based on different levels of initial pipe embedment; (c) large amplitude displacements as the buckle forms; (d) repeated cyclic behaviour.

Figure 1(a) shows the first load monotonic response from steps 0 to 4, described by the authors as follows

(0–1) First load monotonic breakout (dependent on initial penetration);

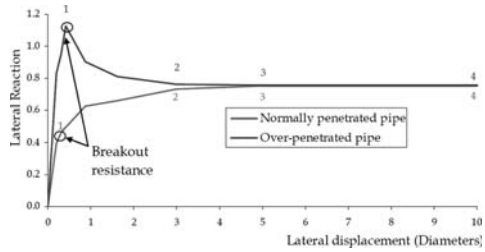

(a) Monotonic Response

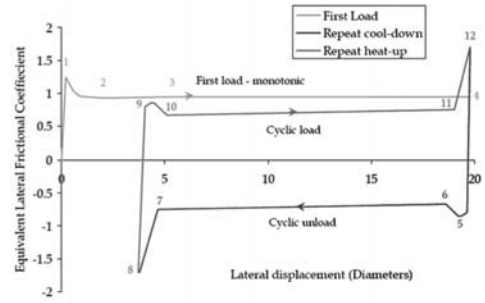

(b) Cyclic Response

Figure 1. Monotonic and cyclic lateral force-displacement response (Bruton et al. 2006).

(1–2) Suction release phase and elevation correction (dependent on initial penetration);
(2–3) Steady accretion phase (increase owing to berm build up or decrease owing to riding-up over some of the berm);
(3–4) Steady state residual friction.

Figure 1(b) shows the cyclic force-displacement response overlaid on the first load monotonic response for steps 5 to 12, described by the authors as follows:

(5–6) Cyclic breakout including suction release from static soil berm;
(6–7) Cyclic phase with a fresh active berm accretion;
(7–8) Berm reaction increases;
(9–10) Cyclic breakout as (5–6);
(10–11) Cyclic accretion (6–7);
(11–12) Cyclic berm interaction (7–8).

Bruton et al. (2008) show the importance that model testing plays in the assessment of pipe-soil interaction, including observations on the failure mechanism during lateral pipe movement, the increase in lateral restraint owing to soil berm formation and the important contrast between light pipe and heavy pipe behaviour. Figure 2 shows the typical forms of lateral pipe response for light and heavy pipes observed in model tests.

Cheuk et al. (2007) report on a series of centrifuge tests conducted to assess the vertical pressure exerted on a pipeline buried in lumpy clay fill when the pipe was moving upward at a constant speed. A model pipe was buried in clay lumps made from natural clay collected from the Gulf of Mexico. The lumpy soil cover was allowed to consolidate for a fixed time period, before vertical extraction was triggered. The resulting uplift resistance was measured for different uplift velocities. Two different consolidation time periods were considered to investigate the potential benefit of a longer waiting period prior to putting the pipeline into operation. Results showed that early commissioning of buried pipelines in under-consolidated lumpy fill could lead to a reduction of soil restraint up to 56%, together with a decrease in the stiffness of the response, as shown in Figure 3. The suction force generated underneath the pipe, which increased with the uplift velocity, was found to be a significant contributor to the overall uplift resistance. Nevertheless, quantitative analysis suggested that the beneficial effect from a higher degree of consolidation was much more significant than that achieved by a high suction force originating from a fast uplift.

The effect of shape and size of the lumps on the consolidation behaviour of lumpy clay backfills and uplift resistance of pipelines has been investigated by Ghahremani & Brennan (2009). Pore pressure measurement during consolidation in small and big cubes confirms that the pore pressures between the lumps reach a stable value earlier in big cubes than in small cubes and the consolidation time of a lumpy backfill with larger lumps is less. The larger lumps were found to provide higher normalised uplift resistance than the small ones. This is shown in Figure 4, where the normalised uplift resistance

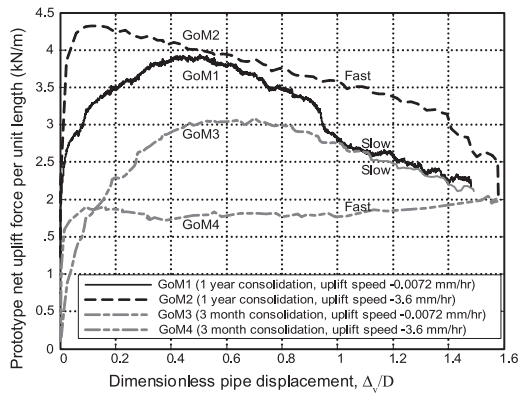

Figure 3. Influence of uplift speed and the degree of consolidation on uplift resistance in lumpy fill (after Cheuk et al. 2007).

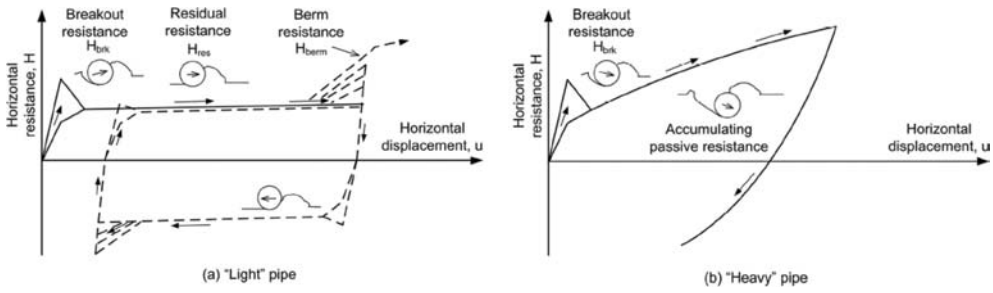

Figure 2. Typical forms of lateral pipe response (after Bruton et al. 2008).

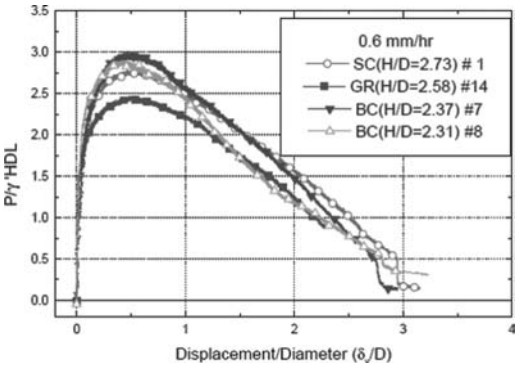

Figure 4. Soil resistance per unit length vs. displacement in slow tests for different lump shapes (after Ghahremani & Brennan 2009).

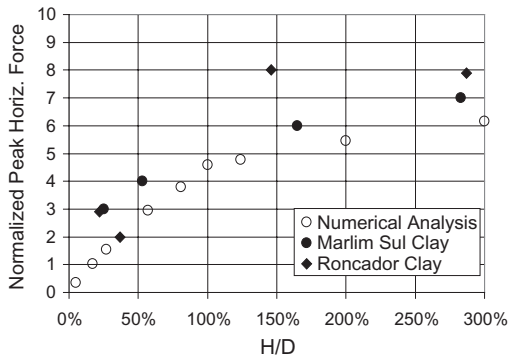

Figure 5. Normalised horizontal forces for physical and numerical simulations in clay (after Oliveira et al. 2009).

is plotted versus different lump shapes for uplift rate of 0.6 mm/hr. The peak uplift resistance is normalised by the weight of the block of the soil above the pipe and the displacement is normalised by the diameter of the pipe. It can be seen that big cubes (BC) resulted in higher resistance than small cubes (SC) and small cubes have higher resistance than grated lumps (GR). This could be the result of different lump interaction mechanisms during consolidation and the arrangement of lumps after consolidation.

Oliveira et al. (2005, 2009) investigated, using centrifuge modelling, a large-scale environmental accident, which occurred in January 2000 when a 17 km long pipeline failed and a million litres of oil spilled into Guanabara Bay (Almeida et al. 2001). A set of centrifuge tests and numerical analyses were carried out on clayey soils from Roncador and Marlim Sul oilfield sites in order to assess the lateral resistance of these soils when loaded laterally in plane strain conditions, simulating the accident conditions.

The centrifuge tests results for clayey soils were normalised in order to make easier any comparison with other data. Force normalisation (N_{Ch}) is obtained through:

$$N_{Ch} = \frac{F_h}{S_u D^* L} \quad (1)$$

where F_h is the measured horizontal peak force, D* is the projection of the pipe bottom contact area with soil at the beginning of the lateral movement and S_u is the T-bar measured undrained shear strength associated with the pipe mid-depth of penetration, or mid-height for full penetration (Oliveira et al. 2006).

Figure 5 shows a comparison between the normalised horizontal forces obtained in the centrifuge tests with the normalised horizontal forces achieved with the numerical simulation using AEEPECD/SIGMA softwares. The physical modelling data showed higher values than the numerical ones, particularly for burial depths over H/D = 100%, but both simulations seems to follow the same trend.

Dingle et al. (2008) also used centrifuge modelling to simulate the behaviour of a section of on-bottom pipeline during vertical embedment and lateral breakout. Image analysis techniques have been used to reveal the internal soil flow at each stage and to link these deformations to plasticity mechanisms. The authors used an artificial soil prepared from commercial kaolin clay mixed with water to form a slurry with a moisture content of 120% and centrifuged to 160 g.

With regard to vertical load-embedment response, the authors concluded that the penetration resistance exceeds predictions based on theoretical plasticity solutions, the discrepancy being most significant at very shallow embedment.

For lateral displacement tests, a brittle breakout response was observed by the authors, followed by upward movement of the pipe towards the soil surface. Simple deformation mechanisms were fitted to the soil flow observed during lateral breakout. Through combination of these mechanisms with the measured loads, the undrained shear strength mobilised at each stage was back-calculated. This analysis revealed that the peak soil strength is not mobilised until after breakout. Suction at the rear of the pipe is lost before slip surfaces in this region are fully developed. Figure 6 shows a comparison of measured resistance and calculated values based on full soil strength.

Finally, the authors highlight the critical uncertainties associated with lateral soil-pipe response: difficulties in comparing large deformation effects

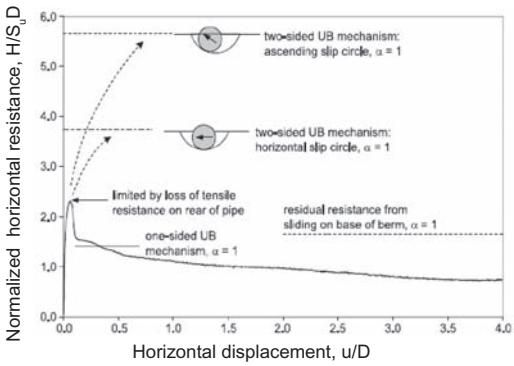

Figure 6. Comparison of measured resistance and calculated values based on full soil strength (after Dingle et al. 2008).

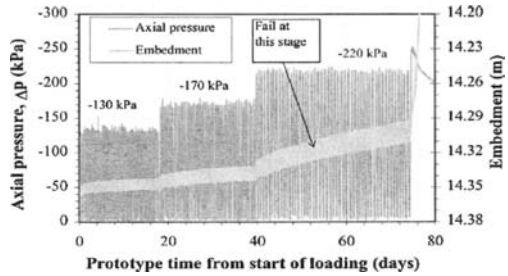

Figure 7. Variations of uplift pressure and embedment of caisson during cyclic loading in NC clay (after Chen & Randolph 2007).

such as berm formation and soil heave with plasticity solutions; relationship between tensile resistance mobilised at the rear of the pipe and the shear strength of the soil; and the complexity of assessing soil strength at very shallow depths.

2.2 *Footings and foundation on soft ground*

Centrifuge studies on the bearing capacity of footings and foundations on soft ground are mostly related to offshore problems and some recent studies are described below.

The vertical pullout capacity and external radial stress changes for suction caissons subjected to sustained loading and cyclic loading have been investigated (Chen & Randolph 2007) in three different kaolin clays, by means of model caissons tested in a centrifuge. The resistance of caissons subjected to sustained loading or cyclic loading is significantly less than that developed under short-term monotonic undrained loading, owing to reductions in both the external shaft friction and end bearing resistance. Figure 7 shows one example of variations of uplift pressure and embedment of a caisson during cyclic loading in NC clay. These have been quantified in terms of an external friction ratio α and an end-bearing factor, N_c. For sustained loading, the ratios of holding capacity relative to that for monotonic undrained loading lay in the range 72 to 85%. The external α value varied between 0.67 and 0.75, while the corresponding N_c value ranged from 7.5 to 9.4. For cyclic loading, the capacity ratio was 72 to 86%. The external α value was 0.65 to 0.80, and the derived N_c value was 6.4 to 9.0.

Gouvernec et al. (2009) used a beam centrifuge to investigate the response of shallow-skirted foundations in lightly over-consolidated clay to concentric transient and sustained uplift. Special attention was given to the influence of the ratio d/D of skirt depth to foundation diameter to mobilise undrained reverse end bearing. They found that doubling the foundation embedment ratio, d/D, from 0.15 to 0.3 led to a 150% increase in undrained uplift resistance V_u measured at a relative displacement w/D = 0.02, and a 250% increase in ultimate uplift capacity, V_{uULT}. Bearing capacity factors, N_c, for undrained uplift of 3.6 and 8.9 were recorded for the foundations with embedment ratios d/D = 0.15 and 0.3 respectively. Comparison with theoretical bearing capacity factors and other centrifuge tests indicated between 30% and 50% of reverse end bearing capacity was mobilised for the foundation with an embedment ratio d/D = 0.15, and 70 to 100% of reverse end bearing was mobilised for the foundation with an embedment ratio d/D = 0.3.

Figure 8 shows the undrained uplift resistance measured by the load cell plotted against relative uplift displacement w/D. Uplift resistance has been taken as the load cell reading, divided by the plan area of the foundation tests with the shorter skirted foundation (prefixed B1: B1T1, B1T4 and B1T5) and three tests with the longer skirted foundation (prefixed B2: B2T1, B2T2 and B2T3) are shown.

The loss in anchor embedment during keying for a vertically installed plate anchor in uniform and NC soils has been investigated by Song et al. (2009) using centrifuge tests and numerical FE modelling. The influence factors studied include anchor geometry, anchor submerged unit weight, and pullout angle. In the centrifuge tests, the plate anchor rotation was observed via transparent soil model tests. The anchor geometry and submerged unit weight affect anchor keying, and parameters representing these influences were combined as a normalized anchor geometry factor. By using this anchor geometry factor, the loss in anchor embedment can be predicted for vertical pullout of the

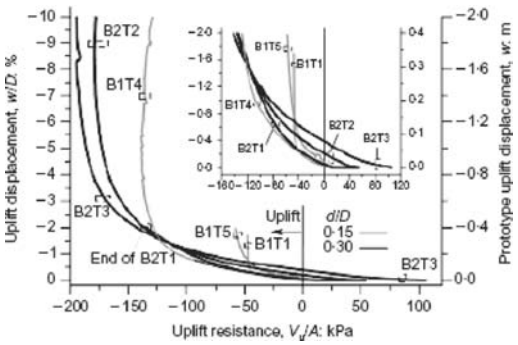

Figure 8. Undrained uplift resistance (after Gouvernec et al. 2009).

anchor. The loss in anchor embedment was found to decrease with decreasing pullout angle in a linear manner. The gradient of the linear relationship was independent of the thickness ratio, t/B, of the anchor.

Onshore studies on the bearing capacity of foundation on soft ground problems have also been studied by centrifuge modelling. These include, for instance, studies of vertical uplift capacity of footings (Lehane et al. 2008) and tower foundations (Rattley et al. 2008).

2.3 *Embankments*

The usefulness of physical modelling in soft ground engineering regarding embankments is exemplified well by the centrifuge modelling studies of the New Orleans levees, which failed during Hurricane Katrina (Sasanakul et al. 2008; Ubilla et al. 2008). Soil profiles in these sites and models were carefully prepared and consisted of a lacustrine clay layer underlying peat layers. A beach sand deposit was found underneath the fine-grained sediments. Four levees were modelled in the centrifuge tests: the London Avenue North and South levees, the 17th Street Canal levee, and the Orleans Canal levee. The first three levees failed, but not the last one. None of the levees was overtopped by the storm surge. Important lessons were learned from a comprehensive campaign of centrifuge tests carried out in two different centrifuge facilities.

The key factor of the failure mechanism of the levees was the formation of a gap between the flooded side of the levee and the sheet pile wall. This gap triggered an increase of the water pressure below the protected side of the levees and, therefore, a reduction of the effective stress at the foundation at that section of the levee, reducing the foundation strength as the loading of the sheet pile was increasing. Failure progress for the London North and South levees is summarised in Figure 9: (a) canal water rise; (b) crack formation; (c) development of full lateral hydrostatic pressure on the wall and increase in pore pressure under the levee (uplift) weakening of the levee foundation; (d) failure of the levee system.

The 17th Street Canal levee failed when the cracking led to a translational (sliding) failure in the clay layer commencing at the foot the sheet pile wall. This was a large horizontal translation that progressed landward through the top of the clay layer and caused the failure of the levee, as shown in Figure 10.

The levee along the southern portion of the Orleans Canal was also modelled in centrifuge tests but failure did not take place as it was subjected to less hydrostatic pressure than those acting at the three other levees.

Very good agreement was observed between the field observations in the four levees and the four sets of centrifuge tests, which confirm the effectiveness of the centrifuge tool in modelling complex problems of soil structure systems for failure and non-failure conditions. The recommendation for future design was to drive the sheet pile much deeper into the sand below the peat layer.

2.4 *Slopes*

To assess the impact of a debris flow on a pipeline, a slide modelling facility has been developed (Boylan et al. 2009) using the geotechnical drum centrifuge at UWA to model the run-out transition process of a submarine slide triggered in an intact block of clay. The experiment involves run-out of an intact block along a model seabed in the geotechnical drum centrifuge at UWA. Specific monitoring techniques including miniature site investigation tools, pore pressure measurement devices, surface profiling tools, and slide impact load measurement instruments have been developed specifically. These devices are used to characterise a very soft seabed and slide before, during and after a slide event, and to record the development of pore pressures within the seabed and the slide, to identify the impact load that results from a slide and to assess the level of erosion of the seabed by the slide. The experimental concept is outlined in Figure 11.

A new device has been developed to measure the operative strength of the runout material during the slide. This cantilever loading device (CLD) monitors the dynamic load from a passing slide, from which the operative shear strength can be inferred. The CLD records the resistance created by soil flow around a vertical cylinder held rigidly in the slide path, as shown in Figure 12.

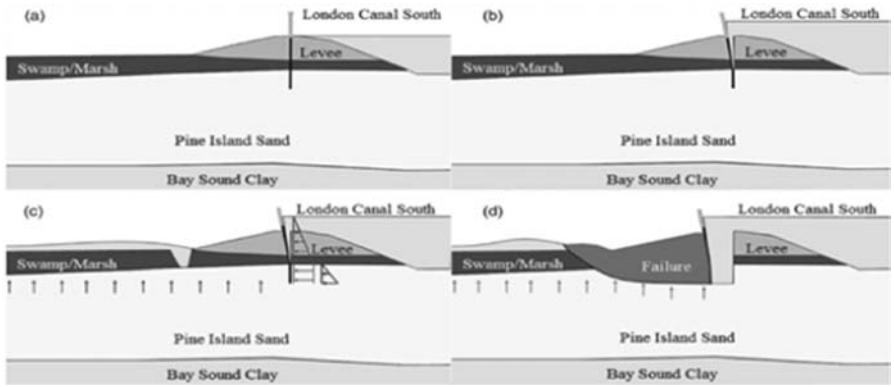

Figure 9. Failure progress for the London South levees as observed in centrifuge tests (after Ubilla et al. 2008).

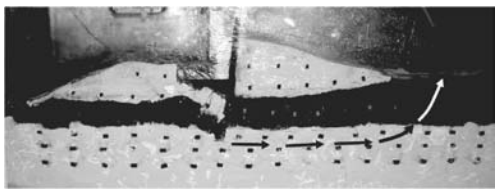

Figure 10. Translational failure pattern observed in centrifuge tests of the 17th Street Canal levee (Sasanakul et al. 2008).

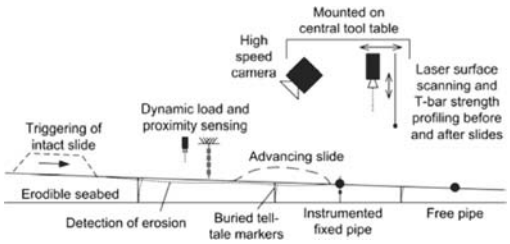

Figure 11. Debris flow impact on a pipeline: experimental concept implemented in centrifuge modelling (after Boylan et al. 2009).

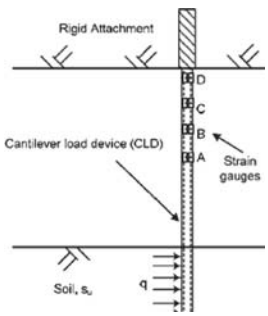

Figure 12. New device to measure the strength of the runout material during the slide (after Boylan et al. 2009).

3 CONSOLIDATION, PRELOADING AND VACUUM PRELOADING (*CONTRIBUTED BY INDRARATNA*)

3.1 *Performance of soft clay foundations stabilized by prefabricated vertical drains*

Due to the rapid increase in population and associated development activities in congested coastal areas, construction activities have often become concentrated in low-lying marshy areas that contain highly compressible weak organic and peaty soils of varying thickness (Indraratna et al. 1992). It is pertinent to stabilize the soft clays before commencing any construction activities, in order to prevent unacceptable differential settlements. In the case of thick soil deposits, preloading has been a most successful ground improvement technique in low-lying areas. It involves loading the ground surface to induce most of the primary settlement that the ground is expected to experience upon the application of post-construction loading (Indraratna & Redana 2000). Most surcharge embankments are usually raised as a multi-stage exercise with rest periods provided between the loading stages to prevent the risk of undrained failure (Jamiolkowski et al. 1983). In order to shorten the consolidation time by significantly decreasing the seepage path length, installation of sand drains and geosynthetic prefabricated vertical drains (PVDs) has been used in conjunction with surcharge embankment (Indraratna et al. 2005a). The smear zone during drain installation can decrease the surrounding soil permeability hence retarding the rate of consolidation (Bo et al. 2003). Application of vacuum load can further accelerate the rate of settlement, and this compensates for the adverse effects of smear and well resistance (Indraratna et al. 2005b).

In this Section, the smear zone determination and the effect of vacuum preloading are discussed

based on large scale physical models. For comparing with laboratory observations, the equivalent 2-D plane strain solution is described, which includes the effects of smear zone caused by mandrel driven vertical drains. The equivalent permeability coefficients are incorporated in finite element subroutines based on employing the modified Cam-clay theory. Finite element modelling is conducted to predict the excess pore pressures, lateral and vertical displacements. A case history is also discussed and analysed, at the site of the New Bangkok International Airport (Thailand) and the predictions are compared with the available field data.

3.1.1 *Prototype drain modelling using a large-scale consolidometer*

The performance of prefabricated vertical drains (PVDs) has been extensively studied at the University of Wollongong, Australia by employing large-scale laboratory models (Fig. 13). The internal diameter and the overall height of the testing chamber are 650 mm and 1000 mm, respectively. The loading system consists of an air compressor, and the consolidation settlement is monitored using a Linear Variable Differential Transducer (LVDT) placed above the piston. Strain gauge type pore pressure transducers are used to measure the excess pore water pressures at different locations both radially outwards from the central drains and with depth.

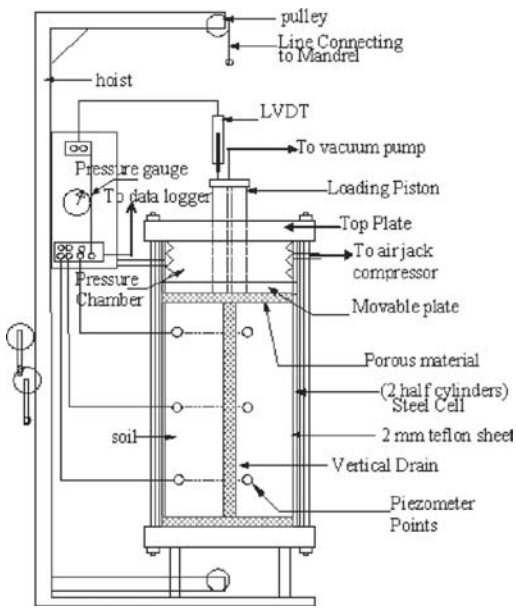

Figure 13. Schematic of large-scale consolidation apparatus (after Indraratna & Redana 1998).

3.1.1.1 Smear zone determination due to vertical drain installation

The smear zone extent can be determined either by permeability variation or water content variation along the radial distance (Indraratna & Redana 1998; Sathananthan & Indraratna 2006). Figure 14a indicates the variation of the ratio of the horizontal to vertical permeabilities (k_h/k_v) at different consolidation pressures along the radial distance, obtained from a single-drain physical model test. The variation of the water content with radial distance is shown in Figure 15 for an applied pressure of 200 kPa. As expected, the water content decreases towards the drain, and also the water content is greater towards the bottom of the cell at all radial locations.

Based on these curves, the extent of the smear zone can be estimated to be around 2.5 times the equivalent mandrel radius. Since this is a 1:1 scale testing of the PVD in the real soil, there is no need for the application of similitude parameters. This agrees well with the estimated extent of smear zone based on both the k_h/k_v ratio (Fig. 14a).

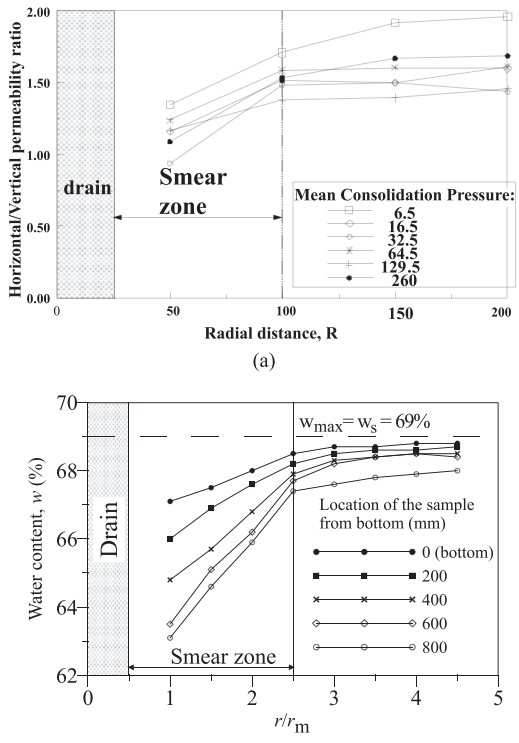

Figure 14. (a) Ratio of k_h/k_v along the radial distance from the central drain (after Indraratna & Redana 1998) (b) Variation of water content with depth and radial distance for an applied pressure of 200 kPa (after Sathananthan & Indraratna 2006).

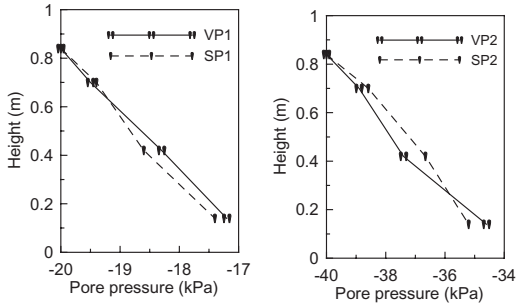

Figure 15. Distributions of measured negative pore water pressure along drain boundary in laboratory testing (a) 20 kPa vacuum pressure and (b) 40 kPa vacuum pressure.

It can be seen that the average value of k_h/k_v starts to decrease considerably from 1.65 (outside smear zone) to 1.1 (within smear zone). It implies that the permeability ratio between undisturbed ground and the smear zone (k_h/k_h') is approximately 1.5 and the extent of smear zone (r_s) is 4–5 times the radius of the vertical drain (r_w). It should be noted that the k_h/k_h' ratio in the field can vary from 1.5 to 10, depending on the type of drain and soils as well as installation procedures (Saye 2003).

3.1.1.2 Physical model for evaluating vacuum pressure propagation along a PVD

In the case of short vertical drains, pore pressure measurements in the physical model taken at a few points along the drain clearly showed that the vacuum pressure not only propagates immediately, but it decreases down the drain length. The loss of vacuum at the bottom of the drain is approximately 15–20% of the applied vacuum at the surface. It is noted that the rate of development of vacuum pressure within the drain may depend on the length and type of PVD (core and filter properties), nevertheless some field studies suggest that it develops rapidly, even if the PVD is long (Bo et al. 2003).

Based on the above observation, Indraratna et al. (2005a) proposed the new radial consolidation theory, which incorporated the vacuum pressure distribution effect as follows:

$$\frac{\bar{u}}{\sigma_1} = \left(1 + \frac{(1+k_1)p_{0,ax}}{2\sigma_1}\right)\exp\left(\frac{-8T_{h,ax}}{\mu_{ax}}\right) - \frac{(1+k_1)p_{0,ax}}{2\sigma_1} \tag{2}$$

$$\mu_{ax} \approx \left[\ln\left(\frac{n}{s}\right) + \frac{k_{h,ax}}{k_{s,ax}}\ln(s) - \frac{3}{4}\right] \tag{3}$$

where, $\bar{u}$ = average excess pore water pressure for the unit cell, VPR = vacuum pressure ratio, VPR = p_0/σ_1, k_1 = ratio between vacuum pressure at the bottom and at the top of vertical drain, n = ratio r_e/r_w under axisymmetric conditions, k_h = horizontal permeability coefficient in the undisturbed zone and k_s = horizontal permeability coefficient in the smear zone.

3.2 *Equivalent plane strain consolidation theory for a 1:1 physical model of a PVD*

In order to investigate the behaviour of an entire embankment, finite element analysis can be carried out based on the 2D plane strain assumption, whereas the true consolidation around vertical drains occurs under axisymmetric conditions. Indraratna et al. (2005a) suggested that the *equivalence* between the 2-D plane strain analysis and 3-D axisymmetric condition needs to be established to obtain realistic predictions. Indraratna et al. (2005a) proposed the conversion procedures based on Figure 16 by changing an axisymmetric unit cell for each drain into an equivalent parallel drain wall by altering the coefficient of soil permeability and drain geometry, such that the time-consolidation curve remained the same for both cases. In this procedure, the half width of the drain b_w and half width of the smear zone b_s remain the same as their axisymmetric radii r_w and r_s, respectively.

The equivalent permeability in the smear zone can be expressed as:

$$\frac{k_{hp}'}{k_{hp}} = \frac{\beta}{\frac{k_{hp}}{k_h}\left[\ln\left(\frac{n}{s}\right) + \left(\frac{k_h}{k_h'}\right)\ln(s) - 0.75\right] - \alpha} \tag{4}$$

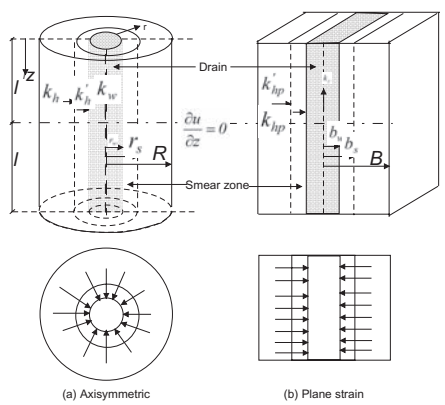

Figure 16. Conversion of an axisymmetric unit cell into plane strain condition (after Indraratna & Redana 2000).

If the effect of smear is ignored in Equation 1, then the simplified ratio of plane strain to axisymmetric permeability in the undisturbed zone becomes the same as that proposed by Hird et al. (1992):

$$\frac{k_{hp}}{k_h} = \frac{0.67}{[\ln(n) - 0.75]} \quad (5)$$

3.3 *Application of smear characteristics and vacuum pressure propagation in a real-life embankment*

3.3.1 *Embankment characteristics*

The Second Bangkok International Airport is situated about 30 km from the city of Bangkok, Thailand. The site consists of 1–1.5 m thick weathered crust (OCR > 2) overlying very soft normally consolidated clay. Underneath the medium clay layer, a light brown stiffer clay layer (OCR = 1) is found at a depth of 10–21 m (Indraratna et al. 2000). The groundwater level was located at 0.5 m below the surface.

The moisture content of the very soft clay layer varies from 80 to 100%, whereas in the lower clay deposits (10–14 m), the water content varies from 50 to 80%. The plastic limits and liquid limits of the soil in each layer were in the range of 80 to 100% and 20 to 40%, respectively.

Several trial embankments were built at this site. One of them (TV1, area 40 × 40 m^2) was constructed with PVDs and further stabilized by vacuum pressure application (Indraratna et al. 2005c). Figure 17 shows the vertical cross section and field instrument positions for the embankment. PVDs of 15 m length with a vacuum pressure membrane system have been installed. The array of instrumentation includes piezometers, surface settlement plates, multipoint extensometers, inclinometers, and observation wells.

The vertical drains were installed in a triangular pattern at a spacing of 1 m (Mebra drains, 100 mm × 3 mm). The PVDs were installed using a steel mandrel, that was statically pushed into the soil without any vibration. Although more gradual than dynamic loading, this method was employed to reduce the extent of smear zone as much as possible. The extent of the smear zone with depth was estimated based on laboratory evaluation, as explained earlier.

3.4 *Multi-drain analysis using FEM incorporating proposed equivalent plane strain model*

In order to investigate the performance of a real-life embankment, the consolidation behaviour was analysed using the finite element software ABAQUS (Indraratna et al. 2005c). The *equivalent* plane strain model (Eqs. 4–5) and the modified Cam-clay theory (Roscoe & Burland 1968) have been adopted in the FEM analysis. According to Indraratna & Redana (1997), the ratios of k_h/k_s and d_s/d_w determined from the laboratory models are approximately 1.5–2.0 and 3–4, respectively, but in practice these ratios can vary from 1.5 to 6 depending on the types of drain, mandrel size and shape and installation procedures used (Indraratna & Redana 2000; Saye 2003). The ratios of k_h/k_s and d_s/d_w for this case study were assumed to be 2 and 6, respectively. For modern PVDs, the discharge capacity (q_w) is usually very high and therefore the role of well resistance can often be neglected (Indraratna & Redana 2000).

The 8-node bi-quadratic displacement and bilinear pore pressure elements were employed in the analysis (Fig. 18), and half of the embankment by symmetry simulated as shown in Figure 18. The incremental surcharge loading was applied at the upper boundary capturing (a) smear effects

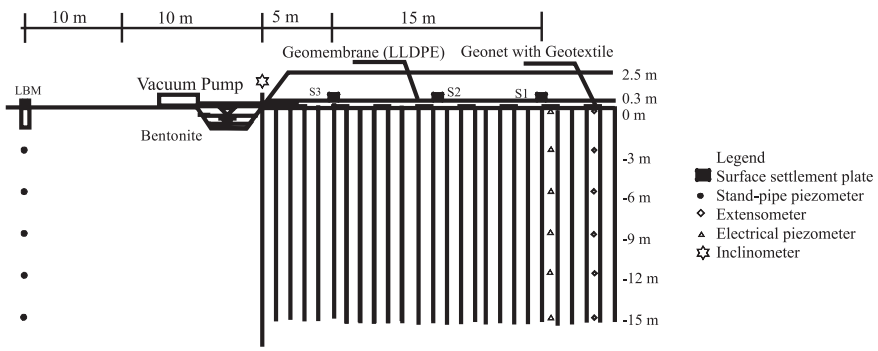

Figure 17. Cross section of embankment TV1 and location of monitoring system (after Indraratna et al. 2005c).

and (b) vacuum pressure propagation. The following 4 distinct scenarios were examined under the equivalent 2D multi-drain analysis (Indraratna et al. 2005c):

Model A: Conventional surcharge only—no vacuum application,

Model B: Vacuum pressure variation adopted from field measurements and made to decrease along the the drain length (zero at the drain bottom),

Model C: Any vacuum pressure loss is ignored, (i.e. –60 kPa vacuum pressure kept constant); vacuum pressure is assumed to be zero at the PVD bottom and varies linearly along the drain length, and

Model D: vacuum pressure kept constant throughout the soil layer.

Figure 19 compares surface settlement between the predictions and measurements (centreline). Prediction using Model B is found to be in accordance with the field data. Comparing all the different vacuum pressure conditions, Models A and D provide the lowest and highest settlement, respectively. Vacuum application in tandem with a PVD system can significantly accelerate the process of consolidation, whereby, most of the primary consolidation can be achieved within 4 months.

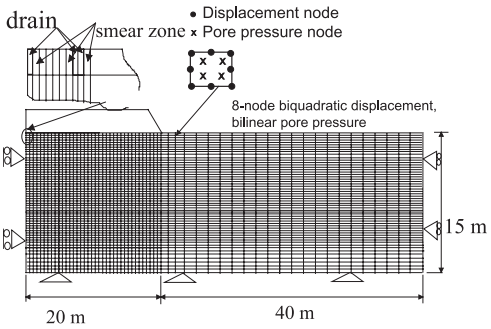

Figure 18. Finite element mesh for plane strain analysis (after Indraratna et al. 2005c).

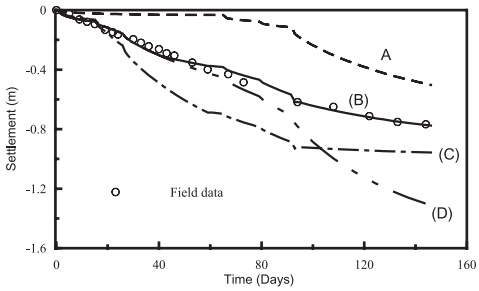

Figure 19. Surface settlement time curves of embankment TV1 (after Indraratna et al. 2005c).

In contrast, the conventional surchage with the same equivalent pressure requires more time to complete primary consolidation (after 5 months). As shown by Model C, a higher settlement can be obtained, if any loss of vacuum pressure can be prevented.

Figure 20 shows the predicted and measured excess pore water pressures. The field observations are closest to Model B predictions. This implied that the assumption of linearly decreasing time-dependent vacuum pressure along the drain length is reasonably justified. Excess pore pressure generated from the vacuum application is less than the conventional case, which enables the embankment to be raised at a higher rate than a conventional construction employing only surcharge pressure.

The predicted and measured lateral movements (end of embankment construction) are illustrated in Figure 21. The observed lateral displacements

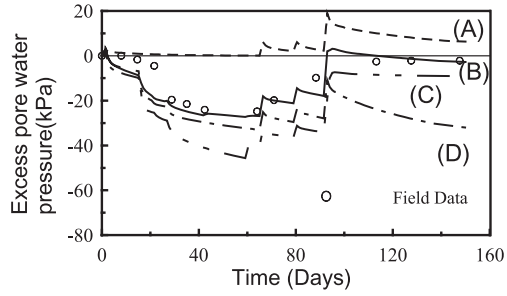

Figure 20. Variation of excess pore water pressure 3 m deep below the surface and 0.5 m away from centreline for Embankment TV1 (after Indraratna et al. 2005c).

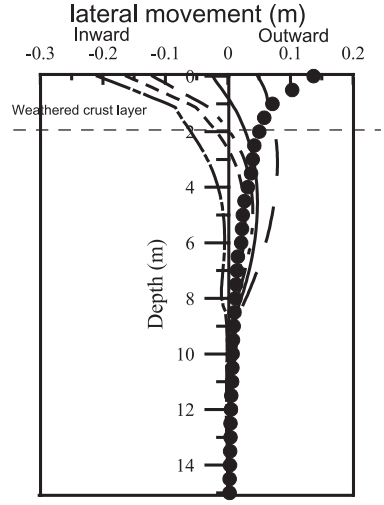

Figure 21. Calculated and measured lateral displacements distribution with depth (after Indraratna et al. 2005c).

do not agree well with any of the vacuum pressure models. At the middle of the soft clay layer (4–5 m deep), the predictions from Models B and C are the closest to the field data. Towards to the surface, the field data do not agree with the 'inward' lateral displacements predicted by both Models B and C. This discrepancy between the FEM and the field measurements is more evident in the surface weathered crust (0–2 m).

4 GROUND IMPROVEMENT (*CONTRIBUTED BY LEE*)

4.1 *Overview*

A detailed review on the application of centrifuge modelling to ground improvement has been presented by Kusakabe (2002). The objective of this section is to update this review and perhaps enhance the coverage of certain aspects. It will not cover vertical drain, preloading and vacuum preloading methods, which have already been discussed above.

4.1.1 *Chemical improvement*

Chemical ground improvement are widely used for foundation support in areas which are underlain by soft soils. It is also widely used as a means of temporary support in underground construction works in a densely built urban environment. For example, the collapse of the Nicoll Highway in Singapore (COI,2005) started after the removal of a sacrificial jet grout layer, which was used as an underground strut. The most commonly used chemical admixture is probably cement, either in a powder or slurry form.

There are two main approaches to introduce cement into the soil matrix. They are deep mixing and jet grouting. The former introduces and mixes cement slurry or powder into the soil matrix by a rotating mixing tool (e.g. Babasaki et al. 1996; Bruce et al. 2001) whereas the latter involves breaking up the soil matrix by a high velocity grout or water jet with concurrent introduction of cement grout (e.g., Gallavresi 1992; Chia & Tan 1993). Lee et al. (2005) noted that, although both methods involve introduction of cement into the ground, the relative composition of soil, cement and water obtained by the two methods can be quite different. In general, deep mixing often results in higher soil-cement and water-cement mass ratios because of the smaller amounts of cements introduced into the ground and the larger amount of soil retained.

Most of the studies on chemical improvement to date were conducted to study the performance of the improved ground. These included seismic performance, failure characteristics and mechanisms as well as settlement performance (e.g. Inagaki et al. 2002; Takahashi et al. 2006; Tanaka et al. 2006; Kitazume 2006; Hayashi & Nishimoto 2006; Yin & Fang 2006). In all of them, the model deep mixed ground was premixed under 1 g-conditions and allowed to cure in moulds before being placed in the model. The detailed features of the improved ground, such as the overlapping improved soil columns are not modelled. This procedure is clearly very different from that used in the field. It is almost certain that, in all of the models, a high degree of uniformity was achieved in the improved ground. This state-of-the-art is very similar to that reported by Kusakabe (2002) and indicates that, while the volume of studies appears to have increased significantly, the objectives and technology has not changed significantly.

In addition, there was no reported study in both international conferences on the performance of chemically improved soil as excavation support. This is despite the fact that chemically improved ground is now widely used in urban areas for excavation support (e.g. Nakagawa et al. 1996; COI 2005). The only reported studies on this problem are Goh (2003) and Zhang et al. (2008). Both involved preparing the improved soil layer under 1 g conditions in a mould.

It is well-known that significant heterogeneity can be induced into the improved ground in the process of chemical improvement. For instance, for dry lime improvement method, Larsson et al. (2005a & b) showed that significant point-to-point variation can result. In a similar way, significant non-uniformities can result from chemical

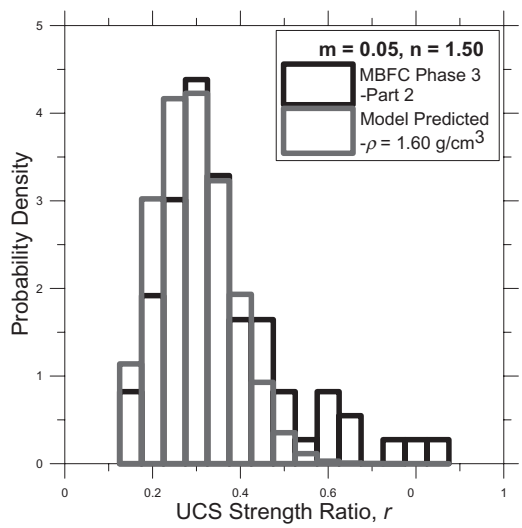

Figure 22. Measured (black lines) and predicted (red lines) unconfined compressive strength distribution in Marina Bay Financial Centre construction project.

improvement using cement slurry. Figure 22 shows the distribution of unconfined compression strength of cement-improved Singapore marine clay taken from Phase 3 of the deep mixing works at the Marina Bay Financial Centre in Singapore. In this figure, the unconfined compressive strength ratio r is obtained by dividing the measured core strength by a reference strength of 6 MPa. As can be seen, the unconfined compressive strength varies from about 700 kPa to about 5 MPa.

The non-uniformity may not be completely random. For instance, based on field tests on soil-cement columns, Sakai et al. (1994) reported a generally trend of variation in strength in a radial direction, the strength being higher in the column's centre and decreased when it moved to the edges.

The columnar structure and non-uniformity are believed to have significant effects on the performance of the improved ground. For example, Nakagawa et al. (1996) reported a coefficient of horizontal subgrade reaction, which amounts to only 3.0% to 13% of the weighted average value based on core strength.

Partly because of the significant variation in strength of the improved soil and the need to ensure a very safe design, the design field strength of the stabilized soil is generally several times less than the strength obtained in laboratory by mixing the same relative amounts of soil and cement (e.g. Nishida et al. 1996). This is often needed to ensure that a sufficient percentage of the cores have strength which exceeds the design value.

In order to study the factors affecting the COV of the treated soil, Lee et al. (2006b) conducted a study to examine the possibility of using centrifuge modelling to simulate the deep mixing process. The first part involved studying the feasibility of scaling the "wet" deep mixing process in the centrifuge. By considering the various dimensionless groups, Lee et al. (2006b) concluded that centrifuge modelling would automatically lead to a consistent scaling of all the relevant forces, except for the viscous forces, which would be over-scaled in the model if cement slurry is used as the model binder liquid. Lee et al. (2006b) proposed using a binder with a lower viscosity such as zinc chloride, which enables the viscosity to be approximately scaled.

Using zinc chloride as the binder, Lee et al. (2006; 2009) conducted a series of centrifuge model tests to investigate the effects of the blade rotation number (CDIT 2002) and slurry density. Figure 23 shows a single-shaft model mixing tool used in the study. The results show that the concentration COV is indeed significantly affected by the blade rotation number. More importantly, for binder density of 1300 kg/m^3 and 1500 kg/m^3, the COV appears to level off for rotation number above about 300 rev/m. This is roughly consistent with the minimum blade rotation number of 360 rev/m recommended by CDIT (2002). More importantly, the results also show that the binder density also has a very significant effect on the COV and that, for really uniform mixing, the binder density should be approximately equal to that of the soil. With the benefit of hindsight, this is not surprising; density differential has been well-recognized to be an important factor that inhibits good mixing. The study is still continuing on other factors, which may affect the COV, such as the soil type, soil state (e.g. over-consolidation ratio), RPM and profile of the mixing blades.

Using a relation between the strength of the treated soil and its soil:water:cement ratios (e.g. Lee et al. 2005), the above concentration data can

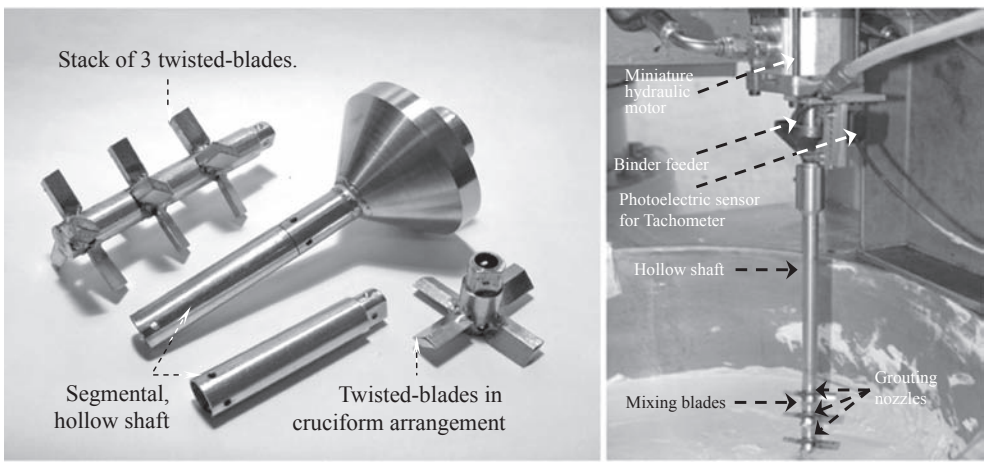

Figure 23. Centrifuge model deep mixing tool.

be converted into strength data. Figure 22 compares the field-measured unconfined compressive strength distribution from the Marina Bay Financial Centre with that predicted using the above framework. As can be seen, some differences do exist, especially at the top end of the strength distribution. However, agreement is generally reasonable and both the predicted and field-measured distributions show a hump around an unconfined compressive strength of about 1800 kPa and a lower limit of about 750 kPa. This is useful in design as a framework for predicting what operating parameters would be needed in deep mixing; at present, such operating parameters are often obtained by trial and error on the site itself. Secondly, one may surmise that, by incorporating such distributions into a constitutive model, one may be able to conduct a series of stochastic finite element analyses, which enables the performance characteristics such as ground movement to be studied on a probabilistic basis. Further study is currently on-going to examine the effects of in-situ water content, soil type and RPM on the mixing quality.

Apart from centrifuge modelling, 1 g miniature deep mixing experiments have also been reported (e.g. Dong et al. 1996; Al-Tabbaa & Evans 1999). However, because of the inherent scale distortion between 1 g small scale models and a large-scale prototype, it is not exactly certain as to what the small model actually represents. Using dimensional analysis, Lee et al. (2010) showed that, in 1 g model tests using cement slurry as the model tracer liquid, the viscous forces will be over-scaled in the model. This may lead to a spurious deterioration in the model mixing quality. Al-Tabbaa & Evans (1999) noted, in 1 g model tests, that their geometrically similar model auger "*produced far more variability between the top and base halves of the columns: in the made ground, the UCS of the top sample was half that of the base sample, while in the sand and gravel the top sample was 50% stronger than the base sample*". One may surmise that a possible cause of the mixing problem reported by Al-Tabbaa & Evans (1999) using their geometrically similar auger is viscous over-scaling leading to deterioration in mixing quality.

4.1.2 *Sand compaction piles*

Sand compaction piles are widely used as a ground improvement measure for reclamation works in near-shore and foreshore areas as well as for onshore works where the ground improvement and disturbance induced by the compaction pile grid is of no major consequence e.g. in sites which are located far from existing buildings and infrastructure, which would be sensitive to ground improvement. A comprehensive review of centrifuge model research on sand compaction piles has been presented by Kusakabe (2002). What the following sections seek to do is to provide an update on the status of sand compaction pile research and modelling technology.

Kusakabe (2002) noted that centrifuge model sand compaction piles were commonly prepared using two different approaches, namely by pluviating dry sand into a pre-drilled hole in the model clay bed and by the "frozen pile method". The "frozen pile method" is a name used by Lee et al. (2001) to refer to an approach which involves inserting frozen miniature columns of saturated sand into pre-drilled holes in the clay bed as sand compaction piles.

As noted by Kusakabe (2002), a large body of research has been conducted using the "frozen pile method", which till today, remains the most widely used method (e.g. Lee et al. 2006a). These include penetration resistance of the improved ground as well as performance of structures such as caissons, which were founded on ground improved using sand compaction piles.

However, at least two geotechnical research groups have, in recent years, been experimenting with in-flight sand pile installation. These are the geotechnical groups in the National University of Singapore (NUS) and ETH Zurich. Using an in-flight sand pile installer mounted on an X-Y table on a beam centrifuge, Ng et al. (1998), Lee et al. (2001, 2002, 2004) studied the changes in overall performance, pore pressure and stresses in a soft clay bed. Ng et al. (1998) and Lee et al. (2001) reported differences in models in which sand piles were installed using the "frozen pile method" and those in which sand piles were installed in-flight. Models in which sand piles were installed in-flight generally show a stiffer response to both vertical and lateral deformation and a wider settlement trough. Lee et al. (2001) attributed the differences to the coupling between the sand pile and the soft clay. The high-g installation process involves a significant amount of lateral displacement, leading to increase in lateral stress in the soft ground and thereby enhancing the coupling between the sand pile and soft clay. On the other hand, in the "frozen pile method" the frozen sand pile may shrink slightly as its thaws, leading to a weaker soil-pile interface.

Lee et al. (2002, 2004) also investigated the pore pressure and stress changes in the soft clay during sand pile installation. Based on centrifuge model data, Lee et al. (2004) reported that plane strain cavity expansion theory appears to give a reasonably good estimate of the build-up in pore pressure and total radial stress at large depths, but significantly over-estimates the build-up in pore pressure and total radial stress at shallow depth. The deviation from the estimates by plane strain cavity expansion theory is dependent upon the depth

and radial distance. Better matching was obtained using a semi-empirical correction, which is based on two limits, namely plane strain at large depth and constant vertical stress nearer to the ground surface. However, there remains a significant radial distance effect, which cannot be explained by plane cavity expansion theories alone.

The peak radial total stress increment and excess pore pressure during jack-in follow a similar trend to the post-installation values, when compared with cavity expansion theory. However, the residual jack-in radial total stress and pore pressure is much smaller than that predicted by cavity expansion theory. This may be due to the stress relief that follows in the wake of a blunt penetrator being pushed into the ground.

On the basis of their findings, Lee et al. (2004) postulated that, in order to mobilize significant set-up of stress in the improved ground, one may require substantial further cavity expansion during the sand injection stage of sand pile installation. Installing a sand pile that has the same diameter as the casing may not mobilize much set-up in the ground. It also means that, for the same sand pile diameter, a smaller casing is likely to be able to generate larger set-up than a larger casing

Lee et al. (2004) also proposed that the cumulative radial total stress increment at a given location due to the installation of multiple piles in a grid may be reasonably estimated by superimposing the increments due to the installation of each pile. On the other hand, pore pressure build-up is shown to be less readily superimposed, possibly because the shear-induced component of excess pore pressure does not increase linearly and infinitely with deviator stress.

The above studies relate mainly to changes in stresses and pore pressure due to sand pile installation. More recently, Yi et al. (2010) added a T-bar penetrometer onto the X-Y Table so that in-flight strength measurements can be made. The emphasis of Yi et al.'s (2010) study was on the significance of pore pressure dissipation and pile group effects. Instead of using marine clay for the soft clay bed, Yi et al. (2010) used kaolin, the coefficient of consolidation of which is about 5 to 10 times that of Singapore marine clay. Two different installation sequences were used to study the consolidation influence. The first involved consecutive installation of successive piles, in which the time interval between installations was kept to the minimum required for adjusting the X-Y table. This ensured that excess pore pressure dissipation between successive pile installation is kept to a minimum. In the second sequence, the piles were installed with 45 minutes interval between successive installations. Pore pressure records showed that this interval would permit full dissipation of excess pore pressures. For the same pile group layout, installing the pile with a long time interval in between leads to a larger increase in the strength. This was attributed to the difference in the degree of dissipation of excess pore pressures between separate installations. Allowing a larger degree of pore pressure dissipation introduces more significant set-up effects that contribute to a larger strength gain. It should be noted that Yi et al.'s (2010) strength measurements are probably better regarded as some form of average rather than point values, given that the size of the T-bar is not insignificant compared to the space in between the piles.

It should be noted that, prior to Yi et al. (2010), Juneja (2002) had also reported preliminary evidence of strength gains of about 40% of the in-situ shear strength from sand piles installed in Singapore marine clay. Given that Singapore marine clay is much less permeable than kaolin, this would imply that, even under undrained conditions, some amount of strength gain is likely to occur, which would also be consistent with the improvement in performance reported by Lee et al. (2001).

The geotechnical group at ETH Zurich developed an in-flight sand pile installer on the central shaft of a drum centrifuge (Weber et al., 2006, 2009). The space constraint on a drum centrifuge is even more significant than that on a beam centrifuge and the success of the ETH group indicates that, with appropriate innovation, a considerable amount of miniaturization can be obtained.

Weber et al. (2009) noted that the interface between the sand pile and the clay comprises of at least two different zones, a penetration zone and a smear zone before the densification zone. The penetration zone consisted of a mixture of granular particles and clay material. Weber et al. (2009) reported that the thickness of the penetration zone was about 1/3 of the sand column radius, but indicated that this is likely to be dependent upon the grain size of the sand, stiffness and strength of the clay and load applied to the soil.

The smear zone is strongly sheared and remoulded due to the installation process of the stone column. Its thickness was also about 1/3 of the radius of the sand column. Beyond the smear zone lies the densification zone. There was no visible microstructural change in this zone, but pore size was reduced according to a hyperbolic relationship. The outer radius of the disturbed zone is about 2.5 times the sand column radius.

One may surmise that all three zones could not have been reproduced using the "frozen pile method". In particular, the penetration zone may play an important role in the coupling between the sand pile and the soft clay. As Lee et al. (2001) has noted, the use of the "frozen pile" method appear

to result in deterioration in coupling between the sand pile and soft clay.

Apart from centrifuge modelling, sand compaction piles have also been studied using triaxial testing. Kim et al. (2004) used a 1 g cylindrical soil model to examine the interaction between sand columns and clay in the SCP-treated ground. The soil box is a cylindrical cell measuring 550 mm in height and 500 mm in diameter. This housed miniature sand piles and clay. Uniform loading was imposed on the top surface of the improved ground via the compressed air. Several pressure cells were placed in the sand column and clay at different locations throughout the sample's thickness. Displacement gauges were installed at the similar locations to measure the soil movements. The experiments indicated an increase of stress concentration ratio with the depth. In response to the uniform, flexible loading, sand and clay were observed to settle differently. The differential settlement could be lessened by the increasing area replacement ratio.

Kim et al. (2006) also reported another series of experiments to investigate the stress concentration mechanism within a unit cell. The test setup consisted of one sand column placed at the centre of the cylindrical container using the "frozen pile" method, surrounded by clay. Load was applied on the top of the improved ground through the loading piston (i.e. rigid loading). Kim et al. (2006) noticed that the settlement reduction factor seemed independent of the applied stress. The stress concentration ratio was strongly related with the area replacement ratio and the relative density of sand column.

Both of these studies used the "frozen pile" method to install the sand piles. Thus, it is unlikely that the installation effects observed using in-flight installation could have been accounted for. However, one interesting feature of these studies is that transducers were embedded inside the sand pile, which allowed the stresses to be measured.

4.1.3 *Lessons learnt*

The above discussion shows that there are a number of approaches to studying ground improvement effects via physical modelling. The most commonly used way is to represent the improved ground on a large-scale, while ignoring the details of the ground improvement process and its effect on the improved ground. In such cases, the improved ground is usually treated as a uniform body and features introduced by the improvement process are often ignored.

On the other hand, one can also consider the same problem on a smaller size and examine the effects of the improvement process on the improved ground. This question leads to alternative approaches, which place greater emphasis on modelling the improvement process. The multitude of methods illustrates the innovation which has been occurring in the sphere of physical modelling with respect to ground improvement. The question of which method is better is probably as difficult as it is irrelevant because, in all likelihood, all methods are useful. The consideration of the problem on a large scale is probably useful from the viewpoint of determining broad performance characteristics of the improved ground compared to the unimproved ground. On the other hand, if one is interested in some of the deeper mechanics related to the improvement processes, then greater attention may be required in modelling the improvement process.

5 EXCAVATIONS AND UNDERGROUND CONSTRUCTION (*CONTRIBUTED BY LEE*)

5.1 *Excavations*

Excavation in soft clay is an area which has been well-studied since the 1990's (e.g. Kimura et al. 1994). Various methods have been developed for simulating excavations. The simplest of this is to pre-excavate the soil at 1 g and then bring the model up to a high-g level to simulate the increase in overburden stress (e.g. Zhu & Yi 1988; Liu 2002). This method is now largely discontinued owing to the fact that it subjects the model to large load-unload cycles, which are not present in the prototype. For instance, Gaudin et al. (2002) noted that wall movements occur during the unload cycles (i.e. deceleration phases), which is evidently spurious.

Another method involved the drainage of heavy fluid (e.g. Bolton & Powrie 1987, Powrie et al. 1994). Prior to excavation, support pressure within the pre-dug excavation was provided by the heavy liquid held within a rubber bag. Excavation was simulated by progressively draining the heavy liquid from the rubber bag. This provides better control of progressive excavation. However, it suffers from two drawbacks. Firstly, the zinc chloride solution imposes a K_0 of 1.0. This may be reasonably representative of heavily over-consolidated soil, but not of soft soil, where the K_0 is usually significantly less than 1.0. In such cases, the vertical and lateral earth pressures cannot be balanced simultaneously. Because of the imbalance in earth pressure, some amount of movement often occurs during the increase in g-level stage, making interpretation of results difficult. Secondly, the heavy liquid cannot simulate the development of passive earth pressure within the excavation area since all the soil has already removed.

Allersma (1998) used another approach, which employs a pre-embedded geotextile band to remove horizontal soil layers. The vertical stress may be well controlled by this method since the soil is removed layer by layer, but the horizontal earth pressure may be reduced by the geotextile band.

The above shortcomings lend impetus to the development of in-flight excavation technology. The first in-flight soil excavator was reported by Kimura et al. (1994) and uses a cutting blade to scrape layers of soil from the excavation area. Subsequent developments using this scraping approach have also been reported by Loh et al. (1998), Gaudin (2002) and König (2002). Toyosawa et al. (1998) also implemented in-flight soil removal, but by using a screw auger instead of a scraping blade.

The above developments do not deal with the model of the earth support system. In most studies, the wall is often installed into a pre-cut slot under 1 g conditions. This does not simulate the installation process of the wall. Powrie et al. (1994) simulated the excavation of diaphragm wall panels by draining sodium chloride solution from pre-cut slots in a model soil bed.

Another aspect of deep excavation is the installation and preloading of struts. Bolton and Powrie (1987) used a pre-installed but non-preloaded prop at model ground surface level to simulate a single-propped wall. This enables the top of the wall to be idealized as a fixed hinge in back-analysis, but it does not really simulate the complex sequence of strut installation and preloading which take place during construction of an actual strutted excavation.

In recent years, efforts have been made into the development of in-flight strutting systems. Goh (2003) reported the development of a system for installing and preloading a single strut in-flight in conjunction with in-flight excavation.

All the above indicates that, over the years, there have been very significant advances in the development of modelling technology and equipment for in-flight excavation and support systems. Nonetheless, real excavations are often even more complex. The developments summarized so far relate mainly to modelling half of a symmetric trench excavation. The only published research investigation, which relates to modelling an excavation in three-dimensions, is Loh et al. (1998)'s study of a corner excavation. Real excavations are more complicated than those studied in many ways. For instance, they may not be symmetrical. Diagonal struts, rather than cross-struts, may be used in corners. All these provide motivation for onward and sustained development of centrifuge modelling technologies.

In addition to complexities in construction sequences, there may be other challenges involved in modelling real excavations. For instance, multi-strutted excavations are often highly constrained in terms of ground movement. In such situations, the small strain behaviour of soils may significantly affect ground movement. In most centrifuge models, reconstituted soils are used; these may not reflect the behaviour of in-situ soils. Even with large block models, it is probably not easy to replicate the in-situ structure, stress history and stress state of the soil completely. To illustrate, consider a centrifuge model constructed out of an undisturbed normally consolidated soil block extracted from a depth of 12 m below ground surface (e.g. Liu 2002). At all points within this block, the soil has been subjected to a maximum effective stress corresponding to 12 m depth. Thus, in a centrifuge model, say at 100 g, all points corresponding to prototype depth of less than 12 m will behave as over-consolidated soil. On the other hand, all points corresponding to prototype depth of greater than 12 m will undergo virgin consolidation, and in-situ structure may be lost in the process. Thus, even in such a block model, in-situ conditions may only be reproduced at one depth.

The approaches which have been adopted in model studies of deep excavations appear to reflect an awareness of these problems. Most of the studies conducted to date were directed towards the following aspects of the deep excavation and retaining system:

a. Stability and failure mechanisms e.g. El Nahas & Takemura (2002).
b. Performance comparison and trend study, usually at a largely qualitative level e.g. McNamara & Taylor (2002).
c. Validation of analytical or computational results e.g. Wu et al. (2002b).

Liu (2002) attempted to evaluate ground movement or settlement directly using centrifuge models but concluded that the measured ground surface settlement of the retained soil was unrealistically high, which they attributed to the shortcoming of the "increase-in-g" method, discussed earlier, used in the study. In view of the challenges in reproducing in-situ soil behaviour using block samples or reconstituted soil, one may, in fact, surmise that direct simulation of ground movement using a centrifuge model is likely to pose significant difficulties. A more viable approach may be to relate model ground movement to some model material parameters such as modulus or strength mobilization factor via numerical or simplified mechanistic calculations, and then use the calculations to predict in-situ ground movement using in-situ parameters.

5.2 *Tunnelling*

The development of modelling technology for tunnelling problems mirrors, to a large extent, that for excavations. However, the development of tunnel modelling technology may be even more challenging that for deep excavations, owing to the more severe space constraint within a tunnel.

One of the earliest methods used for modelling tunnel excavation is by reduction in compressed air pressure within a pre-cut tunnel (Mair 1979). This method remains widely used, even in recent years (e.g. Wu et al. 2002a; Yao et al. 2006, Bilotta et al. 2006). The compressed air method has several shortcomings. Firstly, the vertical and lateral components of the pressure on the tunnel wall are equally, so that $K_0 = 1$. Secondly, there is no pressure gradient between the crown and invert, so that the pressure on the crown is equal to that on the invert. For deep tunnels, the absence of a pressure differential may not be significant. However, for shallow tunnel, there is, in reality, significant difference in crown and invert pressure. Thirdly, the use of compressed air does not allow driving of the tunnel to be modelled.

A variant of the compressed air method is the heavy liquid method (Yeo et al. 2010). In this method, a heavy liquid such as zinc chloride is used in place of compressed air. Figure 24 shows the schematic of a model set-up, used by Yeo et al. (2010), in which a heavy liquid is used for tunnel support. As Figures 24 and 25 show, this model set-up also involves the installation of forepoles and pipe-arches spanning the unsupported length of the tunnel. The model forepoles were installed using the guide shown in Figure 25 at 1 g. The objective of this study, which is currently on-going, is to examine the effects of forepoles on the stability and failure mechanisms of unlined tunnel headings.

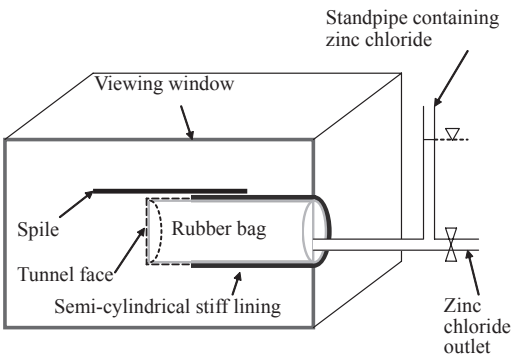

Figure 24. Model tunnel set-up using heavy liquid for tunnel support.

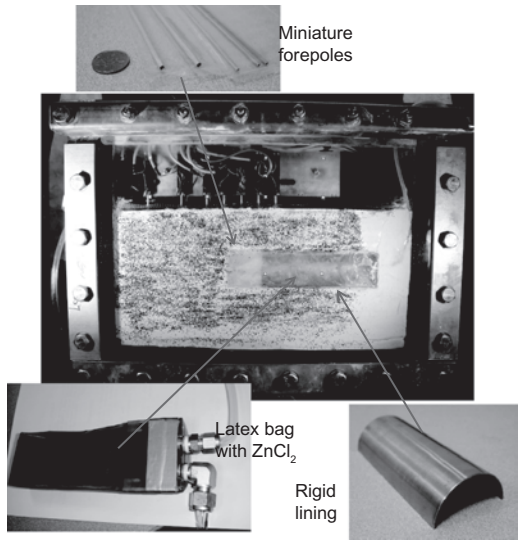

Figure 25. Model set-up for heavy fluid tunnel support.

Other methods have also been developed to model tunnelling in-flight. Nomoto et al. (1994) developed an in-flight shield tunnelling machine, which consisted of a rotary cutting blade at the front of a shield machine pipe to cut the soil at the heading and a screw conveyor to transport the muck out from the model tunnel. Nomoto et al. (1994) also incorporated a lining pipe, which can be pushed forward progressively to simulate installation of lining. Nomoto et al. (1994) experiments were conducted using dry sand, but a similar set-up may conceivably work with soft clays as well.

In tunnelling using a tunnel boring machine, tunnel convergence around the shield is usually limited by the amount of over-cut which affects the gap between the cut section and the shield. However, the ground movement is significantly affected by the earth pressure balance at the tunnel heading and the quality of the grouting between the lining and the soil. Yoshimura et al. (1994) also reported a model shield machine, which is able to simulate changes in the face pressure in-flight.

A similar method, which was implemented in 1 g model tests, was reported by Ahn et al. (2006), who used a 73 mm-diameter screw auger housed within an 80 mm-diameter shield pipe. The tunnelling lining was simulated by a smaller 75 mm-diameter pipe. However, apart from the scale distortion arising from the 1-g conditions, there are several peculiar features of this equipment which may not fully represent field conditions. Firstly, the auger diameter is smaller than the shield pipe diameter. This implies that the cut tunnel diameter

may be less than 80 mm, and the shield pipe has to be forced into a small diameter tunnel. In the field, the cut tunnel is usually slightly larger than the shield, so as to prevent jamming of the shield. This means that there is a small amount of convergence around the shield which is not modelled in the experiment. Secondly, as the Authors noted, the volume loss ratio during liner installation is 12%; this is far larger than that frequently deemed acceptable in the field.

Another method of modelling tunnelling in the laboratory involves the dissolution of a solid chemical infill within the pre-cut tunnel (Sharma et al. 2001). In this method, the tunnel is first pre-cut at 1 g and then infilled with a solid such as polystyrene, which supports the tunnel prior to excavation. Tunnel excavation at high-g is simulated by draining a solvent into the tunnel cavity to dissolve the infill and allowing solvent and infill to flow out through a drainage pipe. Sharma et al.'s (2001) main objective in developing this is to simulate the forward movement of the tunnel heading in a step-by-step fashion. By compartmentalizing the infill and dissolution, tunnel heading excavation can be simulated in a step-by-step progression.

Although this method allows excavation to be segmentalized, it also has drawbacks. Firstly, within a single compartment, the rate and progression of the dissolution process cannot be readily controlled. This may present problems in back-analysis. Secondly, care needs to be exercised in controlling the pressure of the solvent. If this is too high, the tunnel wall may experience a transient over-pressure, which may lead to spurious positive excess pore pressure in the ground.

Non-TBM tunnelling is not necessarily any less challenging. Most non-TBM tunnelling operations involve excavating parts of the tunnel face with progressive lining installation, usually using shotcrete. It is therefore safe to say that we are still some way away from realistically replicating actual tunnelling operations in their entirety.

Furthermore, as in the case of excavations and retaining structures, the approaches that have been used to study tunnelling problems appear to reflect an awareness of current limitations in modelling technology. Most of the experiments to date are directed towards the following aspects:

d. Stability e.g. Bezuijen & van Seters (2002), Wu et al. (2002a).
e. Performance comparison and trend study, usually at a largely qualitative level e.g. Ahn et al. (2006), Yao et al. (2006), Bilotta et al. (2006), Chung et al. (2006).
f. Comparison with existing ground movement relations e.g. Ong et al. (2006).

6 CONCLUSIONS

The foregoing discussion presents some of the ways in which physical modelling has been used to study various classes of problems. In the areas of pipelines, foundations, embankment and slopes, the examples raised show that physical modelling has been used with notable success in problems relating to

1. ultimate capacity or resistance (e.g. pipelines and foundations),
2. failure and instability (e.g. the New Orleans Canal levees), and
3. problems involving very large deformation (e.g. debris flow).

Similarly, in the area of consolidation, large-scale 1 g physical models were shown to be successful in the study of the large disturbance of the soil within the smear zone around the PVD mandrel. The discussion also highlights how physical models can be used together with numerical models to obtain a satisfactory prediction on the behaviour of a trial embankment. Owing to the size limitation of the 1 g physical model, it is not possible to use physical models to study the entire embankment problem. Instead, physical modelling was used to examine a part of the problem, which is not readily addressed by numerical modelling. The findings of the physical modelling exercise are then incorporated into the numerical model to give an overall prediction.

In the area of ground improvement, physical modelling has been used to study the "large-scale" problem of the performance of the improved ground and the "small-scale" problem of the effects of improvement process itself. In terms of the "large-scale" problem, physical modelling has been notably successful in illuminating failure mechanisms and stability characteristics (e.g. Kitazume 2006; Tanaka et al. 2006). For working load performance characteristics, physical modelling results were not often scaled directly to prototype level. Instead, a trend or comparative study is used. Alternatively, physical modelling results are used to provide the mechanistic inspiration for computations, which are then applied to the prototype problem. Similar approaches are also used to study excavations and underground constructions.

The "small-scale" problems, which are studied using centrifuge modelling, are usually those which involve very large displacement, such as mixing processes as well as disturbance, set-up and smearing of soil due to sand pile driving. All these problems are not readily studied using numerical modelling.

All these suggest that, at least in the area of soft clay, physical modelling has contributed

significantly to illuminating problems relating to failure and large displacement. One may also venture to speculate that, apart from the effective stress level and preconsolidation pressure, perhaps, other in-situ factors such as the fabric and structure do not affect these problems as much as they do for problems involving working load conditions. On the other hand, for working load problems, ground movement may be smaller and perhaps affected more by in-situ soil conditions of the soil. For instance, Tan et al. (2002) showed that disturbance to soil samples only minimally affects their strength, as long as effective stress is preserved. On the other hand, the modulus is much more significantly affected and cannot be completely recovered even if effective stress level is reproduced. Thus, whilst centrifuge modelling with remoulded soils may allow in-situ effective stress levels and overconsolidation ratio to be replicated, other in-situ soil condition parameters, which may affect stress-strain behaviour at working load level, may not be so readily replicated. If this is indeed true, then physical modelling may indeed work better under conditions at or near failure or where deformations are large. Numerical modelling, on the other hand, may work better under working load conditions or where strains and deformations are limited. This, if true, would imply that physical and numerical modelling may be better regarded as complementary rather than competitive approaches.

It would also provide impetus to physical modellers to improve their modelling of natural soils. A possible start to this is to develop ways of characterizing, rapidly and reliably, not just the strength, but also some aspects of the stress-strain behaviour, such as a representative modulus, at various points of the soil in the physical model. With this, we would at least know how the stiffness of our remoulded soil models compare with the soils in the field.

ACKNOWLEDGEMENTS

The first Author would like to thank the National University of Singapore for its continuous support in the form of research scholarships to graduate students. Many of these students' works, especially that of Chen-Hui Lee, Jiangtao Yi, Jian Chen and Chong-Hun Yeo, have contributed significantly to the discussion on ground improvement and underground constructions. The NUS research scholarships provided to these students are also gratefully acknowledged.

The second Author wishes to thank the Brazilian Research Council (CNPq), the Rio de Janeiro Research Council (Faperj) and PETROBRAS Oil Company for their continuous support. Thanks are also due to Dr. José Renato Oliveira (IME) and Dr. Maria Cascão Almeida (POLI/UFRJ) for discussions during the preparation of this report. Mr. Ricardo Garske has also contributed with interesting suggestions related to pipeline studies carried out at COPPE-UFRJ.

The third Author also wishes to thank the Australia Research Council (Australia) for its continuous support and the Thailand Airport Authority for providing the trial embankments data. A number of past research students of Prof. Indraratna, namely, Dr. C. Rujikiatkamjorn, Dr. I.W. Redana and Dr. C. Bamunawita have also contributed to the contents of this keynote paper through their research work. Much of the contents reported in this paper here is also described in greater detail in a number of Canadian Geotechnical and ASCE Journals.

REFERENCES

Ahn, S.K., Chapman, D.N., Chan, A.H.C. & Hunt, D.V.L. 2006. Model tests for investigating ground movements caused by multiple tunnelling in soft ground. In *Proceedings of the International Conference on Physical Modelling in Geotechnics (6th ICPMG '06)*, August 2006, Hong Kong SAR, China, 1133–1137.

Allersma, H.G.B. 1998. Development of cheap equipment for small centrifuges. In *Proceedings of International Conference Centrifuge '98,* Sept 1998, 85–90.

Almeida, M.S.S., Costa, A.M., Amaral, C.S., Benjamin, A.C., Noronha, Jr. D.B., Futai, M.M. & Mello, J.R. 2001. Pipeline failure on very soft clay. *3rd International Conference on Soft Soil Engineering*: 131–138. Hong Kong: Balkema.

Al-Tabbaa, A. & Evans, C.W. 1999. Laboratory-scale soil mixing of a contaminated site. *Ground Improvement* 3(3): 119–134.

Babasaki, R., Terashi, M., Suzuki, T., Maekawa, A., Kawamura, M. & Fukazawa, E. 1996. JGS TC Report: Factor influencing the strength of the improved soil. *Grouting and Deep Mixing, Proceedings of IS-Tokyo 96', the Second International Conference on Ground Improvement Geosystems, Tokyo, 14–17 May, Yonekura, Terashi & Shibazaki (eds.)*, Vol. 1, 913–924.

Bezuijen, A. & van Seters, A. 2002. The stability of a tunnel face in soft clay. *Proceedings of the International Conference on Physical Modelling in Geotechnics (ICPMG '02)*, July 2002, St. John's, Newfoundland, Canada, 791–796.

Bilotta, E., Bitetti, B., McNamara, A.M. & Taylor, R. N. 2006. Micropiles to reduce ground movements induced by tunnelling. In *Proceedings of the International Conference on Physical Modelling in Geotechnics (6th ICPMG '06)*, August 2006, Hong Kong SAR, China, 1139–1144.

Bo, M.W., Chu, J., Low, B.K. & Choa, V. 2003. *Soil improvement; prefabricated vertical drain techniques*, Thomson Learning, Singapore.

Bolton, M.D. & Powrie, W. 1987. The collapse of diaphragm walls retaining clay *Géotechnique* 37(3): 335–353.

Boylan, N., Gaudin, C., White, D.J., Randolph, M.F. & Schneider, J.A. 2009. Geotechnical centrifuge modelling techniques for submarine slides, In *Proceedings of the ASME 2009 28th International Conference on Ocean, Offshore and Arctic Engineering OMAE2009*, May 2009, Honolulu, Hawaii, USA.

Bruce, D.A. 2001. Practitioner's guide to the deep mixing method. *Ground Improvement* 5(3): 95–100.

Bruton, D.A.S., White, D.J., Cheuk, J.C.Y., Bolton, M.D. & Carr, M. 2006. Pipe/Soil interaction behavior during lateral buckling, including large-amplitude cyclic displacement test by the SAFEBUCK JIP, *Offshore Technology Conference (OTC17944)*, May 2006, Houston, Texas, U.S.A.

Bruton, D.A.S., White, D.J., Carr, M. & Cheuk, J.C.Y. 2008. Pipe-Soil interaction during lateral buckling and pipeline walking—The SAFEBUCK JIP. *Offshore Technology Conference (OTC19589)*, May 2008, Houston, Texas, U.S.A.

CDIT. 2002. *The deep mixing method: principle design and construction.* Coastal Development Institute of Technology (CDIT), Japan.

Chen, W. & Randolph, M.F. 2007. Uplift capacity of suction caissons under sustained and cyclic loading in soft clay, *Journal of Geotechnical and Geoenvironmental Engineering*, 133(11): 1352–1363.

Cheuk, J.C.Y., Take, W.A., Bolton, M.D., & Oliveira, J.R.M.S. 2007. Soil restraint onbuckling oil and gas pipelines buried in lumpy clay fill, *Engineering Structures* 29: 973–982.

Chia, B.H. & Tan, T.S. 1993. The use of jet grouting in the construction of drains in soft soils. *Innovation in infrastructure development: Proc. 11th Conf. of ASEAN Fed. of Engng. Organisations*, 20–26.

Chung, K.H., Mair, R.J. & Choy, C.K. 2006. Centrifuge modelling of pile-tunnel interaction. In *Proceedings of the International Conference on Physical Modelling in Geotechnics (6th ICPMG '06)*, August 2006, Hong Kong SAR, China, 1151–1156.

COI 2005. *Report of the Committee of Inquiry into the Incident at the MRT Circle Line Worksite that led to the Collapse of the Nicoll Highway on 20 April 2004*, Ministry of Manpower, Singapore.

Dingle, H.R.C., White, D.J., & Gaudin, C. 2008. Mechanisms of pipe embedment and lateral breakout on soft clay, *Canadian Geotechnical Journal* 45: 636–652, May 2008.

Dong, J., Hiroi, K. & Nakamura, K. 1996. Experimental study on behaviour of composite ground improved by deep mixing method under lateral earth pressure. *Grouting and Deep Mixing, Proceedings of IS-Tokyo 96', the Second International Conference on Ground Improvement Geosystems,* Tokyo, May 1996, Vol. 1, 585–590.

El Nahas, A. & Takemura, J. 2002. External stability of open excavations in soft clay with DM self-supported walls. In *Proceedings of the International Conference on Physical Modelling in Geotechnics (ICPMG '02)*, July 2002, St. John's, Newfoundland, Canada, 835–840.

Gallavresi, F. 1992. Grouting improvement of foundation soils. *Grouting, soil improvement and geosynthetics: Proc. Conf. sponsored by Geotech. Engng. Div., ASCE*, Vol. 1, 1–38.

Gaudin, C., Garnier, J., Gaudicheau, P. & Rault, G. 2002. Use of a robot for in-flight excavation in front of an embedded wall. In *Proceedings of the International Conference on Physical Modelling in Geotechnics (ICPMG '02)*, July 2002, St. John's, Newfoundland, Canada, 77–82.

Ghahremani, M. & Brennan, A.J. 2009. Consolidation of lumpy clay backfill over buried pipelines, In *Proceedings of the ASME 2009 28th International Conference on Ocean, Offshore and Arctic Engineering OMAE2009*, May 2009, Honolulu, Hawaii, USA.

Goh, T.L. 2003. *Stabilisation of an Excavation by an Embedded Improved Soil Berm*. Ph.D Thesis, National University of Singapore.

Gourvenec, S., Acosta-Martinez, H.E. & Randolph, M.F. 2009. Experimental study of uplift resistance of shallow skirted foundations in clay under transient and sustained concentric loading, *Géotechnique* 59(6): 525–537.

Hayashi, H. & Nishimoto, S. 2006. Performance of deep mixing method for box culvert foundations. In *Proceedings of the International Conference on Physical Modelling in Geotechnics (6th ICPMG '06)*, August 2006, Hong Kong SAR, China, 507–512.

Hird, C.C., Pyrah, I.C. & Russell, D. 1992. Finite element modelling of vertical drains beneath embankments on soft ground. *Géotechnique* 42(3): 499–511.

Inagaki, M., Abe, T., Yamamoto, M., Nozu, M., Yanagawa, Y. & Li, L. 2002. Behavior of cement deep mixing columns under road embankment. In *Proceedings of the International Conference on Physical Modelling in Geotechnics (ICPMG '02)*, July 2002, St. John's, Newfoundland, Canada, 967–972.

Indraratna, B., Balasubramaniam, A.S. & Balachandran, S. 1992. Performance of test embankment constructed to failure on soft marine clay. *J. Geotech. Eng., ASCE*: 118, 12–33.

Indraratna, B. & Redana, I.W. 1997. Plane Strain Modelling of Smear Effects associated with Vertical Drains. *J. Geotech. & Geoenv. Eng., ASCE* 123(5): 474–478.

Indraratna, B., & Redana, I.W. 1998. Laboratory determination of smear zone due to vertical drain installation. *J. Geotech. Eng., ASCE* 125(1): 96–99.

Indraratna, B. & Redana, I.W. 2000. Numerical modeling of vertical drains with smear and well resistance installed in soft clay. *Canadian Geotechnical Journal* 37: 132–145.

Indraratna, B., Redana, I. & Salim, W. 2000. Behaviour of Soft Clay Foundations stabilised with Vertical Drains. *Int. Conf. on Soft Ground Technology*, Noordwijkerhout, Netherlands, June 2000, 31–41.

Indraratna, B., Rujikiatkamjorn, C., & Sathananthan, I. 2005a. Analytical and numerical solutions for a single vertical drain including the effects of vacuum preloading. *Canadian Geotechnical Journal,* 42: 994–1014.

Indraratna, B., Rujikiatkamjorn, C., & Sathananthan, I. 2005b. Radial consolidation of clay using compressibility indices and varying horizontal permeability. *Canadian Geotechinical Journal*, 42: 1330–1341.

Indraratna, B., Rujikiatkamjorn, C., Balasubramaniam, A.S. & Wijeyakulasuriya, V. 2005c. Predictions and observations of soft clay foundations stabilized with geosynthetic drains and vacuum surcharge. *Ground Improvement—Case Histories Book (Volume 3*),

Edited by Indraratna, B. & Chu, J., Elsevier, London, 199–230.

Jamiolkowski, M., Lancellotta, R. & Wolski, W. 1983. Precompression and speeding up consolidation. In *Proceedings of 8th European Conference on Soil Mechanics and Foundoundtions*, Helsinki, Finland, 3, 1201–1206.

Juneja, A. 2002. *Centrifuge model study of the effects of sand compaction pile installation on soft clay ground*, Ph.D. Thesis, National University of Singapore.

Kim, S.S., Kim, J.K., Byun, K.J. & Sym, S.H. 2004. A case study on the sand compaction pile (SCP) at Pusan Newport Project in Korea. In *Proceedings of the Fourteenth (2004) International Offshore and Polar Engineering Conference*, May 2004, Toulon, France, 477–484.

Kim, S.S., Shin, H.Y., Han, S.J., Kim, J.K. & Lee, M.H. 2006. Estimation of stress concentration characteristics in composite ground reinforced by sand compaction piles with a low replacement ratio. In *Proceedings of the Sixteenth (2006) International Offshore and Polar Engineering Conference*, May 2006, San Francisco, California, USA, 596–603.

Kimura, T., Takemura, J., Hiro-oka, A., Okamura, M. & Park, J. 1994. Excavation in soft clay using an in-flight excavator. In *Proceedings of International Conference Centrifuge '94*, Aug 1994, Singapore, 649–654.

Kitazume, M. 2006. Application of physical modelling for investigating ground failure pattern. In *Proceedings of the International Conference on Physical Modelling in Geotechnics (6th ICPMG '06)*, August 2006, Hong Kong SAR, China, 63–74.

König, D. 2002. Modeling of deep excavation. In *Proceedings of the International Conference on Physical Modelling in Geotechnics (ICPMG '02)*, July 2002, St. John's, Newfoundland, Canada, 83–88.

Kusakabe, O. 2002. Modelling soil improvement methods in soft clay. In *Proceedings of the International Conference on Physical Modelling in Geotechnics (ICPMG '02)*, July 2002, St. John's, Newfoundland, Canada, 31–40.

Larsson, S., Dahlström, M. & Nilsson, B. 2005a. Uniformity of lime-cement columns for deep mixing: a field study. *Ground Improvement* 9(1): 1–15.

Larsson, S., Stille, H. & Olsson, L. 2005b. On horizontal variability in lime-cement columns in deep mixing. *Géotechnique* 55(1): 33–44.

Lee, C.J., Kim, J.S., Yoo, N.J. & Park, B.S. 2006a. Behaviour of sand compaction piles (SCPs) with low replacement ratios. In *Proceedings of the International Conference on Physical Modelling in Geotechnics (6th ICPMG '06)*, August 2006, Hong Kong SAR, China, 539–544.

Lee, F.H., Juneja, A. & Tan, T.S. 2004. Stress and pore pressure changes due to sand compaction pile installation in soft clay. *Géotechnique* 54: 1–16.

Lee, F.H., Juneja, A., Tan, T.S., Yong, K.Y. & Ng, Y.W. 2002. Excess pore pressure due to sand compaction pile installation in soft clay. In *Proceedings of the International Conference on Physical Modelling in Geotechnics (ICPMG '02)*, July 2002, St. John's, Newfoundland, Canada, 955–960.

Lee, F.H., Lee, C.H., Dasari, G.R. & Zheng, J. 2010. Centrifuge Study on Uniformity of Wet Deep Mixing. *International Journal of Physical Modelling in Geotechnics*. (in press).

Lee, F.H., Lee, Y., Chew, S.H. & Yong, K.Y. 2005. Strength and modulus of marine clay-cement mixes. *Journal of Geotechnical And Geoenvironmental Engineering*, *ASCE*, 131(2): 178–186.

Lee, F.H., Lee, C.H. & Dasari, G.R. 2006b. Centrifuge modelling of wet deep mixing processes in soft clays. *Géotechnique* 56(10): 677–691.

Lee, F.H., Ng, Y.W. & Yong, K.Y. 2001. Effects of installation method on sand compaction piles in clay in the centrifuge. *Geotechnical Testing Journal* 24(3): 314–323.

Lehane, B.M., Gaudin, C., Richards, D.J., & Rattley, M.J. 2008. Rate effects on the vertical uplift capacity of footings founded in clay, *Géotechnique* 8(1): 13–21.

Liu, J. 2002. Centrifugal modelling of multi-braced and unbraced excavation failures. In *Proceedings of the International Conference on Physical Modelling in Geotechnics (ICPMG '02)*, July 2002, St. John's, Newfoundland, Canada, 841 - 844.

Loh, C.K., Tan, T.S. & Lee, F.H. 1998. Three-dimensional excavation tests. In *Proceedings of International Conference Centrifuge '98*, Sept 1998, Tokyo, Japan, 649–654.

Mair, R.J. 1979. *Centrifuge modelling of tunnel construction in soft clay*. PhD thesis, University of Cambridge.

McNamara, A.M. & Taylor, R.N. 2002. Use of heave reducing piles to control ground movements around excavations. In *Proceedings of the International Conference on Physical Modelling in Geotechnics (ICPMG '02)*, July 2002, St. John's, Newfoundland, Canada, 847–852.

Nakagawa, S., Kamegaya, I., Kureha, K. & Yoshida, T. 1996. Case History and Behavioural Analyses of Braced Large Scale Open Excavation Area. In *Geotechnical aspects of underground construction in soft ground: proceedings of the international symposium on geotechnical aspects of underground construction in soft ground*, 179–184.

Ng, Y.W., Lee, F.H. & Yong, K.Y. 1998. Development of an in-flight sand compaction piles (SCPs) installer. *Proceedings of International Conference Centrifuge' 98*: 837–843.

Nishida, K., Koga, Y. & Miura, N. (1996). Energy consideration of the dry jet mixing methods. *Grouting and Deep Mixing, Proceedings of IS-Tokyo 96', the Second International Conference on Ground Improvement Geosystems*, Tokyo, 14–17 May, Vol. 1, 643–648.

Nomoto, T., Mito, K., Imamura, S., Ueno, K. & Kusakabe, O. 1994. A miniature shield tunnelling machine for a centrifuge. In *Proceedings of International Conference Centrifuge '94*, Singapore, 699–704.

Ong, C.W., Leung, C.F., Yong, K.Y. & Chow, Y.K. 2006. Pile responses due to tunnelling in clay. In *Proceedings of the International Conference on Physical Modelling in Geotechnics (6th ICPMG '06)*, August 2006, Hong Kong SAR, China, 1177–1182.

Oliveira, J.R.M.S., Almeida, M.C.F., Almeida, M.S.S., Borges, R.G., Amaral, C.S. & Costa, A.M. 2005. Physical and Numerical Modelling of Lateral Buckling of a Pipeline in Very Soft Clay. In *Proceedings of the Int. Symp. on Frontiers Offshore Geotechnics (ISFOG)*, Perth.

Oliveira, J.R.M.S., Almeida, M.S.S., Marques, M.E.S. & Almeida, M.C.F. 2006. Undrained strength of very

soft clay soils used in pipeline studies in the centrifuge. In *Proceedings of the International Conference on Physical Modelling in Geotechnics (6th ICPMG '06)*, August 2006, Hong Kong SAR, China.

Oliveira, J.R.M.S., Borges, R.G., Feitoza, J., Almeida, M.C.F. & Almeida, M.S.S. 2009. Geotechnical response of pipelines shallowly embedded in clayey and sandy soils, *Rio Pipeline Conference & Exposition 2009*, IBP1508–09.

Powrie, W., Richards, D.J. & Kantartzi, C. 1994. Modelling diaphragm wall installation and excavation process. In *Proceedings of International Conference Centrifuge '94*, Aug 1994, 655–661.

Rattley, M.J., Richards, D.J. & Lehane, B.M. (2008). Uplift Performance of Transmission Tower Foundations Embedded in Clay, *Journal of Geotechnical and Geoenvironmental Engineering, ASCE*, April 2008: 531–540.

Sakai, S., Nakano, K. & Hayashi. Y. 1994. Quality of the Soil Cement Columns Constructed by the Single Rod Type Soil Improvement Rig: Report 2. *Summaries of technical papers of Annual Meeting Architectural Institute of Japan. B, Structures I 1994:1517–1518. URL http://ci.nii.ac.jp/naid/110004204161/en/, (accessed 24 Mar 2008, paper in Japanese)*.

Sasanakul, I., Vanadit-Ellis, W., Sharp, M., Abdoun, T., Ubilla, J., Steedman, S. & Stone, K. 2008. New Orleans Levee System Performance during Hurricane Katrina: 17th Street Canal and Orleans Canal North, In *ASCE Journal of Geotechnical and Geoenvironmental Engineering. Special Issue on the Performance of Geo-Systems during Hurricane Katrina*, 134(5): 657–667.

Sathananthan, I. & Indraratna, B. 2006. Laboratory Evaluation of Smear Zone and Correlation between Permeability and Moisture Content, *J. of Geotechnical & Geoenvironmental Engineering, ASCE* 132(7): 942–945.

Saye, S.R. 2003. Assessment of soil disturbance by the installation of displacement sand drains and prefabricated vertical drains. *Geotechnical Special Publication No. 119*, ASCE, 325–362.

Sharma, J.S., Bolton, M.D. & Boyle, R.E. 2001. A new technique for simulation of tunnel excavation in a centrifuge. *Geotechnical Testing Journal* 24(4): 343–349.

Song, Z., Hu, Y., O' Loughlin, C. & Randolph, M.F. 2009. Loss in Anchor Embedment during Plate Anchor Keying in Clay, In *Journal of Geotechnical and Geoenvironmental Engineering ASCE*, October 2009, 1475–1485.

Takahashi, H., Kitazume, M. & Ishibashi, S. 2006. Effect of deep mixing wall spacing on liquefaction mitigation. In *Proceedings of the International Conference on Physical Modelling in Geotechnics (6th ICPMG '06)*, August 2006, Hong Kong SAR, China, 585–590.

Tan, T.S., Lee, F.H., Chong, P.T. & Tanaka, H. 2002. Effect of Sampling Disturbance on the Strength and Stiffness of Singapore Marine Clay. *Journal Of Geotechnical and Geoenvironmental Engineering*, *ASCE* 128(11): 898–906.

Tanaka, T., Asuma, K., Suemasa, N., Kuboi, K. & Daitoh, K. 2006. Centrifuge model tests on the seismic stability of FGC deep mixing ground. In *Proceedings of the International Conference on Physical Modelling in Geotechnics (6th ICPMG '06)*, August 2006, Hong Kong SAR, China, 1107–1112.

Toyosawa, Y., Horii, N., Tamate, S., Suemasa, N. & Katada, T. 1998. Failure mechanism of anchored retaining wall. In *Proceedings of International Conference Centrifuge '98*, Sept 1998, Tokyo, Japan, 667–672.

Ubilla, J., Abdoun, T., Sasanakul, I., Sharp, M., Steedman, S., & Vanadit-Ellis, W. 2008. New Orleans Levee System Performance during Hurricane Katrina: London Avenue and Orleans Canal South, In *ASCE Journal of Geotechnical and Geoenvironmental Engineering. Special Issue on the Performance of Geo-Systems during Hurricane Katrina* 134(5): 668–680.

Weber, T.M., Laue, J. & Springman, S.M. 2006. Centrifuge modelling of sand compaction piles in soft clay under embankment load. In *Proceedings of the International Conference on Physical Modelling in Geotechnics (6th ICPMG '06)*, August 2006, Hong Kong SAR, China, 603–608.

Weber, T.M., Plötze, M., Laue, J., Peschke, G. & Springman, S.M. 2009. Smear zone identification and soil properties around stone columns constructed in-flight in centrifuge model tests. *Géotechnique* 59(3): 197–206.

Wu, B.R., Lee, C.J. & Chiou, S.Y. 2002a. Prediction of ground movements around parallel tunnels. *Proceedings of the International Conference on Physical Modelling in Geotechnics (ICPMG '02)*, July 2002, St. John's, Newfoundland, Canada, 809–814.

Wu, W., Xu, S. & Zhang, H. 2002b. Studies on mechanism of pile anchor support system in deep pits. In *Proceedings of the International Conference on Physical Modelling in Geotechnics (ICPMG '02)*, July 2002, St. John's, Newfoundland, Canada, 853–857.

Yao, J., Taylor, R.N. & McNamara, A.M. 2006. The effects of bored pile excavation on existing tunnels. In *Proceedings of the International Conference on Physical Modelling in Geotechnics (6th ICPMG '06)*, August 2006, Hong Kong SAR, China, 1195–1200.

Yeo, C.H., Hegde, A., Lee, F.H. & Juneja, A. (2010). Centrifuge modelling of steel pipe umbrella arch for tunnelling in clay. In *Proceedings of the 7th International Conference on Physical Modelling in Geotechnics (ICPMG '10)*. June 2010, Zurich, Switzerland (submitted for publication).

Yi, J., Goh, S.H. & Lee, F.H. 2010. Centrifuge study on the "set-up" effect induced by the sand compaction pile installation. In *Proceedings of the 7th International Conference on Physical Modelling in Geotechnics (ICPMG '10)*. June 2010, Zurich, Switzerland (submitted for publication).

Yin, J.H. & Fang, Z. 2006. Physical modeling of the consolidation of soft soil ground installed with vertical drains or deep cement mixing (DCM) soil columns. In *Proceedings of the International Conference on Physical Modelling in Geotechnics (6th ICPMG '06)*, August 2006, Hong Kong SAR, China, 609–614.

Yoshimura, H., Miyabe, K. & Tohda, J. 1994. Response of a tunnel lining due to an adjacent twin shield tunneling. In *Proceedings of International Conference Centrifuge '94*, Singapore, 693–698.

Zhang, Y.D., Tan, T.S. & Leung, C.F. 2008. Undrained End Bearing Capacity of an Improved Soil Berm in an Excavation. *Soils and Foundations* 48: 433–446.

Zhu, W. & Yi, J. 1988. Application of centrifuge modelling to study a failed quay wall. In *Proceedings International Conference Centrifuge 88*, Paris: 415–419.

Physical Modelling in Geotechnics – Springman, Laue & Seward (eds)
© 2010 Taylor & Francis Group, London, ISBN 978-0-415-59288-8

Physical modelling with industry—overview of practices and benefits

C. Gaudin & D.J. White
Centre for Offshore Foundation Systems, University of Western Australia, Perth, Australia

A. Bezuijen & P.E.L. Schaminée
Deltares, Delft, The Netherlands

J. Garnier
Laboratoire Central des Ponts et Chaussées, Nantes, France

ABSTRACT: Collaboration with industry has become a significant part of the activity of physical modelling research centres over the last decade. This results from mutual needs from industry partners to gain access to expertise and capabilities not existing in the industry and from research institutions to gain insight in practical research and to secure funding to support long-term experimental developments. The paper presents experiences shared by three research institutions, the Centre for Offshore Foundation Systems (COFS) at UWA, Deltares and the Laboratoire Central des Ponts et Chaussées (LCPC) in collaborating with industry. The different forms of collaboration and interaction are discussed and the various benefits of industry collaborations are evaluated and discussed.

1 INTRODUCTION

1.1 *Physical modelling and industry*

Geotechnical physical modelling, and in particular centrifuge modelling, is often conducted at Research Institutes (RI) as part of a contract or collaboration with industry, for design or for research and development. This type of physical modelling forms an increasingly important part of the activity of many research institutes, and in some areas of industry it represents an important design tool. For the Symposium on the Application of Centrifuge Modelling to Geotechnical Design, held in Manchester in 1984, W.H. Craig wrote that:

> *"The larger or more novel a design project is, the more attractive are the potential benefits of realistic model testing as an* integral *part of the design process… …that model can be useful and cost effective in contributing to the expedient development and assessment of a design and to its subsequent acceptance, refinement or rejection."*

Craig (1984) reviewed the design studies conducted using the Manchester centrifuge during the preceding 12 years. Subsequent reviews of other applications of physical modelling to geotechnical design are presented by Murff (1996) and Martin (2001).

These reviews highlight the technical contributions of physical modelling to the practice of geotechnical design. There are other types of benefit that arise from this form of collaboration, which are explored in this chapter. The purpose of the paper is to present the practice and benefits of collaboration between industry and institutes that host large physical modelling facilities. It is useful to reflect on this practice, since industry collaboration potentially provides the necessary sustenance of large facilities. Indeed, in the closing sentence of his 1984 review, Craig wrote:

> *"If centrifuge work is to continue, it should have a positive role* beyond *phenomenological studies and the development of design rules by parametric variations in idealised, non specific models."*

One interpretation of this statement is that it was intended to highlight that there is only a finite number of idealised centrifuge tests to be conducted for phenomenological studies. However, the wide range of topics and the large number of papers presented in this conference suggest that there remains no shortage of phenomenological studies to be tackled.

An alternative interpretation is that Craig was proposing that the other benefits which arise from interaction with industry (for both parties)

would sustain centrifuge activity, as much as would purely scientific enquiry. In this paper, we explore the benefits and best practice of industrial collaboration in greater depth. We have attempted to describe the less tangible outcomes of collaborative physical modelling, and propose some aspects that could be described as best practice. These observations are based on our experience at three long-established centrifuge modelling facilities that have close engagement with industry.

1.2 *Background to RI-industry relationships*

Three types of funding can be distinguished for physical modelling research:

1. Competitive public research funding from fundamental or applied research. This type of research is especially important for physical modelling centres related to universities, such as COFS.
2. Project oriented research commissioned by the government. This type of funding is of importance for the Deltares physical modelling centre and for the LCPC.
3. Direct industry funded research, which is of importance for the three centres.

With the general trend of decreasing public research funding, research groups are increasingly reliant on industry support to stabilise their operating budgets. This trend is observed worldwide at geotechnical physical modelling centres, but also across various fields of research and science (Lillywhite et al. 2005). Consequently, the recent years have seen an increasing interaction between universities and research centres, defined here as research institutions), and industry. This relationship has yet to be analysed.

Meanwhile, the relationship between research and industry is recognised as vital for the development of innovation and to be an increasingly significant area of research. Although analysts and policymakers are becoming more interested in understanding it and measuring its benefits, little research has been undertaken so far (Scott et al. 2001).

The main focus of the research performed has been on measuring the benefits flowing from RI-industry collaboration to the wider community (Lillywhite et al. 2005), on the impact of industry collaboration on academic research (Banal-Estanol et al. 2008), and on the benefits for both RI and industry (Lee 2000).

It appears that the quantification of the benefits of RI-industry relationship is a complex process, which is difficult to determine using simple models. It is however recognised that both participants realise significant benefit, some of which is expected and some of which is not (Lee 2000). The industry partner gains benefit by (i) gaining access to new research and discoveries, (ii) solving specific technical or design problems, (iii) re-orienting their research agenda and (iv) recruiting graduates from the universities. Researchers also benefit from collaboration with industry by (i) bringing economic benefit to their institutions, securing funding for students and equipment, (ii) gaining insight into topical areas in which to pursue fundamental research, (iii) gaining insight into practical problems and industry concerns, and (iv) increasing publication levels.

Some of these benefits are still, however, debated, and they do not necessarily apply across all disciplines. In particular, the impact of an RI-industry relationship on academic publications, which has become the principal parameter to evaluate academic performance, has been discussed extensively by Banal-Estanol et al. (2008). Averaged across all disciplines, it appears that researchers with no industrial involvement are likely to be those with the least research output. However, very high levels of industrial involvement and confidential research may affect research productivity by reducing the number of publications.

The practices and benefits of RI-industry relationship within the geotechnical physical modelling community have not previously been documented, beside the numerous papers describing the technical outcomes of research projects funded by industry. This paper attempts to provide an overview of the current practices in engaging with industry supported by key data from three different centrifuge centres—COFS/UWA in Australia (Centre for Offshore Foundation Systems), Deltares in The Netherlands and LCPC in France (Laboratoire Central des Ponts et Chaussées)—in order to evaluate the benefits that may arise for both RI and industry.

As RI-industry relationships are expected to increase even more in the next few years, the paper also aims to establish the ground for a wider study and survey, the outcomes of which will be disseminated to academia, industry and funding institutions with the wider objectives of (i) highlighting for industry to potential benefits of increased engagement with academia, (ii) advising funding institutions of the potential impact of supporting RI-industry collaborations and (iii) suggesting methods to achieve the first two objectives to academia.

2 ENGAGING IN INDUSTRY COLLABORATION

2.1 *Motivations and approach*

Motivations for RIs to collaborate with industry are numerous, and indeed vary, depending on the nature of the institutions: either universities, public

research centres or private research centres. The main motivations identified by COFS, which is a research centre, integrated into a University, are in decreasing order of importance:

1. To secure funding to perform research, to maintain strong technical support and to maintain the technological level of the facility.
2. To gain insight into practical problems that are relevant for future research projects and teaching.
3. To train postgraduate students and create job placement opportunities.
4. To establish contacts with industry and improve our track record of industry interaction for future funding applications. This motivation is specific to the Australian funding system, with joint RI-industry funding applications (Australian Research Council, ARC Linkage) exhibiting a significant higher success rate that solely academic funding application (ARC Discovery) (respectively 50% and 20%).

Deltares is founded with the aim to be a bridge between fundamental research, as it is performed in universities, and applications, as they are commissioned by government and industry. This means that performing physical model tests for industry is part of its 'raison d'être'. Being a different style of institute, there is also some difference in the motivation (order), compared with COFS:

1. To implement academic knowledge into industry projects.
2. To increase fundamental research by industry, using contacts with industry and improve our track record of industry interaction for future funding applications.
3. To gain insight into practical problems that are relevant for future research projects.
4 To work on an international level and prove that the centrifuge is a useful tool for solving geotechnical problems.

LCPC is a third and different example of Research Institute, since this laboratory is under the regulatory authority of two ministries: the Ministry in charge of research and teaching on one side and the Ministry in charge of ecology, energy and sustainable development on the other. It has to try to meet two rather different obligations and is assessed according to two different criteria:

1. To carry out high level scientific research in civil and environmental engineering and to produce scientific papers that will be published in international journals.
2. To carry out applied research to answer social and end-user demands and needs, and to disseminate research results usable by engineers in practice.

This situation may appear to be uncomfortable but actually has a very significant positive influence. It forces the laboratory and its researchers and engineers to develop academic research programmes with the aim of solving very practical questions. Links and cooperation with industry are both natural and vital for all departments of LCPC.

As the motivations are different between the three centres, so is the approach to initiate collaboration with industry. COFS, which is specialised in offshore geotechnics, has engaged over the last five years by adopting an active approach, which can be summarised around the following three aspects:

1. A significant presence in industry focused conferences such as the Offshore Technology Conference (OTC), International Symposium on Offshore and Polar Engineering (ISOPE) and International Conference on Ocean, Offshore and Artic Engineering (OMAE) (in the offshore area) with the presentation of papers describing past industry collaboration and research projects suitable to attract industry attention.
2. The organisation of specific events to facilitate contact with industry such as 'showcase' or 'Open Day' events at the RI or presentations within the seminar series organised by the local engineering professional body.
3. The development of targeted physical modelling courses within the curriculum of the university and the training of students on the facility.

While the first two are aiming at initiating collaboration with industry on a short term basis, the third one aims to increase the awareness of the possibilities and capabilities of physical modelling progressively within the engineering community.

The Deltares approach uses primarily the network of its employees to acquire industry projects. The total scope of activities is wider than offshore. As a consequence, the main activities of Deltares to acquire industry project collaboration are:

1. A significant presence in persons and publications at physical modelling conferences and general geotechnical conferences.
2. Regular meetings between the personnel responsible for the physical modelling with the division directors in the 'model team' to discuss what new leads were established and what must be the follow up to transform these leads into contracts. As a result of this, there is close contact between the 'experimental modellers' and the project leaders, who have the contacts with the clients.
3. The creation of a 'knowledge centre' between Deltares and the Delft University of Technology, where it is possible that students perform tests in the Deltares centrifuge for their projects and/or play a role in industry projects.

As with COFS, the purpose of the last item is to increase the awareness of the possibilities of physical modelling in the longer term.

The LCPC approach used to rely on direct interaction with major industry. Since 1985, when its geotechnical centrifuge was put in operation, LCPC was awarded direct research contracts with industrial partners, including large centrifuge modelling programmes. Most of these industry projects come from oil companies (North American or French) and relate to problems of foundation or anchoring of offshore structures.

Recently, the approach has changed and LCPC relies mainly on new funding schemes developed at a national level to increase the involvement of industry in research in all domains of science.

- In January 2007, the Agence Nationale de la Recherche (ANR) (France's National Research Agency) was created with missions of founding selected projects on a competitive basis each year (www.agence-nationale-recherche.fr). Its annual budget is around one billion Euros and six domains are covered: biology and health; ecosystems and sustainable development; durable energy and environment; engineering and processing, ICT, and human sciences. The presence among the partners of at least one industrial company is required in most ANR calls. As examples, the LCPC centrifuge group is currently cooperating with industry in ANR funded projects on cyclic loading of piles (SOLCYP) and on the vulnerability of constructions to earthquakes (ARVISE).
- In July 2005, 67 competitiveness cluster labels have been attributed to pools of companies, research centres and educational institutions working in partnership (www.competitivite.gouv.fr). Twice a year, these clusters may submit cooperative research projects to get funding from FUI (Fond Unique Interministériel). These projects must involve at least two industry partners and must be managed by an industrial partner. The fund coming from five ministries contains 495 millions Euros for the period 2009–2011.
- Another way of linking industry and public RI exists in France for civil engineering and allows the initiation of 4 year collaborative research projects called PN for a "National Project". The participation of industrial partners is required and the Ministry in charge of research provides 25% of the total cost of the project. The LCPC centrifuge group was, or is, strongly contributing to several PN projects including FOREVER (micropiles), ASIRI (soil reinforcement).

It should be mentioned that, more than the previous programmes, the European Commission's Seventh Framework Programme (FP7) is also designed with the objective of increasing the participation of industry and the private funding of R&D. The calls for "Research for the benefit of SMEs" (small and medium size enterprises) and "Joint Technology Initiatives" are examples of such programmes.

2.2 *Contracting*

Contracting with industry for physical modelling projects varies with industry partners, RIs and national legislation. Two typical options are usually available for an industry seeking research collaboration with RIs. It can either liaise directly with a RI already known by the industry or with an international reputation, or send a request for proposal on a specific project to targeted RIs. In the small community engaged in the particular area of physical modelling experience shows that previous successful relationships, high reputation and quality of the expertise is in most cases more important than the cost of the projects.

In the more formal case where a request for proposal is send to various RIs, some elements are usually included to ensure a fair competition between the RIs:

1. The content required in the proposal is described by the client and if possible also the number of pages in which it should be presented.
2. The required experimental programme (which may include the number of tests to be performed, the instrumentation…) is presented with information about how the tests must be reported and the timeline of the project.
3. Details about how the project must be quoted (as a lump sum, cost per tests and man hours…) are provided.
4. A deadline for the proposal to be submitted is started.
5. The duration of the evaluation period is given to the bidders, who are also informed about the weighting factors between fee and technical proposal in case the technical proposal and fee proposal are evaluated separately.

2.3 *Structure of collaboration*

From an RI perspective, a collaboration between RI and industry means that the industry-oriented project is either fully or partially funded by the industry partner. For the case of the centrifuge facilities presented here, the cost associated with the project includes the cost associated with running the experiments (including potential developments) and the cost associated with the time spent by the researchers on the project. The level of support, the structure of the collaboration

(i.e. the type of contract) and the way the projects are administrated depends both on the projects to be undertaken and on the type of the collaborating industry. Three different types of collaboration can however be indentified:

1. *Type 1*: A contract with a company on a project basis, favouring a one-to-one interaction. This type of structure usually supposes that the project is fully funded by the company, which accounts for development of devices and running the experiments, but also for researcher's man-hours. The projects, spun over a few weeks up to some months (or a couple of years, though it is exceptional), aim at providing design solutions or performance data for numerical analysis calibration for specific issues. The project is administrated by the RI. Outcomes and intellectual property (IP) arisen from the projects are the sole property of the company, which may issue a non-disclosure agreement, although there maybe some particular cases where the company is willing to transfer the IP to the project administrator. The main purpose of this type of collaboration is to provide applicable solutions directly for the industry partner. The activity is essentially a testing service provided by the RI and there is limited opportunity for research or innovation during the collaboration. It can also be difficult, especially for the university centres, to mobilise suitably skilled personnel to carry out this kind of short-term contract work, unless they can be employed on other responsibilities when this type of collaboration is not underway.
2. *Type 2*: A linkage association, where the project is funded by both the company and the RI, and maybe be supported by a third party, such as a national funding institution (NFI). This is the scheme for ARC Linkage Projects in Australia, for some FP7 EU funded projects in Europe, for STW (foundation for applied research) and for COB (the centre of underground construction) in the Netherlands. The support from the RI and industry partner usually includes all cost associated with the experimental and in-kind contribution in terms of man-hours. The project spans over a longer period, which might be up to 3 years, and is not usually case focused. It aims at developing novel solutions potentially leading to new patents or the development and validation of design methodologies. The project may be managed by the third supporting party or by the RI, who has to report regularly to both the industry partner and the third supporting party (if any). The IP is shared by the RI and the industry partner. The main advantages of the type 2 collaboration is that it usually results in a significant level of innovation, involving several researchers, with the project providing sufficient funding to employ specific staff. The outcomes of this type of project are often directly applicable by the industry, although over a longer period of time compared to type 1 collaborations, given the duration of the project.
3. *Type 3*: A Joint Industry Project (JIP) involving more than one company. The project usually aims at developing understanding or design solutions for a specific problem common to all participants and span over a few years. Each partner contributes financially to the project in equal proportion. Additional support might be provided by a national funding institution, which will be responsible for the administrative management of the project (such as the French ANR, the Western Australian MERIWA funding agency, or again STW in the Netherlands). The IP is shared by all participants, who may decide to limit or prohibit its dissemination. The main advantages of the type 3 collaboration are similar to type 2, although the outcomes may not be directly applied by industry if the overall aim of the project is relatively fundamental research, for example to develop an understanding of a broad problem.

Table 1 summarises the different types of RI-industry collaborations of each type (from the three centres point of view).

Advantages and disadvantages of each type of collaboration (as perceived by the three centres) are summarised in Table 2. While type 1 allows delivers direct and immediate outcomes, it usually results in a low level of scientific innovation (although it may require a high level of innovation from a physical modelling point of view). In contrast, type 2 and type 3 may result in high innovation but have deferred and potentially indirect outcomes.

Type 2 and 3 may also require additional research personnel. This point may be perceived as an advantage as it allows training of new researchers on physical modelling activities, but it may also be perceived as a disadvantage if recruitment is an issue.

Table 1. Type of RI-industry collaboration and key parameters.

Type	Industry support	Project length	Project management	IP ownership
1	100%	1–24 months	RI	Industry
2	20–80%	12–36 months	RI/NFI	Joined
3	80–100%	6–60 months	RI/NFI	Joined or Industry

Table 2. Advantages and disadvantages of each type of collaboration.

Type	Research personnel	Scientific innovation	Applicability of outcomes
1	Existing	Low	Direct and immediate
2	Existing may add specifically employed	High	Direct and deferred
3	Existing may add specifically employed	High	Indirect/ direct and deferred

Table 3. Distribution of RI-industry collaboration type.

Type	COFS	Deltares	LCPC
1	82%	40%	42%
2	9%	50%	3%
3	9%	10%	55%

Table 3 presents the distribution of the three types of collaboration between the three research centres considered.

It is interesting to note the differences between the three centres, which probably take their roots in a combination of the size and structure of the centres, national legislation, the geographical location and the working culture.

COFS has a larger percentage of type 1 collaborations, mainly due to its significant involvement in the current offshore developments on the North West Shelf of Western Australia, and also due to the small size of its facility (1.8 m in radius) and operating structure (highly decentralised), which permits a quick reaction to any industry issues, which is beneficial for type 1 collaborations.

In contrast, Deltares has a higher of type 2 collaborations. In the Netherlands, government and industry have initiated several organisations that stimulate applied research (COB, STW, former Delft Cluster). In the new Deltares organisation, the government supplies research money to Deltares, but Deltares has to prove that the money is spent on relevant projects for society. Quite often this is done by asking for co-financing by other parties (this can be industry, or government organisations). In this way, this type of funding lies between type 2 and type 3, but is places here as type 2.

The rather larger percentage of type 3 contracts at LCPC is due to the new French system of planning and funding research, as described in section 2.1 with the annual calls for proposals to ANR and FUI.

The type 2 and type 3 collaborations are more sought after by RIs as they are perceived to be the most rewarding, both in term of financial impact (long term secured funding) and academic impact (publications and patents). Experience shows however that the benefit of the type 1 collaborations should not be ignored, as they usually create opportunities to establish an initial relationship with an industry partner and may be used as a first step to the establishments of a type 2 or type 3 collaboration.

2.4 *Industry partners*

The collaboration between RI and industry may be undertaken at different levels and between different types of industry partners. Industry partners are usually of two kinds:

1. A geotechnical engineering company, which may feature its own R&D department and which is developing and providing geotechnical solutions for the wider community.
2. A geotechnical consulting company, who may act either on its own initiative, or as a technical expert for an engineering company.

Experiences shared by the three RIs are, however, quite different. Relationships with industry appear to be independent of the industry partners for Deltares and LCPC, while it is an important parameter for COFS, notably for the structure of collaboration.

While the type of industry partner does not usually modify the type of collaboration in substance, it may affect the administrative management of the project. When collaborating with a geotechnical consulting company, who acts for a larger client (for example an oil company or a major construction firm), most of the administrative management of the project is transferred to the consulting company. In contrast, collaborating with a large client usually implies that the administrative management of the project is the responsibility of the RI. The workload associated with the administrative management may be significant and requires dedicated personal within the RI, especially with a major geotechnical company for whom contracting documents must follow specific legal procedures. Note that, when dealing with foreign industry partners, national legislation may add to the complexity of the contracting documents.

3 BENEFIT AND EXPERIENCE

While benefits from RI-Industry collaborations are always perceived as valuable, they are actually difficult to quantify, either from the RI side or from the industry perspective. Beyond the evident measure of the benefits through the amount of funding collected, and the number of publications produced,

the following section lists the benefits for both RI and industry as they are perceived by the three research centres from their own experience.

3.1 *Benefits and experience for academics*

The benefits are indeed linked to the motivations and their respective importance depends on the specific needs of each centre. They can be grouped in three items:

1. Benefit to research support.
2. Benefit to portfolio.
3. Benefit for teaching and students.

Since physical modelling for geotechnical is a costly experimental activity, the first and second point is perceived critical by the three centres as it allows funding to be secured for technical developments that will benefit subsequent activities.

The third point is also of importance for Deltares and COFS.

As mentioned before, for Deltares the portfolio of research is of importance to show that it is a RI that serves needs of both the national and international industry and governments. It is also seen to be of equal importance for COFS to be competitive in being awarded National Competitive Grants.

Although Deltares is not a teaching centre, the Dutch government supports student access to research facilities outside the university. This is a rather new development that is facilitated by the 'knowledge centre' that has been established between Deltares and Delft University. As COFS is a research centre within a University, it benefits from knowledge from industry, which is useful for teaching and creating job opportunities for students.

There is a consensus between the three RIs, that benefits for RIs, but also for industry, are maximised over a longer life span project, with projects typically spanning over 3 to 5 years (with collaborations of type 2 or 3), offering the greater benefits for all of the three aspects presented above. If type 1 projects may result in very valuable outcomes in a short period of time, without necessity for a longer research period and a different type of collaboration, they are mostly project-specific, while longer projects generally apply for a wider range of issues.

Benefits appear also to be maximised by frequent interactions with the industry partner, with projects building up on the outcomes of previous one, hence delivering faster and greater benefits.

3.2 *Benefits and experience for industry*

Benefits for industry are harder to quantify without performing a comprehensive survey of industry partners. However, feedback gathered by the three RIs from their own experience indicates that the most important benefits, as perceived by industry partners, are:

1. Gaining access to expertise and capabilities not existing in industry.
2. Input for developing new products and solutions.
3. Gaining access to new research.
4. To validate their numerical models.

In contrast to benefits for RIs emerging from collaboration, benefits for industry seem to be more tangible for short term projects (of type 1) than for longer lasting projects. Although the financial commitment for the industry partners is more important (as they solely fund the project), the return is more easily quantifiable and justifiable. Typical short term type 1 collaboration usually focuses on assisting in design, where the optimisation of a geotechnical solution may return significant financial benefit, sometimes a few orders of magnitude higher than the initial investment.

Although they are still seen as significant, the benefits for industry are less perceptible for long term projects as the financial return is either not immediate or not easily quantifiable. Possible benefits are that a JIP helps to introduce new products or new design methods into practice. Validation of design by physical modelling can be very helpful to get products or design methods accepted. A very long term JIP (>25 years) that existed between Dutch dredging contractors and the former institutes that now make Deltares, showed that apart from increased knowledge of dredging (that helped to make these contractors world leading) another, more or less unexpected benefit emerged: the people from the dredging parties involved started to talk the same technical language. This significantly facilitated the possibilities to work together in consortia in various projects.

3.3 *Intellectual property and publications*

The management of intellectual property (IP), which includes publications and patents, is seen as the most important, but also the most contentious part by both the RI and the industry partner. Problems may arise from the different perspective partners have about IP.

Publications are usually seen by RIs as public knowledge and may be a necessity, notably for academic RIs, while confidentiality of the research outcomes may be perceived as a key parameter by the industry partner for industrial competition. In the Netherlands, type 3 research is quite often what is called pre-competitive research. It provides the basis on which various parties can develop their own applications.

The management of a patent is a different issue as it may be perceived by both the RIs and the industry partner as a significant source of income and a way to protect their research outcomes. The following sections present a brief and limited overview of the perception the three centres have of IP and its benefits.

3.3.1 *Publications*

From the RI perspective, publication is an important benefit that an RI-Industry collaboration may raise, as it is the one the most used to evaluate research performance.

In order to evaluate the impact of RI-Industry collaboration on publication, it is suggested that a to publication index PI is created as follows:

$$PI = (\text{No. of journal papers} \times 3 + \text{No. of conference papers})/(\text{No. of people involved} \times \text{the number of days of physical modelling activity}) \times 365.$$

The coefficient 3 applied to journal papers reflects the fact that they are valued more than conference papers in the academic community.

This coefficient is obviously rather crude and will need some improvement to be used as a valuable indicator for the future, but it gives a preliminary indication of how many papers are generated from a project by a single researcher over a year and permits research outcomes from RI-industry relationships to be quantified.

Table 4 presents the publication index, calculated over the last 6 years, for each centrifuge centre and for each type of collaboration.

The difference between centres reflects the requirements for each institution which are of a different nature. More interestingly, differences between the types of collaboration highlight the fact that for COFS notably, longer collaborations result in a better publication index and, as such, should be favoured by RIs if academic output is the main consideration in liaising with industry. Note that this also may be due to the fact that a significant portion of type 1 collaboration has strict confidentiality clauses, hence reducing significantly the PI. This relation is less clear for Deltares and LCPC.

Regardless of the type of collaboration and the differences between centres, Table 4 demonstrates that industry relationship leads to significant number of publications and, as such, does not have a detrimental effect on research outcomes of RIs.

Table 4. Publication index PI.

Type of academic-industry collaboration	COFS	Deltares	LCPC
Type 1	1.1	2.5	2.3
Type 2	9.4	4.1	–
Type 3	8.5	–	4.5

3.3.2 *Patents*

When the research project results in the development of a new solution for a geotechnical problem, patents may be actively sought by both Industry partner and RIs, as a way to generate income from the research performed, but more often as a way to protect research outcomes from the use of a third party.

The management of patents is simpler than the management of publications, as the patent protects contractually the rights of all partners. Experiences from the three RIs considered here is limited with a very few numbers of patents generated to date. However, maximising patent outcomes may need to be a strategy for the future to attract and develop industry relationships.

4 EXAMPLES OF COLLABORATION WITH INDUSTRY

The different opinions expressed above are illustrated by an example from each of the research centres considered here, with a particular focus on the structure of the collaboration established and the benefits generated for both partners.

4.1 *COFS*

The example presented relates to a project performed in 2007 in collaboration with Keppel Offshore and Marine Technology Centre PTE LTD in order to understand the mechanism governing jetted spudcan extraction (Gaudin et al. 2009) and to provide recommendations for successful in-situ jetted extraction (Bienen et al. 2009).

The collaboration was of type 1, as defined in Section 2.2. The contract was signed between the University of Western Australia and Keppel Offshore and Marine Technology Centre PTE LTD, following Australian legislation. Contract elements included the scope of the study, the experimental programme to be performed, the schedule of the project, the deliverables from the project and a clause defining the ownership of IP. Pricing was established on a lump sum basis.

The project administrative management was the responsibility of COFS. It was agreed by contract that the IP from this project would by owned by COFS, with authorisation to publish. By courtesy, COFS informed the industry partner of all publications related to the project. The project ran over four months and involved two senior academics in addition to the support of three technicians. A junior academic joined the project in a second stage of the study.

The benefits for COFS that arose from this project were as follows:

- The development of new modelling techniques which were subsequently used on other projects and to establish collaborations with other industry partners.
- An insight into issues encountered by industry for this type of foundation, which subsequently helped to orient some of the academic research undertaken at COFS.
- The confirmation of an ongoing good relationship with Keppel following a previous project, and resulting in a second collaboration of type 2 dealing with the development of a new foundation concept.
- A significant academic impact with 2 journal papers and 2 conference papers published.

Similarly, the benefits identified by the industry partner were:

- An insight into COFS capabilities and expertise in performing centrifuge tests and developing solutions to solve practical issues.
- A methodology to determine the flow rate required to achieve successful jetted spudcan extraction.
- An on-going successful relationship with COFS.

The project was seen by both parties as having substantial benefits, mainly because the project was performed with a mutual understanding of the needs and benefits anticipated by each party. While COFS ensured that outcomes were delivered as expected and in time, providing value for the industry partner, Keppel understood COFS requirement for publications and training and the need to complement its own research.

4.2 *Deltares*

Physical modelling in geotechnics is often associated with centrifugal research but this is not always necessary, as will be shown in this example. The research described was commissioned as a type 3 research collaboration by 3 companies, who distribute natural gas in the Netherlands and one manufacturer of connections between the gas pipes and houses. The research was performed in various contracts starting in 2002 and is still ongoing, although with time gaps between the contracts.

Settling soil around houses built on pile foundations in the Netherlands causes differential settlements. This is a problem for the service pipes for natural gas that make the connection between the house and the supply pipeline in the street. The connection between the service pipes and the house has to be able to overcome differential settlements of up to 1 m. Several constructions

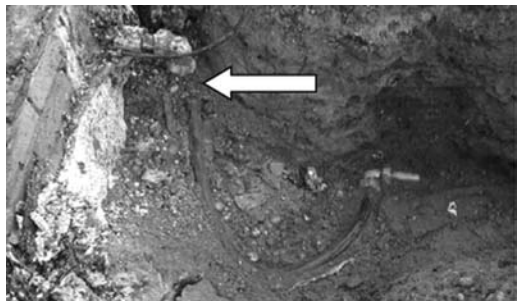

Figure 1. Broken connection in supply pipe that caused a gas explosion, which destroyed a house, August 2003 (Viethöfer & Bezuijen 2006).

that had been developed in the past were tested in a full scale physical model and this research received significantly more attention after an explosion had occurred because such a connection had failed (see Figure 1).

It appeared that most of the constructions, based on insights from the past, were not strong enough to overcome the differential settlements without the risk of leakage.

One manufacturer used the results to develop a new type of connection that, in the same physical model test, appeared superior to the existing connections. This resulted in contracts for more than 125.000 connections in total for the manufacturer, the only one with a tested system.

The advantage for the distributing companies is that they can show that they use now tested connections and that the risk of leakage (with all possible consequences) is minimised.

The advantage for the RI is that they are now established as the testing institute for this type of connections and tests are planned for larger gas pipes, electricity connections etc.

More details on the tests are presented by Viehöfer & Bezuijen (2006).

4.3 *LCPC*

One example of a type 3 project is the French programme SOLCYP that started in 2008 for 4 years (www.pnsolcyp.org). The project was submitted to the ANR (National Research Agency) in response to the call for proposals in 2007. It links 9 partners including 3 companies, 5 research centres and one administrative coordinator.

The project deals with the response of piles to horizontal or vertical cyclic loads. Several approaches are used: physical modelling (in a centrifuge and in a calibration chamber), field pile loading tests and numerical modelling.

The main objective of the project is to develop and propose a method that could be used in

practice to take the effects of cyclic loads into account when designing deep foundations.

The centrifuge test programme is being carried out in the LCPC facility. Two soils are used (clay and sand). Vertical and horizontal cyclic loads are applied to the model piles.

For the horizontal loads, the aim is to gather experimental data on the effects of cyclic loading sequences on the pile head deflection and the maximum bending moment, since these are the two parameters needed by engineers for designing the piles.

The idea is to suggest calculating the pile deflection and the maximum bending moment under the maximum lateral load in a first step using the classical techniques proposed in all codes of practice. The effects of the cycles could then be taken into account by applying multipliers on the obtained values of deflection and moment.

When more information is required on the response of the pile, a complete study must be performed using cyclic P-y reaction curves. The centrifuge tests may also provide information on the effects of the cyclic sequences on the P-y curves, as already shown by Rosquoet et al. (2007).

It is also expected that, at the end of the project, multiplier coefficients will be proposed (depending of course on the number and characteristics of the cyclic loads) to be applied:

– directly to the pile head deflection or bending moment for the simplest cases;
– on the P-y curves for the more complex ones.

The advantage for the industrial partners of the project is to obtain experimental data to be used to develop an official design method recognised by all control offices. In France, any proposed foundation system must indeed be checked by a control office that based its decision on recognized and official designing rules. Without the agreement of the control office, the insurance company will not insure the construction or the building and the project will abort.

For the LCPC, besides the benefit of contributing to improve the code of practice leading to safer and cheaper foundation systems and then establishing centrifuge modelling as a valuable tool in assisting to design, new experimental devices and procedures were developed, increasing the capabilities and potential of the group.

5 CONCLUSIONS

5.1 *Summary*

The paper presented experiences of three physical modelling faculties in collaborating with industry partners. Despite obvious differences in dealing with industry due to the nature of each centre and their geographic localisation, some important points, shared by the three facilities have been identified as follows:

1. The three centres are engaged with industry and industry collaborations represent an important part of their activity.
2. The industry relationship does not affect negatively the overall research activity. On the contrary, the three centres experience significant benefits in engaging with industry.
3. Benefits experienced by the three centres include notably new insights for fundamental research, development of specific capabilities useful for further research, but also more academic outcomes such as publications and patents, as would also result for academic research.

In general, industry collaborations appear to be extremely valuable and are actively sought by the three centres.

The paper also proposes some tools to monitor and quantify outcomes from industry collaborations. Thought there is clearly room for improvement in the future, these tools are a first attempt to provide information about RIs-Industry collaboration. It is the authors' opinion that these tools will become indispensable in the future for the evaluation of the performance of RIs by funding institutions and to develop long term strategy to attract and develop further collaborations with industry.

5.2 *Criteria for successful relationship*

From the experience of the three centres considered in this paper, some key elements have been identified, which must be accounted for to ensure a successful relationship for both the industry partner and the RIs.

– The RIs must exhibit reactivity and adaptability to cope with the ever changing needs of industry.
– The RIs must understand the needs and requirements of industry, which has to survive in a competitive environment, notably in terms of protection of the intellectual property, even if it may conflict with the needs and requirements of the RIs.
– The outcomes delivered must correspond to those expected by the industry partners. This does not mean that the results must be those expected by the industry partner, but that the deliverables and the research outcomes correspond to those agreed between the RI and the industry partner.

– Frequent two-way communication throughout the project is a necessity to ensure that both parties understand each other needs and requirements and update, if necessary, details of the research project, which by nature, always contain uncertainties.

A successful collaboration with an industry partner is always the best way to engage further and more fruitful collaborations.

5.3 *Strategy for the future*

Geotechnical projects, and consequently physical modelling projects associated with them, are becoming increasingly complex, requiring complex testing procedures, expensive instrumentation and highly qualified personal. It is anticipated that this will result, in the near future, in RIs specialising in specific research areas. COFS is an example of a centre that focuses on offshore geotechnics, while Deltares has decided to focus on the behaviour of soft-soils and protection against flooding and LCPC is expect in the behaviour of granular material under cyclic loading.

As a consequence, it is anticipated that more collaboration between the various research centres will become necessary in the future to be able to answer more complex issues. As an example, centrifuge tests at one RI can be combined with 1-g tests at another RI. This will require better knowledge of each other capabilities, but also standardisation of equipment, procedures, data handling and, so that a model developed one RI may be tested at another RI, if required.

This should ensure the further establishment of physical modelling as a valuable tool to assist industry in the design process and in solving practical issues.

REFERENCES

Banal-Estanol A., Jofre-Boent M. & Meissner C. 2008. *The impact of industry collaboration on academic research output: A dynamic panal data analysis*. Personal communication.

Bienen B., Gaudin C. & Cassidy M.J. 2009. The influence of pull-out load on the efficiency of jetting during spudcan extraction. *Applied Ocean Research* 31: 201–211.

Craig W.H. 1984. Centrifuge modelling for site-specific prototypes. *Proc. of Symp. On Application of Centrifuge Modelling to Geotechnical Design. Manchester, UK*: 473–489.

Gaudin C., Bienen B. & Cassidy M.J. 2009. The mechanism of jetting extraction of spudcan in soft clay. *Géotechnique*. (under review).

Lee Y.S. 2000. The Sustainability of University-Industry Research Collaboration: An Assessment of Behavioral Outcomes. *Journal of Technology Transfer* 25: 111–133.

Lillywhite J.M., Hawkes J. & Libbin J. 2005. *Measuring net benefits resulting from university-industry collaboration: An example from the New Mexico Chile Task Force*. Western Economics Forum.

Martin C.M. 2001. Impact of centrifuge modelling on offshore foundation design. In S.M. Springman (ed), Proc of the Int. Work. On Constitutive and Centrifuge Modelling: Two Extremes. Monte-Verita, Switzerland. A.A. Balkema: 135–154.

Martin B.R. & Tang P. 2007. *The benefits from publicly funded research*. Science and Technology Policy Research, Univeristy of Sussex, paper No. 161.

Murff, J.D. 1996. The geotechnical centrifuge in offshore engineering. *Proc. Offshore Technology Conf., Houston*, OTC 8265.

Rosquoet F., Thorel L., Garnier J. & Canepa Y. 2007. Lateral cyclic loading of sand-installed piles, *Soils & Foundations*, Paper No. 3284, 47(5): 821–832.

Scott A., Steyn G., Geuna A., Brusoni S. & Steinmueller W.E. 2001. *The Economic Returns to Basic Research and the Benefits of University-Industry Relationships: a Literature Review and Update of Findings*. Report prepared for the Office of Science and Technology, November 2001. Brighton: SPRU, 2001: 33.

Viehöfer T.C. & Bezuijen A. 2006. Testing service pipes in settling soil. In C.W.W. Ng et al. (eds), *Proc. Int. Conf. on Physical Modelling in Geotechnics, Hong Kong*: 765–770.

This page intentionally left blank

Physical Modelling in Geotechnics – Springman, Laue & Seward (eds)
© 2010 Taylor & Francis Group, London, ISBN 978-0-415-59288-8

Development of teaching resources for physical modelling community

S.P.G. Madabhushi, U. Cilingir & M.E. Stringer
Department of Engineering, University of Cambridge, UK

ABSTRACT: Physical modelling of interesting geotechnical problems has helped clarify behaviours and failure mechanisms of many civil engineering systems. Interesting visual information from physical modelling can also be used in teaching to foster interest in geotechnical engineering and recruit young researchers to our field. With this intention, the Teaching Committee of TC2 developed a web-based teaching resources centre. In this paper, the development and organisation of the resource centre using Wordpress. Wordpress is an open-source content management system which allows user content to be edited and site administration to be controlled remotely via a built-in interface. Example data from a centrifuge test on shallow foundations which could be used for undergraduate or graduate level courses is presented and its use illustrated. A discussion on the development of wiki-style addition to the resource centre for commonly used physical model terms is also presented.

1 INTRODUCTION

Physical modelling in geotechnical engineering research has grown steadily over the past few decades. With improvements in computing and instrumentation more and more laboratories are getting involved in physical modelling and this activity is now truly worldwide. However to sustain this activity, a steady stream of undergraduate and graduate students who are well-trained in physical modelling techniques is required. To this end there is a need to introduce physical modelling in undergraduate and graduate teaching firstly to impress on the critical issues in Soil Mechanics (such as the non-linear behaviour of soils), and secondly to demonstrate the usefulness and strengths of physical modelling. These aims can be achieved by creating a well documented and curated set of teaching resources that can be used by geotechnical teachers worldwide to introduce their students to physical modelling.

The TC2 sub-committee on teaching has attempted to create such a web-based resource. This paper introduces some of the key aspects of the teaching resources. As with the development of any of the resources of this type, the key issue is the sustainable development and addition of new material to ensure wide usage of the resources by the geotechnical teaching community. To enable the ease with which the resources can be maintained and new material can be appended, the WorldPress.org platform has been adopted. The technical details of the platform and examples of the resources currently available are presented in this paper.

2 TYPES OF INFORMATION ON THE WEBSITE

The website is envisaged to be a comprehensive site containing teaching resources which will be useful for both academics preparing courses and also to students who are new to the art of geotechnical physical modelling. The current web address of the site is: www.tc2teaching.org

Some of the content which can be found on the website is now described.

2.1 *Physical modelling*

A collection of information has been assembled, creating the main knowledge base of the website. Pages describe some of the possibilities that physical modelling can offer, the different types of physical modelling tests, as well as some popular techniques used by researchers such as "particle image velocimetry." This section of the website also includes descriptions of common instruments, which enables new students to quickly understand the different types of devices which they may wish to use in experiments. It must be pointed out this is just the 'early' framework and more information will be added by researchers and users in due course. In Figure 1 a screen shot of the currently available explanations for physical modelling terms are presented. There is also an opportunity for the visitors to leave comments or make suggestions using the space as shown in Figure 1. These comments are moderated periodically by the web administrator and necessary changes or additions

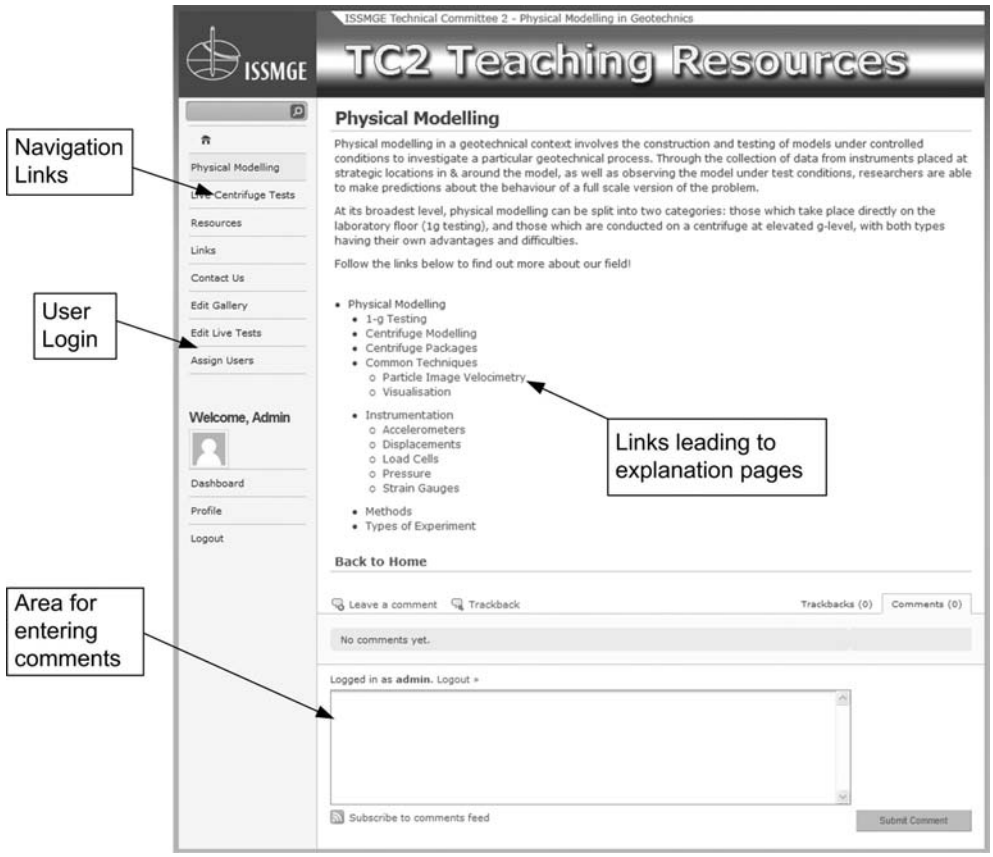

Figure 1. Screenshot showing the physical modelling techniques.

to the website are made. This allows for continuous growth of the available resources.

2.2 *Images & video*

A set of images are collected and stored in individual galleries on the website. Each image is accompanied with a description which should provide both the context for the image and technical insight to the scenario.

Similarly, a collection of videos is made available on the website, which is accompanied with descriptive text explaining the test being undertaken and any specific physical modelling issues which were faced and solved. In Figure 2, a screen shot of the current image gallery is shown.

2.3 *Datasets*

A section of the website is used for making data available for teaching purposes. Data stored in this section will typically be from coursework exercises. Each data set will have its own page, on which a description of what the data is used for will be included. The data itself and any associated information for carrying out analysis, for example task briefs, can be directly downloaded from the webpage. An example of centrifuge test data on shallow foundations on a sand layer is presented in Sec.4 and its use is illustrated.

2.4 *Publication list*

A set of pages have been created to list journal, conference papers and presentations relevant to the teaching of physical modelling. These pages are designed to be helpful for academics creating new courses or reviewing existing course content.

In addition, text books with particular emphasis on the aspects of geotechnical physical modelling are listed.

In the case of books and papers, each entry is accompanied by its abstract and also the reference information. This was done to protect the

Figure 2. Screen shot of teaching resources webpage showing the image gallery.

copyright of the journals, books and conference proceedings on the relevant material.

In the case of presentations, the content can be downloaded directly from the website.

2.5 *Live centrifuge tests*

Increasingly it is possible to have tele-participations capabilities for centres/laboratories with physical modelling capabilities to allow remote user participation. These tele-participation facilities are described in some detail by Madabhushi et al. (2010). The teaching resources website aims to bring in links to all facilities which have tele-participation facilities.

A dashboard has been created which gives an overview of any centrifuge experiments or 1-g testing being carried out at physical modelling centres which have live video streams available. The dashboard operates a traffic light system which indicates whether tests are live (green), are being prepared (amber) or have finished (red) as well as an estimated time, date and short description of the test. Clicking on an individual centre takes the user to a centre-specific page which gives the links to the centre's own webpage and live stream. The page also gives information about the research activities of the centre and also the live stream activity. The list of centres and the publication of test description and timings will be the responsibility of the individual centres. After the website's launch, centres will be able to request an account, which will allow access to the pages where the information is entered.

3 DEVELOPMENT AND ORGANISATION OF WEB RESOURCES

The website has been built using Wordpress, which is a content management system (CMS), licensed under the GPL (General Public License). CMSs enable quick and easy publication of dynamic websites, with users entering web-content through a user-interface. Administrators can extend the basic functionality of the site (for example restricting access to certain pages) by selecting from a wide range of open-source or commercial "plugins". Alternatively, the user can write their own code to provide additional website functionality or page templates. Page templates and functions developed specifically for this website were written in PHP (Personal Home Page)—a language which was originally based on the C programming language and developed to enable dynamic web pages. Dynamic web pages are so called because on their own they do not hold all of the content. Instead, they are like a framework which places the information given to it. This information is obtained by the web server, which queries a database in order to return content appropriate to the context in which the web page has been accessed. Once set

up, dynamic pages make running a website much simpler since they automatically keep themselves up to date by pulling the appropriate content out of the database. A database has been created using the open-source database software, MySQL (name of the program) to hold the dynamic web content for the TC2 web resources site.

In order to facilitate the addition of certain content, the website has been created with both open access and restricted access areas. Figures 1 and 2 display screenshots taken of the website as seen by a guest on the website.

3.1 *Unrestricted areas*

All of the website's information and resources are made freely available to guests of the website. A site navigation bar is placed on the left side of the screen to enable users to access the different areas of the site.

In order to promote discussion on topics, users can make comments on individual pages after entering basic identification details, such as a name and email (Note: the email address is not displayed publically) After moderation by the website administrators, the comments will appear on the webpage for future guests to see and respond to. Since the aim of allowing comments is to promote discussion, the moderation process will only remove inappropriate, abusive or irrelevant (spam) comments.

3.2 *Restricted access areas*

Users of the website who will add either pictures or update their centre's live testing information are able to request a user account with additional privileges. Users granted access will be able to log in to access additional pages, which appear in the navigation menu on the left of the screen. These pages allow the user to directly upload images and their associated descriptions to the website. In addition, users can post information about upcoming tests on their live video stream and change the status of the test.

The enhanced user accounts are available by request to the webmasters, whose email is available on the "Contact Us" page.

Users who wish to upload videos, data or individual page information can contact the webmasters, who will prepare and publish the information on the website.

4 EXAMPLE ON USE OF CURATED DATA

This section describes a sample exercise, which has been used in a taught graduate module on geotechnical centrifuge modelling at the University of Cambridge. It describes the example problem, presents the raw data, details the anticipated processing of the raw data by students and gives the conclusions which the students are expected to draw.

The data from the experiment carried out by students in 2009 is made available on the website in the "Data" section.

4.1 *Description of the experiment*

The sample problem involved the modelling of a shallow foundation on a beam centrifuge. A foundation loading test was carried out at different g-levels using the 10 m Turner beam centrifuge at the Schofield Centrifuge Centre, University of Cambridge. The Turner beam centrifuge is 10 m in diameter with a capacity of 150 g-tons and was described by Schofield (1980). A dry sand layer of 350 mm height was poured in a cylindrical model container of 850 mm diameter. The relative density of the sand was around 50%. The footing models, which are made of high strength aluminium alloy, were placed on the surface of the sand without any embedment. Load was applied vertically on the footing by a 2D actuator capable of exerting 10 kN of force. Details of the 2-D actuator are discussed by Haigh et al. (2010). The actuator was attached on the top of the model container. Displacement of the footing and the load exerted by the 2D actuator was measured using a linear variable differential transformer (LVDT) and an axial load cell respectively. Data acquisition was carried out using DasyLab with a sample rate of 1000 Hz. The schematic layout of the experiments is shown in Figure 3. Two circular footing models were used. Each model was tested at four different g-levels.

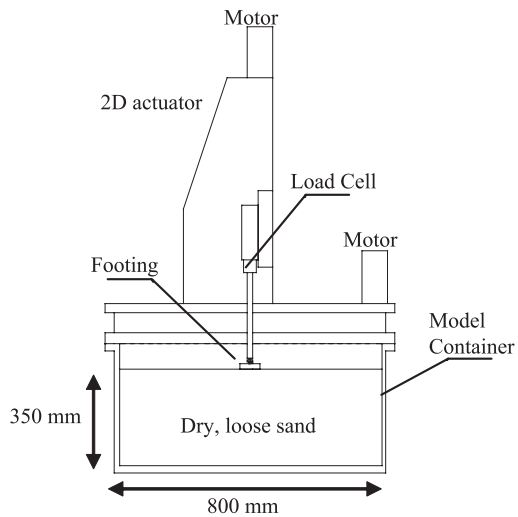

Figure 3. Schematic drawing of the experimental layout.

Table 1 lists the footing sizes and g-levels at which they were tested. Each test was ended when approximately 25 mm of vertical displacement had been achieved. At this point, the footing was retracted from the soil and the centrifuge was then spun-up to the next required g-level and the actuator repositioned. The footing was moved sideways to ensure the new test was not affected by the previous test area; for example from any compaction which may have occurred. After the tests had been completed at all four g-levels, the centrifuge was stopped and the second footing model was attached to the actuator. The same procedure was used for subsequent tests.

Students were expected to complete the following tasks for their course work:

- Draw the prototype being modelled in the centrifuge tests
- Plot the curves of foundation load versus vertical displacement from filtered data obtained in each centrifuge test
- Discuss the differences in the observed bearing capacity between the different sized prototype footings
- Discuss the modelling of models attempted in these centrifuge tests and confirm if the data is consistent with this principle.
- Estimate the bearing capacity resistance using analytical calculations and compare this to the centrifuge test results.

4.2 *Anticipated processing by students and comparison with analytical solutions*

The first task is to draw the prototype models corresponding to each model listed in Table 1. Students are expected to calculate the prototype size of each model according to the scaling laws proposed by Schofield (1981). The next task is to process the raw data obtained in the experiments, which consists of an array with three columns: elapsed time, footing displacement (in volts) and the applied axial load (in volts).

Table 1. Centrifuge test configurations.

Test number	Footing size (mm)	Centrifugal acceleration (g)
1	125	10
2	125	20
3	125	30
4	125	40
5	62.5	20
6	62.5	40
7	62.5	60
8	62.5	80

Students were expected to convert the raw data, which is given in volts, to physical quantities by multiplying the numbers with the calibration factors listed in Table 2. The calibration factors were supplied prior to the centrifuge tests.

The second step in processing the data is to filter it using MATLAB. There are various filtering options available in MATLAB for post processing. In this particular example, an 8th order Butterworth filter was used. Figure 4 shows typical results obtained from one of the centrifuge tests. If MATLAB is not available or is not preferred, simple filtering techniques can be used. For example performing a running average on the data points.

Table 2. Channels and associated calibration factors.

Channel	Measuring	Unit	Calibration factor
1	Time	s	N/A
2	Displacement	V	10 mm/V
3	Load	V	13191 N/V

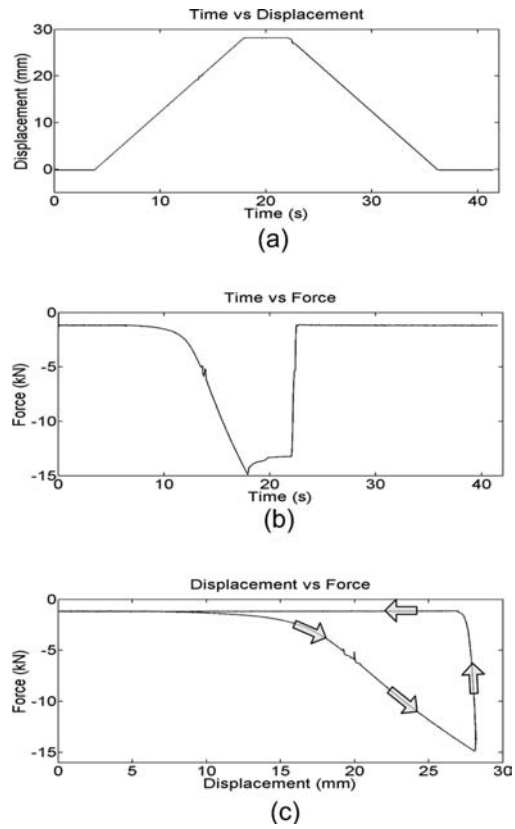

Figure 4. Typical results at model scale: (a) time vs displacement (b) time vs force (c) displacement vs force.

After processing all the results, students are expected to calculate the vertical stiffness of the ground in each test. This can be done by selecting an allowable serviceability limit on the settlements and finding the corresponding vertical load. Vertical stress exerted on the soil can simply be calculated by dividing the load by the footing area. The strain should also be found. This can be done by dividing the settlements by a characteristic depth below the footing, typically one footing diameter.

The results were also expected to be compared with analytical solutions. Differences in bearing capacity of different size prototype footings were to be calculated using well known bearing capacity solutions.

4.3 *Conclusions to be drawn by the student*

Students are expected to reach the following conclusions at the end of the exercise by discussing the differences in bearing capacity of different size footings and by talking about the concept of modelling of models attempted in the centrifuge tests:

- Stress-strain relationship should be similar between two models of the same prototype. If the results deviate from predictions, then the student should question the validity of the results and discuss the reasons of the observed deviation. Often, these deviation results from local variations in the soil model, particle size effects resulted from using a small footing, failure to set two footing tests sufficiently apart from each other.
- The results should show that the stiffness of the ground measured by footing tests increases as the size of the footing and the vertical force increase.
- The bearing capacity should increase as the size of the footing increases. The student is expected to explain why this is the case by referring to the footings of different sizes and hence different depths of influence.
- Bearing capacity calculations should be compared with the test results and the reasons of any deviation shall be discussed accordingly.

5 DISCUSSION ON WIKI-STYLE CONTENT

This section presents a discussion on wiki-style addition to the teaching resources website which is moderated against malicious and unsolicited posts. The aim of such an addition would be to encourage users to share their knowledge on commonly used terminology regarding the physical modelling techniques in geotechnical engineering. Students, both undergraduate and graduate, and others, who are new to physical modelling methods, would benefit from this openly available and editable content. However, the amount of user freedom and the restrictions on who is allowed to put new content and who is allowed to edit and monitor is a delicate issue which needs to be discussed thoroughly.

A complete freedom on editing and moderating the website content might expose people, who are new to physical modelling, to false or biased knowledge. It might be argued that this false or biased knowledge would be picked up and corrected timely by other users. However, it should be noted that this type of self-control on the webpage may only be possible if the volume of users is big enough to fix the problematic content before inexperienced physical modellers start to use them. Therefore, it is suggested that certain users, who are known to be experts in their individual fields, should be encouraged to contribute to the moderation and editing of this wiki-style user content. It is also suggested that uploaded content would be supported by references to related publications. It is relatively easy for the web administrator to give editing rights to the experts using the present website architecture.

6 CONCLUSIONS

It would be very useful to have a common resources pool of physical modelling techniques and curated test data. Such a resource would be valuable to the teachers of geotechnical engineering who wish to introduce their students to physical modelling. An open-source content-management based website was developed that brings together such resources. This paper presents the main features of the web resources currently available. A wiki-style future growth through user participation, but moderated by experts in the field, is anticipated.

REFERENCES

Haigh, S.K., Houghton, N.E., Lam, S.Y., Li, Z. & Wallbridge, P.J. 2010. Development of a 2D servo-actuator for novel centrifuge modelling, *Proc. 7th International Conference on Physical Modelling in Geotechnics, Zurich, Switzerland.*

Madabhushi, S.P.G., Haigh, S.K., Ali, A., Williams, M., Ojaghi, M., Lamata, I., Blakeborough, T., Taylor, C. & Dietz, M. 2010. Distributed testing of soil-structure systems using web-based applications, *Proc. 7th International Conference on Physical Modelling in Geotechhnics, Zurich, Switzerland.*

Schofield, A.N. 1980. Cambridge Geotechnical Centrifuge Operations. *Geotechnique* 30(1): 227–268.

Schofield, A.N. 1981. Dynamic and earthquake geotechnical centrifuge modelling. In Prakash, S. (ed) *Proceedings, International Conference on Recent Advances in Geotechnical Earthquake Engineering and Soil Dynamics, St. Louis, 26 April–3 May*, University of Missouri-Rolla.

Physical Modelling in Geotechnics – Springman, Laue & Seward (eds)
© 2010 Taylor & Francis Group, London, ISBN 978-0-415-59288-8

STREAM: A method to facilitate efficient data exchange and archiving

P.E.L. Schaminée
Deltares, Delft, The Netherlands

A.A. Klapwijk
NCIM, Leidschendam, The Netherlands

D.J. White
COFS UWA, Perth, Australia

ABSTRACT: The results of physical experiments are complex and valuable. To facilitate efficient exchange and archiving of test results STREAM has been developed. STREAM means Standardized Test Results Exchange and Archiving Method. A formal distinction is made between the description of the information and the data itself. Standardizing the format of the description file for a given type of test—the so-called Testdefinition—instead of the data files themselves, permits the utilization of generic software tools and data formats for documentation, reporting and data storage. The formal breakdown of a test into five phases—the so-called SMARF phases—has several benefits: (i) testing activities are structured, (ii) it simplifies the process of documentation, and (iii) it facilitates a structured data handling process. These complete, consistent, fully-checked and quality-assured files may be easily utilized by personnel who were not directly involved in the conduct of the tests.

1 INTRODUCTION

Everywhere are needs for an efficient way to exchange and to archive information. In this paper the focus is on information obtained by means of experimental testing. In general a test is performed in a test set up designed by engineers. They may be involved in the current program of tests, or they may have long since moved on, with the test activity becoming standardized and routine. During testing, the actual values (the instrument readings, or observations) are obtained by operators. These values are analyzed and reported by experimental specialists (often someone different to the operator). Then, it is usual for the reported values to be transferred to a client, who will use a selection of the results for calculations, and so on. It is important to observe that at different stages different people are involved, who all use the results for their specific purposes. It is a small step to recognize that they all want a different set of information to be archived for later use. This is in contrast with the idea that one single standard data file for all types of test fits all purposes.

In this paper a method is described for the exchange and storage of data from single tests. The method considers the initial set-up of the experiment through the gathering of raw data until the factual report of the test results (which may involve some level of interpretation and collation of the raw measurements).

The reasons that the method has been developed are (i) to improve the quality of the reported and stored test results, (ii) to minimize the effort required to apply the method and (iii) to maximize the benefit of using the method. The method was developed with many types of geotechnical tests in mind, spanning from routine laboratory tests (e.g. a moisture content determination) through to complex centrifuge model tests. It is equally applicable to experimental activity that is conducted in the field.

The method described in this paper is centred around two new elements:

1. A chronology that captures the activity involved in any form of experimental activity: SMARF (Set-up, Measurement, Analysis, Reporting, Filing—see Section 2);
2. A method that structures information generated throughout the SMARF process: STREAM (Standardized Test Results Exchange and Archive Method—see Section 3).

STREAM uses a standard format for defining types of tests and accepts several formats for

storing the corresponding data. The purpose is to allow the results of a single test to be collated as a complete set of information, which can be accessed by anyone who has the corresponding standard definition. There are two different kinds of information involved:

1. The values of the quantities to be exchanged (i.e. the readings of one test). These are stored in a separate data file for each test.
2. The precise description of these quantities (i.e. an explanation of what the readings are of, in a standard way, comprehensible by any user). These descriptions of the quantities for a type of test are stored in a so-called Testdefinition, which is a document that is formatted in a standard way.

In STREAM, conversion between various formats of data files is accepted and various formats of data file are already implemented. In addition a program—the so-called Testdefiner®—is available to easily create a Testdefinition and a Matlab® library has been created to make optimum use of STREAM.

2 THE CONCEPT OF SMARF

It is useful first to note some difficulties that commonly arise with data handling during the process of obtaining experimental results. Firstly, different personnel are involved at different stages of the activity. Also, if multiple tests of the same kind are conducted at different times, different users may undertake them. The resulting data may be stored in different ways and it may also be measured in different ways (which may not be documented).

To resolve these differences may require double-handling of information before it is finally reported (for example, transferring information from spreadsheets of different formats, or between some combination of multiple lab notebooks and multiple spreadsheets). In other cases, if the procedures are ill-defined and not logged then the resulting data may be inconsistent—as a simple example, if different oven temperatures were used but not noted during moisture content determinations.

The SMARF concept identifies five chronologically-ordered phases from the design of a test to its factual reporting. These phases lead to the SMARF acronym—set-up, measurement, analysis, reporting and filing.

- *Set-up phase* in which the equipment and samples are prepared;
- *Measurement phase* in which the actual experiment takes place, i.e. the gathering of sensor readings;
- *Analysis phase* in which the recordings are analyzed and new derived quantities are calculated or key values at particular times are extracted;
- *Reporting phase* in which both the measured and calculated results are presented attractively by means of figures, tables, etc;
- *Filing phase* in which the results are prepared for long term storage and future accessing.

The SMARF concept provided moments to transfer to a next phase by means of a well defined phase report. At this moment the current set of data for a particular test can be stored in a data file and 'frozen'. The format and operation of STREAM is specifically developed for transfer of experimental test results. The target is to facilitate well-defined storage and exchange of properly-described data during these processes.

3 THE CONCEPT OF STREAM

The STREAM method, linked to the SMARF chronology, is meant to be useful for both simple standardized common tests (i.e. a moisture content measurement) and very complex custom tests (i.e. a geotechnical centrifuge test). In the case of performing a geotechnical centrifuge investigation, the test series consists only of a limited number of tests which use the same Testdefinition. Even then the method must be efficient and beneficial if it is to prove desirable for users to apply.

Documentation of exchanged or archived results is an integral part of the process. Tests of the same type share the same procedures and therefore share the same documentation with respect to the description of quantities and equipment. It was concluded that the method can be optimized by using the shared information for tests of the same type. Therefore, only one Testdefinition is created for all tests of the same type. All values (i.e. readings) from each single test are stored in a separate data file.

In STREAM the five SMARF-phases are defined separately. In the Testdefinition it is clear in which of the five SMARF phases an item is created. An item is referred to as a test result or

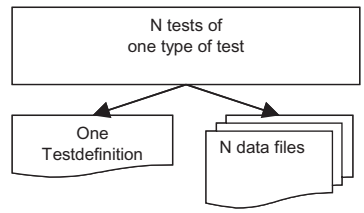

Figure 1. Relation between a Testdefinition and the corresponding data files.

analysis result to be exchanged. Using the Testdefinition each data file can be checked before entering the next SMARF phase for completeness and correctness.

The SMARF process is set out in Figure 2, indicating broadly the different steps that are conducted at each stage. The data file is updated throughout the test, as the experiment moves through the SMARF phases.

A side effect is that this allows reuse of (parts of) common measurement or analysis definitions. The concept of the five SMARF-phases has proved to be efficient (i) with respect to process of defining a test, because the kind of information to be exchanged and archived can be optimized for each phase and (ii) with respect to the completeness after each phase, because it is well documented which items are required in later phases.

When the one of the phases changes, which might be the case when new insights are gained, the Testdefinition also has to be changed. However it becomes very easy to redo processing a test from a well described point. For example, the best way to analyze and report a test may only be established, after the last test of a short series.

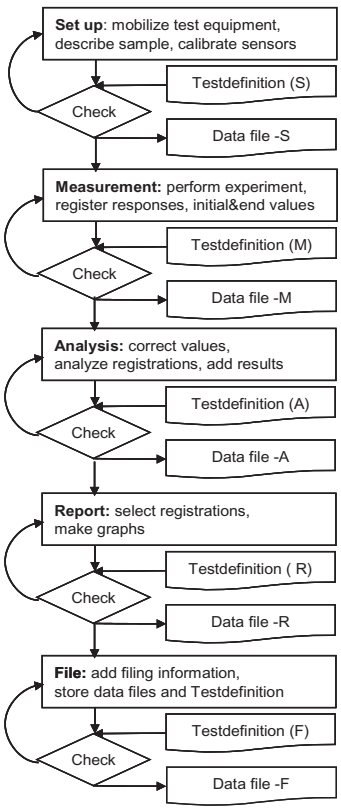

Figure 2. Flow diagram of one test.

All persons involved of defining one or more phases will use the Testdefiner to edit the single Testdefinition which corresponds to that test. When the type of test is completely new, an empty template has to be used. However, when a Testdefinition for a similar type of tests already exists, sets of items can be copied from previous Testdefinitions. Even the client can be involved in the process of defining a test, because he can easily be informed about the items and their definition using the information concerning the report-phase in the Testdefinition.

4 USING STREAM: AN EXAMPLE

In this section STREAM is illustrated by applying it to an example test. Imagine a test to determine the moisture content of a sand sample as a function of time and suppose the test procedure consists of weighing a moist sample in a bin placed in an oven until it is dry. The use of STREAM starts by describing all items to be obtained in the five SMARF phases.

In the set up phase the mass of the empty bin has to be determined and the sand has to be classified. In Figure 3 a screen shot from the Testdefiner interface is shown.

Figure 3 shows that the quantity "mass of the empty bin" requires a unique reference in the Testdefinition, here chosen as 'EmptyBinMass'—the so called *shortname*. No other quantity is allowed with the same shortname in this Testdefinition. In the address field at the top are the *phase* (set up), the *type* of data (a number) and the *category* ('equipment') are visible. The available phases and types are set by the Testdefiner and the relevant ones for each quantity are selected by the user. The category name is defined by the user. The purpose of the category name is to permit the user to group sets of items within a phase. Clicking an other tab will open new pages to enter information about the item EmptyBinMass, such as how it should be measured, the valid range (i.e. minimum and maximum values). This information is used to check the data file.

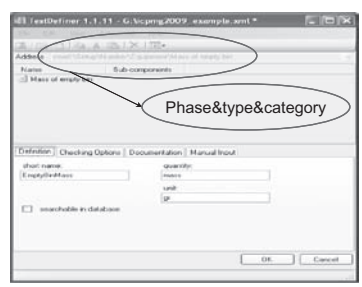

Figure 3. Graphical user interface in Testdefiner® for item.

The next step is defining the measurement phase. During this phase the mass of the bin together with the mass of the moist sand has to be determined as a function of time. So, time and mass are to be measured, these are quantities with more than one observation: these are called *columns*. Figure 4 shows a Testdefiner input screen for a column.

That sensor values in columns often require more information than a single number—for example, they should be accompanied by the location of the transducer in the experiment and the calibration information of the sensor.

In the analysis phase some calculations have to be performed to calculate the moisture content as a function of time, from the measured weight. The result of this analysis will be stored in a new *column* item 'MoistureContent'. Figure 5 is a screen view of its documentation tab in the Testdefiner.

The procedure—that is, the formula to be applied to calculate the moisture content—is described in the documentation field, and refers to other items in the Testdefinition by their shortnames. It becomes clear that for the analysis the EmptyBinMass is essential, so this item must be stored in the data file after the set up phase.

When preferably all phases, but at least the set up and measurement phases are defined, the data acquisition system can be set up to store the information directly in the correct format. In most cases a simple conversion program will be required to convert the data file produced by the

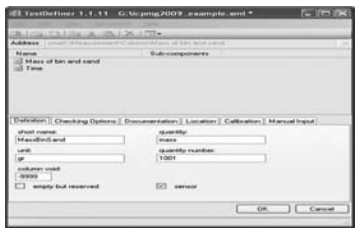

Figure 4. GUI in Testdefiner for a column quantity.

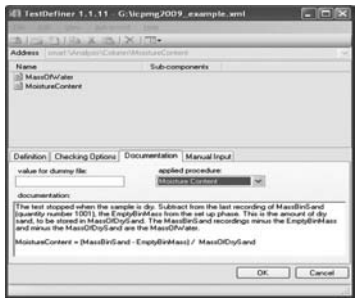

Figure 5. GUI in Testdefiner for documentation.

data acquisition (DAQ) system into a STREAM data file that conforms with the Testdefinition. Suitable conversion routines have been written for the DAQ systems at Deltares and COFS/UWA.

When the measurement phase has ended and the data is stored in a STREAM data file, it is checked for completeness and correctness. For example, the existence of all defined *column* items can be checked and the *column* data can be compared with the instrument range limits. When the file passes these checks, it can be 'frozen', to prevent it from being changed, and transferred to the analysis phase.

The analysis procedure is mostly known beforehand, the Testdefinition can also be complete and presumably also most of the analysis software is in place. The STREAM library allows efficient importing of information from or export of information to a STREAM data file. The main characteristic of the library is that all references to the information in the data file are made by using the shortnames defined in the Testdefinition. The implementation is by reading and writing the data file through the corresponding Testdefinition. All of the items that have been defined in the Testdefinition can be accessed. This guarantees that all information in a data file is described in the Testdefinition all the time. When all analysis is ready, it can be checked for completeness and correctness and, when it passes these checks, can be frozen as an analysis data file. Based on the frozen file a selection will be made for the report to the client. This selection can be presented and sent to the customer and the data file can be archived.

However, when analyzing the first test of a new type of test, it might become apparent that new items have to be created and defined within the Testdefinition. Describing these new items instantly in an update of the Testdefinition, allows all standard STREAM tools to be used continuously. It is recognized that the Testdefiner should function in a user friendly way. The next tests of the same type might lead to modification in the items set in the Testdefinition. In this case the stringent 'borders' between the phases, especially between the measurement and analysis phase, permit new analysis to be performed based on previously frozen measurement files. For this reason the STREAM library facilitates batch processing.

After the last test in a series, all of the tests can be easily processed using the same software because all items are well described in the Testdefinition and all values are available in the (frozen) data files.

5 ABOUT THE TESTDEFINITION

All STREAM Testdefinitions have the same standardized structure and are written as an XML file.

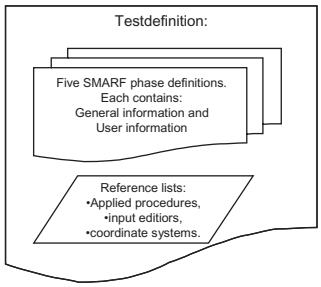

Figure 6. Types of information in a Testdefinition.

The Testdefinition does not store the data itself, but contains a structured list of the data elements, and additional information that helps the user to correctly perform the test, input the resulting data in a datafile, to describe the applied formulae and procedures and to check corresponding data files for correctness (Figure 6).

Each Testdefinition consists of two classes of information: general and user-defined. In the following paragraphs both are described in detail.

5.1 *General information*

General information is unconditionally required for all data files and is therefore predefined. These general information items are well defined. They can be grouped in three categories: (i) file tracing, i.e. information to identify for example the organization where the test was performed, the person responsible for the test (ii) test description, i.e. the reference to the corresponding Testdefinition, (iii) data format description, i.e. information on the characters used as column and record separators in the data file.

5.2 *User-defined information*

The users have to define each item they want to exchange and store in the data file separately. STREAM provides the user three types of information (i) numbers, which can be used for information such as the duration of the test, the temperature of the oven and the target centrifuge g-level, (ii) strings, which can be used for names of standards, equipment, procedures, people and text labels and (iii) columns, which are a set of numbers belonging to one quantity: in most cases a series of measurements of a quantity varying through time.

The information to describe each item depends on the type of information. For example, each number or column requires a unit in contrast to a string which does not. To facilitate the user to describe each item, the program Testdefiner is available. It guides the user and stores the information in the correct XML-based Testdefinition format.

6 ABOUT THE DATA FILE

During the search for a standard data file format it became clear that only the specific application of the data determines the most suitable format. For example, the DIGGS data format is tailored for road maintenance (with its strong links to GIS databases), the XML language is very useful for structured data exchange (where many single data values, each with a different definition, are collated) and worksheets in a tabular program (such as Excel) are very useful for intuitive interpretation, and for storing time histories of transducer data. Similar tests will be performed for different applications; therefore the STREAM method for defining and structuring data has to be application-independent.

So, it was concluded that the exchange method has to incorporate conversion of data files, instead of one standard format fitting all uses. Once the Testdefinition is set up, correct conversion tools can be easy developed Currently STREAM is implemented with a GEF formatted data file and an MS Excel data file.

Each STREAM data file contains all of the results from a single test and is regarded as an independent entity. The method does not provide the means to describe relations between tests, other than belonging to the same type of test. For example, the method does not relate tests from the same location as a GIS-database application would do.

7 STREAM AND STAND ALONE TOOLS

For the Testdefinition two stand alone tools have been developed, the Testdefiner® and a report tool. As described above, a wide range of information is required to define each item in a Testdefinition completely. The Testdefiner supports the user to enter all required information by a structured graphical user interface. Input accelerators are the capabilities to copy parts of existing Testdefinitions, to copy information from a single quantity using automated counters to maintain required uniqueness. The Testdefiner is programmed in C#. The resulting Testdefinition is a structured XML file that conforms to the STREAM Testdefinition format. In a Testdefinition all information describing the data file is available. However, being an XML file it is not directly suitable for a summary of this description in a factual report. The Testdefinition report tool constructs excerpts from a Testdefinition that can be included into Word or Excel documents.

Specific stand alone tools are also available for presenting and interpretation data files in the GEF format, which has been developed over many years since the GEF format was first created in 1999. There are two tools to reduce the number of readings (or instrument scans) of a GEF file, one by only keeping the n-th row of data and one by graphically selecting a continuous part of the data. The GEFviewer®, is a powerful plotting tool.

8 FUTURE DEVELOPMENTS FOR TC2

The STREAM method was developed (and is continuing to develop) by means of Deltares funding. During this development process both the use at Deltares and the potential use in the international geotechnical community (as defined by the working group for data exchange and archiving of TC2 of ICCSGME) were taken into account. Since no additional funding is expected, no developments solely for working group purposes can be honored. However, it has been attempted to provide a platform which is as flexible as possible. A user software exchange library can be easily arranged based on the basic functions, library and tools provided. Some of the expected developments for the various aspects of STREAM are described below.

- *The concept.* The concept of a definition file and corresponding data files is an essential part of STREAM and will not be changed.
- *The Testdefinition*. All non-user item information in a Testdefinition has to be agreed upon. It will be brought in line with international data models for geological testing, especially with the accuracy of identifying parameters such as the location. These modifications have to be made due to integration of the concept into a national governmental program to make a Dutch national database for hydrological and geotechnical parameters.
- *The Testdefiner*. The Testdefiner itself will be adapted for the modifications described above. The interface may evolve through user feedback.
- *The collection of Testdefinitions*. Each Testdefinition is defined by the people involved with a type of test. If, for example, TC2 agrees a standard type of testing for a routine event, such as a model CPT or T-bar penetrometer test, a standard Testdefinition can be agreed upon. In this case it might be appropriate to make this Testdefinition available by means of a TC2 or ISSGME web site. It might also be useful to make only parts of definitions standard. For example, what particular properties of the centrifuge being used have to be stored. This can be defined by means of the concepts of Testdefinitions as well.
- *The Matlab® STREAM system library*. The basic functions make use of Deltares software. It is expected that the library of STREAM functions will be made freely available. The underlying software will be delivered in a shielded form.
- *The Matlab® STREAM user library*. This is a new development: a public site to exchange generic functions. However, when there are plenty of tools and functions available, the benefit of using STREAM increases and the possibility to exchange test results is enhanced.
- *The GEF library*. This library is now widely used in the Netherlands and supports several field testing exchange formats, so it will remain available. The increase of tools available for GEF will partly depend on the growth of the STREAM libraries described above.

9 CONCLUSIONS

The concept of a standard description document—a Testdefinition—for each type of geotechnical test provides significant benefits to experimentalists. It provides a method that can

1. streamline experimental activity;
2. improve its quality;
3. lead to well-documented tests;
4. archived in a time-proof manner.

The Testdefinition provides a structure for logging and storing in a structured form all of the information that arises from any geotechnical test—ranging from a simple moisture content determination to a complex centrifuge model.

The structure of the Testdefinition is divided into a chronology that reflects the different stages of experimental activity, given by the acronym SMARF—Set-up; Measurement; Analysis; Reporting and Filing. By dividing the experimental activity into this chronology, there are clear gateways at which the experiment advances to the next stage. At each gateway the completeness and quality of the data can be automatically checked according to criteria within the Testdefinition.

Software tools for generating the documentation for defining and inputting test data have been developed and are described in this paper. A basic Matlab library to import, export and convert data based on the Testdefinition is available.

This approach also facilitates the process of defining specific minimum standards for the information to be stored, particularly for cases where no standard currently exists such as centrifuge model tests. It is regarded as an advantage that these standards can develop gradually in time, leading to easier exchange and more efficient interpretation of test results.

2 *Similitude*

This page intentionally left blank

Physical Modelling in Geotechnics – Springman, Laue & Seward (eds)
© 2010 Taylor & Francis Group, London, ISBN 978-0-415-59288-8

Scaling of hydraulic processes

A. Bezuijen
Deltares/Delft University of Technology, Delft, The Netherlands

R.S. Steedman
Steedman & Associates Ltd, London, England

ABSTRACT: The paper reviews the scaling of hydraulic processes in centrifuge model tests under increased acceleration fields. Scaling relations used for the design and interpretation of model tests are found to be complex and affected by a wide range of variables. Classical scaling relations applied to slow, consolidation conditions or rapid dynamic conditions are developed into a comprehensive set of scaling techniques for laminar and turbulent flow. It is found that the interpretation of any given model test requires very careful consideration to ensure that key decisions such as the scaling of grain size or the viscosity of the pore fluid permit the best interpretation of the model data. Examples are given of the scaling of waves, turbulent and laminar flow, and erosion processes.

1 INTRODUCTION

The interpretation of physical model tests carried out in a centrifuge requires a comprehensive understanding of the effects of the increased acceleration field on the relationships governing the phenomena being investigated. The importance of achieving a common basis to the interpretation of centrifuge experiments was illustrated by the publication of a catalogue of scaling laws by TC2 of the ISSMGE (Garnier et al. 2007). One field of scaling relations that is still to be fully documented is the scaling of hydraulic processes. The analytical investigation was carried out by the authors and was used to support the design of a wave generator, tests on micro-stability of sand grains on a slope with an outward directed hydraulic gradient (Bezuijen et al. 2006) and tests on piping (Beek et al. 2010a).

The paper addresses the scaling rules for waves, laminar and turbulent flow, single grain and bulk erosion and is illustrated by examples. The basis for the development of the scaling relations for flow is the Forchheimer equation, and empirical relations to calculate the coefficients in this equation using the porosity and grain size. This empirical relation is comparable to the Ergun equation (Bird et al. 1960) but modified to be more appropriate to the problem of soil particles subject to a range of hydraulic flow conditions. The analysis provides a framework for the design and interpretation of (centrifuge) model tests of hydraulic processes in geotechnical applications, such as flow through dikes or flow over or out of soil slopes. The solutions proposed address conditions of laminar, turbulent and intermediate flow.

2 HYDRAULIC NUMBERS

The classical assumption in centrifuge testing is that the lengths in the model are N times smaller than the length in prototype, where N is the scale factor. The stresses are the same in model and prototype and that implies that the acceleration is N times higher in the model compared to the prototype. Kinematics lead then to the following set of scaling equations:

$$L_{s,m} = \frac{1}{N} L_{s,p} \qquad a_m = N a_p \tag{1,2}$$

$$t_{s,m} = \frac{1}{N} t_{s,p} \qquad u_{s,m} = u_{s,p} \tag{3,4}$$

$_m$: indicates model
$_p$: indicates prototype

where L_s is the characteristic length dimension, a the acceleration, g the acceleration of gravity, t_s the characteristic time and u_s the characteristic velocity (velocity for dynamic effects). Other scaling relations are possible, as will be discussed below.

The consequences of this classical approach on the Froude number (F) and the Reynolds number (R), two key numbers governing hydraulic phenomena in the model and prototype, may be readily deduced. These numbers are expressed in the form:

$$F = \frac{u_o}{\sqrt{a L_s}} \qquad R = \frac{\rho u_o L_s}{\mu} \tag{5,6}$$

where u_0 is the velocity of flow, μ the dynamic viscosity, ρ the density of the liquid and L_s (in this general formula) the typical dimension of a flow canal.

Using the scaling relations set out in Equations 1–4 it is clear that although the Froude number is unchanged in model and prototype, the Reynolds number requires that for exact similitude the viscosity of the model fluid has to be N times *lower* than the viscosity in the prototype. Where the fluid in the prototype is water this is clearly impractical and, as a consequence, although hydraulic processes where Froude scaling is dominant (such as water waves) can be scaled down easily in a centrifuge, the scaling rules cannot be followed exactly in situations where Reynolds scaling is dominant. This does not invalidate the model, but may affect its interpretation, as discussed below.

3 WAVES

The shape of a wave approaching a slope depends on the breaker parameter, see Figure 1.

The breaker parameter (ξ) is expressed as:

$$\xi = \tan\alpha / \sqrt{H/L} \tag{7}$$

where α is the slope angle, H the wave height and L the wave length. To scale breaking waves in a centrifuge, ξ must be constant in model and prototype. Using the kinematic scaling rules set out in Equations 1–4, it is clear that the wave frequency must be N times higher in the model than in the prototype. This presents a real challenge in a centrifuge at high g.

Table 1 shows prototype and 1:50 centrifuge model values for a wave with a wave height of 2 m and a wave steepness of 6%. The required model wave frequency of around 10 Hz is relatively high for a wave generator and it would require a sophisticated hydraulic servo system to create irregular waves.

Furthermore, although much reduced, the wave length in the centrifuge in this example is still 0.67 m, which is large compared to the typical dimensions of a model container. To avoid standing waves in the tank in which the waves are generated, the distance between the wave generator and the target (such as a levee or an offshore structure) should be several wave lengths at least. Typically, a container several meters in length would be necessary. Most centrifuges cannot accommodate such a large container and this makes it complicated to include waves in centrifuge tests.

Thus, although straightforward from a scaling perspective, the high frequency of shorter waves and the length of the run up necessary to model longer waves require careful consideration in a typical centrifuge container. Depending on the orientation, angular velocity and dimensions of the model container, an assessment should also be made of any possible distortion of the shape of the waves by Coriolis effects.

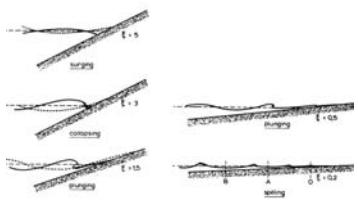

Figure 1. Types of breakers as a function of the breaker parameter ξ according to Battjes (1974).

Table 1. Waves in prototype and 1:50 centrifuge model.

	Prototype	Centrifuge	Scale
Wave height (m)	2	0.04	N
Wave steepness (-)	0.06	0.06	1
Wave length (m)	33.33	0.67	N
Wave period (s)	5.38	0.11	N

4 PERMEABILITY

4.1 *Forchheimer relation*

Flow through granular material is described by the Forchheimer relation (Bear 1988), which may be expressed as:

$$i = av_f + bv_f^2 \tag{8a}$$

where i is the hydraulic gradient and v_f the filter velocity. The terms a and b are the Forchheimer constants. a has the dimension (s/m) and b (s/m)^2. In the case of granular material the parameters a and b can be approximated as (Adel 1989):

$$a = 160\frac{\nu}{g}\frac{(1-n)^2}{n^3 d_{15}^2} \quad \text{and} \quad b = \frac{2.2}{gn^2 d_{15}} \tag{8b}$$

where ν is the kinematic viscosity, n the porosity, d_{15} the diameter of the grains of the granular material with 15% (by weight) of the grains being smaller and g the acceleration due to gravity.

Equation 8 embraces both laminar and turbulent flow. The parameters a and b have different dimensions and therefore it is difficult to assess directly the influence of these parameters on the permeability of the granular matrix. To investigate this, Equation (8) was first rewritten using Darcy's law. Assuming:

$$u = k \cdot i \tag{9}$$

then Equation 8a may be written as:

$$k = \frac{-a + a\sqrt{1 + 4bi/a^2}}{2bi} \tag{10}$$

Equation 10 provides insight into the effect of turbulent flow on permeability, which is seen here to depend on the hydraulic gradient. Since for small values of y, $(1 + y)^{0.5} \approx 1 + 0.5y$. Equation 10 reduces for small values of bi/a^2 (laminar flow) to:

$$k = 1/a \tag{11}$$

For large values of bi/a^2 (turbulent flow) Equation 10 reduces to:

$$k = 1/\sqrt{bi} \tag{12}$$

Substituting the empirical relations for a and b from Equation 8b, the permeability (and thus the flow velocity) for laminar flow is seen to be proportional to d_{15}^2 (as commonly assumed) but for turbulent flow the permeability is proportional to $\sqrt{d_{15}}$. Grain size therefore has a much larger influence on the permeability in a laminar flow regime than in the case of turbulent flow, where the influence of the grain size is much smaller.

This approach may then be used to confirm whether, for any given grain size (d_{15}) and flow velocity in the model, laminar, turbulent or mixed flow conditions will be consistent with the prototype. Figure 2 shows how the different flow states (laminar, mixed or turbulent) are related to hydraulic gradient, flow velocity and grain size.

4.2 *Consequences for scaling*

The flow velocity should be the same in model and prototype (Equation 4). Since the pressure gradient is N times higher in the model this means that the permeability should be N times lower. However, scaling the grain size by N (consistent with the linear scale) would mean that the permeability in the model would be much too low. Reducing the viscosity of the pore fluid by a factor of N to compensate for a reduced grain size is not an option where water is the pore fluid. It is common anyway in geotechnical models to use roughly the same grain size where possible (e.g. coarse/fine sand, silt or clay).

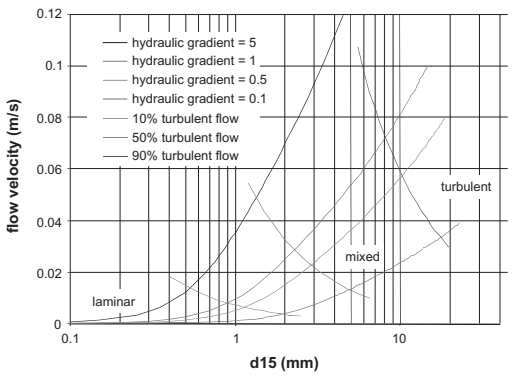

Figure 2. Flow velocity as a function of the grain size for a porosity of 0.4 and a kinematic viscosity of 1×10^{-6} m²/s.

If grain size is maintained constant, then scaling of the permeability for laminar flow requires that the viscosity be N times higher in the model. However, Equation 8 shows that if turbulent flow (when parameter b dominates) is an important consideration in the model, then changing the viscosity is not appropriate. Instead, scaling the grain size linearly with N will be necessary to give the same flow velocity in the model (under a pressure gradient N times higher) as in the prototype. However, this introduces a new complication, in that Reynold's number will then be reduced by N in the model, compared to the prototype resulting in a possible transition from turbulent to laminar flow. This may require further consideration.

At the other end of the scale, where flow is presumed to be laminar, this analysis also provides useful guidance for model design where it is intended to ignore the requirements of Equation 4. A common example is the use of the centrifuge for consolidation. In model tests involving consolidation, it is typical that the prototype grain size is very small, the model grains are not scaled and the model fluid viscosity is not increased. Equation 3 and 4 then become:

$$t_{s,m} = \frac{1}{N^2} t_{s,p} \qquad u_{s,m} = N u_{s,p} \tag{13,14}$$

The consequence of the increase in flow velocity on the model may then be checked using the approach in Section 4.1 and the equivalent to Figure 2 for the actual model material. (For example, if the grain size and pore fluid viscosity are unchanged, then Reynold's number will be increased by N.)

Table 2 summarises the different combinations of scaling relations needed to correctly interpret different hydraulic conditions in a centrifuge model with

Table 2. Scaling of grain size and its influence on the scaling of flow velocity and time for laminar and turbulent flow. The combination in gray may be used in dynamic conditions.

Scaling of grain size (d_{15}):	[-]	$1/\sqrt{N}$	1/N
Laminar flow/water			
k_m/k_p	1	1/N	$1/N^2$
$t_{s,m}/t_{s,p}$	$1/N^2$	1/N	1
$u_{s,m}/u_{s,p}$	N	1	1/N
Lam. flow/viscous liquid, (where $\nu_m = N\nu_p$)			
k_m/k_p	1/N	$1/N^2$	$1/N^3$
$t_{s,m}/t_{s,p}$	1/N	1	N
$u_{s,m}/u_{s,p}$	1	1/N	$1/N^2$
Turbulent flow/water			
k_m/k_p	$1/\sqrt{N}$	$1/N^{0.75}$	1/N
$t_{s,m}/t_{s,p}$	$1/(N\sqrt{N})$	$1/N^{1.25}$	1/N
$u_{s,m}/u_{s,p}$	$\sqrt{N}$	$N^{0.25}$	1

a characteristic grain size d_{15}. The purpose of the table is to show how mixed or turbulent flow may distort the interpretation of a model designed using the classical laminar flow assumption. In general all combinations as shown in Table 2 are possible. It is clear that linear scaling of grain size is the simplest approach to the modelling of turbulent flow.

5 EROSION AND PIPING

5.1 *Single and bulk grain erosion*

Erosion may be divided into single grain erosion and bulk erosion (van Rhee 2002). Single grain erosion is characterised by flow over a granular (e.g. sand) layer, where the flow is sufficient to pick up individual grains one by one with no interaction between the grains and the sand layer underneath. Examples are sand erosion in rivers and on beaches.

During bulk erosion (such as during dredging operations), the erosion rate is so high that groundwater flow in the sand layer also affects the erosion rate. For sand particles to be removed in saturated conditions at high speed, it is necessary that the porosity of the upper part of the sand layer increases and this can only occur when there is a water flow into the sand.

For the purposes of this paper, the analysis has been limited to single grain erosion. Again, there is a difference between laminar and turbulent flow.

5.1.1 *Erosion—laminar flow*

Where there is no scaling of the grains, the weight of the grains will be N times higher in the model compared to the prototype. To exert a comparable erosive force on the grain in the model and the prototype means that the pressure gradient has to be N times higher. Since this is a direct consequence of adopting a 1/N linear scale at Ng, with or without a high viscosity liquid, then single grain erosion under laminar flow conditions should be correctly scaled. This result was confirmed experimentally by Bezuijen & Den Adel (2006), although different findings from recent experiments (Beek et al, 2010b) suggests that the result depends on the geometry of the problem. The interpretation of erosion in laminar flow models is very complex for some geometries, as discussed in Section 5.2 below.

5.1.2 *Erosion—turbulent flow*

The scaling rules for single grain erosion under 1 g conditions were presented by Van Rhee (2002):

$$E = \kappa \cdot \rho_s \sqrt{\Delta g D} \left[\frac{f_0}{8 \Delta g D} (u^2 - u_{cr}^2) \right]^{\alpha} \qquad (15)$$

where E is the erosion rate, κ a coefficient, ρ_s the density of the grains, $\Delta = (\rho_s - \rho)/\rho$ with ρ the density of water, D the diameter of the grains, f_0 the Darcy-Weisbach friction coefficient (dimensionless), u the flow velocity, u_{cr} the critical flow velocity when erosion starts and α is an exponent (1.5 according to van Rijn 1984).

Following this approach for centrifuge conditions (substituting Ng for g) shows that single grain erosion will be correctly scaled under turbulent flow provided the grain size is scaled down by 1/N. This gives the same erosion rate in the model as in the prototype, as should be the case given the same velocities in model and prototype. This is an important result because it means that the shaping of gravel beaches associated with failure of breakwaters can be studied in a centrifuge.

This finding may be explored further using the Shields parameter θ, a dimensionless shear stress developed by normalising the shear force derived from the flow by the resistance of the grains (based on density and dimension). This parameter can be expressed for centrifuge conditions under Ng as:

$$\theta = \frac{\tau}{(\rho_s - \rho) NgD} = \frac{u_*^2}{\Delta NgD} \text{ with } u_* = \sqrt{\frac{f}{8}} u \qquad (16)$$

where, in addition to the terms defined above, τ is the shear stress exerted on the bed and u_* is the friction or shear velocity (the square root of the bed shear stress divided by ρ) and f the friction coefficient. This parameter depends on the geometry of the problem and Reynolds number but is independent of the g level itself.

Experimental data show that the Shields parameter may be considered broadly constant for sand grains above values of the boundary Reynold's number $u_* D/\nu$ of around 5. (Below this value, in laminar flow conditions, it increases sharply.) The critical Shields parameter θ_{cr} is the value of the Shields parameter θ when the grains start moving, i.e. where $u = u_{cr}$ in Equation 17. It is clear from Equation 17 that if the grain size is not scaled and the Shields parameter is constant, then the critical velocity will be $\sqrt{N}$ times greater in a centrifuge model at Ng. For the critical flow velocity to be the same in model and prototype and assuming again that the Shields parameter is roughly constant over the range of Reynold's number between model and prototype, then the scaling of single grain erosion close to the critical velocity in turbulent flow conditions will only be correct if the grain size is reduced by 1/N.

5.2 *Piping*

Piping is an erosion mechanism caused by excessive hydraulic gradients. Figure 3 illustrates a typical field problem where piping allows grains from an underlying permeable sand layer to be eroded as hydraulic gradients below a dike become too large.

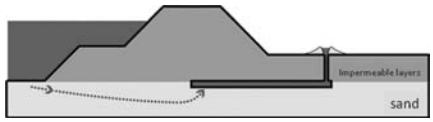

Figure 3. Sketch illustrating typical piping mechanism.

Quite often small 'craters' are seen on the downstream side of dikes (as in Figure 3), but the last dike failure in the Netherlands considered to be caused by piping dates back to the 19th century. Beek et al. (2010a) report results from centrifuge model tests investigating piping and it is clearly important for this paper to review how the scaling relations may apply to this phenomenon.

A particular feature of piping erosion that affects its potential to be modelled in a centrifuge is the rather unusual length-scaling for this mechanism, which may be explained by flow velocity differences in the sand layer. A flownet for a 2-dimensional semi-infinite aquifer, with an impermeable dam on top, is shown in Figure 4.

Usually the average gradient $H/(2b)$ in Figure 4 is used to see whether or not piping is critical (values between 0.05 and 0.2). However, it will be the gradient at the downstream outflow that determines whether or not piping starts. According to Polybarinova-Kochina (1962) the flow velocity (v) directly underneath the dam may be defined by the relation:

$$v = \frac{kH}{\pi\sqrt{x^2 - b^2}} \tag{17}$$

where x is the distance from the centreline in the middle between the points B and C in Figure 4. It may be assumed that erosion of sand will start when v exceeds a certain value. However, this relationship is clearly insufficient on its own to assess the local length scale near the exit, as the value of v tends to infinity when x approaches b.

An alternative criterion that can be used instead is to assume that sand grains will only move at the point C in Figure 4 when over a certain distance between $x = b$ and $x = x_0$ (where $x_0 > b$) the total discharge is larger than a certain value. The total discharge between $x = b$ and $x = x_0$ may be written as:

$$Q = \frac{kH}{\pi}\ln\left(\frac{x_0 + \sqrt{x_0^2 - b^2}}{b}\right) \tag{18}$$

For small values of $x_0 - b = \Delta x$, and noting that $\ln(1 + \Delta y) \approx \Delta y$, then the average hydraulic gradient ($i_a = Q/(k\Delta x)$) may be approximated as:

$$i_a = \frac{H}{b\pi}\sqrt{\frac{2b}{\Delta x}} \tag{19}$$

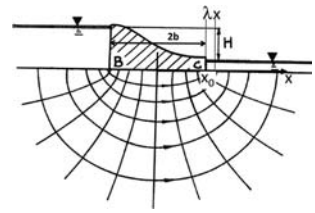

Figure 4. Sketch for groundwater flow calculation.

It is further assumed that for any given sand, i_a must reach a certain threshold value in order to loosen the grains to start the piping process. This implies that there needs to be a certain average gradient over a given number of grains, independent of the scale of the flow net, to start the piping.

The consequence of Equation 19 is that there will be a length scale effect in the piping process. A limiting value of H/b found in a model test will be higher than the limiting value of H/b in prototype, because i_a is constant both in model and prototype and $b/(\Delta x)$ is larger in prototype.

A scale dependency was also found in model tests (Silvis 1991 and Beek et al. 2010b). However, the dependency itself was not the same as predicted by the formulae above. According to Equation 19, for models of decreasing size, for a given value of i_a, H/b will increase with the square root of the decrease in b (and hence with the square root of the increase in N, the scale), but instead the data showed an increase to the 1/3 power, a smaller rate of increase than expected, although still significant.

One explanation for this discrepancy is that the experiments were more focussed on the formation of a channel underneath the impermeable layer as sketched in Figure 4, rather than on the initiation of piping at the exit point. It is likely that during the formation of a channel below the impermeable layer the flownet would be significantly different from the Polibarinova-Kochina ideal.

The model tests reported by Bezuijen & Den Adel (2006) and discussed in Section 5.1.1 above appeared to confirm that single grain erosion under laminar flow was correctly scaled. However, in the data presented by Beek et al. (2010a) the critical hydraulic gradient was found to reduce with g level rather than remain constant, as would be expected using the same model dimensions and grain size at various g levels. Instead it appeared that there was a decrease in the critical gradient underneath the dam with increasing g level, see Figure 5.

It is possible that this is a complexity introduced as a consequence of the increase in Reynold's number and reduction in the Shields parameter with increasing g level in the laminar flow conditions existing below the impermeable layer. The reduction in Shields parameter may partially offset the increase in critical velocity and thus affect the

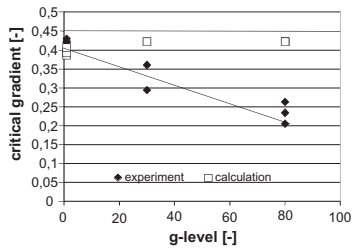

Figure 5. Critical gradient as a function of g level. Taken from Beek et al. (2010a), modified.

critical hydraulic gradient. Further work is needed to resolve these different interpretations.

For field applications, the increase in H/b found by Beek et al. (2010b) for a given value of i_a raises questions over the use of Bligh's (1910) assumption, that H/b is independent from b. Following Bligh's approach could lead to the underestimation of the critical hydraulic gradient underneath the dam, if the same value of H/b derived from a small dam is used for a much larger structure: an unsafe assumption.

The modelling of piping phenomena in a centrifuge model is complex and requires the scaling of grain size to ensure that the single grain erosion under turbulent flow is realistically reproduced. Without this, interpretation of the model data in prototype terms is very complex. The singular nature of the initiation of piping and the transient condition that follows until a steady state erosive process has developed is a further problem for the interpretation of the model test. It is not clear from the data reviewed for this paper that the results of centrifuge model tests can yet be used directly in the field to predict reliably the onset of piping.

6 CONCLUSIONS

This review of the scaling laws for certain hydraulic processes commonly experienced in geotechnical centrifuge models leads to the following conclusions:

- Froude scaling is no problem in a centrifuge. In principle wave generation is possible, but there are some technical challenges, certainly irregular waves are generated or when wave reflections have to be compensated for.
- Exact Reynolds scaling as would be necessary for dynamic processes is not possible. A compromise has to be found depending on the process studied.
- Laminar flow can in principle be studied in a linear scale centrifuge model test using the same grains and viscous fluid or using normal water and grains scaled with the square root of the model scale.
- Turbulent flow can best be scaled by scaling down the grains proportionally to the model scale. This result presents the opportunity to scale down large blocks (for example as in a breakwater) in a centrifuge.
- Modelling of erosion phenomena requires very careful consideration of the flow conditions and particularly whether the erosion process is steady-state or transient and whether it is occurring under laminar or turbulent conditions. The conventional option of scaling grain size introduces additional complexity which makes interpretation of the experimental results challenging.
- Scale modelling of hydraulic processes on the centrifuge is very difficult when the solution of the flow equation leads to flow singularities, because the scale of the grains compared to the dimensions of the structure is then of importance. An example of this is the initiation of piping.

REFERENCES

Adel den, H. 1989. *Re-analysing permeability experiments with the Forchheimer relation (in Dutch)*. GeoDelft report CO-272553/56.

Battjes, J.A. 1974. Computation of set-up, longshore currents, run-up and overtopping due to wind-generated waves. *Comm. on Hydraulics, Dept. of Civil Eng., Delft University of Technology*. Report 74–4.

Bear, J. 1988. *Dynamics of Fluids in Porous Media*. Dover Publications Inc. New York.

Beek, V.M., van, Bezuijen, A. & Zwanenburg, C. 2010a. Piping: Centrifuge experiments on scaling effects and levee stability. *7th International Conference on Physical Modelling in Geotechnics*. Zurich.

Beek, V.M., van, Knoeff, J.G., Rietdijk, J., Sellmeijer, J.B. & Lopez De La Cruz, J. 2010b. Influence of sand characteristics and scale on the piping process—experiments and multivariate analysis. *7th Int. Conf. on Physical Modelling in Geotechnics.* Zurich.

Bezuijen, A. & Den Adel, H. 2006. Dike failure due to surface erosion Ng and 1 g tests. *Proc. 6th Int. Conf. on Physical Modelling in Geotechnics.* Hong Kong.

Bird, R.B., Stewart, W. & Lightfoot, E.N. 1960. *Transport phenomena*. New York. John Wiley & Sons.

Bligh, W.G. 1910. Dams Barrages and Weirs on Porous Foundations. *Engineering News.* 64(26):708–710.

Garnier, J., Gaudin, C., Springman, S., Culligan, P.J., Goodings, D., Konig, D., Kutter, B., Phillips, R., Randolph, M.F. & Thorel, L. 2007. Catalogue of scaling laws and similitude questions in geotechnical centrifuge modelling. *International Journal of Physical Modelling in Geotechnics.* 7(3):1–23.

Polubarinova-Kochina, P.Y.A. 1962. *Theory of groundwater movement*. Translated from the Russian by J.M. Roger de Weist. Princeton University Press.

Silvis, F. 1991. *Verification Piping Model; experiments in the Delta flume.* Evaluation report (in Dutch) Delft Geotechnics Report. CO317710/7.

Rhee, C. van 2002. *On the sedimentation process in a trailing suction hopper dredger.* Delft University of Technology. Netherlands.

Rijn, L.C van. 1984. Sediment pick-up functions. *J.Hydraul. Eng.* 110:1495–1502.

Physical Modelling in Geotechnics – Springman, Laue & Seward (eds)
© 2010 Taylor & Francis Group, London, ISBN 978-0-415-59288-8

A virtual rain simulator for droplet transport in a centrifuge

B. Caicedo & J. Tristancho
Department of Civil and Environmental Engineering, Universidad de los Andes, Bogotá, Colombia

ABSTRACT: Rain is one of the most important sources of geotechnical problems, as for example in slope stability, shallow foundations, pavements and others. Simulating rain in centrifuge models looks easy using nozzles developed for agricultural purposes; these nozzles produce droplets that simulate rain. However due to the presence of factors such as Coriolis force, drag on the droplets, evaporation, and wind around the model, the prediction of the distribution pattern of droplets over the model is a difficult task. For this reason, the conception of a rain device for centrifuge, producing homogeneous rain distribution, is only possible after a tedious experimental process of trial and error. This paper presents a virtual rain generator for centrifuge developed to help in the conception of raining devices in a centrifuge.

1 INTRODUCTION

Rain simulation in centrifuge is helpful to model geotechnical problems where the interaction between the rain and the soil plays an important role: slope stability (Kimura et al. 1991), expansive soils, soil drainage, etc. Most of the devices producing rain in centrifuge are nozzles generating droplets. These droplets are affected by the Coriolis and drag forces, as well as by evaporation processes. As a result, the characteristics of the simulated rain depend on a huge number of parameters: centrifuge acceleration, centrifuge radius, position and direction of the nozzle, injection pressure, wind velocity, temperature and relative humidity. Therefore, the design of a rain generation device that assures a homogeneous distribution of rain in centrifuge models is a difficult task, made by trial and error.

The objective of this paper is to present a numerical simulation model that mimics the behavior of droplets in the spray cloud, expressed from a hydraulic nozzle in a rotating frame. The initial size and corresponding velocity of each droplet ejected is obtained using a random generator, based on physical measurements. The transport model uses an effective drag coefficient that accounts for aerodynamic drag, air entrainment and mutual interference of droplets, in addition to evaporation effects and vertical wind velocity fluctuations. Simulated targets collect the droplets at different positions below the virtual nozzle, to study deposition patterns. This virtual rain generator allows several nozzles to be placed in specific positions and directions. The optimal position of nozzles working simultaneously allows different rain intensities to be simulated, and optimizes the droplets homogeneity on the target surfaces.

2 KINEMATICS OF A BODY IN A ROTATING FRAME

To illustrate the kinematics of body in a rotating frame, a flat horizontal turntable rotating at a constant rate is considered, described by angular velocity ω. A man throws a body on this table, in any direction, considering that no net forces act on it.

The kinematics of the body can be described in different ways, depending on the position of the observer (Fig. 1):

- For observer B (inertial frame), the body moves at constant velocity describing a rectilinear trajectory.
- On the other hand, for observer A, on the rotating frame, it appears that the body trajectory seems to be spiral (Fig. 2). From his point of view, it looks as though there is a force acting on it.

Such a force is "fictitious". In fact, the acceleration of the body is caused exclusively by the motion of the observer. According to the observer on the rotating frame, there appears to be a force with one component pointing outwards and another directed around. The "fictitious" force seen by the observer A in vector notation is, (Lewowski et al. 1999):

$$\vec{F}_{\text{Fict}} = -m\vec{\omega} \times (\vec{\omega} \times \vec{\rho}) - 2m\vec{\omega} \times \vec{v} \quad (1)$$

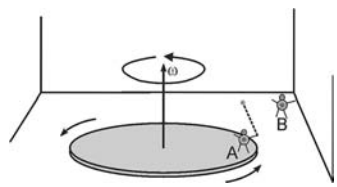

Figure 1. Trajectory of a body in a rotating and a non-rotating frame.

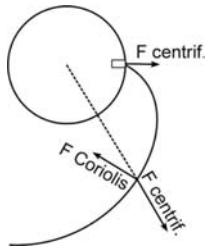

Figure 2. Curvilinear trajectory observed in the rotating frame.

where $\boldsymbol{v}$ is the velocity as seen in the rotating frame (that is, as seen by the observer A). The angular velocity vector of the rotating frame is ω and it points vertically out of the rotating axis (Fig. 3):

$$\vec{\omega} = \hat{z}\omega \tag{2}$$

considering that the initial position of the body is (ρ, 0) in radial coordinates, and using the relationships:

$$\vec{\rho} = \hat{\rho}\rho, \quad \hat{z} \times \hat{\rho} = \hat{\theta}, \quad \text{and} \quad \hat{z} \times \hat{\theta} = -\hat{\rho} \tag{3}$$

then the centrifugal force is represented by:

$$\vec{F}_{cent} = m\omega^2\rho\hat{\rho} \tag{4}$$

If the velocity, as seen in the rotating frame, is:

$$\vec{v} = \hat{\rho}v_\rho + \hat{\theta}v_\theta \tag{5}$$

Then, the Coriolis force becomes:

$$\vec{F}_{Cor} = 2m\omega(\hat{\rho}v_\theta - \hat{\theta}v_\rho) \tag{6}$$

and the fictitious force necessary to describe the curvilinear trajectory of the body in a rotating frame is:

$$\vec{F}_{Fict} = m(\omega^2\rho + 2\omega v_\theta)\hat{\rho} - 2m\omega v_\rho\hat{\theta} \tag{7}$$

Note that there are two components in the radial direction: the centrifugal and the Coriolis force, and one component on the angular direction that depends only on the Coriolis force.

3 NUMERICAL MODEL OF RAINFALL IN A CENTRIFUGE

3.1 *Kinematics of a droplet in a centrifuge*

Nozzles used for agricultural purposes are suitable for reproducing rain in centrifuge. These nozzles eject droplets that propagate in all directions of a three-dimensional frame. Cylindrical coordinates are appropriate to analyze the kinematics of a droplet.

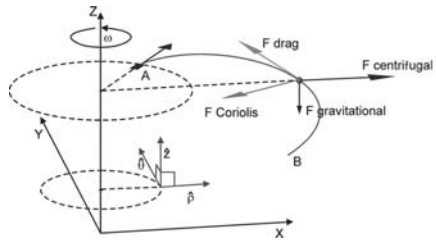

Figure 3. Trajectory of a droplet in a rotating frame.

Consider a droplet ejected from point A (Fig. 3) in a radial direction within a frame rotating with constant angular velocity ω around z-axis. For an observer located at point A, the droplet describes a curvilinear trajectory as a result of the different forces that act on it: the gravitational force in the z direction, the centrifugal force on radial direction, and the Coriolis force on radial and tangential directions. Also, drag forces have to be considered in the analysis due to the high velocity of the droplets once ejected from the nozzle (Sidhamed et al. 2005).

3.2 *Conservation of momentum*

Take a droplet located at (ρ, θ, z) in a cylindrical rotating frame (Fig. 3), and consider that its velocity relative to the rotating frame is given by:

$$\vec{V}_d = \hat{\rho}v_\rho + \hat{\theta}v_\theta + \hat{z}v_z \tag{8}$$

The trajectory of the droplet in the rotating frame is affected by the centrifuge, gravity, Coriolis and drag forces. These forces are:

$$\vec{F}_{grav} = -m_d g\hat{z} \tag{9}$$

$$\vec{F}_{cent} = m_d\omega^2\rho\hat{\rho} \tag{10}$$

$$\vec{F}_{Cor} = 2m_d\omega(\hat{\rho}v_\theta - \hat{\theta}v_\rho) \tag{11}$$

Here m_d is the mass of the droplet. The drag force acts in the opposite direction to the relative velocity between the droplet and the air above the model. The drag force of a droplet has been proposed by Sureshkumar et al. (1997), in the rotating frame as:

$$\vec{F}_{drag} = -C_D\left(\frac{\pi D_d^2}{4}\right)\left(\frac{\rho_a W^2}{2}\right)(R_\rho\hat{\rho} + R_\theta\hat{\theta} + R_z\hat{z}) \tag{12}$$

Here C_D is the drag coefficient, D_d is the diameter of the droplet, ρ_a is the air density, W is the magnitude of the relative velocity between the air and the droplet, and R_ρ, R_θ, and R_z are the direction cosines of each component of the relative velocity

in the cylindrical frame. The magnitude of the relative velocity between the air and the droplet is:

$$W = [(v_\rho - v_{\rho(air)})^2 + (v_\theta - v_{\theta(air)})^2 + (v_z - v_{z(air)})^2]^{1/2} \quad (13)$$

and each direction cosine of the relative velocity is:

$$R_\rho = \frac{(v_\rho - v_{\rho(air)})}{W} \quad (14)$$

$$R_\theta = \frac{(v_\theta - v_{\theta(air)})}{W} \quad (15)$$

$$R_z = \frac{(v_z - v_{z(air)})}{W} \quad (16)$$

The flow of air over a model in a centrifuge is extremely complex, since it is affected by all the components of the machine. For this reason, it is necessary to take precautions concerning the air flow, in order to apply artificial rain under controlled characteristics.

Well controlled conditions for air flow in a beam centrifuge are possible by covering the model with an appropriate device. If the model is covered, the motion of the air occupying the space above of the surface of the soil is induced by the motion of the model and the cover. As a result, the model and the air above it rotate in unison with constant angular velocity ω about z axis. However this assumption is only a first approximation of the air flow problem. In fact, if there is a gradient of temperature, a vortex will appear as a result of the Coriolis forces. Nevertheless the velocity of these vortices is low compared with the velocity of the droplet (Vargas et al. 2002). For this reason, the model considers, as a first approximation, zero relative velocity between the surface of the model and the air. In other words, the numerical model considers that the air and the physical model rotate in unison.

The droplets generated by the nozzles used to simulate rain are small in diameter; as a result the droplets can evaporate in flight and even disappear. Under these circumstances, the mass of the droplets changes during raining. Therefore the momentum balance is represented by:

$$\frac{d(m_d \vec{V}_d)}{dt} = -m_d \frac{\partial \vec{V}_d}{dt} + \vec{V}_d \frac{\partial m_d}{dt} \quad (17)$$

Considering the forces affecting the droplet (Equations 9 to 12), the first term of the conservation equation of momentum is:

$$m_d \frac{d(\vec{V}_d)}{dt} = -m_d g\hat{z} + m_d \omega^2 \rho\hat{\rho} + 2m_d \omega(\hat{\rho}v_\theta - \hat{\theta}v_\rho) - C_D\left(\frac{\pi D_d^2}{4}\right)\left(\frac{\rho_a W^2}{2}\right)(R_\rho\hat{\rho} + R_\theta\hat{\theta} + R \quad (18)$$

3.3 *Conservation of droplet mass*

The mass of the droplets reduces as the droplets evaporate. The equation to calculate the rate of change of droplet mass due to evaporation used here was proposed by Ranz and Marshall (1952), Goering et al. (1972), Thompson & Ley (1983) and Sidhamed et al. (2005). This equation, in terms of droplet diameter (in μm), is given below.

$$\frac{dD_d}{dt} = 2\left(\frac{M_v}{M_a}\right)\left(\frac{D_v}{D_d}\right)\left(\frac{\rho_a}{\rho_L}\right)\left(\frac{\Delta P}{P_a}\right)(2 + 0.55N_{sc}^{1/3}N_{re}^{1/2}) \quad (19)$$

Here D_d is the droplet diameter in μm, M_v is the molecular mass of vapour diffusing from the droplet, M_a is the molecular mass of air, D_v is the diffusion coefficient of vapour in air in m²/s, ρ_a is the density of air, ρ_L is the density of water, ΔP is the difference between saturation vapour pressure at the drop surface and vapour pressure in the surrounding air, P_a is the partial pressure of air, $N_{sc} = \mu_d/\rho_a D_v$ is the Schmidt number, $N_{re} = D_{ra}W/\mu_a$ is the Reynolds number, and μ_a is the absolute viscosity of air.

The temperature of the droplet is close to the wet temperature of air, (Thompson & Ley 1983), under this consideration the pressure difference ΔP can be expressed as follows, (Sidahmed et al. 2005):

$$\Delta P = 67(T_{wb} - T_{db}) \quad (20)$$

Where T_{wb}, and T_{db} are the wet and dry bulb temperatures of air in °C.

The second term of the conservation equation of momentum is then:

$$\vec{V}_d \frac{\partial m_d}{dt} = \vec{V}_d\left(\rho_L \frac{1}{2}\pi D_d^2 \frac{dD_d}{dt}\right) \quad (21)$$

3.4 *Droplet trajectory*

The accelerations of the droplet in each direction of the cylindrical rotating frame are obtained from Equations 18 and 21, as follows:

$$\frac{dv_\rho}{dt} = \omega^2\rho + 2\omega v_\theta - \frac{3}{4}\left(\frac{C_D}{D_d}\right)\left(\frac{\rho_a W^2}{\rho_w}\right)R_\rho - \frac{3v_\rho}{D_d}\frac{dD_d}{dt} \quad (22)$$

$$\frac{dv_\theta}{dt} = -2\omega v_\rho - \frac{3}{4}\left(\frac{C_D}{D_d}\right)\left(\frac{\rho_a W^2}{\rho_w}\right)R_\theta - \frac{3v_\theta}{D_d}\frac{dD_d}{dt} \quad (23)$$

$$\frac{dv_z}{dt} = -g - \frac{3}{4}\left(\frac{C_D}{D_d}\right)\left(\frac{\rho_a W^2}{\rho_w}\right)R_z - \frac{3v_z}{D_d}\frac{dD_d}{dt} \quad (24)$$

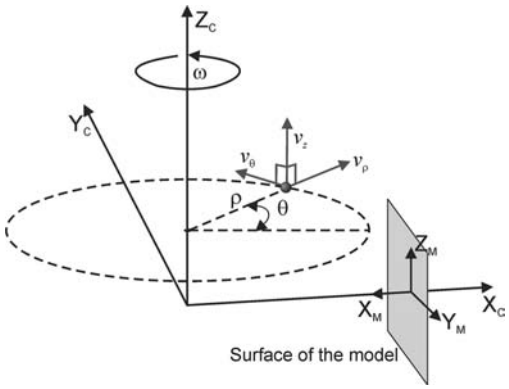

Figure 4. Global Cartesian rotating frame and model local Cartesian frame.

Introducing a rotating Cartesian frame, the centrifuge frame is suitable for analyzing the droplet trajectory (Fig. 4). The z-axis (Z_C) of this global Cartesian frame coincides with the centrifuge rotating axle, and the x-axis (X_C) is coincident with the arm of the centrifuge.

The droplet position in a global Cartesian rotating frame is calculated from the velocities in the rotating cylindrical frame as follows:

$$\frac{dx_C}{dt} = v_\rho \cos\theta - v_\theta \sin\theta \tag{25}$$

$$\frac{dy_C}{dt} = v_\rho \sin\theta + v_\theta \cos\theta \tag{26}$$

$$\frac{dz_C}{dt} = v_z \tag{27}$$

Finally, the relative position of droplets in a model Cartesian frame, (X_M, Y_M, Z_M) having its origin in the intersection between the global x-axis and the surface of the model is given below, (Fig. 4):

$$x_M = x_{\text{model}} - x_C \tag{28}$$

$$y_M = -y_C \tag{29}$$

$$z_M = z_C \tag{30}$$

4 BOUNDARY AND INITIAL CONDITIONS

4.1 *Nozzle position*

A method to assure an adequate distribution of droplets in centrifuge is including a number of nozzles in adequate location and direction, depending on the shape of the model (Kimura et al. 1991). Thus, it's possible to include different nozzles located at (X_i, Y_i, Z_i) on the Cartesian frame of the model in the numerical virtual rain generator. Furthermore, the axis of each nozzle can be rotated with respect to the model Cartesian frame by the angles (α_i, β_i, γ_i), as indicated in Figure 5.

4.2 *Direction of ejection*

The virtual rain generator is made of nozzles projecting water in a rectangular pattern (Fig. 6). This pattern is defined by two opening angles of the spray: $\delta_{\max}$ and $\lambda_{\max}$.

The direction along which a droplet is injected is defined by two angles δ_j ($-\delta_{\max}/2 < \delta_j < \delta_{\max}/2$), and λ_j ($-\lambda_{\max}/2 < \lambda_j < \lambda_{\max}/2$). Montecarlo simulation is used to generate the initial trajectory of each droplet.

4.3 *Drop size and velocity spectra*

For each type of nozzle it is important to measure the drop size spectra. The measures carried out by Sidhamed (2005), show that the drop size spectra can be described using a log-normal probability distribution function. The numerical model proposed in this paper uses a Montecarlo generation algorithm to obtain the drop size spectra. Figure 7

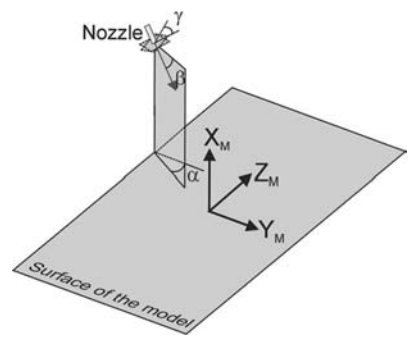

Figure 5. Nozzle position in the model Cartesian Frame.

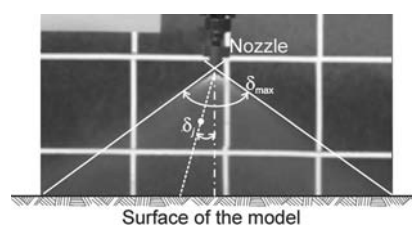

Figure 6. Schematic showing the opening angles of ejection from the nozzle.

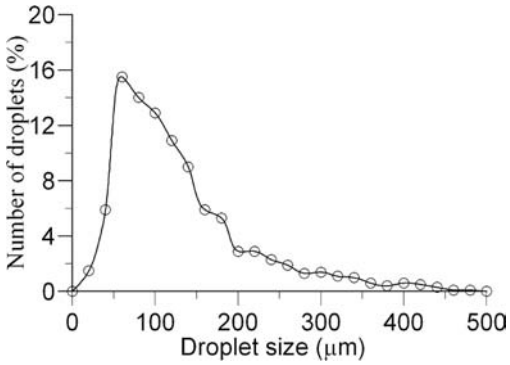

Figure 7. Droplet size spectra from the Montecarlo simulation.

shows the droplet spectra used in the virtual rain generator.

The ejection velocity of the nozzle depends on the injection pressure through the Bernoulli equation:

$$V_0 = C_V \sqrt{\frac{2\Delta p}{\rho_w}} \tag{31}$$

Here, C_V is the coefficient of velocity for the nozzle. Equation 31 is useful for calculating the mean velocity of the droplets, in this case a probability distribution function is adopted as well and the velocity of each droplet is obtained using Montecarlo simulation.

4.4 *Virtual target model*

To collect the spray droplets ejected by the virtual nozzle and to study their distribution patterns and the deposition characteristics, it is necessary to define a virtual target. The virtual target is a flat surface in this paper, i.e. the surface of the model.

5 RESULTS AND DISCUSSION

The initial virtual tests of the numerical model concern the estimation of the effect of the centrifuge acceleration and the size of the centrifuge arm. Six virtual tests were carried out with centrifuge accelerations of 100 g, 50 g and 20 g, and two centrifuge radius of 5.5 m and 1.9 m. The target area was the surface of the model that is a rectangular region having 40 cm ∗ 60 cm, and the nozzle was located vertically 15 cm above the centre of the target surface. Table 1 presents the input values for the parameters used in the model.

Figures 8 and 9 show the trajectories of the droplets for the different virtual tests, these show

Table 1. Input values for the model.

Input parameter	Value
Nozzle opening angle	118°
Mean droplet velocity	6 m/s
Standard deviation of droplet velocity	1.2 m/s
Mean droplet diameter	10^{-4} m
Standard deviation of droplet diameter	$5 * 10^{-5}$ m

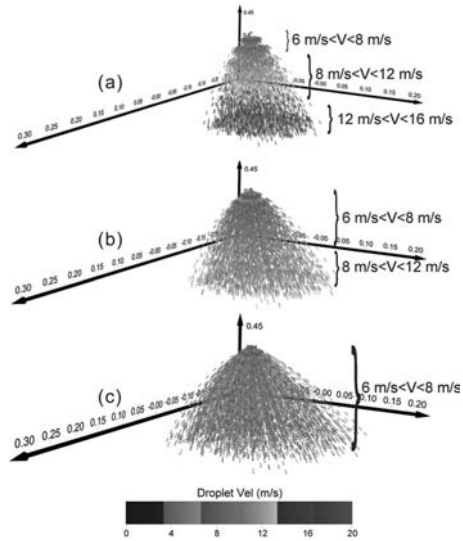

Figure 8. Rain trajectories for a 5.5 m centrifuge radius and centrifuge accelerations of: (a) 100 g, (b) 50 g, and (c) 20 g.

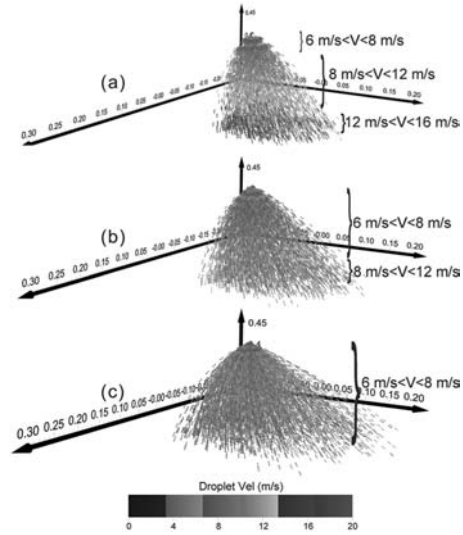

Figure 9. Rain trajectories for a 1.9 m centrifuge radius and centrifuge accelerations of: (a) 100 g, (b) 50 g, and (c) 20 g.

the higher the acceleration level, the higher the droplet velocity at impact. In fact, for the tests carried out at 100 g, the impact velocity is around 14 m/s, while the impact velocity is around 8 m/s for the tests at 20 g. These results show that for the tests carried out at higher centrifuge accelerations, the centrifuge force is dominant over the Coriolis force. The radius of the centrifuge has an influence too; so that the Coriolis force is higher for the tests carried out with a centrifuge radius of 1.9 m, than in the case of a centrifuge with a 5.5 m radius. As a result, the deviation from the ejection point is higher on the tests with 1.9 m radius. The velocities shown in Figures 8 and 9 are relative velocities in the rotating frame that are different to velocities in the inertial frame.

Figure 10 shows the droplet impacts on the surface of the model. The deviation of the droplet impact is clearly noticeable in this figure, in the direction of the Coriolis force, and a slight deviation in the direction of gravity. The droplets in the tests with higher acceleration are smaller than the droplets in the lower acceleration tests. This is the result of the greater evaporation on the higher acceleration tests, due to the higher droplet velocity.

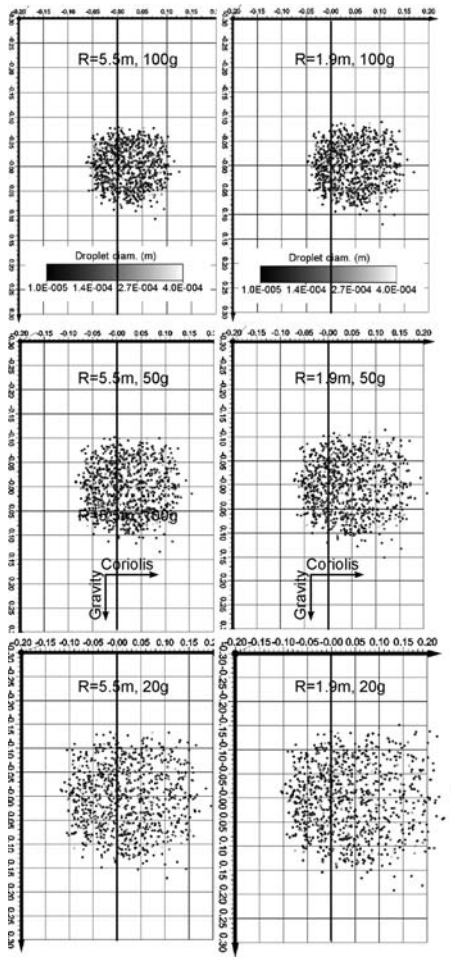

Figure 10. Droplet impact points.

6 CONCLUSIONS

This paper presents a numerical model to calculate droplet transport in a rotating frame. The model reveals that producing homogeneous rain in centrifuge depends on a huge set of parameters. For this reason, this model will be a useful tool for better conception of centrifuge raining devices, once it is calibrated.

The results presented in this paper use the characteristics of raining devices reported in different papers (Sidahmed et al. 2005). The validation process underway at the University of Los Andes is intended to characterize the nozzles in terms of droplets velocities and diameters, and physical models on centrifuge at different g levels are carried out to validate the impact pattern of the droplets.

REFERENCES

Goering, C.E., Bode, L.E. & Gebhardt, M.R. 1972. Mathematical modeling of spray droplet deceleration and evaporation. *Transactions of the ASAE* 15(2): 220–225.

Kimura, T., Takemura, J., Suemasa, N. & Hirooka, A. 1991. Failure of fills due to rain fall. In Ko et al. (eds), *Centrifuge 91, Int. Conf., Boulder, CO*, 509–516. Rotterdam: Balkema.

Lewowski, T., Lewoska, L. & Mazur, P. 1999. Measurement of the effect of Coriolis and centrifugal forces on the trajectory of a body in a rotating frame. *Eur. J. Phys*. 20: 109–116.

Ranz, W.E. & Marshall, W.R. Jr. 1952. Evaporation from drops: Part I. *Chemical Engineering Prog*. 48(3): 141–146.

Sidahmed, M.M., Taher, M.D. & Brown, R.B. 2005. A virtual nozzle for simulation of spray generation and droplet transport. *Journal of Biosystems Engineering* 92(3): 295–307.

Thompson, N. & Ley, A.J. 1983. Estimating drift using a randomwalk model of evaporating drops. *Journal of Agricultural Engineering Research* 28: 261–419.

Vargas, M., Ramos, E., Ascanio, G. & Espejel, R. 2002. A centrifuge for studies of fluid dynamics phenomena in a rotating frame of reference. *Rev. Mex. de Fís*. 48(3): 255–266.

Physical Modelling in Geotechnics – Springman, Laue & Seward (eds)
© 2010 Taylor & Francis Group, London, ISBN 978-0-415-59288-8

Potentialities and challenges of centrifuge modelling on unsaturated soils

B. Caicedo & J. Tristancho
Department of Civil and Environmental Engineering, Universidad de los Andes, Bogotá, Colombia

L. Thorel
Laboratoire Central des Ponts et Chaussées, Nantes, France

ABSTRACT: The behavior of geotechnical structures located near the soil surface is highly influenced by unsaturated soil conditions. Some researches about the potentialities of centrifuge modeling of geotechnical problems involving unsaturated soils are presented, with a focus on scaling laws, soil preparation, instrumentation and atmospheric actuators. Finally some ideas to improve the practice of centrifuge modeling with unsaturated soils are presented.

1 INTRODUCTION

Centrifuge technique has been widely used to model geotechnical structures mainly when the free surface or the stress gradient plays an important role on the structure's behavior. Most of these models have been carried out using mainly saturated clays or dry sands. However the behavior of geotechnical structures located near the soil surface is highly influenced by the water content of the soil located near the surface where the soil is frequently unsaturated.

Experimental complexities related with unsaturated soils are well known in laboratory. Concerning centrifuge modeling these complexities are enhanced, however the potentialities of centrifuge modeling of geotechnical problems involving unsaturated soils may well justify the additional effort.

On the contrary of many centrifuge applications, very few data is available on scaling laws for unsaturated soils (Garnier et al. 2007). This paper presents the results of several authors on scaling laws related to unsaturated soils as well as the results of some models carried out on unsaturated soils. The problems related with soil preparation, instrumentation and atmospheric actuators are highlighted, as well as successful experiences found in the literature. Finally some ideas to improve the practice of centrifuge modeling with unsaturated soils are presented.

2 SCALING LAWS FOR UNSATURATED SOILS IN CENTRIFUGE

2.1 *General considerations*

Experiments carried out using geotechnical centrifuge generally fall in two categories: those designed to investigate process using the centrifuge field as a tool (centrifuge testing), and those that are performed to reproduce data to predict behavior of geotechnical process (centrifuge modeling). This last category makes use of scaling of the results of centrifuge experiments (the model scale) to the problem under investigation (the prototype scale).

A powerful means to analyze the scaling laws, when the mathematical description of the process is well established, is the inspectional analysis (Barry et al. 2001). This analysis involves mapping the equation controlling the process in a non dimensional form. However inspectional analysis relies on the invariance of the physical law under changes of scale (Brikhoff 1960).

Modeling of models (Schofield 1980) can be used when the theoretical model is not available or to validate the scaling laws obtained using inspectional analysis. This technique involves measures at different acceleration levels so that scaling laws can be inferred directly from the measured data.

2.2 *Validation of scaling laws for non-deformable unsaturated soils*

Prototype-model scaling in unsaturated porous media that undergo negligible consolidation in the centrifuge has received much attention previously. Several authors (e.g. Barry et al. 2001; Culligan et al. 1997; Burkhart et al. 2000; Crançon et al. 2000, 2001, Khalifa et al. 2000; Rezzoug et al. 2000 a,b; Knight et al. 2000; Soga & Comoulos 2000; Thorel et al. 2000; Depountis et al. 2001) have presented scaling analysis for porous media flow in unsaturated soils.

Three processes are relevant on scaling laws of flow in unsaturated soils having negligible volume changes: the flow velocity or the discharge, the

dynamics of the evolution of water content or saturation, and the water content profile at equilibrium.

The suction curve of a soil depends on its fabric and mineralogy, these two factors controls the pore sizes and the absorption of water. Furthermore the ions in water affect the osmotic suction.

Due to the complexities of unsaturated soils, it is better to use in the model the same soil than the prototype. In other words, to use a soil having the same mineralogy, reproducing the same fabric and uses the same water. Under these conditions the suction curve is conserved and the profile of water content at equilibrium in a soil column is scaled in the same ratio than the length. In fact, considering a soil column subjected to capillary infiltration (Fig. 1), the pore water pressure in two homologous points A_p and A_m, located at heights Z_p and $Z_m = Z_p/n$ are the same:

$$u_p = \rho_w g Z_p \tag{1}$$

$$u_m = \rho_w g n Z_m = \rho_w g n \frac{Z_p}{n} \tag{2}$$

Considerable efforts has been done during the NECER project (Garnier et al. 2000), to validate the scaling law for capillary rise. For example, Figure 2a shows the results reported by Thorel et al. (2000) concerning the profile of water content in capillary rise for different centrifuge levels. Figure 2b shows the good agreement for all the results reported in prototype scale using 1/*n* as scale factor.

The flow of water in unsaturated soil is commonly described using generalized Darcy's law

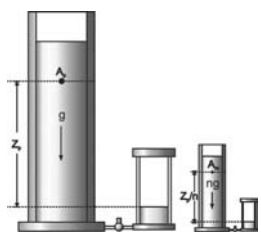

Figure 1. Capillary rise in prototype and in model scales.

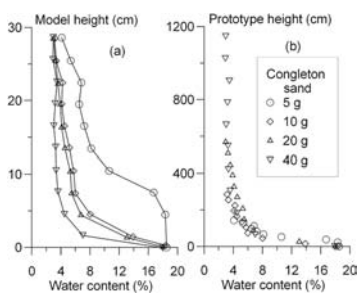

Figure 2. Capillary height for different g levels: (a) model, (b) prototype (Thorel et al. 2000).

(Darcy 1856: Buckingham 1907; Richards 1931; Childs & Collis George 1950):

$$v_w = K_w \frac{\partial H}{\partial z} \tag{3}$$

In this equation H is the hydraulic potential, K_w is the unsaturated permeability, and z the direction of flow. The coefficient of permeability, K_w, is a function of any two of three possible volume-mass properties (Lloret & Alonso 1980):

$$K_w = K_w(S, e) \text{ or } K_w = K_w(e, w) \text{ or } K_w = K_w(w, S) \tag{4}$$

If the model and the prototype have the same permeability and the pore water pressure is conserved in homothetic points, the flow of water in the prototype and in the model are:

$$v_{wp} = K_w \frac{\partial H}{\partial z_p} \quad \text{and} \quad v_{wm} = K_w \frac{\partial H}{\partial z_m} \tag{5}$$

Then:

$$v_{wm} = n v_{wp} \tag{6}$$

Figure 3 shows the results reported by Thorel et al. (2000) concerning the flow of water during capillary rise tests at different g levels. Good agreement is observed using *n* as a scaling factor.

The evolution of water content in unsaturated soils is done by the Richard's equation (1931):

$$\frac{\partial \theta_w}{\partial t} = \frac{\partial}{\partial z}\left[K_w \frac{\partial H}{\partial z} \right] \tag{7}$$

In this case the double derivation about z, implies that the evolution of the water content as a function of time is scaled with a factor of n^2 (Lord 1999):

$$\left(\frac{\partial \theta_w}{\partial t} \right)_m = n^2 \left(\frac{\partial \theta_w}{\partial t} \right)_p \tag{8}$$

Figure 4 shows the results reported by Rezzoug et al. (2000a) concerning the dynamic of the

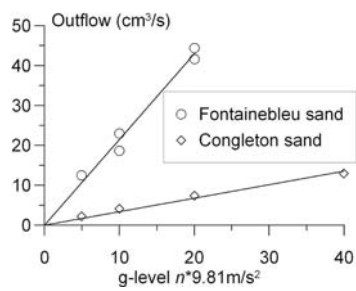

Figure 3. Drainage flow versus g-level (Thorel et al. 2000).

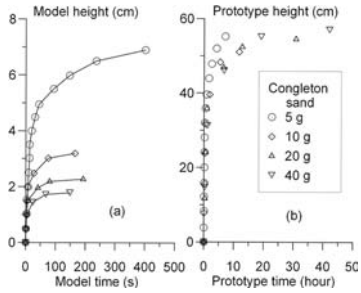

Figure 4. Capillary rise versus time: (a) model, (b) prototype (Rezzoug et al. 2000a).

capillary rise as a function of time, and the good agreement of the n^2 scale factor.

2.3 *Validation of scaling laws for deformable soils*

Most of studies relating scaling laws applied for unsaturated soils have been done on sands having little or negligible volumetric changes on infiltration. Concerning unsaturated deformable soils, Bear et al. (1984) studied the centrifugal filtration in unsaturated deformable soil, and Caicedo et al. (2006) presented a validation of the scaling laws for expansive soils.

Volumetric changes in unsaturated soils depend on the variation of total stress and suction (Fredlund & Rahardjo 1993). Discussions about the best way to take into account suction and total stress in volumetric changes on unsaturated soils are very active. However most authors agree with taking separately the role of total stress and suction, for example Fredlund & Rahardjo (1993) propose for the volumetric changes the following equation:

$$\frac{\partial \varepsilon_v}{\partial t} = m_1^s \frac{\partial(\sigma - u_a)}{\partial t} + m_2^s \frac{\partial(u_a - u_w)}{\partial t} \tag{9}$$

Where m_1^s is the coefficient of volume change with respect to a change in net stress (σ-u_w); and m_2^s is the coefficient of volume change with respect to a change in matric suction (u_a-u_w). The change of matric suction with time is controlled by equation 7. As a result if the change in net stress is null, the relationship of volumetric strain between the model and the prototype is:

$$\left(\frac{\partial \varepsilon_v}{\partial t}\right)_m = n^2 \left(\frac{\partial \varepsilon_v}{\partial t}\right)_p \tag{10}$$

This result is valid too when there is a change in net stress, however if the change in net stress is the result of an external load, the loading velocity must be scaled with a factor of n^2.

The displacement ΔH of the surface of a soil column is:

$$\Delta H = \int \varepsilon_v dz \tag{11}$$

As the volumetric change is conserved in the model and in the prototype, the scale factor for displacement is:

$$\Delta H_p = n \Delta H_m \tag{12}$$

The results reported by Caicedo et al. (2006) confirm these scaling relationships for expansive soils. These results concern the modeling of a 10 m high soil column of overconsolidated lacustrine soil from the "Sabana de Bogotá". The expansion was measured when applying a total inundation of 1 m high at the start of modeling (Fig.5). The soil column was modeled with accelerations of 100 g, 200 g, and 400 g.

Figure 6 shows the expansion displacement in prototype scale using as scale factors n for heave and n^2 for time. These curves show the good agreement obtained using these scale factors.

Concerning expansion, the water content profile is an appropriate parameter that reflects the evolution of expansion in depth. To verify that the soil conditions along the depth are the same in the different models, the water content was measured taking out soil samples at different depth and at the same prototype time for the 200 g and 400 g models. Figure 7 shows the good agreement of the water content profile for the tests performed at 200 g and 400 g.

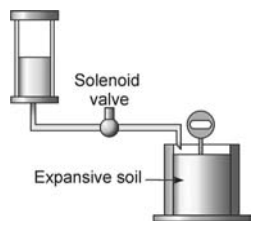

Figure 5. Schematic draw of expansion tests.

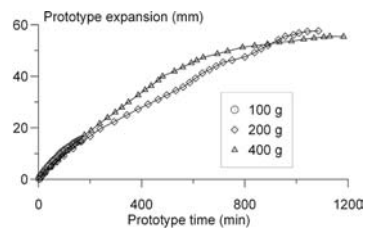

Figure 6. Prototype expansion for different g levels.

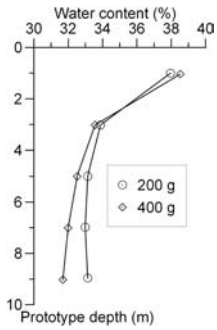

Figure 7. Prototype water content profile for 200 and 400 g.

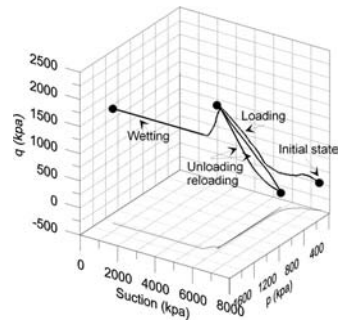

Figure 8. Stress–suction history of a Kaolin under vertical stress compaction.

3 PREPARATION OF SOILS

Physical modeling of unsaturated soils has heightened the need for soil preparation techniques suitable to predict the behavior of soils during the test.

Some studies have been carried out in order to establish controlled methodologies to reproduce intermediate unsaturated soils. These procedures could be grouped in two main techniques: (i) the inclusion of a cementing material in sandy soils (Abdulla & Goodings 1994; Dupas & Pecker 1979; Ismail et al. 2000), and (ii) mixtures of clay and sand compacted by uniaxial compression (Kimura et al. 1994; Boussaid et al. 2005; Murillo et al. 2009).

However the previously mentioned methods suffer from some limitations mainly concerning the possibility of controlling the stress path during compaction. By using traditional compaction techniques using blows or kneading, the stress path determination during compaction is difficult. Although uniaxial compression allows soil preparation under controlled vertical stress, the whole stress path remains unknown. However the behavior of compacted unsaturated soils having expansive or collapsible behavior is strongly dependent on their negative pore water pressure and their stress-suction history.

An alternative to identify the stress-suction history during compaction is the use of suction monitored apparatus (triaxial or oedometer). These apparatus allows the characterization of unsaturated soils in a fraction of time compared with suction controlled apparatus (Blatz & Graham 2003; Jotisankasa et al. 2007).

This kind of apparatus makes possible to assess the stress-suction state and the history of an unsaturated soil on vertical stress compaction. Furthermore it is possible to establish the best preparation procedure to obtain soils having different behavior. For example, Figure 8 shows the stress–suction trajectory of kaolin during compaction, this compaction was made applying a first loading stage and then a cycle of unloading and reloading. Finally the sample is saturated to assess its behavior during wetting.

Although preparation of unsaturated soils for physical modeling by vertical stress compaction is a useful technique, this method is only valid for modeling compacted soils. In fact this technique doesn't replicate the fabric of natural unsaturated soils. For this reason there is a need of developing new preparation techniques that replicates in a better way the unsaturation process in the field, for example reducing phreatic level or drying from the surface.

4 INSTRUMENTATION

4.1 *Suction sensors*

The measure of suction in unsaturated soils is a difficult task for the following reasons:

- It doesn't exist sensors covering the broad range of suction values of unsaturated soils (Table 1).
- Direct measurements of suction have to deal with cavitation.
- The response time of the sensors varies in a broad range.

All these difficulties are enhanced in centrifuge modeling due to the presence of the acceleration field and the need for miniaturization.

For physical modeling in centrifuge the use of standard tensiometers have been reported by Chiu et al. (2005), high performance tensiometers have been tested in centrifuge during the MUSE project (Lourenço et al. 2006; Muñoz et al. 2011). The measurements carried out with tensiometers in centrifuge are consistent with those carried out in laboratory. However, the tensiometers cavitate at a lower maximum sustainable suction at an elevated g-level (Chiu et al. 2005).

Psychrometers have been tested in centrifuge by Tristancho & Caicedo (2008) using a CR7 Campbell data acquisition system installed in the centrifuge arm. The results reported by Tristancho & Caicedo (2008) show that consistent measurements

Table 1. Devices for measuring soil suction.

Suction sensor	Range (MPa)
Hygrometer	10–90
Psychrometer	0.5–6.5
High performance tensiometer	0–2
Standard tensiometer	0–0.09

can be obtained using psychrometers in isothermal conditions under temperature gradients. The offset measured in the psychrometer grows and therefore the measure is less accurate.

4.2 *Water content sensors*

Different devices for measuring water content in centrifuge have been tested (Gunzel et al. 2003), such as capacitive sensors (Dupas et al. 2000), or TDR sensors (Crançon et al. 2000, 2001).

The principle of capacitive sensors is based on the variation of the relative dielectric permittivity of soil, κ, and the contrast between water ($\kappa = 80$), soil ($\kappa = 4$ to 10), and air ($\kappa = 1$). The electronic circuit to measure the dielectric permittivity in water content sensors is a variable frequency oscillator using an inductor and a variable capacitor. Although measures using capacitive sensors are reliable, careful calibration is needed because the readings depend on the shape of the electrodes and on the type of soil.

The technique to measure water content based on the time domain reflectometry, TDR, is based on the propagation velocities of the waves in the porous medium. As the presence of water in the medium affects the speed of the electromagnetic wave, the energy which does not become dissipated in the medium and returns to its source depends on the water content. The accuracy of TDR measurements depends on precise measurement of time and careful calibration with the relative volumetric content of water around the probe. However TDR sensors in centrifuge models have to deal with the problem of its size. In fact the principle treasuring technique of the TDR sensors makes its miniaturization difficult.

5 ACTUATORS

Mechanical actuators like load actuators or robots designed to work on traditional centrifuge models on dry or saturated soils are useful to work on unsaturated soils. However the most challenging actuators for centrifuge models on unsaturated soils are atmospheric actuators. These actuators try to replicate a number of atmospheric variables to study the soil response under particular environmental conditions.

The complexity of the atmospheric actuators depends on the number of environmental variables that are reproduced. For example the following actuators have been used in centrifuge modeling:

- Rain actuators (Kimura et al. 1991).
- Rain and relative humidity environmental chamber (Take & Bolton 2002).
- Rain, relative humidity, wind, temperature and radiation in environmental chamber (Tristancho & Caicedo 2008).

Atmospheric actuators offer interesting possibilities of studying the behavior of geotechnical structures under extreme environmental conditions. However the replication of atmospheric variables respecting scaling laws need a complex control system on the actuators, this particular point is under development nowadays.

6 CONCLUSIONS

This paper deals with the physical modeling of unsaturated soils, both considered in the cases of non-compressible and compressible. An overview on soil preparation, instrumentation and actuators used for experiments on unsaturated soil has been presented.

The challenge is to perform new experiments with engineering applications, taking into account water migration in unsaturated soils.

REFERENCES

Abdulla, W.A. & Goodings, D.J. 1994. Study of sinkholes in weakly cemented sand. *Centrifuge 94*, Leung, Lee and Tan(eds) Balkema, Rotterdam: 797–802.

Barry, D., Lisle, I., Prommer, H., Parlange, J., Sander, G. & Griffioen, J. 2001. Similitude applied to centrifugal scaling of unsaturated flow. *Water Resour. Res.* 37(10): 2471–2479.

Bear, J., Corapcioglu, M.Y. & Balakrishna, J. 1984. Modeling of centrifugal filtration in unsaturated deformable porous media. *Adv. Water. Resour*. 7: 150–167.

Birkhoff, G. 1960. *Hydrodynamics* 2nd ed. Princeton Univ. Press, Princeton N.J.

Blatz, J.A. & Graham, J. 2003. Elastic—plastic modelling of unsaturated soil using results from a new triaxial tests with controlled suction. *Géotechnique* 53(1): 113–122.

Boussaid, K., Thorel, L., Garnier, J., Ferber V. & David J.P. 2005. Comportement mécanique de sols intermediaries reconstitutes: Influence de la teneur en eau et du percentage d'argile. *Congrès francais de mécanique*, Troyes, France.

Buckingham, E. 1907. Studies of the movement of soil moisture. *U:S:D:A: Bur. Of Soils, Bulletin* No. 38.

Burkhart, S., Davies, M.C.R, Depountis, N., Harris, C. & Williams, K.P. 2000. Scaling laws for infiltration and drainage tests using a Geotechnical Centrifuge. In

Physical Modeling and Testing in Environmental Geotechnics. Garnier, Thorel, Haza Eds: 191–198.

Caicedo, B., Medina, C. & Cacique, A. 2006. Validation of time scale factor of expansive soils in centrifuge modeling. In *Physical modeling in Geotechnics* ICPMG 06, Ng, Zhang & Wang (eds.): 273–277.

Childs, E.C. & Collis-George, N. 1950. The permeability of porous materials. *Proc. Royal Soc*. Vol 201 A: 392–405.

Chiu, C., Cui, Y., Delage, P., de Laure, E. & Haza, E. 2005. Lessons learnt from suction monitoring during centrifuge modeling. *Advanced Experimental Unsaturated Soil Mechanics*. Tarantini, Romero, Cui Eds. Taylor & Francis: 3–8.

Crançon, P., Guy, C. & Pili, E. 2000. Modeling of capillary rise and water retention in centrifuge tests using TDR. In *Physical Modeling and Testing in Environmental Geotechnics*. Garnier, Thorel, Haza Eds: 199–206.

Crançon, P., Thorel, L. & Garnier, J. 2001. Flows in unsaturated soils: experiments and physical modelling in geotechnical centrifuge. *XVth ICSMGE.* Istambul 27–31 août 01: 569–574 (in French).

Culligan, O., Barry, D. & Parlange, J. 1997. Scaling unstable infiltration in the vadose zone. *Can. Geot. J*. 34: 466–470.

Darcy, H. 1856. *Histoire des fontaines publiques de Dijon*. Paris Dalmont: 590–594.

Depountis, N., Davies, M.C.R., Harris, C., Burkhart, S., Thorel, L., Rezzoug, A., König, D., Merrifield, C. & Craig, W.H. 2001 Centrifuge modelling of capillary rise, *Engineering Geology* 60(1–4): 95–106.

Dupas, A., Cottineau, L.M., Thorel, L. & Garnier, J. 2000. Capacitive sensor for water content measurement in centrifuged porous media. In *Phys. Modeling & Testing in Environmental Geotech.*. Garnier, Thorel, Haza Eds: 11–17.

Dupas, J.M. & Pecker, A. 1979. Static and dynamic properties of sand—cement. *ASCE Journal of Geotechnical Engineering* 105 GT3: 419–436.

Fredlund, D.G. & Rahardjo, H. 1993. *Soil mechanics for unsaturated soils.* John Wiley & Sons (ed.).

Garnier, J., Gaudin, C., Springman, S.M., Culligan, P.J., Goodings, D., Konig, D., Kutter, B., Phillips, R., Randolph, M.F. & Thorel, L. 2007 Catalogue of scaling laws and similitude questions in geotechnical centrifuge modelling. *Int. J. Physical Modelling in Geotechnics* 7(3): 1–24.

Garnier, J., Thorel, L. & Haza, E. (ed.). 2000. *Physical modeling and testing in environmental geotechnics*. Network of European Centrifuges for Environmental Geotechnic Research. Laboratoire Central des Ponts et Chaussées: 392.

Günzel, F.K., Craig, W.H., Crançon, P., Cottineau, L.-M., Kechavarzi, C., Lynch, R., Merrifield, C.M., Oung, O., Schenkeveld, F.M., Soga, K., Thorel, L. & Weststrate, F.A. 2003 Evaluation of Probes and Techniques for Water Content Monitoring in Geotechnical Centrifuge Models. *Int. J. Physical Modelling in Geotechnics* 3(1): 31–43.

Ismail, M.A., Joer, H.A. & Randolph, M.F. 2000. Sample preparation technique for artificially cemented soils. *ASTM Geotech. Testing J.* 23(2): 171–177.

Jotisankasa, A., Ridley, A. & Coop, M. 2007. Collapse behavior of compacted silty clay in suction-monitored oedometer apparatus. *J. Geot. & Geoenv. Engng*. July: 867–877.

Khalifa, A., Garnier, J., Thomas, P. & Rault, G. 2000. Scaling laws of water flow in centrifuge models. In *Physical Modeling and Testing in Environmental Geotechnics*. Garnier, Thorel, Haza Eds: 207–216.

Kimura, T., Takemura, J., Hiro-Oka, A. & Okamura, M. 1994. Mechanical behaviour of intermediate soils. *Centrifuge 94.* Singapore, Leung et al. (Ed), Balkema: 13–24.

Kimura, T., Takemura, J., Suemasa, N. & Hirooka, A. 1991. Failure Of Fills Due To Rain Fall. *Centrifuge 91*, International Conference, Boulder Colorado: 509–516.

Knight, M.A., Cooke, A.B. & Mitchell, R.J. 2000. Scaling of movement and fate of contaminant releases in the vadose zone by centrifuge modeling. In *Physical Modeling and Testing in Environmental Geotechnics*. Garnier, Thorel, Haza Eds: 233–242.

Lloret, A. & Alonso, E. 1980. Consolidation of unsaturated soils including swelling and collapse behavior. *Géotechnique* 30(4): 449–477.

Lord, A.E. 1999. Capillary flow in the geotechnical centrifuge. *Geotech. Testing J., ASTM* 22(4): 292–300.

Lourenço, S.D.N, Gallipoli, D., Toll, D.G & Evans, F.D. 2006. Development of a commercial tensiometer for triaxial testing of unsaturated soils. *Geotechnical Special Publication Nº 147, ASCE,* Reston 2: 1875–1886.

Muñoz, J.J., Casini, F., Lourenço, S., Vaunat, J., Pereira, J.-M., Thorel, L., Garnier, J., Delage, P; Alonso, E. & Gallipoli, D. 2011 Centrifuge modelling of a shallow foundation on an unsaturated compacted silt. *Géotechnique*. (submitted).

Murillo, C., Thorel, L. & Caicedo, B. 2009. Spectral analysis of surface waves method to assess shear wave velocity within centrifuge models. *J.Applied .Geophysiscs* 68: 135–145.

Rezzoug, A., Konig, D. & Trantafylidis, Th. 2000a. Scaling laws in centrifuge modeling for capillary rise in soils. In *Physical Modeling and Testing in Environmental Geotechnics*. Garnier, Thorel, Haza Eds: 217–224.

Rezzoug, A., Konig, D. & Trantafylidis, Th. 2000b. Numerical analysis of scaling laws for capillary rise in soils. In *Physical Modeling and Testing in Environmental Geotechnics*. Garnier, Thorel, Haza Eds: 217–224.

Richards, L.A., 1931. Capillary conduction of liquids in porous mediums. *Physics* 1: 318–333.

Schofield, A.N. 1980. Cambridge geotechnical centrifuge operations. *Géotechnique* 30: 227–268.

Soga, K. & Comoulos, H. 2000. Some remarks on water movement in homogeneous unsaturated soils in relation to centrifuge testing. In *Phys. Modeling & Testing in Environmental Geotechnics*. Garnier, Thorel, Haza Eds: 243–250.

Take, W.A. & Bolton, M.D. 2002. The use of centrifuge modelling to investigate progressive failure of over consolidated clay embankments. In *Constitutive and Centrifuge Modelling: Two Extremes*, Springman (ed): 191–197.

Thorel, L., Noblet, S., Garnier, J. & Bisson, A. 2000. Capillary rise and drainage flow through a centrifuged porous medium. In *Physical Modeling and Testing in Environmental Geotechnics*. Garnier, Thorel, Haza Eds: 251–258.

Tristancho, J. & Caicedo, B. 2008. Climatic chamber to model soil atmosphere interaction in the centrifuge. In *Unsaturated Soils, Advances in Geo-Engineering,* Toll et al (eds), Taylor & Francis: 117–121.

Physical Modelling in Geotechnics – Springman, Laue & Seward (eds)
© 2010 Taylor & Francis Group, London, ISBN 978-0-415-59288-8

Influence of fluid viscosity on the response of buried structures in earthquakes

S.C. Chian & S.P.G. Madabhushi
University of Cambridge, Schofield Centre, Cambridge, UK

ABSTRACT: The use of high viscous pore fluid has been widely established to match the rate of excess pore pressure generation and subsequent dissipation in dynamic centrifuge tests. The appropriate viscosity is linked to the geometric and gravity scaling factors which corresponds to the use of pore fluid of 'N' cSt in a 'N'g centrifuge test. The use of either water (1 cSt) or pore fluid lower than 'N' cSt can influence the behaviour of soil liquefaction in a centrifuge test. In this paper, the floatation of a tunnel following soil liquefaction is investigated using pore fluids with two different viscosities. The results show that the uplift displacement of the tunnel is significantly affected by the pore fluid viscosity.

1 INTRODUCTION

1.1 *Seismic damage to underground structures*

Past earthquakes in Japan (Seed 1970) and the United States (Bardet & Davis 1999) have identified damage susceptibility of underground structures including large buried pipelines and tanks. Studies by Yang et al. (2004) and Sun et al. (2008) have indicated the likelihood of significant damage by floatation in liquefiable soils. This issue of floatation failure of underground structures poses risk of high human casualties and property losses.

During liquefaction, the shear strength of a saturated cohesionless soil is reduced dramatically due to increase in pore water pressure. In addition, due to the nature of a relatively lower unit weight of tunnel than the surrounding soil, tunnels and other underground lifelines may float due to their buoyancy.

1.2 *Physical modelling of earthquakes*

In geotechnical centrifuge modelling, it is essential to replicate identical stress and strain as in the prototype scale. A scaled model is made to correspond with the prototype at the pre-determined centrifuge g-level. As shown in Table 1, a 1:N model will experiences the same stress-strain condition as the prototype when subjected to a centrifugal acceleration of N × g level (Schofield 1980, 1981).

Table 1 describes a conflict in the time scaling between the dynamic and consolidation events. In order to overcome this inconsistency, the saturated hydraulic conductivity of sand may be reduced by increasing the pore fluid viscosity. However by doing so, concerns were raised about the alterations to damping effects to the soil-fluid phase. Ellis et al. (2000) studied the effects with resonant column tests on sand and determined that the soil skeleton damping is dominant at strains above 0.02%, which masked the negligible increase in viscous damping of the higher viscosity fluid.

Table 1. Centrifuge scaling laws.

Parameter	Model/Prototype	Dimensions
Length	1/N	L
Acceleration	N	LT^{-2}
Velocity	1	LT^{-1}
Strain	1	1
Stress	1	$ML^{-1}T^{-2}$
Force	$1/N^2$	MLT^{-2}
Mass	$1/N^3$	M
Seepage velocity	N	LT^{-1}
Time (Seepage)	$1/N^2$	T
Time (Dynamic)	1/N	T

In centrifuge tests of a tower structure, rapid dissipation of excess pore pressures was observed in sand saturated in water, but the damping characteristics were similar in water and viscous fluid tests (Madabhushi 1994). Likewise, the use of water was found to prevent high pore pressure generation in sand foundations below gravel embankments, thereby lowering the crest settlement of embankment significantly (Peiris et al. 1998).

In this paper, centrifuge tests were conducted to investigate the effects of viscosity on the floatation of buried structures. Comparison between the uses of different pore fluid viscosities at varying buried depth of circular tunnels will be discussed with respect to their uplift displacements. The soil's

responses are depicted with accelerations and pore pressures.

2 CENTRIFUGE TESTING

2.1 *Model preparation*

The models were prepared in a 670 mm (L) × 250 mm (W) × 430 mm (H) Equivalent Shear Beam (ESB) box consisting of aluminium and rubber rings which allows the box to deform comparable to the soil in the box. The design and performance compliance of the ESB Box were mentioned in Zeng & Schofield (1996) and Teymur (2002).

Sand was prepared to the relative density (D_R) of approximately 45% using the sand pluviation method with the automatic sand pourer. The relative density of the sand was adjusted by varying the flow rate and drop height of the nozzle to the desired pour location. Calibration details to produce loose sand samples were described by Chian et al. (2010). The Sable HN31 Hostun sand was used in the models. The properties of the sand are indicated in Table 2.

Instrumentations such as accelerometers (ACC) and pore pressure transducers (PPT) were placed at specific pre-determined depths and locations as shown in Figure 1. All dimensions in this paper are in 'mm' and are shown at model scale.

Tunnels were buried at known depth in the sand to ascertain the difference in the response of tunnels with their buried depth. Securing supports were also put in place so as to avoid any accidental movement of the tunnels prior to centrifuge testing.

After sand pouring was completed, these sands were saturated with high viscous methyl cellulose fluid prepared at the desired viscosity (cSt) equivalent to the centrifuge g-level in the first instance, so as to satisfy the scaling laws. The second model was saturated with low pore fluid viscosity of a ninth of the first model's value as shown in Table 3. Two tunnels were suitable to be placed in the model

Table 2. Properties of Hostun sand.

Properties	Values
Φ_{crit}	33°*
D_{10}	0.209 mm
D_{50}	0.335 mm
D_{60}	0.365 mm
e_{min}	0.555
e_{max}	1.01*
G_s	2.65*

* after Mitrani (2006).

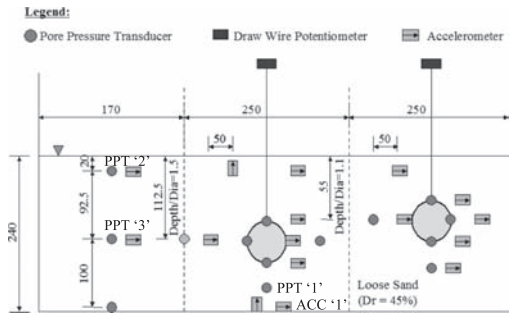

Figure 1. Location of instruments.

Table 3. Test configurations.

Description	DC-02	DC-04
Prototype tunnel diameter	5 m	5 m
Prototype buried depth	7.5 m (1.5 × Dia.) & 5.5 m (1.1 Dia.)	7.5 m (1.5 × Dia.) & 5.5 m (1.1 Dia.)
Pore Fluid viscosity	66.7 cSt	7.4 cSt

as the difference in centrifugal radial gravity field varies by less than 0.34% with the use of a 10 m diameter Turner beam centrifuge.

2.2 *Test procedure*

After model preparation was completed, the model package accompanied with the Stored Angular Momentum (SAM) actuator was loaded in one arm of the beam centrifuge, while the other arm loaded with an equivalent counterweight. The SAM actuator is capable of applying strong lateral motions to a centrifuge package up to a peak ground acceleration (PGA) of 0.3 g in a 100 g centrifuge test (Madabhushi et al. 1998).

During the test, the centrifuge was spun up at intervals of 10 g till the desired g-level of 66.7 g. An earthquake of predetermined magnitude was then fired. Real-time data were acquired via the Centrifuge Data Acquisition System (CDAQS) and transferred to the computer in the control room. The displacements of the buried tunnels were determined before firing a stronger earthquake. After all planned earthquakes have been fired, the centrifuge was slowed and brought to a halt. The tested centrifuge package was then visually examined for further leads on the failure mechanisms.

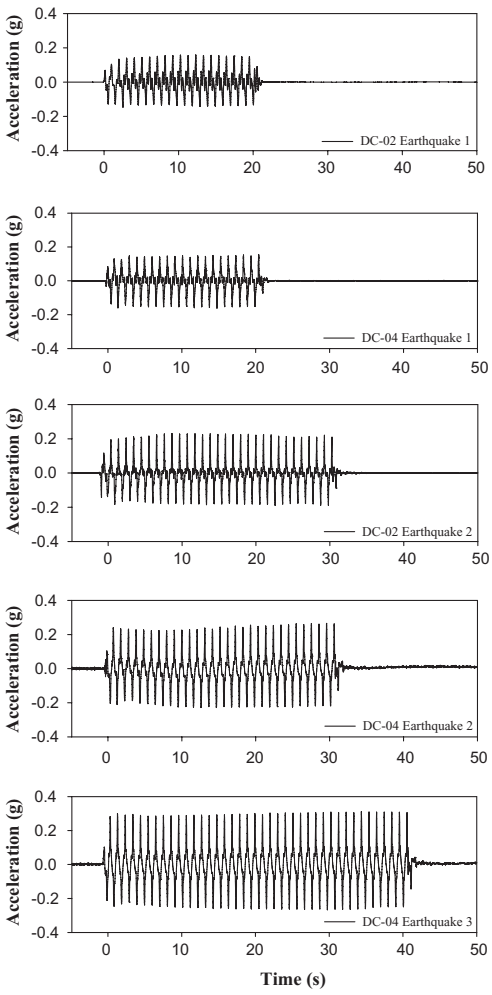

Figure 2. Input earthquake motion at the base of centrifuge models at ACC '1'.

Figure 2 shows the input motion of the earthquake in these tests. These earthquake loadings of each test were comparable in magnitude with PGAs of approximately 0.15 g, 0.24 g and 0.30 g and durations of 20 s, 30 s and 40 s in the first, second and third earthquakes respectively.

3 RESULTS

3.1 *Pore pressure generation and dissipation*

Both centrifuge tests registered an increase in pore pressures with the onset of cyclic earthquake loading. Both tests showed similar peak excess pore pressure generation as illustrated in Figure 3. This demonstrates that the pore pressure generation was unaffected by pore fluid viscosity.

However, due to the low viscosity, migration of fluid was less restrictive. As such, high excess pore pressure was able to dissipate quickly upwards to the soil surface being the sole means of drainage path. The excess pore pressure dissipation was so pronounced that it was observed even during the earthquake loading. In addition, a sharp decrease in pore pressure was observed in DC-04 immediately after the earthquake, thereby indicating the soil's inability to retain high excess pore pressure during post-earthquake.

At the soil surface, the pore fluid migrated quickly towards the free surface. However, a drop in excess pore pressure near the soil surface was not possible because the pore fluid from deeper region would arrive at the shallower region. As a result, excess pore pressure near the soil surface was retained for a longer duration as shown in Figure 4.

3.2 *Floatation of tunnel*

The change in viscosity can also be used to assess the effect of the soil's saturated hydraulic conductivity on the floatation of buried structures. Referring to Eq. 1, saturated hydraulic conductivity is affected by the soil's pore geometry as well as the fluid viscosity and soil porosity (Nutting 1930).

$$K_{sat} = \frac{g}{\nu} \cdot k_i \tag{1}$$

where K_{sat} is the saturated hydraulic conductivity, k_i is the intrinsic permeability of the soil, ρ and μ are the fluid density and kinematic viscosity respectively, and g is the gravitational constant.

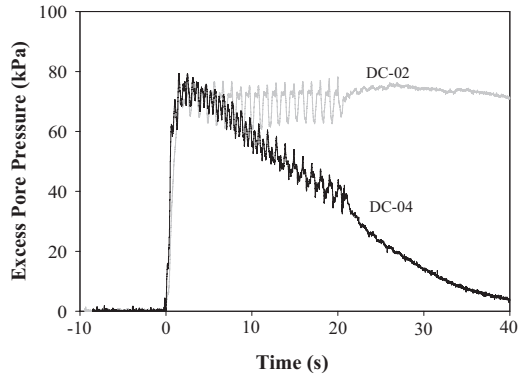

Figure 3. Excess pore pressure near base of centrifuge models at PPT '1'.

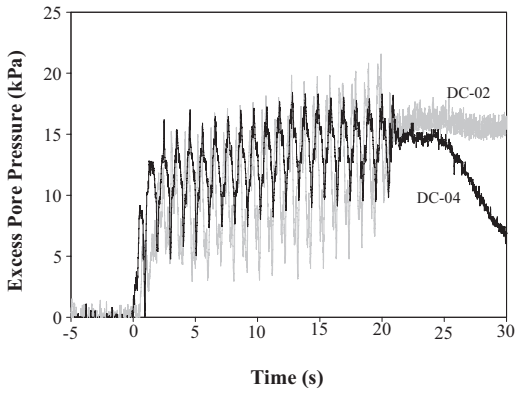

Figure 4. Retention of excess pore pressure near surface of soil at PPT '2'.

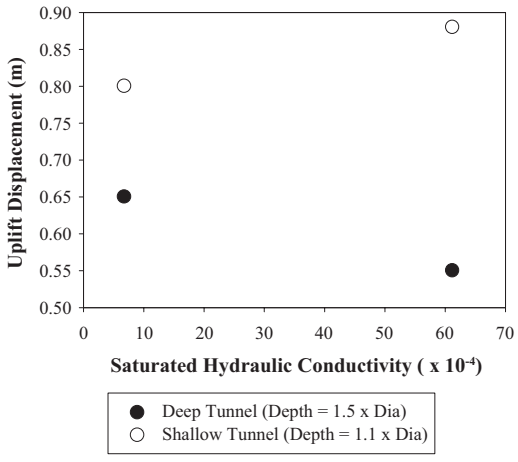

Figure 5. Uplift displacements of tunnels at varying saturated hydraulic conductivity.

The saturated hydraulic conductivity for a given soil becomes lower when the fluid is more viscous. The use of a ninth (7.4 cSt) of the initial pore fluid viscosity (66.7 cSt) would result in an increase in the saturated hydraulic conductivity by nine-folds.

A higher saturated hydraulic conductivity encourages pore fluid mitigation. This may promote uplift displacement of tunnel when adequate saturated hydraulic conductivity permits rapid filling of displaced void with pore fluid. As a result, the shallow tunnel displaced more ™ in DC-04 than in DC-02 as indicated in Figure 5. However, the deep tunnel showed a lower uplift displacement instead. This is due to the rapid dissipation of pore pressures at deep regions as depicted in Figure 3. Recovery of the soil's shear strength took place during the reduction of excess

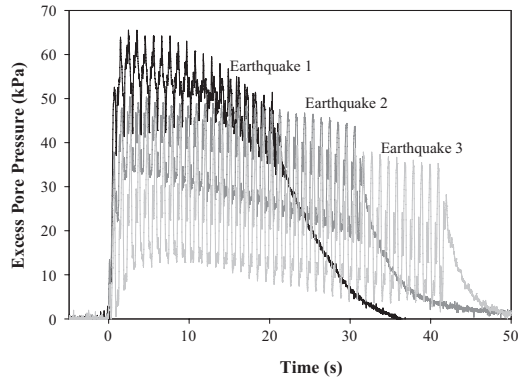

Figure 6. Reduction of peak pore pressures with subsequent earthquakes in DC-04 at PPT '3'.

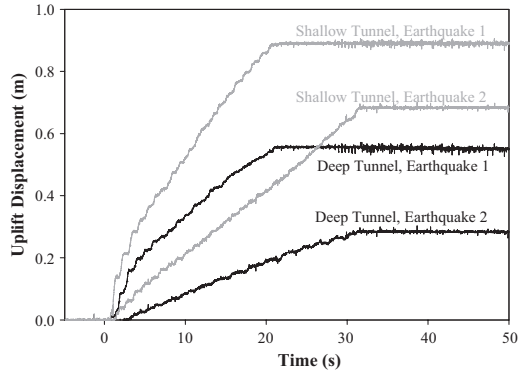

Figure 7. Impact of subsequent earthquakes to uplift displacement in DC-04.

pore pressure which discouraged the progress of floatation.

In subsequent earthquakes, the peak excess pore pressure decreased with the number of earthquakes as illustrated in Figure 6. Given the reduced excess pore pressure, the floatation of tunnels in DC-04 in subsequent earthquakes were less significant as compared to the first earthquake loading. This is verified in Figure 7. Furthermore, the deeper tunnel was also presumed to be affected more substantially than the shallow tunnel. However, such effect would be somewhat influenced by the smaller magnitude of uplift due to heavier overlying soil above the tunnel.

4 CONCLUSION

The use of lower viscosity pore fluid is shown to affect the floatation of tunnels significantly. The lower viscous pore fluid leads to a higher saturated

hydraulic conductivity, which encourages pore fluid migration. This results in an increase in uplift displacement of tunnel as portrayed in the centrifuge tests. Such effect is most obvious for shallow buried structures. In the case of deep buried structures, the rapid dissipation of excess pore pressure dominates which leads to a reduction in uplift displacement due to the recovery of the soil's shear strength. Use of correct viscosity of pore fluid is therefore important for accurate modelling of tunnel uplift in liquefaction problems.

REFERENCES

Bardet, J.P. & Davis, C.A. 1999. Responses of large-diameter buried pipes to earthquakes. In Seco e Pinto (ed), *Earthquake Geotechnical Engineering*: 973–986. Rotterdam.

Chian, S.C., Stringer, M.E. & Madabhushi, S.P.G. 2010. Use of automatic sand pourer for loose sand models. *Int. Conf. On Physical Modelling in Geotechnics*, Zurich, 28 June–1 July 2010. Rotterdam: Balkema.

Ellis, E.A., Soga, K., Bransby, M.F. & Sato, M. 2000. Resonant column testing of sands with different viscosity pore fluids. *ASCE Journal of Geotechnical and Geoenvironmental Engineering* 126(1): 10–17.

Madabhushi, S.P.G. 1994. Effect of pore fluid in dynamic centrifuge modelling. *Proc. Centrifuge '94*, Singapore, 31 August–2 September 1994: 127–132. Taylor & Francis.

Madabhushi, S.P.G., Schofield, A.N. & Lesley, S. 1998. A new stored angular momentum based earthquake actuator. *Proc. Centrifuge '98,* Tokyo, 23–25 September 1998: 111–116. Rotterdam: Balkema.

Mitrani, H. 2006. *Liquefaction remediation techniques for existing buildings*. PhD Thesis, Cambridge University.

Nutting, P.G. 1930. Physical analysis of oil sands, *American Association of Petroleum Geologist Bulletin* 14: 1337–1349.

Peiris, L.M.N., Madabhushi, S.P.G. & Schofield, A.N. 1998. Dynamic behaviour of gravel embankments on loose saturated sand. *Proc. Centrifuge '98,* Tokyo, 23–25 September 1998: 263–270. Rotterdam: Balkema.

Schofield, A.N. 1980. Cambridge geotechnical centrifuge operations. *Geotechnique* 25(4): 743–761.

Schofield, A.N. 1981. Dynamic and earthquake geotechnical centrifuge modeling. *Proc. Int. Conf. on Recent Advances in Geotechnical Earthquake Engineering and Soil Dynamics*, St Louis, 26 April–3 May 1981. 3: 1081–1100.

Seed, H.B. 1970. Soil problems and soil behaviour. In R.L. Wiegel (ed.), *Earthquake Engineering*, Chapter 10, Prentice-Hall, Englewood Cliffs, New Jersey: 227–252.

Sun, Y., Klein, S., Caulfield, J., Romero, V. & Wong, J. 2008. Seismic analyses of the Bay Tunnel. *Proc. Int. Conf. On Geotechnical Earthquake Engineering and Soil Dynamics IV*, Sacramento, 18–22 May 2008: 1–11.

Teymur, B.T. 2002. *Boundary effects in dynamic centrifuge modelling*. PhD Thesis, Cambridge University.

Yang, D., Naesgaard, E., Byrne, P.M., Adalier, K. & Abdoun, T. 2004. Numerical model verification and calibration of George Massey Tunnel using centrifuge models. *Canadian Geotechnical Journal* 41: 921–942.

Zeng, X. & Schofield, A.N. 1996. Design and performance of an equivalent shear beam container for earthquake centrifuge modelling. *Geotechnique* 46(1): 83–102.

This page intentionally left blank

Physical Modelling in Geotechnics – Springman, Laue & Seward (eds)
© 2010 Taylor & Francis Group, London, ISBN 978-0-415-59288-8

Use of automatic sand pourers for loose sand models

S.C. Chian, M.E. Stringer & S.P.G. Madabhushi
University of Cambridge, Schofield Centre, Cambridge, UK

ABSTRACT: The consistency of laboratory sand model preparation for physical testing is a fundamental criterion in representing identical geotechnical issues at prototype scale. This objective led to the development of robotic apparatus to eliminate the non-uniformity in manual pouring. Previous studies have shown consistent sand models with high relative density between 50 to 90% produced by the automatic moving-hopper sand pourer at the University of Cambridge, based primarily on a linear correlation to flow rate. However, in the case of loose samples, the influence of other parameters, particularly the drop height, becomes more apparent. In this paper, findings on the effect of flow rate and drop height are discussed in relation to the layer thickness and relative density of loose sand samples. Design charts are presented to illustrate their relationships. The effect of these factors on different sand types is also covered to extend the use of the equipment.

1 INTRODUCTION

Geotechnical centrifuge modelling has been increasingly popular in the past few decades. Given the nature of testing soils in small scale physical models, accurate, consistent and repeatable sand preparation is essential to represent soil properties in the field. Inconsistency in preparation would result in a large variation in results in the centrifuge tests. Tests on shaking tables can also benefit with more uniform reproduction of models. These merits have motivated many researchers in the development of robotic sand pouring apparatus. Research centres with such facilities include the Hokkaido University in Japan (Miura & Toki 1982), University of British Columbia in Canada (Vaid & Negussey 1984), Laboratoire Central des Ponts et Chaussees (LCPC) in France (Garnier & Cottineau 1988), Technical University Delft in the Netherlands (Allersma 1990), and the National Central University in Taiwan (Chen et al. 1998).

The sand pourer in Cambridge is a travelling pluviator and is designed to be fully automated requiring no intervention from the operator. The components of the apparatus were constructed with available off-the-shelf units and commercial computer control software so as to lower development costs. Details on the design philosophy were presented by Madabhushi et al. (2006).

In addition, previous studies by Zhao et al. (2006) have shown the capability of the automatic sand pourer in producing consistent dense sand samples with relative densities between 50 to 90%. Lower relative densities were not achievable with the multiple sieving arrangements. Therefore, loose samples continued to be prepared with a manual hopper which posed difficulties in ensuring consistent flow rate and drop height.

This paper aims to extend the existing apparatus to achieve consistent low relative density sand samples. The preparation of low relative density samples is particularly important in liquefaction studies in geotechnical earthquake engineering. Over 50 calibration tests were conducted with varying drop height and nozzle diameter. Different types of sand were also included to investigate the grain size effects and the consistency of loose samples.

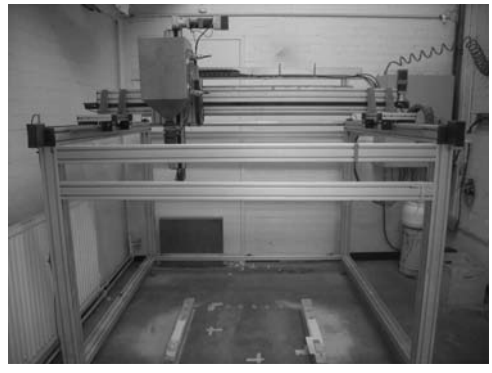

Figure 1. The automatic sand pourer at the University of Cambridge.

2 METHODOLOGY

2.1 *Sand pluviation*

Sand pluviation is employed in the series of calibration tests reported in this paper. Reproducible and uniform sand samples can be achieved with this method as confirmed by Miura & Toki (1982). In their paper, comparisons were made between pluviation and various manual sample preparation methods such as the tapping, flask and rodding. These manual preparation methods were shown to produce significant variation of relative densities between different operators as compared to pluviation due to human skill dependency.

Apart from these merits, the pluviation method can achieve a wide range of relative densities. The effect of particle size segregation is reduced significantly. Zhao et al. (2006) found that the relative density of the sample varies most with the sand flow rate, while varying the drop height has relatively minor effect. The use of sieves at high flow rates also causes sieves to be inundated and blocked. In addition, given that the automatic sand pourer uses a moving hopper and a stationary receiving container, loose samples can be poured without issues of variations in the sand caused by machine vibration and the moving platform. Travelling pluviators can be operated without sieves as it is able to move the nozzle over the area of interest (Amat 2007). Based on these findings, the use of sieves is avoided in the tests. Furthermore, the removal of sieve allows higher sand flow rate per unit area to be achieved which may lead to lower relative density sand samples to be produced. The paths of travel by the hopper are as illustrated in Figure 2.

2.2 *Sand properties and testing accessories*

The types of sand commonly used in Cambridge's centrifuge tests and 1-g experiments are namely, the Fraction E Leighton Buzzard silica sand and the Sable HN31 Hostun silica sand. Their properties are shown in Table 1.

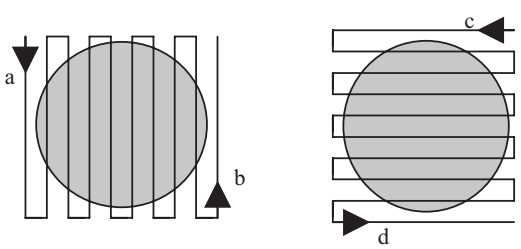

Figure 2. Travel paths of pour (after Zhao et al. 2006).

Table 1. Properties of Fraction E and Hostun sands.

Properties	Fraction E	Hostun
Φ_{crit}	32°*	33°**
D_{10}	0.0993 mm	0.209 mm
D_{50}	0.195 mm	0.335 mm
D_{60}	0.218 mm	0.365 mm
e_{min}	0.613*	0.555**
e_{max}	1.014*	1.01**
G_s	2.65*	2.65**

*after Tan 1990.
**after Mitrani 2006.

A typical round calibration container was used in these tests. Flow irregularities may arise at the edges of travel; hence the travel paths were extended over the boundary of the container to avoid such irregularities. The rim of the container was tapered outwards to minimize disturbances from the boundary effects as suggested by Zhao et al. (2006).

The tests covered a wide range of drop height ranging from 300 mm to 1150 mm. The nozzle diameters used in these tests were 5, 6, 7 and 9 mm.

2.3 *Test procedure*

Sand was poured through the nozzle as the hopper transits across the container in the travel path as illustrated in Figure 2. Each cycle of pour was considered as having travelled from a to b, followed by from c to d. Hence, the plan area will be covered twice in a cycle. The drop height of pour was kept constant by raising the hopper vertically by the thickness of sand deposited in each cycle.

3 TEST RESULTS

3.1 *Overview*

The calibration tests have shown a consistent relationship between drop height and nozzle diameter with the relative density obtained. The relative density achieved ranges from 27.2% to 72.5% and 36.9% to 82.9% for Fraction E and Hostun sands respectively.

3.2 *Influence of drop height*

Each type of sand offers information on their unique influence of drop height to the relative density achieved with a given nozzle diameter. A low drop height leads to a low fall velocity which in turn results in a loosely packed arrangement.

The theoretical fall velocity is computed based on the expression in Eq. 1 (Chapra 2005).

$$v = \sqrt{\frac{m \cdot g}{\rho \times A \times C_d}} \cdot \tanh\left(\frac{t}{\sqrt{\frac{m}{g \cdot \rho \times A \times C_d}}} \right) \quad (1)$$

where v is the fall velocity, m is the mass of the sand grain, g is the acceleration due to gravity, ρ is the density of air, A is the projected area of the sand grain, C_d is the drag coefficient, and t is the elapsed time of the fall.

For simplicity, the sand grains are assumed to be spherical ($C_d = 0.47$) in the above computation. Given a specific drop height, the elapsed time can be estimated with Eq. 2.

$$t = \sqrt{\frac{m}{g \cdot \rho \cdot A \cdot C_d}} \cdot \arccos h\left(e^{\frac{h \cdot \rho \cdot A \cdot C_d}{m}} \right) \quad (2)$$

where h is the drop height.

The fall velocity will achieve terminal velocity as soon as the forces acting on the sand grain is in equilibrium. However, given the low drop height, terminal velocity was not achieved for both sands. Figure 3 illustrates their theoretical fall velocities. Given the smaller average particle size, the fall velocity for Fraction E is lower and also likely to attain terminal velocity earlier than the Hostun sand.

3.3 *Influence of nozzle diameter*

As shown in Zhao et al. (2006), the nozzle diameter alters the relative density. This is extended with the use of two types of sand to investigate the grain size effects. A larger nozzle diameter leads to a steep increase in flow rate as shown in Figure 4.

Similar to the decrease in drop height, a larger flow rate also leads to a lower relative density. The reason for the lower relative density is likely due to the larger flow area of the nozzle, thereby resulting in a minimal bouncing and subsequent rearrangement of the sand particles.

3.4 *Influence of sand type*

The type of sand also influences the relative density obtained. Despite having differing e_{max} and e_{min} values, the relative densities obtained from the two types of sand would ideally show a similar trend. However, the results from these tests showed otherwise. Each type of sand portrayed their individual distinctive trend especially with the use of small nozzle diameters. The relative density curves for both sands obtained with a 5 mm nozzle diameter are presented in Figure 5.

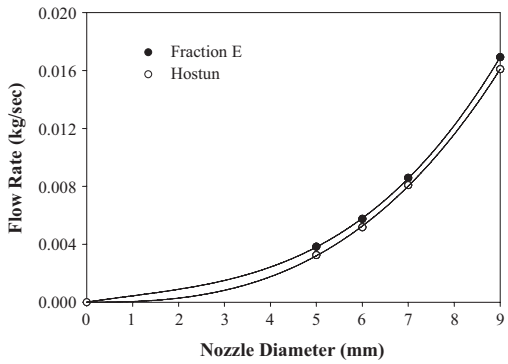

Figure 4. Flow rates for Fraction E and Hostun sands.

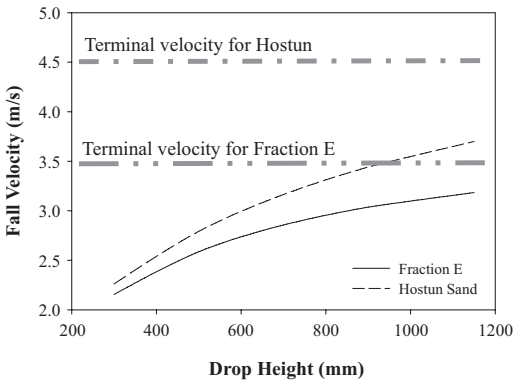

Figure 3. Theoretical fall velocities of sand with drop height.

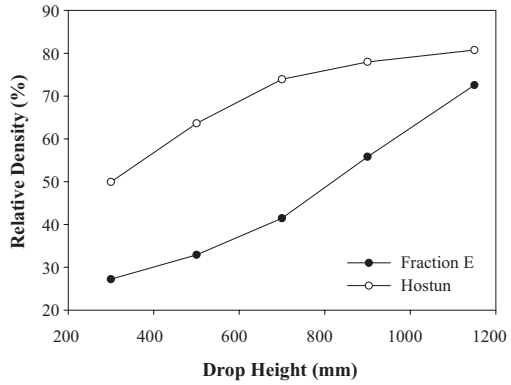

Figure 5. Relative densities with 5 mm nozzle diameter fitting.

The relative density curve for the Hostun sand resembles a leftward shifting of the Fraction E curve. Furthermore, despite the differing trends, the results still showed persistence of an inverse relationship between flow rate and relative density between the two types of sand.

Fraction E sand generally produces higher flow rates than Hostun sand for all nozzle diameters as illustrated in Figure 4. Hence, this could have led to the Fraction E sand achieving a consistently lower relative density than the Hostun sand across all drop heights.

Alternatively, the lower relative density achieved may be due to the difference in particle size distribution of the sands. The finer Fraction E sand produces a relatively lower relative density as compared to the coarser Hostun sand. Figure 6 illustrates the particle size distribution curves for the two types of sand obtained with an accusizer and following the procedure of the Single Particle Optical Sizing (SPOS) method outlined by White (2002).

3.5 *Design charts*

These calibration tests are part of the effort to provide design charts for the convenience of researchers using the automatic sand pourer. The available nozzle diameter fittings and drop height are investigated. Figures 7 and 8 show these design charts for Fraction E and Hostun sands respectively.

It was postulated by Zhao et al. (2006) that the varying the drop height has a minor effect on the relative density when using the multiple sieve arrangement. The relative density obtained was also assumed to be linearly correlated to the flow rate. However, Figures 7 and 8 showed that the influence of drop height becomes more apparent without the use of sieves. In addition, the relative density did not follow a linear relationship with flow rate in these tests.

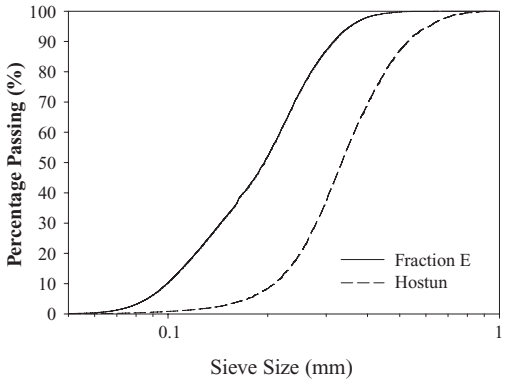

Figure 6. Particle size distribution for Fraction E and Hostun sand.

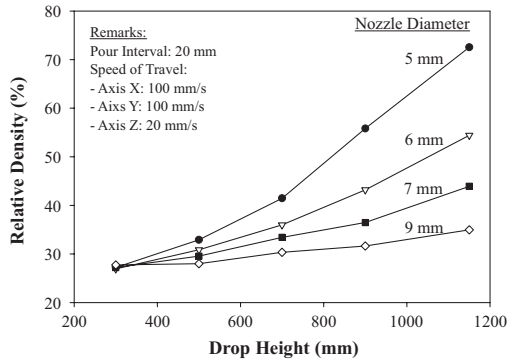

Figure 7. Design chart to achieve specific relative density with Fraction E sand.

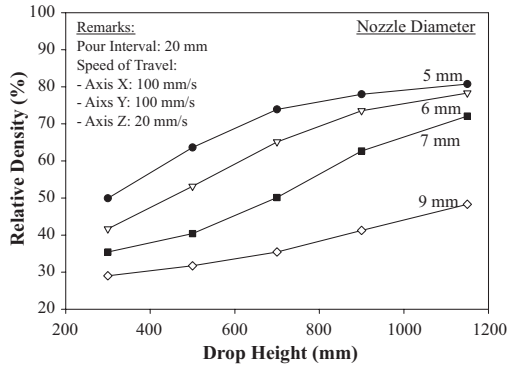

Figure 8. Design chart to achieve specific relative density with Hostun sand.

In order to fully utilise the automation of the sand pourer, a good estimation of the number of pour cycles required to achieve a desired thickness of sand is essential. This is particularly useful for placement of instruments at specific depths of the sand. Similarly, these can be realised with charts indicating the approximate pour thicknesses for different nozzle diameters at varying drop heights. Figures 9 and 10 provide the information to achieve the above purposes. These figures are to be referred with the charts in Figures 7 and 8.

As observed in these figure, Fraction E generally produces a slightly thicker pour per cycle. This is in agreement with the higher flow rate illustrated in Figure 5. The influence of increased relative density with drop height is also reflected in these figures with downward-trending lines.

3.6 *Relationship between sand properties and apparatus parameters*

In the first instance, the relative density curves shown in Figures 7 and 8 may not show visible

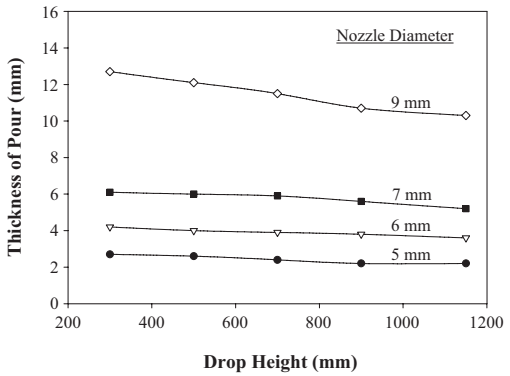

Figure 9. Design chart to estimate thickness of pour with Fraction E sand.

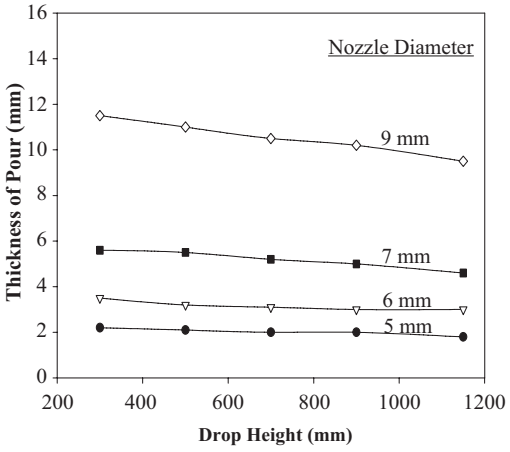

Figure 10. Design chart to estimate thickness of pour with Hostun sand.

patterns in comparison with one another. However, they do level off at extreme high and low values of relative densities. This is expected as extra effort is required to compact very dense sand samples, especially with the limitation of fall velocities of the sand grains approaching the terminal velocity. Likewise, there is a constraint on the minimum relative density governed by the sand grain arrangement obtainable from the pluviation technique. The relative density curves would therefore turn out to be in a sigmoid-like function (an S-curve shape). Given the operating limits of the apparatus, the relative density curves obtained may not portray the complete upper and lower limits achievable with the type of sand. Hence, the data illustrated in the design charts in Figures 7 and 8 reflect only a portion of the complete S-curve. Since the sand pourer is mainly used for preparation of small scale models, the limits of the drop height and nozzle diameter investigated are sufficient for laboratory research purposes.

4 CONCLUSIONS

The results demonstrate that the automatic sand pourer is capable of producing repeatable loose sand samples at specific relative densities. Smaller sand grain sizes can offer a lower relative density. Design charts are produced for each of the sand investigated. They allow varying relative densities of sand layers to be laid with desired sand thickness within the constraints of available drop height and flow rate. Instruments may also be placed at specific thicknesses of the sand with ease. The tests conducted also revealed that the relative density curves follow a generalised sigmoid-like function with levelling off at extreme high and low values of relative density.

REFERENCES

Allersma, H.G.B. 1990. *Centrifuge research TUD computer controlled sand pluviation machine.* Report No. 325. Delft University of Technology, Delft, Netherlands.

Amat, A.S. 2007. *Elastic stiffness moduli of Hostun sand.* University of Bristol, UK.

Chapra, S.C. 2005. *Applied numerical methods with MATLAB for scientists and engineers*. MacGraw-Hill, New York.

Chen, H.T., Lee C.J. & Chen, H.W. 1998. The traveling pluviation appartatus for sand specimen preparation. *Proc. Centrifuge 98, Tokyo, 23–25 September 1998*. 143–148. Rotterdam: Balkema.

Garnier, J. & Cottineau, L.M. 1988. La centrifugeuse du LCPC: Moyens de préparation des modèles et instrumentation. In Corte (ed). *Proc. Centrifuge 88, Paris, 25–27 April 1988*. 83–90. Rotterdam: Balkema.

Madabhushi, S.P.G., Houghton, N.E. & Haigh, S.K. 2006. A new automatic sand pourer for model preparation at University of Cambridge. *Int. Conf. on Physical Modelling in Geotechnics, Hong Kong, 3–8 August 2006*: 217–222. Rotterdam: Balkema.

Mitrani, H. 2006. *Liquefaction remediation techniques for existing buildings*. Cambridge University.

Miura, S. & Toki, S. 1982. A sample preparation method and its effect on static and cyclic deformation-strength properties of sand. *Soils and Foundations.* 22(1):61–77.

Tan, F.S.C. 1990. *Centrifuge and theoretical modelling of conical footings on sand*. Cambridge University.

Vaid, V.P. & Negussey, D. 1984. Relative density of pluviated sand samples. *Soils and Foundations.* 24(2):101–105.

White, D.J. 2002. The measurement of particle size distribution using the Single Particle Optical Sizing (SPOS) method. *Technical Report, CUED/D-SOILS/TR321*. University of Cambridge, UK.

Zhao, Y., Gafar, K., Elshafie, M.Z.E.B., Deeks, A.D., Knappett, J.A. & Madabhushi, S.P.G. 2006. Calibration and use of a new automatic sand pourer. *Int. Conf. on Physical Modelling in Geotechnics, Hong Kong, 3–8 August 2006*. 265–270. Rotterdam: Balkema.

This page intentionally left blank

Physical Modelling in Geotechnics – Springman, Laue & Seward (eds)
© 2010 Taylor & Francis Group, London, ISBN 978-0-415-59288-8

Physical modeling of kinematic pile-soil interaction under seismic conditions

L. Dihoru, S. Bhattacharya, C.A. Taylor & D. Muir Wood
University of Bristol, Bristol, UK

F. Moccia & A.L. Simonelli
University of Sannio, Benevento, Italy

G. Mylonakis
University of Patras, Patras, Greece

ABSTRACT: A series of shaking table tests were carried out to study the kinematic response of flexible piles in layered soil deposits under seismic excitation. These tests were carried out in a deformable shear stack where the dynamic responses of the pile and the free field were recorded for various seismic inputs, soil configurations and pile head boundary conditions. The pile bending moments were measured along the length of the pile using strain gauges. The bending moment profiles are compared with the predictions made by three theoretical models of kinematic pile-soil interaction: (a) Dobry & O'Rourke (1983); (b) Mylonakis et al. (1997) and (c) Nikolaou et al. (2001). This study showed that the theoretical models predicted the maximum kinematic pile response with a variable degree of success. The observed differences can be attributed to the limitation imposed by the idealizations in the respective model regarding the non-linear nature of the soil.

1 INTRODUCTION

1.1 *Context of the research*

Piles are often used in moderate to high seismic areas to support structures (buildings and bridges) where the soil is inadequate to carry the load on its own. In these seismic areas, piles often pass through shallow loose and/or soft soil deposits and rest on competent end bearing soils. Post-earthquake reconnaissance work (Mexico City 1985; Kobe 1995) has shown that a large number of pile-supported buildings built in layered soils suffered significant settlement and tilting and that in several cases pile damage has occurred close to interfaces separating layers with very different shear moduli. It is widely acknowledged that piles are affected by both the movement of the superstructure, i.e. inertial forces, and the kinematic bending moments induced by the surrounding soil. Recent building codes (Eurocode 8) include pile design provisions that account for the combined effect of both mechanisms. One of the challenges faced by the engineers lies in the prediction of the maximum bending moment in the pile at an interface having a sharp stiffness contrast.

1.2 *Effect of soil conditions on pile response*

The effect of local soil conditions on the observed magnitude and patterns of seismic damage to buildings have been studied extensively in the last four decades. A synergetic relationship between earthquake engineering and soil dynamics research has developed, with soil geometric and stiffness characteristics becoming important parameters in the seismic design of structures. The shearing stress-strain behaviour of soils, in particular the shear modulus G (γ) and the damping ratio β (γ) were found to be the properties that affect most the dynamics of soil-structure interaction at small, medium and large strains γ.

A large number of analytical and numerical methods have been proposed for evaluating the dynamic lateral response of piles (simplified methods, Winkler foundation models, finite element/boundary element methods).

1.3 *Research objectives*

This paper presents a set of experimental results from a program of dynamic pile testing carried out on the earthquake simulator at Bristol University.

The research was carried out within the framework of the RELUIS (Rette di Laboratori Universitari Ingegneria Seismica) project. A small scale model pile was installed in a shear stack containing several granular material configurations. The shear stack was subjected to real seismic inputs while the free-field motion and the bending response of the pile were measured. Three classic theoretical models of soil-pile interaction (Dobry & O'Rourke 1983; Mylonakis et al. 1997 and Nikolaou et al. 2001) were employed in evaluating the soil-pile kinematic interaction. A comparison was made between the experimental and the theoretically-simulated results of pile bending.

2 SEISMIC TESTING OF A PHYSICAL MODEL OF SOIL-PILE INTERACTION

2.1 *Scaling laws and properties of the soil*

The small scale model employed in this study was based on a reference numerical prototype (Figure 1) used in a number of previous parametric studies (Mylonakis et al. 1997; Nikolaou et al. 2001 and Sica et al. 2007). The prototype is a simplified two-layered profile consisting of a top layer of soft clay and a bottom layer of medium density gravel overlying the bedrock. The prototype shear wave velocities are v_{s1} = 100 m/s (top) and v_{s2} = 400 m/s (bottom) and the resulting profile can be classified as subsoil type D, according to Eurocode 8 (EN-1998-1 2003). It is worth noting that Eurocode 8 recognizes the importance of kinematic interaction for structures embedded in soil profiles with high stiffness contrast between consecutive layers. The Poisson's ratio and the thickness of the soil were the same for the two prototype layers ($\nu_1 = \nu_2 = 0.4$ respectively $h_1 = h_2 = 15$ m). The prototype subsoil profile has a total thickness of 30 m, and contains a concrete pile of diameter d = 600 mm, length l = 20 m and Young's modulus E_p = 25 GPa. Each soil layer is characterised by its thickness h, density ρ, shear wave velocity v_s, Poisson's ratio ν, and damping ratio β.

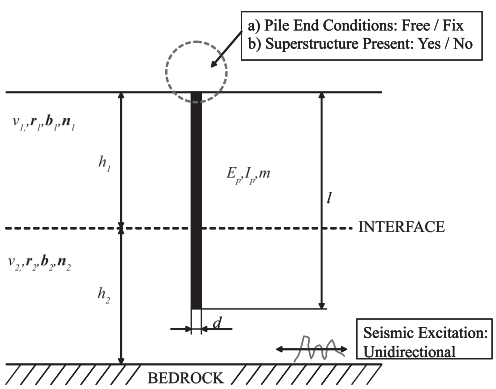

Figure 1. Reference prototype employed in the study.

It is important to mention that this research employed dry sands as model materials for the soil profile. While recognizing the difference in properties between clay, gravel and sands, the main objective of this study was to achieve a similar stiffness contrast between the two layers for model and prototype.

The experimental work made use of an existing shear stack of length 1190 mm, width 550 mm and height 818 mm (Figure 2). The ratio between the prototype soil depth (30 m) and the shear stack height (0.8 m) gave the fundamental scale factor for length (n = 37.5) which governed all the compliance laws employed in modeling (Table 1).

The details regarding the physical and geometrical similitude between the model and the prototype have already been described (Dihoru et al. 2009). A strain-gauged 6063-T6 HE9TF aluminium alloy model pile (E_{Al} = 70 GPa, outer diameter D_0 = 22.23 mm, length l = 0.75 m, thickness t = 0.71 mm) was installed in the centre of the stack

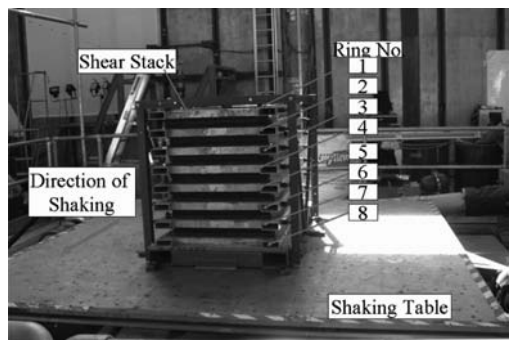

Figure 2. Shear stack installed on the earthquake simulator.

Table 1. Scale factors for single gravity models (Muir Wood 2002).

Variable	Scale factor	Magnitude
Length	n_l	n^{-1}
Density	n_ρ	1
Stiffness	n_G	$n^{-0.5}$
Acceleration	n_g	1
Stress	$n_\rho n_g n_l$	n^{-1}
Strain	$n_\rho n_g n_l / n_G$	$n^{-0.5}$
Displacement	$n_\rho n_g n_l^2 / n_G$	$n^{-1.5}$
Velocity	$n_g n_l (n_\rho / n_G)^{0.5}$	$n^{-0.75}$
Dynamic time	$n_l (n_\rho / n_G)^{0.5}$	$n^{-0.75}$
Frequency	$(n_l)^{-1} (n_\rho / n_G)^{-0.5}$	$n^{0.75}$
Shear wave velocity	$(n_\rho / n_G)^{-0.5}$	$n^{-0.25}$

and the model soil was deposited by dry pluviation from a drum suspended above the shear stack. The materials employed in soil modeling were Leighton Buzzard (LB) sand BS881-131, Fraction E (D_{50} = 0.142 mm, G_s = 2640 kg/m^3, e_{min} = 0.613, e_{max} = 1.014) and LB sand BS881-131, Fraction B (D_{50} = 0.82 mm, G_s = 2640 kg/m^3, e_{min} = 0.486, e_{max} = 0.78). The reference values for e_{min} and e_{max} for the sands are given in Tan 1990.

A number of granular material configurations were tested out of which only one will be investigated in this paper. The model soil configuration presented here consisted of a 0.4 m thick top layer of LB- Fraction E and 0.4 m thick bottom layer of sand mixture containing 85% LB-Fraction B and 15% LB-Fraction E (by mass).The pluviation procedure aimed to obtain two layers of significantly different packing density (loose top layer and dense bottom layer) in order to physically model a high stiffness contrast. Exploratory modal tests were carried out to determine the shear wave velocity in the two layers. Pulse half-sinusoidal signals of 10 Hz frequency and 10V amplitude were generated by the shaking table in the horizontal direction. The travel time of the shear wave between various accelerometers embedded in sand at precise locations was employed in computing the shear wave velocity and the shear stiffness of the sand layers. The experimentally achieved stiffness values were G_1 = 9 MPa (top layer) and G_2 = 32 MPa, respectively. The following set of instruments were employed for measuring the dynamic behaviour of the model: accelerometers embedded in sand for the free field response, accelerometers installed on the outer rings of the stack for the shear stack response and strain gauges installed at eight different ordinates on the pile for the pile bending response.

2.2 *Experimental layout and physical modelling*

A schematic layout of the experiments showing the soil layering and the boundary conditions of the pile head are shown in Figure 3.

Figure 4 shows the instrumented (strain gauged) pile.

Acceleration records from the Italian strong motion database (Scassera et al. 2008) have been used as input motions for the experimental and the numerical work. The seismic inputs have been chosen in such a way that their original peak ground acceleration values are as close as possible to the reference maximum peak acceleration on soil type A of the selected seismic zone. The following seismic records were employed: Friuli (1976) (TMZ records) and Irpinia (1980) (STU records). The inputs were frequency scaled, while their amplitude was kept unscaled. Two scaling factors were employed in frequency scaling, i.e. 2 and 12 (Table 2).

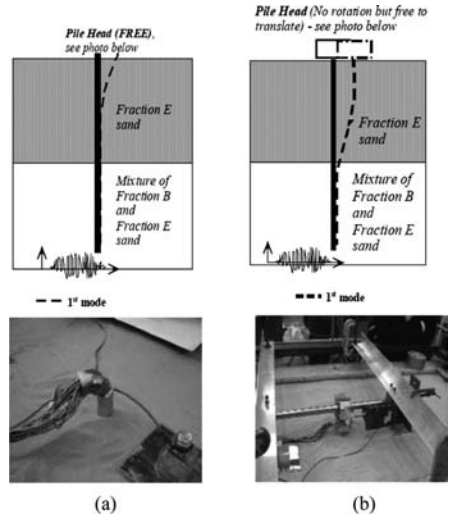

Figure 3. Schematic diagram of (a) the free end boundary condition of the pile (top) and photo of the pile head (bottom). (b): the fixed head (free to translate but fix against rotation-top) and photo (bottom).

Figure 4. Strain gauged pile.

Table 2 shows the features of the seismic input for two scaling factors (2 and 12). Other details associated with the tests can be found in Dihoru et al. (2009).

The unscaled version of the strong motion data is shown in Figures 5 and 6.

Table 2. Details of the employed seismic inputs.

Input motion	Scaling factor	Δt scaled	PGA	Arias intensity
		s	g	m/s
STU 000	12	0.0002	0.3	0.0925
STU 000	2	0.0012	0.3	0.5548
TMZ 270	12	0.0004	0.3	0.0961
TMZ 270	2	0.0025	0.3	0.6007

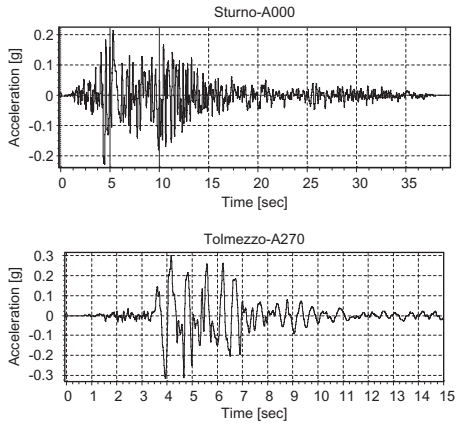

Figure 5. Acceleration time history: STU unscaled (top) and TMZ unscaled (bottom).

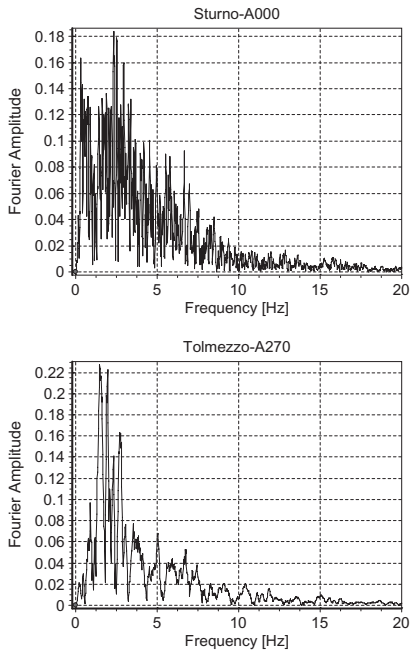

Figure 6. FFT of the STU signal (top) and TMZ (bottom).

3 THEORETICAL METHODS FOR COMPUTING BENDING MOMENTS AT THE INTERFACE

In this paper, the experimental results are compared with theoretical predictions made via a linear elastic method and via a non-linear method based on an equivalent linear procedure, respectively.

Linear analysis: In this type of analysis, the pile and the soil are assumed to be in the linear elastic region. The analysis was based on the SPIAB ('Soil Pile Interaction Analysis') code (Mylonakis 1995). The theoretical bending moment values were compared with the experimental results. It is worth observing that, when subjected to a strong earthquake, the soil will no longer be in the linear elastic range. However, a linear elastic analysis was considered useful in the initial stage of the investigation.

Non-linear analysis: In this type of analysis, the non linear behavior of the soil is represented by an equivalent linear elastic model which accounts for soil stiffness and damping ratio values consistent to the earthquake-induced level of shear strain. This is still a crude representation of the actual soil response under earthquakes, but it is certainly more realistic than the linear elastic model. An equivalent linear site-response analyses of the subsoil has been carried out using EERA (Equivalent-linear Earthquake Response Analysis, Bardet et al. 2000). The equivalent stiffness and damping parameters obtained via EERA were used as inputs in the SPIAB analysis. The next section compares the simulated results with the experimental ones.

4 COMPARISON BETWEEN EXPERIMENTAL RESULTS AND THEORETICAL PREDICTIONS

Figure 7 compares the experimental bending moments with simulated results obtained via EERA and SPIAB. The equivalent values for stiffness and damping for the two layers obtained via EERA were employed as input parameters in the SPIAB analysis. The ratio of shear modulus of the top layer to the shear modulus of the bottom layer was 9:37. The kinematic bending moments were normalized by the yielding moment of the pile (M_y). The bending moments were found to be influenced by the boundary conditions of the pile head and by the input motion. The equivalent linear elastic analysis method (EERA and SPIAB) predicted the shape of the bending moment profile reasonably well.

The experimental and the SPIAB maximum bending moments at the interface were also compared with the predictions made via two analytical